Curtin Medical School

Development of Novel Nanocosmeceuticals for Skin Delivery

Thellie Ponto

0000-0002-0234-0653

This thesis is presented for the Degree of
Doctor of Philosophy
of
Curtin University

March 2022

DECLARATION

To the best of my knowledge and belief, this thesis contains no material previously published by any other person except where due acknowledgment has been made.

This thesis contains no material which has been accepted for the award of any other degree or diploma in any university.

Animal Ethics The research presented and reported in this thesis was conducted in compliance with the National Health and Medical Research Council Australian code for the care and use of animals for scientific purposes 8th edition (2013). Ethical approval was not required, as advised by the Curtin University Animal Ethics Committee, as all animals used in the project were stillborn at birth and collected by veterinarians.

Human Ethics The research presented and reported in this thesis was conducted in accordance with the National Health and Medical Research Council National Statement on Ethical Conduct in Human Research (2007) – updated in March 2014. The clinical study conducted in this thesis received human research ethics approval from the Curtin University Human Research Ethics Committee (EC00262), Approval Number #HSE2019–0521. The trial was registered on Australia and New Zealand Clinical Trials Registry (ANZCTR), Approval Number #ACTRN12619001547134.

Signature: _____

Date: 25/ 03 / 2022

ABSTRACT

Nanocosmeceuticals combine active cosmetic ingredients integrated with nanotechnology to enhance sensory, physicochemical and therapeutic properties. Nanocosmeceuticals carriers have diverse sub-micron sized forms (10 nm to 1000 nm) such as nano and microemulsions, vesicles and particles used in the topical delivery of cosmeceutical ingredients. This research focused on developing novel nanocosmeceutical formulations to target delivery to the skin, enhance the stability of actives, and improve sensory properties on the skin. Nano/microemulsions were developed for two natural product active cosmeceutical compounds, with different physicochemical properties and thus formulation challenges. These were fully assessed for their physical characteristics, stability, skin delivery and efficacy. Quality by Design (QbD) principles were applied, and materials were chosen based on their physicochemical properties and safety profile.

Chapter 1 of the thesis presents a critical review of the current literature on topical nanocosmeceuticals and their application to human skin.

Chapter 2 describes the development of nano-creams containing caffeine (CAF) to manage cellulite. These formulations of 2% CAF were developed using a range of oils, surfactants, and chemical penetration enhancers and fabrication methodologies. A target product profile (TPP) was generated and optimal formulations were developed using a low energy method to meet the TPP. Physical characteristics were characterised, including organoleptic properties, pH, droplet size distribution, and viscosity. The optimal CAF nanoemulsion exhibited a particle size of 425.00 ± 5.37 nm, pH 5.64 ± 0.01, and viscosity of 8814 ± 1050 Pa.s. In vitro permeation testing (IVPT) of the developed formulations and a topical marketed 2% CAF cream were conducted in Franz-type diffusion cells using newborn piglet skin. The steady-state CAF flux (Jss) for the optimised formulation was 8.829 ± 1.472 µg/cm²/h compared with 2.827 ± 0.555 µg/cm²/h for the marketed 2% CAF semisolid topical cream. The optimised 2% CAF formulation containing lanolin (LAN) was chosen for clinical testing.

Chapter 3 describes the development of a standardised method for scoring the severity of cellulite in female participants' posterior thighs region and evaluating the method's reliability. This tool was then used as a primary efficacy measure in the clinical trial. In Stage 1 of the study, five evaluators were provided with written instructions outlining the steps to be followed

in the assessment process and conducted their evaluations independently, recording a score for the numbered images of each participant. After a 4-week interval, each evaluator repeated their assessment using the same images presented randomly. No additional training was provided. In Stage 2 of the study, 2 evaluators received additional training and practice in scoring the photographic images. They scored the images independently, but when there was a discrepancy between scores, a third person acted as a moderator and assigned a moderated score for the images. This scoring and moderation process was repeated after 4 weeks on the same set of images presented in random order. In stage 1, the inter-rater reliability ($ICC_{2,5}$) was 0.838 (95% CI: 0.700–0.922) and test/retest $ICC_{3,1}$ values ranged from 0.360 – 0.990. In stage 2 (following further training), the inter-rater reliability for 2 evaluators improved to 0.978, and the test/retest reliability of the moderated scoring method improved to 0.993.

Chapter 4 describes the clinical trial conducted to determine the effect of the optimised CAF nano-cream formulation on cellulite appearance, thigh circumference, and skinfold thickness. The clinical trial was approved by the Ethics Committee of Curtin University (HSE2019-0521) and registered on the Australian New Zealand Clinical Trials Register (ACTRN12619001547134). 24 healthy females were recruited, aged between 18 to 55 years, with a BMI > 22 and the presence of at least mild cellulite. A double-blind, randomised placebo-controlled paired trial was conducted where each volunteer applied active and placebo cream to regions on each of the upper thighs, twice daily for 12 weeks. The effect of the cream on skin appearance was monitored over 12 weeks. The primary outcome measures were reduced cellulite scores from 3.96 (95% CI: 3.16-4.76) to 2.50 (95% CI: 1.70-3.30) (active) compared with placebo from 3.88 (95% CI: 3.08-4.67) to 2.83 (95% CI: 2.03-3.63). The effect sizes (ES) indicated a moderate effect for active CAF nano-cream formulation (ES = 0.475), whilst placebo (ES = 0.286) had a small effect.

Chapter 5 describes the development of self nano-emulsifying drug delivery systems (SNEDDS) for skin delivery of astaxanthin (ASX), a potent natural antioxidant. The formulations were characterised for physical appearance, viscosity, refractive index, stability, and antioxidant activity of ASX. SNEDDS-ASX skin penetration/permeation was determined across porcine skin mounted by IVPT. ASX was quantified in the stratum corneum (SC), the epidermis-dermis-follicle region (E+D+F) and the receptor compartment. Terpenes (D-

limonene, geraniol and farnesol) were included in the SNEDDS formulations to evaluate their potential skin penetration enhancement. All SNEDDS formulations had droplets in the 20 nm range with low polydispersity. SNEDDS-L1 (no terpene) significantly increased ASX penetration to the SC and the (E+D+F) compared to an ASX in oil solution and a commercial ASX facial serum product. The SNEDDS containing D-limonene gave the highest ASX permeation enhancement with 3.34 and 3.79 times the amount in the SC and E+D+F, respectively, compared to a similarly applied dose of ASX in oil. We concluded that SNEDDS provide an effective formulation strategy for the enhanced skin penetration of a highly lipophilic molecule. When applied to ASX, it can offer topical formulations for UV protection anti-ageing and inflammatory conditions of the skin.

The doctoral research conducted in this thesis contributes to a better understanding of the development of nanocosmeceuticals and their interaction with the skin. The formulation development approach, materials used and low energy fabrication methodology offer promising formulations for skin delivery applications in dermatological and cosmetics.

LIST OF PUBLICATIONS AND CONFERENCE ABSTRACTS

Publications:

- Jhanker, Y., Mbano, M. N., **Ponto, T**., Espartero, L. J. L., Yamada, M., Prow, T., Benson, H. A. E. (2021). Comparison of Physical Enhancement Technologies in the Skin Permeation of Methyl Amino Levulinic Acid (mALA). *International Journal of Pharmaceutics*, 610, 121258. doi: 10.1016/j.ijpharm.2021.121258
- **Ponto, T**., Latter, G., Luna, G., Leite-Silva, V. R., Wright, A., Benson, H. A. E. (2021). Novel Self-Nano-Emulsifying Drug Delivery Systems Containing Astaxanthin for Topical Skin Delivery. *Pharmaceutics*, 12(2),108. doi:10.3390/pharmaceutics13050649
- Nastiti, C. M. R. R., **Ponto, T**., Mohammed, Y., Roberts, M. S., Benson, H. A. E. (2020). Novel Nanocarriers for Targeted Topical Skin Delivery of the Antioxidant Resveratrol. *Pharmaceutics*, 12(2),108. doi:10.3390/pharmaceutics12020108
- Nastiti, C. M. R. R*., **Ponto, T***., Abd, E., Grice, J. E., Benson, H. A. E., & Roberts, M. S. (2017). Topical Nano and Microemulsions for Skin Delivery. *Pharmaceutics*, 9(4), 37. doi:10.3390/pharmaceutics9040037

  *equal contribution

Conference Abstracts:

- **Perspectives in Percutaneous Penetration, La Grande Motte, France, April 2022**

  Targeted Topical Delivery of Caffeine in the Management of Cellulite: Novel Cosmetic Formulation Development, Characterisation and Clinical Evaluation
- **Controlled Release Society Virtual Annual Meeting, USA Chapter, July 2021**

  Formulation Development for Topical Skin Delivery of Astaxanthin
- **Drug Delivery Australia (DDA) Virtual Conference, Australia, November 2020**

  The Reliability of a Standardised Tool for Evaluating Cellulite in the Posterior Thigh

- **Mark Liveris Seminar, Curtin University, Perth, Australia, September 2018**

  Development of Lipid-Based Nanoemulsions of Caffeine: Preliminary Formulation Design, Characterisation and In Vitro Release Determination by Two Different Methods

ACKNOWLEDGEMENTS

Praise to Lord Jesus Christ, for His great love, blessings and miracles throughout my life and many thanks to my beloved parents, especially to my mother, who always brings my name into her prayer with her amazing faith. I am incredibly grateful to the Ponto's family for always supporting and being proud of me.

I am extremely grateful to the Australian Government and Curtin University for providing financial support through the Australian Government Research Training Program Scholarship.

I would love to express my sincere gratitude to Associate Professor Heather Benson and her husband, Professor Anthony Wright, for their patience, excellent supervision, invaluable knowledge and endless support. I undoubtedly consider myself very lucky to have worked under their guidance and supervision. I am truly blessed to have Prof. Vania Rodrigues Leite-Silva for her guidance in developing my semisolid cream formulations. Her expertise in the cosmetic industry and academics is unquestionable.

I would also like to extend my thanks to Dr Brioni Moore, who was included in my primary supervision team due to the restructuring changes at Curtin University. She offers an excellent mutual relationship, advice, and support throughout my thesis writing process. I would also like to express my appreciation to the Curtin Medical School and Curtin Health Innovation Research Institute (CHIRI), especially Professor Lynne Emmerton, Professor Kevin Batty, Professor John Mamo, Associate Professor Cyril Mamotte, Dr Kylie Munyard and to distinguished thesis examiners for their assistance during my thesis preparation and examination.

My sincere gratitude goes to Professor Michael S. Roberts for extending his support and making me a part of his research group, which was my dream. It is privileged to meet him and collaborate under the Roberts Group at the Translational Research Institute (TRI), Queensland. Through him, I met Associate Professor Heather Benson. I am grateful to have Dr Mohammed Yousuf Hussain and Dr Bhaveshkumar Ramjibhai Panchal for a fantastic opportunity and guidance during my technical training and for assisting me with the Rheology data analysis in UQ.

The completion of my PhD study could not have been possible without the invaluable assistance of Giuseppe Luna, Randy Strack, Jorge Martinez, Dr Victor Chuang, Dr Kim Watkins, Dr Penny Moss, Dr Rob Stuart, Angela Jacques, Rob Walker, Charmaine D Costa, Paul Mannix, Julia Aitken, Petra Behre, Andrea Johnson, other staffs at Curtin University and Portec Veterinary Services Welshpool.

I appreciate the invaluable and constant assistance from my best friends at Curtin University and Queensland University, especially Dr Christofori M.R.R Nastiti, Dr Abolghasem Hedayatkhah, Dr Yeakuty Marzan Jhanker, Dr Behin Sundara Raj, Corina M. Ionescu, Fatima N. Jahan, Gemma Latter, Dr Eman Abd, Dr Shereen Yousef, Susbin Wagle, Shahinda Alsayed and Vinci Mizranita. Many thanks also to my best friends in Perth, especially Rod Ryan and Ariel S. Villanueva.

Last, but foremost, my deep thanks goes to Pietro Lembo for his unconditional love and support throughout this journey. Without you and everything you have done, none of this would be possible.

DEDICATION

"For I know the plans I have for you," declares the Lord, "plans to prosper you and not to harm you, plans to give you hope and a future".

Jeremiah 29:11

This thesis is dedicated to my mum Sriwahyuty, sister Theresia, nieces (Vania, Kimberly, Ivana, Cheryll and Felicia), grandnieces (Keiko and Kelly) and every woman has a passion for learning and is motivated to pursue a career in science, especially in the field of skin, cosmetics and beauty industry.

TABLE OF CONTENTS

ABBREVIATIONS

5-FU	5-fluorouracil
ACT	acetone
AGR	annual growth rate
AHA	alpha-hydroxy acid
AHA	α-hydroxy acid
ALA	α-lipoic acid
API	active pharmaceutical ingredients
ATR-FTIR	attenuated total reflectance fourier transform infra-red
AWT	acoustic wave therapy
CAF	caffeine
cAMP	cyclic adenosine monophosphate
cAMP	cyclic adenosine monophosphate
Co	cosurfactant
CPE	chemical penetration/permeation enhancers
Cryo-TEM	cryogenic-transmission electron microscopy
CS	cell senescence
CSM	cellulite severity measure
CSS	cellulite severity scale
DCM	dichloromethane
DCMS	decylmethyl sulphoxide
DEGEE	diethylene glycol monoethyl ether
DHT	dihydrotestosterone
DHT	dihydrotestosterone
DLS	dynamic light scattering
DMSO	dimethylsulfoxide
DoH	Declaration of Helsinki
DSC	differential scanning calorimetry
EC	emollient cream
EG	emollient gel
EM	emulsion
EMP	elongated microparticles
ER	enhancement ratio
ES	effect size
ES	oestradiol
ESWT	extracorporeal shock waves therapy
EU	eucalyptol
FDA	food and drug administration

FF-TEM	freeze fracture–transmission electron microscopy
GAIS	global aesthetic improvement scale
GCO	green coffee oil
GRAS	generally recognised as safe
GRASE	generally recognised as safe and effective
GROC	global rating of change
HC	hydrocortisone
HEE	high-energy emulsification
HLB	hydrophile-lipophile balance
HPH	high-energy emulsification
HSL	hormone-sensitive lipase
HXN	hexane
ICCs	intraclass correlation coefficients
IPM	isopropyl myristate
IVPT	in vitro permeation testing
KCSS	knee cellulite severity score
LAA	L-ascorbic acid
LAN	lanolin
LC	liquid crystal
LEE	low-energy emulsification
LOD	limit of detection
LOQ	limit of quantification
LPL	lipoprotein lipases
MCT	medium-chain triglycerides
MEs	microemulsions
MFWS	modified fitzpatrick wrinkle scale
MMPs	matrix metalloproteinases
MW	molecular weight
MWD	multi-wavelength
NEs	nanoemulsions
NLCs	nanostructured lipid carriers
NS	no significant
O/W	oil-in-water
O/W/O	oil in water in oil
OA	oleic acid
OS	oxidative stress
PBS	phosphate buffered saline
PCS	photon correlation spectroscopy
PDE	phosphodiesterase
PDI	polydispersity index

PG	propylene glycol
PGs	prostaglandins
PS	phase separation
QELS	quasi-elastic light scattering
QTPP	quality target product profile
RF	radiofrequency
ROS	reactive oxygen species
ROS	reactive oxygen species
RSD	relative standard deviation
S	surfactant
SANS	small angle neutron scattering
SAXS	small angle X-ray scattering
SB	stratum basale
SC	stratum corneum
SCCE	stratum corneum chymotryptic enzyme
SEM	scanning electron microscope
SFT	skinfold fat thickness
SG	stratum granulosum
SL	stratum lucidum
SLNs	solid lipid nanoparticles
SNEDDS	self nano-emulsifying drug delivery systems
SPF	sun protection factor
SS	stratum spinosum
TC	thigh circumference
TEWL	total transepidermal water loss
TR	transcutol®
TS-GS	tissue stabilised-guided subsicion
TTAGGG	telomeres
U.S. FDA	the United States Food and Drug Administration
UPF	UV protection factor
UV	ultraviolet
W/O	water-in-oil
W/O/W	water in oil in water
WSRS	wrinkle severity-rating scale
ZP	dynamic light scattering

LIST OF FIGURES

LIST OF TABLES

Chapter 1.

Nanocosmeceuticals in the Skin: A Literature Review

1.1 Role, challenges, and market opportunities

Throughout human civilisation, there has been a desire to present beauty, an obsession with eternal youth, and a need to revitalise skin wellness. These endeavors contribute to the high demand for innovative cosmetic/cosmeceutical skincare products. Looking back in ancient history, there are many examples of natural products in skincare. Around 4000 BC, Cleopatra, the last Egyptian queen, bathed in sour donkey milk to improve her complexion and make her skin softer and smoother.[1] Woman in ancient Rome rubbed fermented grape skins from the bottom of wine barrels over their skin to exfoliate and improve their skin texture. Greek women also used a combination of lime, sulphur, and mustard to rejuvenate their skin. It is interesting to look at the basis of these natural products used in ancient times.[2-4] Sour milk contains lactic acid; grape skins contain tartaric acid; and the lemon extract contains citric acid, a naturally occurring alpha-hydroxy acid (AHA).[5,6] These acids and their derivatives are now common ingredients of chemical peeling. Archaeologists found evidence that Egyptians used henna to produce a dye that they applied to adorn the palms, soles, cheeks, nails, lips, and hair with art design[1,7]. Kohl was applied as a cosmetic, in the form of dark eyeliner, extending the eyebrows (Ebers Papyrus; 1550 BCE), and as a medicinal collyrium (lotion or wash) to treat eye diseases.[8]

Drs Albert Kligman and Raymond Reed first introduced cosmeceuticals in the late 1970s. They described cosmeceuticals as products that blended cosmetics and active pharmaceutical ingredients (API) to achieve medical effectiveness on personal human appearance, ranging from the skin to body to hair.[9] The first cosmeceutical product contained AHA and was introduced to the United States market in the 1990s.[10] To date, cosmeceuticals are used to treat a range of skin conditions, including photoageing, dark spots, hyperpigmentation, wrinkles, and skin dryness.[11,12] In Japan, cosmeceuticals are called quasi-drugs due to the mixing of pharmacological and non-pharmacological active compounds.[13]

1.1.1 Role of nanotechnology in cosmeceuticals

The European Commission defines nanotechnology as "those areas of science and engineering where phenomena that take place at dimensions in the nanometre scale are utilised in the design, characterisation, production and application of materials, structures, devices and systems".[14] There is evidence of the contributions of nanotechnology to almost every field of science: including physics, biology, chemistry, engineering, computing, and material science.[15] Historically, there is evidence that nanotechnology was used for skincare by ancient Egyptians, Greeks, and Romans when they prepared hair colour formulations. However, over the past 40 years, nanotechnology has become well established as a formulation strategy for personal skincare and health care products in the cosmetic industry: ranging from sunscreens to moisturising lotions and hair products.[11]

Nanocosmeceuticals are used to describe when cosmeceutical active ingredients are incorporated with a nanotechnology delivery system.[12] The goal of nanocosmeceuticals is to develop elegant cosmeceutical products with enhanced active ingredient performance, usually through the rapid penetration of active ingredients into the skin, resulting in improved effectiveness.[12] Nanocosmeceuticals offer several advantages to conventional cosmeceuticals: the potential to enhance delivery to the target site, controlled drug release at the target site, and the ability to improve stability by protecting sensitive active ingredients within the formulation.[11] As a result, nanotechnology-based products provide deeper skin penetration, enhanced skin ageing effects, better UV protection, improved stability, longer-lasting effects and good sensory properties.[11] A variety of different novel nanocarrier approaches have been applied within the cosmeceutical industry, including nanoemulsions (NEs), liposomes, niosomes, solid lipid nanoparticles (SLNs), nanostructured lipid carriers (NLCs), nanocrystals, dendrimers, nanospheres, and nanotubes. The properties of these nanotechnology formulations are described later in the chapter (section 1.3.3). Some of these approaches are well established in commercially available cosmeceutical products, whilst others are in the research and development phase.

1.1.2 Challenges

Concerns have been raised over the safety of nanotechnology-based consumer and personal care products, primarily nanoparticle-based sunscreen products that contain zinc oxide and

titanium dioxide.[16] However, extensive studies of the skin penetration of zinc oxide nanoparticles following application to human volunteers, under a range of application conditions (including massage, bathing and on damaged skin), have failed to show any toxic effects.[17-20] Nevertheless, these concerns along with public perception, have forced the cosmetic industry to consider how nanotechnology is used in cosmetics and ensure comprehensive safety assessments are conducted before the product's launch to market.[16] For consumer protection, all ingredients (including nanomaterials) must be disclosed on the product label, thereby allowing the consumer to make informed decisions regarding product use, taking into account any personal health and safety issues.[16,21] Nanocosmeceutical-based products should be regulated and evaluated for their efficacy and safety in clinical trials, which is a critical step before the market launch.[22] It should be noted that a variety of nanocarriers are utilised in nanocosmecuticals, ranging from solid forms (nanoparticles) to liquids (nanoemulsions, nanovesicles), with the latter being far less controversial from a safety perspective.

1.1.3 Global market and forecasts for nanocosmeceuticals

Two of the major global cosmetic companies, Lancome and Christian Dior, launched their first nanocosmetics in 1986 (Niosomes® and Captures®), with L'Oréal (Revitalift®) following in 2005. The technology is now widely used for cosmeceutical products that target wrinkles, hyperpigmentation, dark spots, photoageing, and skin dryness.[11,21,23]The field of nanocosmetics continues to draw considerable interest from many companies engaged in research and development (R&D) in personal care products for the whole spectrum from baby care to antiageing creams. In 2020, the worldwide beauty and personal care market was valued at USD 483 billion and is predicted to increase to USD 784.6 billion by 2025 (Figure 1.1).[24] This rapid rise in market value is driven by an increasingly ageing population (an estimate that 2.09 billion people will be >60 years of age in 2050), increased affluence, and growing markets in Asian countries (China, Japan, Korea and India), the Middle East, and Africa (predicted annual growth rate (AGR) of 21%).[23]

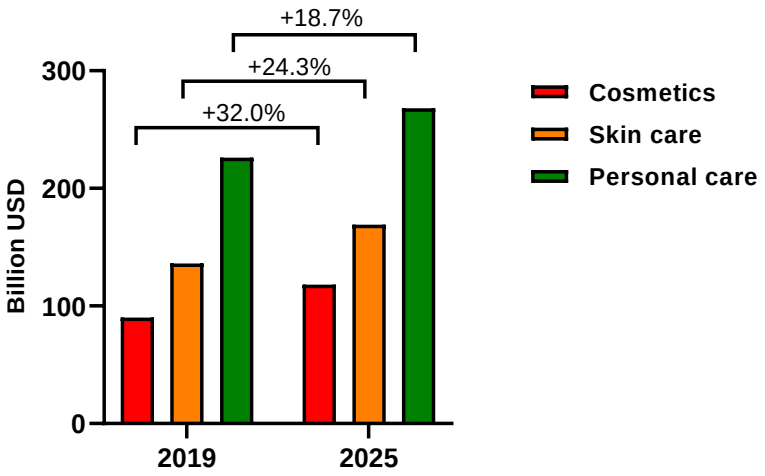

Figure 1.1 A comparative representation of revenue and estimated growth rate of cosmetics (+32%), skincare (+24.3%) and personal care (+18.7%) between 2019 and 2025. Adapted from Roberts et al.[24]

1.2 Skin

The skin is the largest organ in the human body, covering an area of approximately 1.6-1.9 m^2 on an average adult, and accounting for about 10-16% of the total body mass.[25,26] The skin has many important roles including protection, regulation and sensation.[23,27-29] It protects the body from invasion of foreign substances and microorganisms, and prevents excessive water loss from the body. The skin controls heat and moisture flow to and from the surrounding environment (thermoregulation).[30,31] The distribution of nerves in the skin provides sensory properties, including feeling touch, pain, itch, heat and cold temperatures. In addition, due to its unique patterns, the skin on the fingers and palm has been used for human legal identification and recognition using biometric technology.[32]

1.2.1 Skin structure and functions

Epidermis (the outer layer), dermis (the inner layer), and hypodermis are the three main anatomical layers of human skin (Figure 1.2).[33]

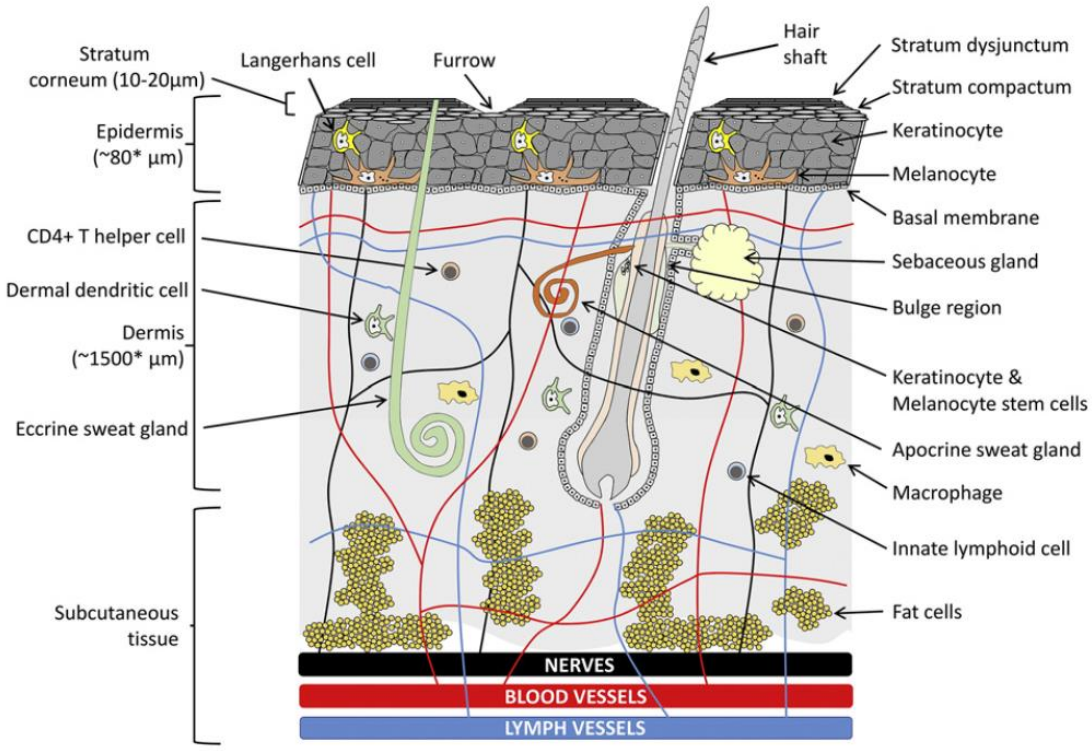

Figure 1.2 A representation of human skin structure in cross-section. The depth of skin layers may vary depending on the body sites and degree of hydration. The figure is reproduced from Roberts et al.[33] with permission

1.2.1.1 Epidermis

The epidermis is a multiple-layered membrane of keratinocytes, with thickness ranging from 0.06 mm (eyelids) to about 0.8 mm (palms and soles).[25] There are five histological layers: (i) the stratum germinativum/basale (SB) at the dermal-epidermal junction, generating new keratinocytes that differentiate through the (ii) stratum spinosum (SS), (iii) stratum granulosum (SG), (iv) stratum lucidum (SL) and (v) stratum corneum (SC) at the skin's outer surface.[34-37] As there are no blood vessels in the epidermis, cells must source nutrients and eliminate waste products by diffusion across the dermo-epidermal layer. Thus cells decline, differentiate, and die as they move further from the basal layer.[38] It takes approximately 28 days for a daughter cell from the SB to move through the various epidermal layers and be shed from the SC. The term "viable epidermis" is often used for the epidermal layers below the stratum corneum, but this terminology is questionable given the degradation within the epidermal layers.

Stratum basale (SB)

The SB, also referred to as the stratum germinativum or basal layer, contains melanocytes, Langerhans cells, and Merkel cells.[25] Melanocytes produce the pigment melanin from tyrosine, which is responsible for hair, eyes, and skin pigmentation. The primary function of melanin is to absorb ultraviolet (UV) radiation and are free radical scavengers in the basal layer. People who have darker skin have more active and efficient melanocytes.[39] Langerhans cells are bone marrow-derived and act as the outermost guard of the cutaneous immune system. They play a role in allergic contact dermatitis.[39] Merkel cells are associated with sensory receptors and are also thought to have a neuroendocrine function.[39]

Stratum spinosum (SS)

The SS, also known as the prickle cell layer, consists of two to six rows of keratinocytes located directly above the basal layer.[25] A combination of the basal and spinous layers is also referred to as the Malpighian layer of the skin. Within this layer, cellular morphology changes from columnar to polygonal cells as the keratinocytes start to differentiate and form keratin tonofilaments interconnected by desmosomes. Desmosomes function as "molecular rivets", adding structural integrity to the epidermis.[40]

Stratum granulosum (SG)

Within the SG, the keratinocytes differentiate, with the polygonal cells starting to flatten in appearance. The presence of hydrolytic enzymes, including stratum corneum chymotryptic enzyme (SCCE), are associated with the desquamation process, whereby a layer of stratum corneum cells are shed from the skin surface each day (on average). Overexpression of these enzymes result in dermatological disorders such as psoriasis and dermatitis.[41,42]

Stratum lucidum (SL)

Within the SL, the cell nuclei and other organelles disintegrate and the cells contain relatively higher levels of keratin protein, are more compact, and flattened in shape. The SL is also considered as a part of the portion of SC, with both layers having a structure composed of an intracellular protein matrix and surrounding lipid lamellae that substantially reduce skin barrier permeability.[39,40]

Stratum corneum (SC)

The SC (10-15 layers; 10-20 µm thick) comprises keratin-rich corneocytes surrounded by multiple lipid bi-layers.[43] The SC has been described as a "brick and mortar system" in which keratinised cells with a polygonal, elongated and flattened shape are embedded in a lipid "mortar-like" matrix.[44] The lipid matrix comprises ceramides, cholesterol, cholesterol sulphate, di-triglycerides, fatty acids and sterol/wax esters.[27,34,45-47] It is this combination of relatively desiccated proteinaceous cells and highly ordered lipid bilayers that provide the main diffusion barrier of the skin.

1.2.1.2 Dermis

The dermis (or corium) is a 3-5 mm layer between the epidermis and hypodermis (subcutaneous fat layers).[25,39] It acts as a source of nourishment and musculoskeletal support to the epidermis.[48] Since the dermis is hydrophilic, it offers little resistance for the permeation of most hydrophilic drugs but may reduce the permeation to deeper tissues of highly lipophilic drugs.[25,38] The dermis consists of collagenous fibre, elastic connective tissue (elastin), and other extracellular components, including blood and lymphatic capillaries, nerve endings, pilosebaceous units (sebaceous glands, hair follicles, and arrector pili muscle) and secretory glands (sweat/eccrine and apocrine). The sebaceous glands secrete sebum composed of a mixture of triglycerides, fatty acids, and waxes that lubricate the skin and maintain a pH of around 5. Sweat glands produce sweat and assist in thermoregulation.[39,40]

1.2.1.3 Hypodermis

The subcutaneous fat layer or hypodermis comprises a network of fat (adipose) tissue, with primary roles in thermal insulation, protection against physical shock and as an energy reservoir.[29]

1.2.2 Skin penetration/permeation

The SC is the main barrier to permeating externally applied substances, microorganisms, and excessive water loss.[39,49,50] Externally applied substances permeate the skin by two main pathways: the transepidermal pathway and the transappendageal (shunt) pathway (Figure 1.3).[51] The transepidermal pathway is the main pathway for skin absorption, with molecules having the potential to follow an intercellular route (between the cells) and/or a transcellular route (through the cells). It is important to note that regardless of the route, substances must

cross intercellular SC lipids, and the tortuous and heterogeneous nature of the SC contributes to its barrier properties.[52] The shunt pathway via hair follicles and sebaceous ducts was first identified by Scheuplein [53] as a pathway for providing drug transport in the early stages of skin absorption before steady-state diffusion is established. Follicular transport has received considerable attention that has provided a better understanding of the mechanism of permeation. Applied substances enter the infundibulum, the open space where the hair emerges, from which absorption can follow one of two routes. Small molecules tend to penetrate the epithelium of the hair shaft into the viable epidermis and dermis in a process termed transfollicular penetration.[54] Large molecules and particles become trapped to form a reservoir, termed the transfollicular pathway.[55] The rich blood supply to the follicle can facilitate absorption.

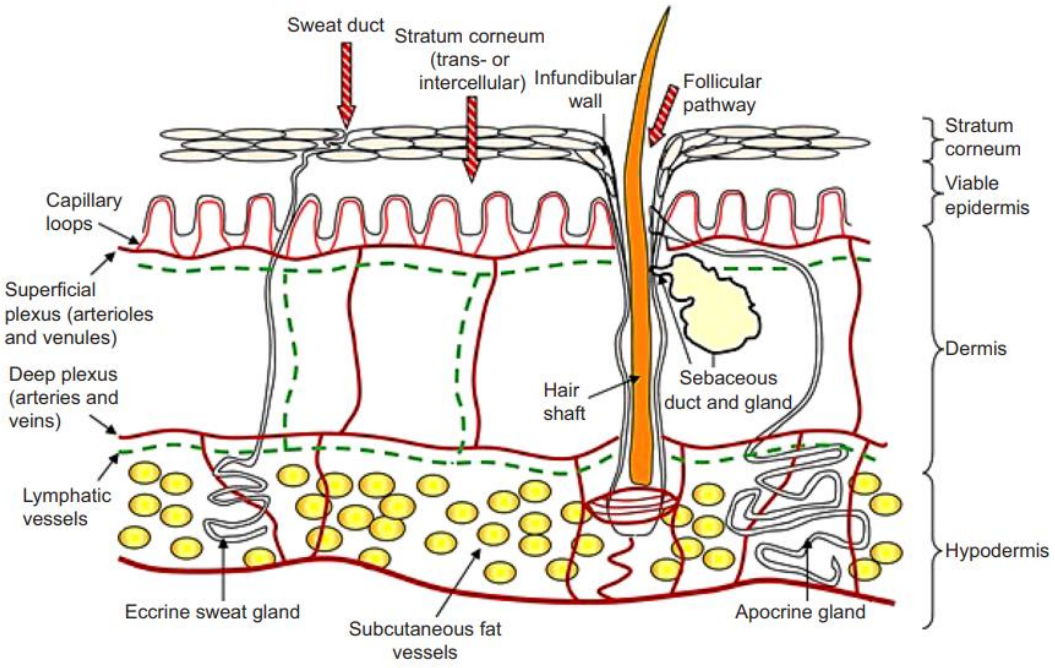

Figure 1.3 A diagrammatic representation of penetration pathways to the skin showing routes of penetration through the sweat duct, directly across the stratum corneum and via follicular pathways. The figure is reproduced from Abd et al.[51] with permission

1.3 Strategies to overcome the skin barrier function

Skin permeation is limited to small (molecular weight MW <~500 Da), soluble (generally low melting point MP) and moderately lipophilic (octanol-water partition coefficient log P in range 0 to 5) compounds. Generating sufficient skin permeation of molecules that do not exhibit these characteristics requires some form of skin penetration enhancement technology. Ideally,

skin penetration/permeation enhancers reduce the skin barrier only temporarily and reversibly and are non-toxic and non-allergenic.[56] Skin penetration/permeation techniques include physical enhancement, non-invasive or minimally invasive technologies, and chemical or formulation-based approaches. Figure 1.4 summarises the technologies that have been applied as skin permeation enhancement techniques.

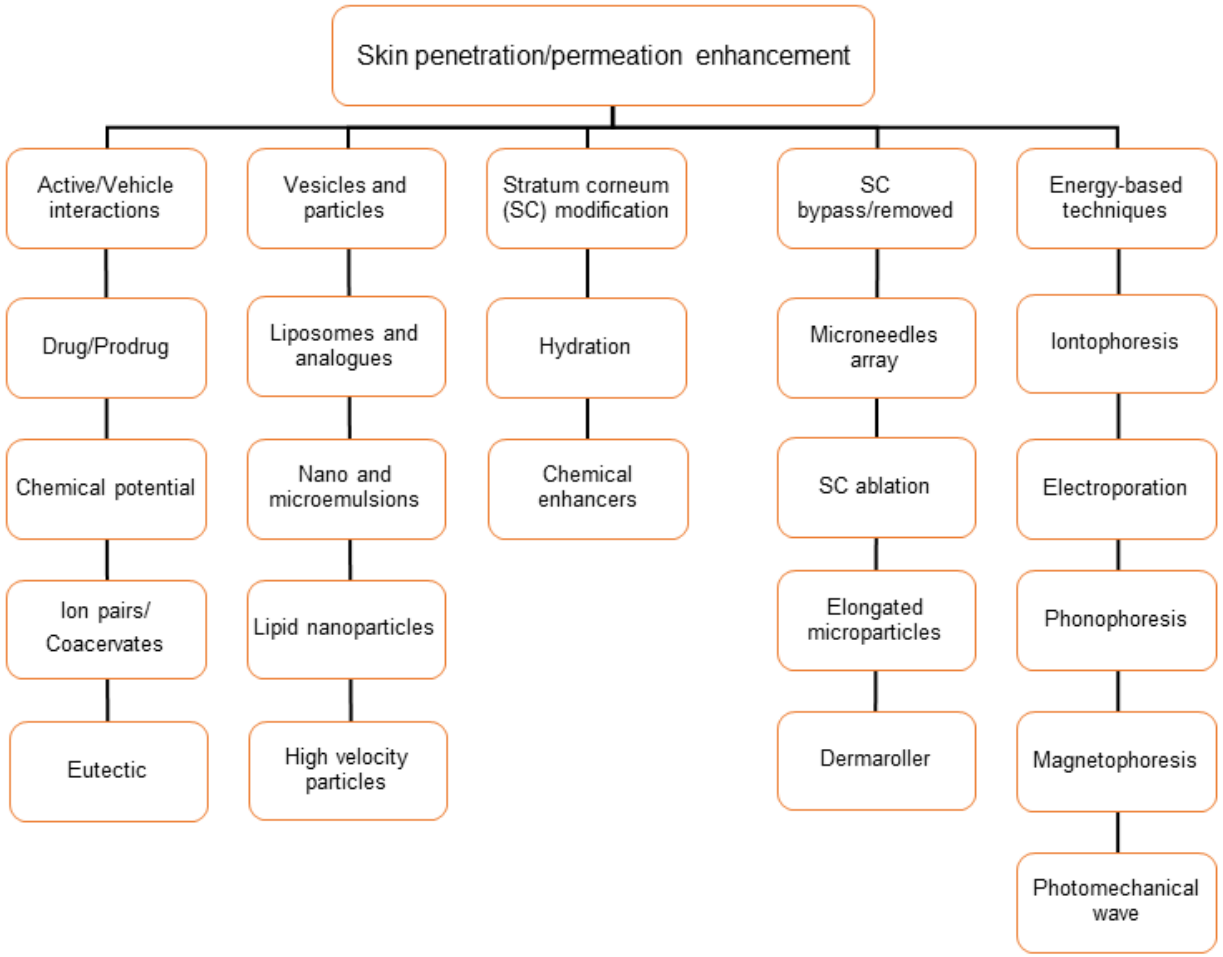

Figure 1.4 Strategies to optimise skin drug penetration/permeation enhancement. Flowchart adapted from Barry[27]

1.3.1 Physical penetration/permeation enhancement

Physical enhancement techniques include energy-based, mechanical-based and velocity based technologies. Energy-based technologies include iontophoresis, sonophoresis/phonophoresis (ultrasound), magnetophoresis, electroporation and laser-assisted delivery.[57-59] Mechanical-based physical enhancement includes microneedles, elongated microparticles (EMP), microdermabrasion and dermaroller.[29] Many excellent reviews of these technologies, their mechanisms of action and applications have been published.[58,60-66] As these techniques are not the focus of the current research, they have not been reviewed in detail in this chapter.

1.3.2 Chemical penetration/permeation enhancement

In general, chemical penetration/permeation enhancers (CPE) improve the solubility of the permeant molecules within the SC and/or increase the fluidity of the intercellular lipid bilayers.[56,67-69] Enhancement can also be achieved by increasing the thermodynamic activity of the permeant in the formulation (for example, by limiting the solubility in the vehicle or supersaturation).[68-70] A wide range of chemical enhancers have been identified, including water, alcohols, amines, dimethylsulfoxide (DMSO), esters, glycols, pyrrolidones, sulphoxides and surfactants.[57,67,68,71-73] CPE are commonly used components in dermal and transdermal delivery for enhancing absorption of both hydrophilic and lipophilic molecules.[67] There are many excellent review articles,[74-76] book chapters[39,40] and indeed whole books[77] devoted to CPE, their mechanism of action and application to skin delivery. In this chapter, the focus is on the CPE techniques that have been investigated in this thesis: propylene glycol (PG), Transcutol®, lanolin (LAN) and terpenes.

1.3.2.1 Glycols

Propylene glycol (propane-1, 2-diol) (PG) is rapidly absorbed into the skin and is widely used in topical formulations at a range of concentrations. It acts as a solvent, increasing solubility within the SC. It has been shown to have multiple action mechanisms and act synergistically with other solvents to enhance skin permeation. Differential scanning calorimetry (DSC) studies have shown that PG interacts with α-keratin in the corneocytes and lipid bilayers[78] to increase diffusion within the SC. X-ray diffraction studies have shown that PG molecules integrate into the hydrophilic regions of the lipid lamellae, increasing lipid fluidity by

incorporating between the polar head groups of the bilayers, and orienting in a perpendicular direction to the bilayer.[79] PG has also demonstrated synergistic enhancement activity with lipophilic enhancers including terpenes[80] and isopropyl myristate.[81]

1.3.2.2 Ether glycols

Transcutol® (TR) is a highly purified form of diethylene glycol monoethyl ether (DEGEE), with similar properties to PG.[71,82] It is a safe hydroalcoholic solubiliser and skin penetration/permeation enhancer without comprising skin integrity.[83-86] Harrison et al.[86] investigated the TR-induced changes in the diffusivity and solubility of a model compound (4-cyanophenol) in human SC using attenuated total reflectance fourier transform infra-red (ATR-FTIR) spectroscopy and measurement of compound flux using Franz diffusion cells. The latter showed that TR enhanced flux by a factor of two. They concluded that the mechanism of PG enhancement of TR was primarily by increased solubility of the penetrant in this SC barrier, based on their ATR-FTIR data. We have previously demonstrated up to a three-times increase in the flux of the antioxidant compound resveratrol by incorporation of TR in microemulsion formulations.[87]

1.3.2.3 Fatty acids

Lanolin (wool fat) is a lipid-rich substance secreted by the sebaceous glands of sheep and used in cosmetic, dermatological and personal care products for its emollient properties. It is composed of cholesterol, ceramides and free fatty acids[88-91] with anhydrous lanolin in conformity with the U.S.P. specifications containing 0.56 % free fatty acid in the form of oleic acid (OA).[92] Olive oil, which has also been used in topical products for its emollient properties, also contains high levels of oleic acid. Oleic acid, a long-chain fatty acid with *cis*-9-octadecenoic acid, is a potent permeation enhancer.[67,72,76] Early DSC studies[93] showed that OA alters the phase transition temperature of the SC lipids with no effect on keratin. The skin permeation enhancement of piroxicam was correlated to the uptake of the OA in the lipid bilayers. Further investigations were carried out by Goodman et al.[94] to assess the effectiveness of a range of enhancers (azone, decylmethyl sulphoxide (DCMS), OA and PG) on permeation of 5-fluorouracil (5-FU) and oestradiol (ES) applied in PG vehicles and water vehicles. Three enhancers (azone, DCMS and OA) had their mechanism of action previously assessed by differential scanning calorimetry (DSC),[95] and showed` effectiveness at low

concentrations. The findings reported a 100-fold increase in the permeation rate (flux) of hydrophilic 5-FU applied in 2% of azone in PG vehicles. Five percent OA in PG enhanced 5-FU permeation was the most effective pretreatment. Using PG alone was less effective than a combination of two enhancers. Data showed that 5% OA in PG promoted ES permeation by more than 10-fold through IVPT using human skin. The results suggested that enhancers effectively enhanced the delivery of a polar drug (5-FU) compared to a non-polar drug (ES). Combination of azone with PG demonstrated a synergetic effect in permeability, compared to an aqueous vehicle; thus, PG itself may play a penetration-enhancing role. The 5-FU results indicated that azone and OA remained in skin tissue. Abd et al.[96,97] investigated the mechanism of action of OA incorporated into microemulsions, on the permeation of caffeine and naproxen into human skin, using in vitro permeation testing (IVPT). They determined the solubility of the active compound in the vehicles and the SC, active compound flux across human epidermal membranes, and uptake of active and vehicle components into the SC. The effect of vehicle pH on the permeation of caffeine and naproxen was also determined to assess the effect of ionisation and hydrophilic nature. It was reported that OA significantly enhanced the skin penetration of caffeine and naproxen, compared to aqueous controls. The permeation enhancement of naproxen increased as the amount of ionised naproxen increased. In addition, the primary mechanism of permeation enhancement of the hydrophilic caffeine was permeation enhancer-induced alteration in diffusivity, rather than effects on SC solubility. In contrast, increased SC solubility drove the increases in the permeation flux of the lipophilic molecule naproxen.[96,97]

1.3.2.4 Terpenes

Terpenes are the volatile constituents of essential oils, extracted from the leaves, fruits, and flowers of a range of plants. Structurally, they consist of repeated isoprene (C_5H_8) units, for example, monoterpenes (C_{10}), sesquiterpenes (C_{15}), diterpenes (C_{20}), and triterpenes (C_{30}) which contain 2, 3, 4 and 6 isoprene units. Terpenes are generally recognised as safe (GRAS), potent chemical enhancers with high penetration enhancement and low systemic toxicity.[67,72,98] Monoterpenes are commonly used as penetration/permeation enhancers due to act reversibly on the skin lipids and low skin irritation at a 1 to 5% concentration.[72,99] Much of the early work on elucidating the mechanism of action of terpenes was undertaken in Brian

Barry's group.[100,101] They showed that terpenes increased drug diffusivity through human epidermal membranes and that the effect correlated empirically with their enhancer activities. The principal mode of action of these accelerants may be described by the lipid-protein-partitioning theory: the terpenes interact with intercellular SC lipids to increase diffusivity, rather than partitioning into the SC or via interaction with keratin in the corneocytes. Abd et al.[96] reported that the terpene eucalyptol (EU) enhanced the skin penetration of CAF and naproxen via increased diffusivity rather than SC solubility.

There is a large body of research investigating the influence of the chemical structure of terpernes and lipophilicity on permeation enhancement effects. Terpenes with a nonpolar group, like limonene, are reported to be better enhancers for lipophilic drugs, while terpenes containing polar groups provide better enhancement for hydrophilic drugs.[56,102]

El-Kattan et al.[103] investigated the effect of 12 terpenes, selected for their range of lipophilicity (log P 1.06-5.36), on the permeation of hydrocortisone (HC) through hairless mouse skin when applied as an alcoholic hydrogel. Flux, cumulative receptor concentration, skin content, and lag time of HC were measured over 24 h. The solubility of HC in the alcoholic hydrogel solvent mixture was determined in the presence of each terpene and compared to the gel with no terpene. The terpene with the highest lipophilicity (nerolidol: log P = 5.36 ± 0.38) enhanced HC flux (35.3-fold over control), compared with a 10.1-fold increase over control for fenchone (log P = 2.13 ± 0.30). There was a linear relationship between the log P of terpenes and the cumulative amount of HC in the receptor after 24 h and lag time (cumulative amount increased and lag time decreased with increasing lipophilicity), but no correlation between the log P of enhancers and HC skin content. An increase in the log P of terpenes correlated with a proportional increase in HC solubility in the formulation solvent mixture. Nastiti et al.[87] showed that there might be potential to target skin regions based on the choice of a terpene. A nanoemulsion containing eugenol showed the highest RSV penetration into the SC and combined epidermis-dermis-follicle skin region. In contrast, limonene-containing nanoemulsion had the highest RSV permeation through the skin.

1.3.3 Nanoformulations for topical/transdermal skin delivery

Colloidal nanocarriers systems are classified into liquid colloidal systems (microemulsions and nanoemulsions) and vesicular carriers (lipid-based nanocarriers): including solid lipid

nanoparticles (SLNs), nanostructured lipid carriers (NLCs) and lipid vesicles with varying degrees of flexibility or deformability in their structure (for example liposomes, transfersomes®, ethosomes, SECosomes, niosomes, invasomes). A schematic representation of the various nano-delivery systems for topical/transdermal delivery is presented in Figure 1.5.

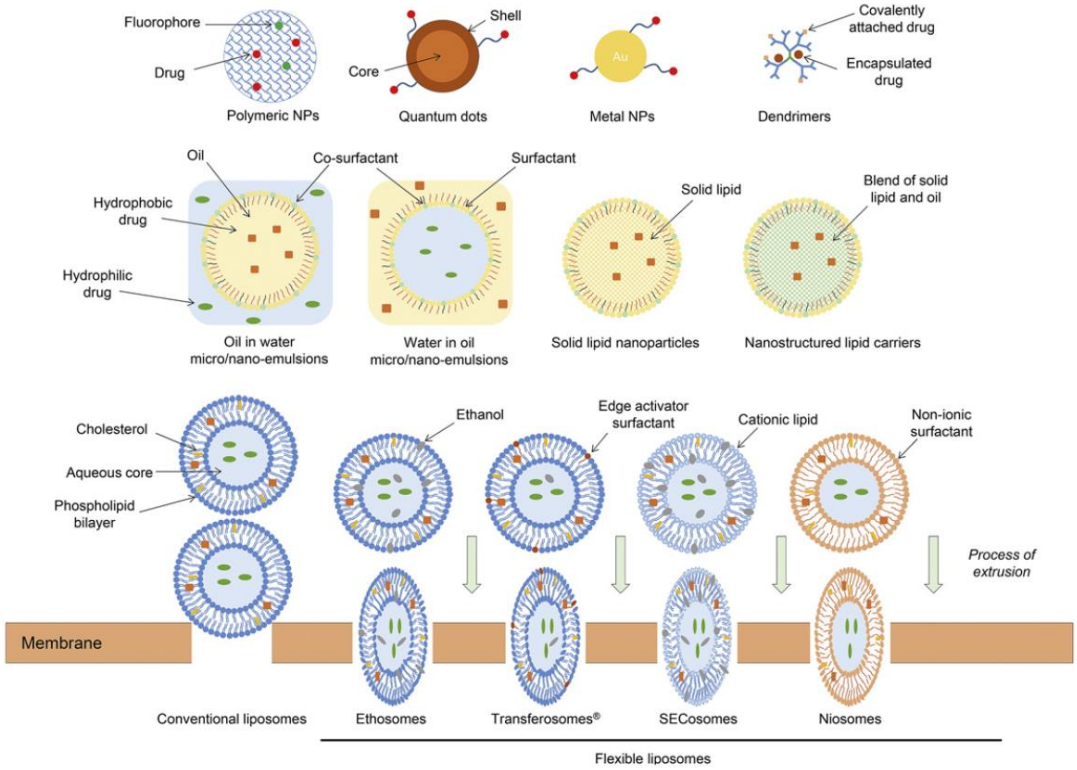

Figure 1.5 Schematic representation of nano-delivery systems for topical/transdermal delivery. Reproduced with permission from Roberts et al.[33]

In this chapter, the review is focused on microemulsions (MEs) and nanoemulsions (NEs) as these are the most frequently utilised nanosystems in cosmetics, cosmeceuticals and personal care products.

MEs are described as an oil and water phase colloidal dispersion system, stabilised by a surfactant (S) /co-surfactant (CoS) mixture to form nanosize (10-100 nm) droplets. They are transparent, monophasic (single-phase), optically isotropic and thermodynamically stable.

NEs are described as a colloidal dispersion system of an oil and water phase, stabilised by a S/CoS mixture to form nanosize (<100 nm) droplets. They are transparent, monophasic (single-phase), and optically isotropic. Phase separation is approximately independent by time; NE is considered as kinetically stable or thermodynamically metastable.[104-106]

Table 1.1. summarises the properties of the types of emulsions commonly used in skin formulations.[106-108]

Table 1.1 Summary of definition, physical properties and method fabrication of macroemulsion, microemulsion and nanoemulsion. Adapted from Nastiti et al.[109]

	Macroemulsion	Microemulsion	Nanoemulsion
Physical description	Coase dispersion	Colloidal dispersion	Colloidal dispersion
Particle size range	>500 nm	<100 nm	<100 nm
Polydispersity	High	Low	Low
Thermodynamic stability	Unstable	Stable	Unstable
Preparation	High energy	Low energy	Low/high energy
Composition: surfactant to oil ratio	Low	High	Moderate
Physical appearance	Creamy	Transparent	Transparent
Viscosity	Semi-solid	Liquid	Liquid

1.3.3.1 Components of topical micro/nanoformulations

Oil Phase

There are three parameters for selecting oil phase components that may influence releasing drug from formulation, solubilising drug in the system leading to loading capacity, and drug permeation through the skin.[110] A wide range of oils can be used, including mineral and vegetable-based oils. Oil substances are medium-chain triglycerides (MCT) such as Labrafac CC® and Labrafac lipophile WL 1349®, containing (caprylic/capric triglyceride); Labrafil M 1944 CS® (mono-, di- and triglycerides and PEG-6 mono- and diesters of oleic (C18:1) acid and viscous oil (α-tocopherol) can be utilised alone or in combination as the oil phase in developing ME/NE. CPEs can be used as components of an oil phase in ME/NE formulations[104], including fatty acids (oleic acid, lauric acid, linoleic acid, myristic acid, etc.); fatty acid esters (isopropyl palmitate, isopropyl myristate, etc.); terpenes (limonene, cineole, eugenol, eucalyptol, menthol, etc.) and short-chain alcohols.

Surfactants

Surfactants are required to generate a stable nano-sized ME/NE by lowering the interfacial tension between the oil and aqueous phases.[109] Surfactants are classified according to their polar head group and classified as amphiphilic compounds; anionic, cationic, non-ionic, and zwitterionic.[111] Non-ionic surfactants are the most commonly used type in topical/transdermal ME/NE due to their lower tendency to cause skin irritation. Surfactants can enhance penetration/permeation into and through the skin by entering the intercellular route and

fluidising, solubilising and extracting the SC lipids. The surfactant penetrates the intercellular lipid matrix, interacting and reversibly binding with keratin filaments, resulting in the disruption of corneocytes.[112-114]

Non-ionic surfactants that are commonly used in topical/transdermal ME/NE,[109,115] include Cetearyl alcohol (mixture of cetyl C16 and stearyl C18 of fatty alcohols), Ceteareth-20 (polyethylene glycol ether of Cetearyl alcohol), Kollipor® RH40 (polyoxyl-40 hydrogenated castor oil), Kolliphor EL® (polyoxyl-35 hydrogenated castor oil), Labrasol® (mixture of mono-, di- and tri-glycerides of C8 and C10 fatty acids, and mono- and di-esters of PEG), Plurol Oleique® (polyglyceryl-3-oleate), Plurol Isostearique® (isostearic acid ester of poly-glycerols and higher oligomers), Sucrose esters, Tween® (polysorbate), Transcutol® P (diethylene glycol monoethyl ether).

Moreover, lecithin is an amphiphilic surfactant that has been widely used to prepare ME/NE formulations by assuring low surface tension. Lecithin is derived from natural compounds (eggs, soy and sunflower seeds); therefore, it is a good candidate for non-toxic and safe ingredients.

Co-surfactants

Co-surfactants aid in reducing the interfacial tension to improve further the stability and solubility of active molecules loaded into ME/NE systems. In addition, co-surfactants play the role of increasing the flexibility and fluidity of the liquid-liquid interface. They decrease its bending stress. Short and medium-chain alcohols and polyglycerol derivatives (for example, ethanol, isopropanol, isopropyl myristate, propylene glycol and Transcutol® are widely used in formulating ME/NEs.

A wide range of materials is used as surfactants and cosurfactants in topical micro/nanoformulations, as shown in Chapter 2 (Table 2.2). In addition, an excellent review focused on the composition and formulation characteristics that affect delivery for topical/transdermal delivery is provided by Lopes.[115]

1.3.3.2 Formulation

MEs and NEs are equilibrated systems that can be oil-in-water (O/W), water-in-oil (W/O), oil in water in oil (O/W/O), water in oil in water (W/O/W) or bicontinuous. Bicontinuous MEs have aqueous and oil phases intertwined and stabilised by flexible surfactant layers or sheets in the areas between the phases.[116] Bicontinuous structures are dynamic and characterised by a higher amphiphilic character, greater fluctuation at the interface, lower interfacial tension, and better solubilising properties than globular MEs.

A pseudo-ternary phase diagram is used as a tool to construct the most suitable ratios of oil, water and the blend of surfactant/co-surfactant at 25°C for microemulsion stability.[117] The effect of various surfactant/co-surfactant weight ratios on the extent of a stable microemulsion area can be easily observed with these diagrams. Based on the titration method, the mixtures of oil, surfactant and co-surfactant is diluted with water phase under mild agitation until the system shows turbidity-to-transparency by visual observation (naked eye).[118-120] For example, Cavalcanti et al.[121] used pseudo-ternary phase diagrams to construct three regions (oil, S/CoS and water) at room temperature. Caprylic/capric triglycerides were used as the oil phase, Brij 52® and Tween 80® as the surfactants, and deionised water as the aqueous phase. Three-phase diagrams were prepared with different ratios of S/Co (Tween 80® and Brij 52®) at 7:3, 8:2 and 9:1 (w/w). The oil phase and the mixture of S/Co blend were carefully mixed followed by water titration until formed a system. The grey area represents the ME systems. In contrast, the white areas represent liquid crystal (LC), emulsion (EM), emollient gel (EG), emollient cream (EC), and phase separation (PS) (Figure 1.6).

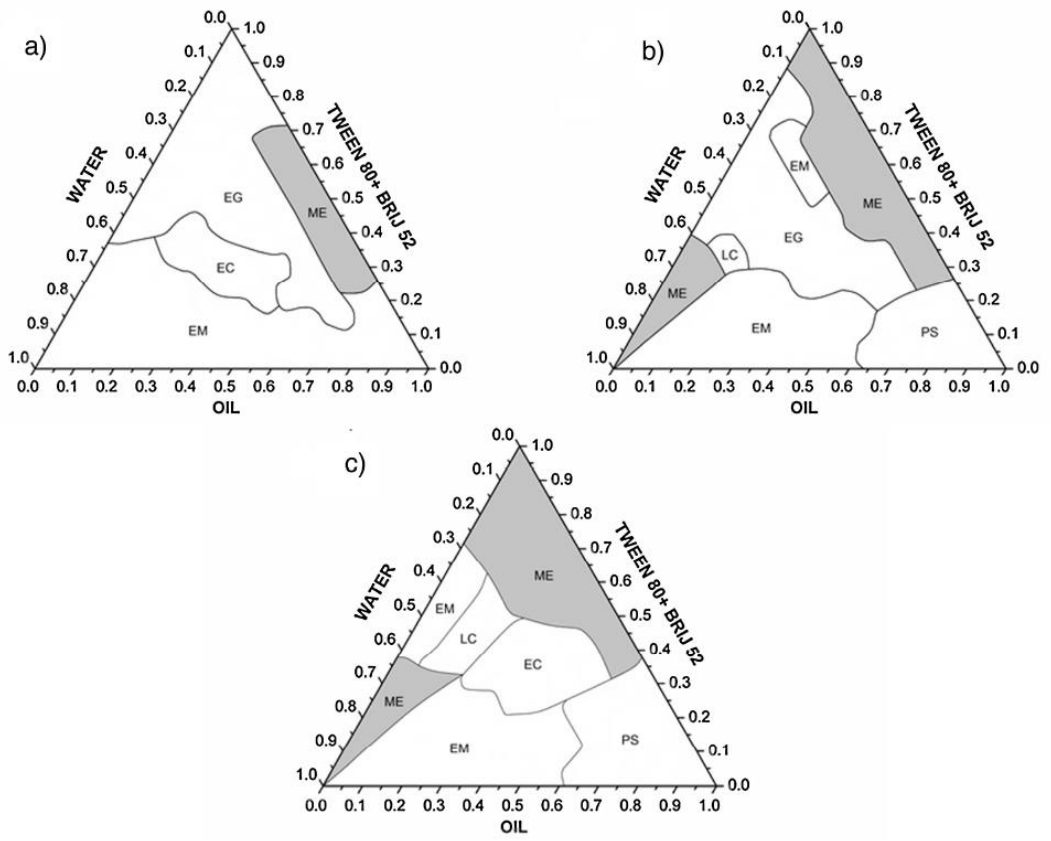

Figure 1.6 Pseudo-ternary phase diagrams of mixed Tween 80® and Brij 52® at 7:3 (a), 8:2 (b) and 9:1 (c) formed together with oil phase and water. Reproduced with permission from Cavalcanti et al.[121]

1.3.3.3 Preparation methods for ME/NE

MEs can be produced spontaneously at the optimal weight ratio of oil, S/CoS, and water with low energy, continuous stirring and often involving temperature. Generally, MEs can convert into NEs with extra energy input. Based on the energy power applied, the NE fabrication method is divided into high-energy emulsification (HEE) and low-energy emulsification (LEE).[104,109] HEE methods use devices to break up the size of the inner phase droplet into uniform nano-sized droplets and reproducible range. Examples of HEE methods include high-pressure homogenisation, microfluidisation, and ultrasonication to break down the oil and water phases, causing them to intersperse and form nanometer-sized droplets (Figure 1.7). This method is not suitable for thermolabile active molecules such as retinoids, proteins and enzymes. High-pressure homogenisation (HPH) is the most widespread method to formulate NEs in the cosmetics, food and pharmaceutical industries.[122-124] The homogeniser supplies high energy (500 to 5000 psi) to the coarse emulsion through a small orifice and generates a

continuous and homogenous flow with a nano-sized droplet. The HPH method offers several advantages compared to microfluidisation and ultrasonication. HPH is easily scaled up with a short fabrication time and free from using organic solvents. It is considered the most feasible for industries in providing higher productivity of final products.

LEE methods involve gentle stirring, heating and phase inversion. In principle, a water-in-oil macroemulsion can transform into an oil-in-water NE using lower energy, either by changing components formulation or temperature (Figure 1.7). Dilution can be used to form a final ME or NE product. Sole et al.[125] reported that dilution of an O/W ME produced NE with a droplet size of 20 nm regardless of the composition of the ME or dilution procedure (incremental or all at once). Dilution can also be used as a LEE method.[125] For example, dilution of an O/W ME with water induces a proportion of the surfactants in the ME to dissolve into the aqueous phase. The surfactant molecules remaining at the oil/water interface cannot maintain the low interfacial tension required for thermodynamic stability, resulting in the ME droplets converting to NE droplets.

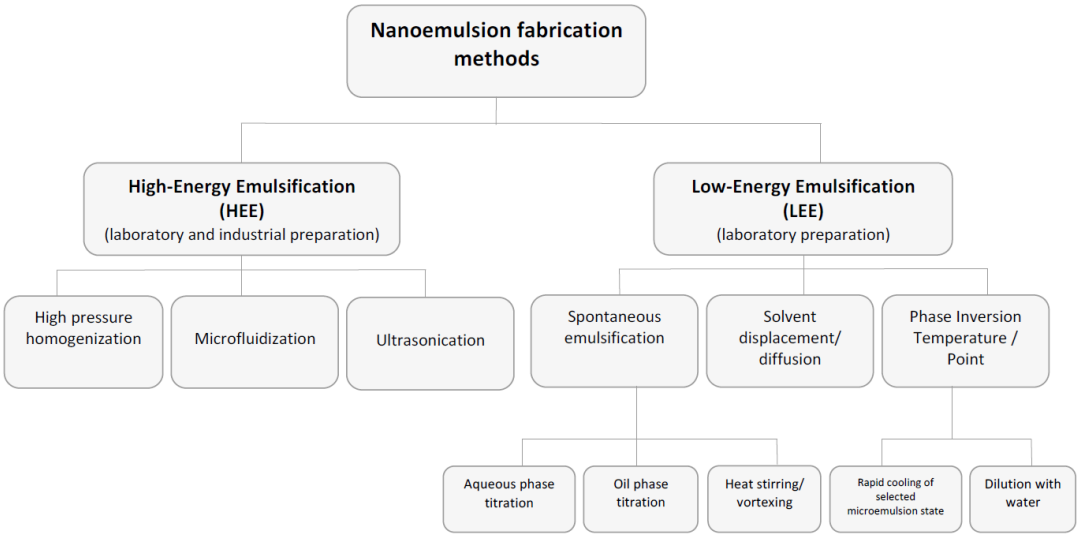

Figure 1.7 Schematic representation of the method of NE preparation. Reproduced with permission from Nastiti et al.[109]

1.3.3.4 Assessment of physical characteristics in MEs and NEs

The characteristics tests performed for topical/transdermal guarantee the successful formation of the ME/NE. The most common characterisation tests are required using technologies:

Particle analysis and morphology

Particle/droplet size, polydispersity index (PDI) and zeta potential (ZP) tests are determined with rapid equipment analysis such as dynamic light scattering (DLS), also known as photon correlation spectroscopy (PCS) or quasi-elastic light scattering (QELS). In principle, DLS analyses the fluctuations in the intensity of scattered laser light when it passes through particles or droplets and converts the signal into a measure of the average particle size and distribution. A number of instruments are available, including the Zetasizer Nano™ ZSP (Malvern, UK). Using a PCS method, the Zetasizer Nano™ ZSP can provide rapid analysis of particle/droplet size (down to about 10,000 nm), the polydispersity (a measure of the broadness of the particle size distribution that indicates the quality or homogeneity of the dispersion) and zeta potential (surface charge). The latter is an important determinant of stability as it indicates the degree of repulsion between the particles in the dispersion. Small-angle X-ray scattering (SAXS) and small-angle neutron scattering (SANS) are useful tools for determining particle size distribution.[126] Freeze fracture–transmission electron microscopy (FF-TEM), scanning electron microscope (SEM), and cryo-TEM permit high-resolution imaging of the system's nanostructure and morphology.[127]

Electrical conductivity

Electrical conductivity measurements provide information on the emulsion structure, with high conductivity values indicating a continuous water phase whilst an oil continuous phase will have low or no conductivity. They can also be used to detect and monitor a phase inversion. Increases in conductivity may demonstrate the percolation transition caused by the attractive interactions between water droplets, characteristic of a bicontinuous structure.[128] Electrical conductivity measurements are simple and inexpensive, involving the insertion of conductometer electrodes into the NE/ME formulation. High conductivity is obtained for a continuous aqueous phase. Phase inversion in response to formulation or temperature change can be monitored by the change in electrical conductivity. They can determine the emulsion type, monitor a phase inversion process and changes in the formulation during preparation or storage, or respond to the formulation or temperature changes.

Viscosity

Viscosity is a crucial factor that influences physical stability and affects drug delivery from ME/NEs.[104,129] Low viscosity NEs have a faster release and rapid skin penetration than high viscosity NEs, but when formulating topical products there is a necessity to ensure they flow on the skin and have good sensory properties. Increasing the water concentration may lead to a lowering of the viscosity, whereas decreasing the surfactant/co-surfactant concentration may increase interfacial tension between the water and oil, causing increased viscosity. Therefore, oil-in-water NEs are usually lower in viscosity than the water-in-oil NEs. The rheological properties of liquid and semisolid NEs and MEs are generally determined using cone and plate type rheometers.

1.3.3.5 Micro and nanoemulsions in topical/transdermal delivery

A recent literature review identified that a wide range of hydrophilic and lipophilic drugs had been delivered into the skin using topical MEs and NEs for transdermal, dermatological and cosmetic/cosmeceutical applications.[109] We reviewed the current literature to evaluate the formulation components, physical characterisation assessments (size, ZP, PDI, viscosity), the in vitro and in vivo skin penetration/permeation evaluations and clinical efficacy. In evaluating the in vitro studies, we considered the experimental methodologies and the skin models used. While human skin is the gold standard, pig and piglet skin is also reasonable. Still, animal skin such as rats, mice, guinea pigs, and rabbits generally over-estimate skin permeation as the skin structure is markedly different to humans. Overall, we showed in our review that NEs and MEs of varied formulation components had demonstrated effective skin delivery for a wide range of lipophilic and hydrophilic active compounds.[109]

In Chapter 2, this literature review is extended to focus on the skin delivery of CAF. A summary of the dosage forms, formula compositions, CAF concentration/amount applied, skin penetration/permeation of topical MEs and NEs are presented.

1.3.3.6 Commercial nanocosmeceuticals

Estée Lauder launched their first innovative cosmetic product (Night Repair Cellular Recovery Complex) in 1982. A decade later, Estée Lauder reformulated the product and launched the cosmetic Advanced Night Repair Protective Recovery Complex. They used a liposome delivery system to neutralise 90% of damaged skin due to external factors (UV exposure,

pollution, etc.), resulting in natural repair of skin damage. Another antiageing product, Perfectionist [CP+] with Poly-Collagen Peptides, peptides and BioSync Activating™ complex to help lift deep wrinkles and correct age spots.[130] L'Oreal has invested USD 600 million on patents for innovative formulas such as "nanosome particles" from total revenue of USD 17 billion.[16] L'Oreal has employed nanotechnology in products such as Revitalift antiwrinkle cream, which contains nanosomes of Pro-Retinol A, and claims that it instantly returns the skin and reduces the appearance of wrinkles. Due to the high absorption rate to deeper skin, the product shows an immediate lifting effect. Besides cosmetic antiwrinkle products, this French company had patented an oil-in-water (O/W) emulsion containing filler in 2006. The emulsion can be extensively incorporated to deliver drugs for cosmetic and dermatological applications. In addition, Lancôme rolled out Rénergie Microlift, an antiageing moisturiser, microfilter containing silica and protein nanoparticles for lifting and tightening skin surface.

There is now a broad range of nanocosmeceuticals-based products available in the market, with examples presented in Table 1.2.

Table 1.2 Summary of nanotechnology-based cosmeceutical products. Adapted from Dhapte-Pawar et al.[23]

Products	Company	Use
A. Liposome		
1. Capture Totale®	Dior	Antiwrinkle effect help in removing blemish and dark spots
2. Advanced Night Repair Protective Recovery Complex	Estee Lauder	As skin repairing agent
3. Clinicians Complex Liposome Face and Neck Lotion	Clinicians Complex	Prevent ageing and help to provide nutrient to the skin
4. Kerstin Florian Rehydrating Liposome day creme	Kerstin Florian	Rehydrate the skin and acts as moisturiser
5. Dermasome®	Microfluidics	Retaining and prevent loss of moisture from the skin
6. Decorte Moisture Liposome Eye Cream	Decorte	Whitening the black skin around the eyes and also help in moisturising
B. Niosome		
1. Niosome+	Lancome	Whitening skin and increase facial look
2. Niosome+ Perfected Age Treatment	Lancome	Removing wrinkle and also help in skin cleansing
3. MayuNiosome Base Cream	Laon Cosmetics	Moisturising and whitening
4. Anti-Age Response Cream	Simply Man Match	Antiwrinkle agent
5. EusuNiosomeMakamPom Whitening Facial Cream	Eusu	Removing and decreasing wrinkle formation
6. Niosome+	Lancome	Whitening skin and increase facial look
C. Solid Lipid Nanoparticles		
1. Allure Body Cream	Chanel	Moisturising the skin and body
2. Soosion Facial Lifting Cream SLN technology	Soosion	Antiwrinkle agent and help in nourishing the skin
3. Phyto NLC Active Cell Repair	SirechEmas	Rejuvenating skin and help in nourishing with decrease in pigmentation

Products		Company	Use
D. Nanoemulsion			
1.	Vital Nanoemulsion A-VC	Marie Louise	Nourishing skin and miniaturisation
2.	Precision-Solution Destressante Solution Nano Emulsion Peaux	Estee Lauder	Moisturising the skin
3.	Coni Hyaluronic Acid and Nanoemulsion Intensive Hydration	Clinicians Complex	Hydrating skin and moisture retention
4.	Phyto-Endophin Hand Cream	Kerstin Florian	Sooth and moisturise the skin
5.	Vitacos Vita-Herb Nona-Vital Skin Toner	Microfluidics	Moisturizing the skin
E. Gold nanoparticles			
1.	ChantecailleNano Gold Energising Eye Serum	Chantecaille	Reducing the ageing process by increasing cell growth
2.	AmeiziiNano Gold Foil Liquid	Ameizil	Repairing damaged skin and moisturszing it with increased fairness
3.	LR Nano Gold and Silk Day Cream	LR	Protect and prevent skin cancer by preventing harmful radiation of sun
4.	O3+ 24 K Gold Gel Cream	O3+	Providing glowing skin and provide shine
5.	Orogold 24K Nano Ultra Silk Serum	Orogold	Prevent moisture loss and keep a healthy skin
F. Nanosphere			
1.	Fresh As A Daisy Body Lotion	Kara Vita	Moisturising the skin and also preventing water loss
2.	Hydralane Ultra Moisturizing Day Cream	Hydralane Paris	Moisturising agent and in retaining moisture inside the skin
3.	Clear It! Complex Mist	Kara Vita	Help to reduce pimples and prevent acne formation
4.	Cell Act DNA Filler Intense Cream	Cell Act Switzerland	Antiwrinkle agent
5.	Nanosphere Plus	Dermaswiss	Potential antiageing agent

1.3.4 Focus applications for this research

The primary focus of this research is topical formulations for the management of skin ageing and wrinkles and cellulite. Therefore, the following section of this chapter provides a brief overview of these conditions, their causes, and potential treatments.

1.3.4.1 Skin ageing

Human skin undergoes physiological changes with advancing age. The main factors that induce the skin ageing process can be intrinsic and extrinsic.[131-133] However, it must be recognised that no factor acts in isolation to contribute to the ageing process and the visible effects, including loss of elasticity (seen as laxity), sagging and wrinkles, change in skin texture and dryness, and localised pigmentation. These ageing processes are accompanied by phenotypic changes in cutaneous cells and structural and functional changes in extracellular matrix components: such as elastin, collagens, and proteoglycans, required to provide elasticity, tensile strength, and hydration of the skin, respectively.

Intrinsic or chronological ageing occurs as a natural consequence of physiological changes and is influenced by genetics. Effects are seen in the epidermis and dermis. There is a reduction in proliferation of cells in the basal layer, resulting in a thinner epidermis and decreased contact surface area between the epidermis and dermis, further reducing the ability for cell proliferation.[134] This decreased cell proliferation affects a range of epidermal cells, including keratinocytes, fibroblasts, and melanocytes, called cellular senescence. Intrinsic age-related changes in the dermis include fewer mast cells and fibroblasts, a reduction in elastin and collagen fibres,[135] and degeneration of oligosaccharides which reduces the ability of the skin to retain water.[136]

Typically symptoms of intrinsic ageing include excessive dry skin, itchy skin, and loss of elastic fibres underlying eye sockets and cheeks.[137] However, there are significant variations in intrinsic ageing due to ethnicity, anatomical site, and hormonal changes.[131,133] For example, wrinkling patterns appears delayed in people of Asian race, compared to Caucasians.[131,138] Black skin also contains larger lipid structures and produces higher melanin levels, thus protecting from sun exposure, leading to photoageing.[139] Ageing skin is more prone to develop on those parts of the body where the skin is thinner. The skin surrounding the eyes (eyelids) can show the earliest signs of premature ageing.[133] The process may be enhanced during

menopause as low estrogen levels (hypoestrogenism) may influence collagen production, promoting thinner skin and decreased hydration.[131] Intrinsic ageing occurs when endogenous damage accumulates due to the increased reactive oxygen species (ROS) formation generated by oxidative cellular metabolism. Telomeres (TTAGGG), short DNA sequences present at the ends of eukaryotic chromosomes, are considered essential elements in the intrinsic ageing process. The enzyme telomerase plays a vital role in longevity.[132]

Extrinsic ageing is related to environmental factors such as air pollution, smoking, poor nutrition, drug and alcohol intake, and sun exposure.[131-133] Of these, smoking and sun exposure are two of the most important extrinsic factors contributing to skin ageing. For example, Kennedy et al.[140] demonstrated a relationship between smoking load and the intensity in the formation of facial wrinkling, attributing smoking to the activation of matrix metalloproteinases (MMPs), which cause a reduction of collagen and elastin in the dermis. However, sun exposure is the most important extrinsic factor, accounting for about 80% of facial ageing.[141] UVB (290-320nm) induces alteration primarily at the epidermal level, while UVA (320-400 nm) penetrates deeply into the dermis and damages the connective tissue. UVB causes DNA damage in melanocytes and keratinocytes and reduces the production of the soluble epidermal factor (ESF) and proteolytic enzymes, leading to skin inflammation after 12 hours of exposure. Whilst epidermal thinning is a feature of intrinsic skin ageing, UV aged skin exhibits epidermal thickening. Type VII collagen production in the keratinocytes is also decreased and as this is important in achoring collagen fibrils at the dermal-epidermal junction, this weakened connection results in wrinkle formation.[142] Exposure to UV radiation leads to upregulation of matrix metalloproteinases (MMPs) production, altering collagen and other extracellular matrix proteins. UVA plays a role in skin photoageing. Photoaged skin is characterised by the formation of deepening wrinkles, uneven skin texture, dyspigmentation (jaundiced skin), increased fragility, impaired wound healing, and the potential for skin cancer. Wrinkles are the most obvious sign of skin ageing and for which cosmetic procedures and topical products are most frequently sought. Both intrinsic and extrinsic ageing factors decrease Laminine 5 in the dermal-epidermal membrane, essential for epidermal cell attachment. Loss of collagen is considered a primary cause of skin ageing and wrinkle formation. Collagen accounts for roughly 90% of the proteins in the human dermis. Laminin 5

binds type VII collagen, forming the anchoring fibrils embedded in the papillary dermis.[143,144] Additionally, Laminin 5 forms a covalent complex that interacts with type IV collagen in the basement membrane.[145]

Human ageing is a complex biological process with complicated mechanisms. A few theories have associated factors with the human ageing process, characterised by a metabolic change in ageing cells,[146,147] gene expression patterns[148] and elevated reactive oxygen species (ROS) levels.[149] The widely accepted theory is the oxidative stress (OS) hypothesis.[135,150,151] OS is considered an imbalance between production and accumulation of ROS*,* resulting in molecular and cellular damage (cellular ageing).[150,152] Additionally, high levels of ROS can damage DNA, lipids and proteins in cells and tissues, causing activation of the p38 pathway. This pathway is essential to control cell proliferation, differentiation, and cell death (apoptosis) in all eukaryotes, from microorganisms to humans. Senescence is biological ageing when a cellular responds to damage and stress.[153] Cell senescence (CS) is a condition where cells irreversibly stop dividing and enter a state of permanent growth arrest without undergoing cell death.[154] Senescence can be induced by unrepaired DNA damage, and an accumulation of DNA damage can trigger telomere shortening. Telomere plays a crucial role in preventing DNA damage and protecting chromosome degradation.[154] When the telomere length reaches below a critical limit and becomes short. As a result, cells undergo senescence and apoptosis, resulting in intrinsic ageing and photoageing the skin.[155]

Inflammation is a protective response in connective tissue when organisms injure tissues, other causes of cell injury (microbes, trauma and toxins), or necrotic cells.[156] Immediately, leukocytes are sent to kill the microbes and minimise necrotic tissue. ROS and inflammation play a role in the apoptosis of endothelial cells. ROS and inflammation are associated with the prostaglandin (PG) biosynthetic pathway.[150,157] PGs are a group of lipid metabolites derived from arachidonic acid produced at the tissue damage site.

Furthermore, PGs are involved in controlling blood flow, blood clot formation, and induction of labour. ROS can also alter genes and protein function to dysregulate intracellular and extracellular homeostasis, leading to allergic and inflammatory skin diseases.[158] Davalli et al.[159] published their review on Novel Molecular Mechanisms, suggesting molecular inflammation plays a crucial role during the process of ageing and ageing-related diseases.

1.3.4.2 Treatment and prevention

There are three categories by which ageing skin is managed, based on the severity of wrinkles (Table 1.3).

Table 1.3 Photoageing therapies. Adapted from Rabe et al.[160]

Primary	Secondary	Tertiary
Photoprotection	Photoprotection	Chemical peelings
	Retinoic acid	Microdermabrasion/microcoblation
	Antioxidants	Laser
	Estrogens	Botulinum toxin
	Growth factors/cytokines	Fillers

The increasing demand for antiageing products is directly proportional to the rapid growth of the elderly population.[10] Therefore, the cosmeceutical industry develops new materials for functional cosmetics, including whitening, antioxidant and antiwrinkle products. Many antiageing products are incorporated with the topical and oral form to treat skin ageing based on active ingredients. The most common active compounds for antiageing cosmeceuticals include AHA, retinoids and antioxidants, and even beyond modern antiageing cosmetics (anti-enzymatic agents).

Photoprotection

Naturally, the skin has two photoprotective components: the melanin located in the epidermis layer and urocanic acid (UCA) presented in SC.[132,161] They both reflect and absorb UVB radiation.[132] An alternative approach to skin protection is avoiding sun exposure in the middle of the day, from 10 am and 4 pm,[160] and wearing sunglasses and hats. Photoprotective clothing with a UV protection factor (UPF) has been designed for sun protection. In addition, healthcare practitioners encourage the application of sunscreens onto the skin to minimise the harmful effects of UV radiation. The efficacy of sunscreens is based on the sun protection factor (SPF). Sunscreens prevent skin cancer and slow skin ageing due to UVA and UVB protection (coverage dose 2 mg/cm^2).[162]

Retinoids

Tretinoin (all-*trans*-retinoic acid) is a nonselective agent that activates retinoic acid receptors (RARs) directly and the retinoid x receptor (RXR) indirectly.[163] Retinoid receptors are nuclear receptors that bind to retinoids. They are mediators for the actions of retinoids to repair UV-induced skin damage, epidermal differentiation and renewal, and increased dermal

collagen.[164] When bound to a retinoid, they act as transcription factors by altering the expression of genes with corresponding response elements. Previously, retinoids were used for acne treatment. Remarkably, tretinoin is a potent active ingredient to treat the signs of ageing in cosmetic form.[133] Many previous topical tretinoins (retinoic acid) were focused on photoageing and skin wrinkle appearance. Kligman et al.[165] investigated the ability of topical tretinoin to enhance the repair of UV damage. Hairless mice were irradiated with UVA and UVB using FS20 sunlamps for 10 weeks. The mice were then treated topically with concentrations of topical tretinoin for either 5 or 10 weeks. The findings found tretinoin stimulated wound repair in UV-induced histology. Topical tretinoin increased fibroblast growth and collagen production in the dermal structure. In addition, Weiss et al.[166] assessed the efficacy of 0.1% topical tretinoin in treating ageing skin. In an 8 to 12 month vehicle-controlled, double-blind study, treatment with 0.1% cream resulted in significant improvement in clinical assessments and histological. Whilst tretinoin improves damaged skin; its use may also expose the skin to allergic reactions in the form of a burning sensation (stinging), peeling or erythema.[133,160]

Antioxidants

Several antioxidants, such as vitamins (A, B3, C and E), α-lipoic acid (ALA), α-hydroxy acid (AHA), coenzyme Q10 (CoQ_{10}), and plant-derived molecules (carotenoids and polyphenols), prevent photoageing secondary to ROS at the cellular level.[133,154,160] Antioxidants inhibit inflammation by reducing the production of transcription factors.[133] Moreover, antioxidants indirectly affect the expression of inflammatory cytokines.[133,167] In this section, we focus on vitamin C (L-ascorbic acid; LAA) due to its potent antioxidant effect.[168] In dermatology, LAA can be used topically to treat photoaged skin.[169] It can also treat hyperpigmentation by inhibiting tyrosinase and stimulating collagen synthesis.[170] Vitamin C is an unstable molecule, having a short half-life. However, this problem is partially overcome by its conversion into its derivatives, including LAA, fully penetrating the cutaneous skin. There is a need to examine the efficacy of LAA when penetrating cutaneous tissues.[133] However, Humbert et al.[171] reported topical vitamin C use led to significant reductions in wrinkle measurements, assessed by optical profilometry in a 6-month double-blind, placebo-controlled, randomised trial.

Life style

Consuming a healthy diet and regular exercise has been shown to play an important role in the expected life span.[172] A healthy lifestyle, in particular, maintaining physical activity reduces comorbidity diseases (hypertension, DM type 2, stroke and cancers).[172,173] Furthermore, nutrition like exercise is important to maintain biological ageing on telomeres health. As previously described, telomere length plays a key role in cell senescence.[174] Sallam et al.[175] reported a relationship between moderate to regular physical exercise and reduction of oxidative stress level. Moreover, there was also an association between physical exercise and longer telomere length.[176,177] The findings revealed physical exercise contributed to protecting the incidence of telomere attrition; however, the mechanisms remained unclear.[178]

Consuming a fibre-rich diet and unsaturated fats (liquid at room temperature) benefits telomere health. For example, regularly eating whole grains and beans can extend longevity.[179] Thomas et al.[180] proved in a mouse experiment that consumed nutrients, such as vitamin C, vitamin E, curcumin, polyphenols and omega-3 fatty acid, had antioxidant and anti-inflammatory effects and were linked with telomere health. Unhealthy eating habits affect the inflammatory state leading to shorter telomere length (telomere attrition), increasing chronic diseases and decreasing lifespan.[181]

1.3.4.3 Cellulite

Cellulite is the "orange peel" or "cottage cheese" appearance of the skin, typically found on the thighs and buttocks. It is not harmful, but many people seek treatment for its unsightly appearance. Fibrous connective tissue connects the skin to the underlying muscle. When fat cells accumulate in this region, they push the skin upwards, but the connective tissue pulls the skin downwards, creating an uneven surface that dimples the skin. The causes of cellulite are not fully understood, but it is known that it is more common in women, is influenced by hormonal and genetic factors[182], and is associated with weight gain. Factors that predispose to cellulite are summarised in Table 1.4.

Table 1.4 Predisposing factors may trigger cellulite development. Adapted from Rao et al.[183] and Khan et al.[184]

Predisposing factors	
Gender	Women are more likely to develop cellulite because of the underlying structure of fat and connective tissue described previously.
Age	Normal anatomical and physiological changes occurring during the postpubertal period result in women developing cellulite. With increased age, atrophy of the epidermis results in increased severity of cellulite.
Genetic predisposition	Women often have a similar body habitus as other women in their family, which theoretically supports the degree and presence of cellulite.
Race	Caucasian women commonly present with cellulite more than Asian or African American women.
Increased subcutaneous fat	The appearance of cellulite is enhanced on the skin's surface due to increased adipose tissue in the subcutaneous layer.
Diet	Diets rich in high carbohydrates can result in hyperinsulinemia and stimulate lipogenesis, resulting in an overall increase of body fat content, thus increasing the development of cellulite.
Sedentary lifestyle	Sustained sitting and/or standing periods may hinder blood circulation, resulting in stasis and microcirculation changes in cellulite-prone areas.
Pregnancy	A surge in certain hormones, such as prolactin and insulin, and an increase in overall fluid volume can stimulate cellulite by lipogenesis and fluid retention

Genetic background is known to play a role in the development of cellulite.[185] It is often found that the presence and degree of cellulite in similar body habitus areas are associated with their family tree. Women tend to develop cellulite because women have a different connective tissue organisational structure to men. Connective tissues are built by collagen, the main protein. The structure of connective tissue looks like a picket fence in women, whereas in men, it looks like a cross-linked fence, holding stronger, evenly fats. Meanwhile, hormones (estrogen and androgen) are more likely to contribute to cellulite formation. Estrogen is known to stimulate lipogenesis, thus inhibiting lipolysis. This may explain why the onset of cellulite at puberty in women is greater than in men. Moreover, a poor diet, including an excessive carbohydrate and fat intake, provokes hyperinsulinemia and stimulates lipogenesis, thus increasing subcutaneous adipose tissue.[183]

Varieties of treatment approaches are available to reduce the appearance of cellulite. These include surgery, lipolysis including cryolipolysis, laser, radiofrequency and acoustic wave therapies. There are also topical creams containing anti-cellulite medications. These treatments will generally be used with recommended lifestyle (increased exercise) and dietary

modification. The treatment of cellulite is described in detail in Chapter 4. The development and clinical evaluation of a novel topical treatment for cellulite is the subject of Chapters 2 to Chapter 4 of this thesis.

1.4 References

1. Benson HA, Roberts MS, Leite-Silva VR, Walters K. *Cosmetic Formulation: Principles and Practice*.1st ed.CRC Press; 2019.https://doi.org/10.1201/9780429190674
2. Fabbrocini G, De Padova MP, Tosti A. Chemical peels: what's new and what isn't new but still works well. *Facial Plast Surg*. 2009;25(05):329-336.doi:10.1055/s-0029-1243082
3. Clark E, Scerri L. Superficial and medium-depth chemical peels. *Clin Dermatol*. 2008;26(2):209-218.doi:10.1016/j.clindermatol.2007.09.015
4. Sarkar R, Mandlewala ZK, Guss LG, et al. The History of Chemical Peels. *Chemical Peels: A Global Perspective*.1st ed. 2019.doi:10.5005/jp/books/18229
5. Brody HJ, Monheit GD, Resnik SS, Alt TH. A history of chemical peeling. *Dermatol Surg*. 2000;26(5):405-409.doi:10.1046/j.1524-4725.2000.00505.x
6. Rajanala S, Vashi NA. Cleopatra and sour milk—the ancient practice of chemical peeling. *JAMA dermatology*. 2017;153(10):1006-1006.doi:10.1001/jamadermatol.2017.3393
7. Honigman R, Castle DJ. Aging and cosmetic enhancement. *Clin Interv Aging*. 2006;1(2):115-119.doi:10.2147/ciia.2006.1.2.115
8. Hirschberg J. *The History of Ophthalmology: Antiquity*. 1st vol. Verlag JP Wayenborgh; 1982. https://doi.org/10.1163/9789004418288_021
9. Reed R. The definition of "cosmeceutical". *J Soc Cosmet Chem*. 1962;13:103-106. https://www.dr-jetskeultee.nl/jetskeultee/download/common/1962_-reed.-r.-the-definition-of-cosmeceutical.pdf
10. Shin K-O, Park H-S. Antiaging Cosmeceuticals in Korea and Open Innovation in the Era of the 4th Industrial Revolution: From Research to Business. *Sustainability*. 2019;11(3):898.doi:10.3390/su11030898
11. Kaul S, Gulati N, Verma D, Mukherjee S, Nagaich U. Role of Nanotechnology in Cosmeceuticals: A Review of Recent Advances. *J Pharm (Cairo)*. 2018;2018:3420204. doi:10.1155/2018/3420204
12. Aziz ZAA, Mohd-Nasir H, Ahmad A, et al. Role of Nanotechnology for Design and Development of Cosmeceutical: Application in Makeup and Skin Care. *Frontiers in Chemistry*. 2019;7(739):1-15.doi:10.3389/fchem.2019.00739
13. Pandey A, Jatana GK, Sonthalia S. *Cosmeceuticals*. StatPearls Publishing, Treasure Island (FL); 2020.http://europepmc.org/abstract/MED/31334943
14. European Commission-Scientific Committee on Emerging and newly identified Health Risks (SCENIHR). *modified Opinion (after public consultation) on The appropriateness of existing methodologies to assess the potential risks associated with engineered and adventitious products of* nanotechnologies;2006. Accessed November 3, 2021. https://ec.europa.eu/health/ph_risk/committees/04_scenihr/docs/scenihr_o_003b.pdf
15. Bayda S, Adeel M, Tuccinardi T, Cordani M, Rizzolio F. The history of nanoscience and nanotechnology: from chemical–physical applications to nanomedicine. *Molecules*. 2020;25(1):112.doi:10.3390/molecules25010112
16. Raj S, Jose S, Sumod US, Sabitha M. Nanotechnology in cosmetics: Opportunities and challenges. *J Pharm Bioallied Sci*. 2012;4(3):186-193.doi:10.4103/0975-7406.99016
17. Holmes AM, Song Z, Moghimi HR, Roberts MS. Relative penetration of zinc oxide and zinc ions into human skin after application of different zinc oxide formulations. *ACS nano*. 2016;10(2):1810-1819.doi:10.1021/acsnano.5b04148
18. Mohammed YH, Holmes A, Haridass IN, et al. Support for the safe use of zinc oxide nanoparticle sunscreens: lack of skin penetration or cellular toxicity after repeated application in volunteers. *J Invest Dermatol*. 2019;139(2):308-315.doi:10.1016/j.jid.2018.08.024
19. Leite-Silva VR, Liu DC, Sanchez WY, et al. Effect of flexing and massage on in vivo human skin penetration and toxicity of zinc oxide nanoparticles. *Nanomedicine*. 2016;11(10):1193-1205.doi:10.1016/j.jid.2018.08.024
20. Mohammed YH, Haridass IN, Grice JE, Benson HAE, Roberts MS. Bathing Does Not Facilitate Human Skin Penetration or Adverse Cellular Effects of Nanoparticulate Zinc Oxide

Sunscreens after Topical Application. *J Invest Dermatol*. 2020;140(8):1656-1659. doi:10.1016/j.jid.2019.12.024
21. Lohani A, Verma A, Joshi H, Yadav N, Karki N. Nanotechnology-Based Cosmeceuticals. *ISRN Dermatology*. 2014;2014:843687.doi:10.1155/2014/843687
22. Souto EB, Fernandes AR, Martins-Gomes C, et al. Nanomaterials for Skin Delivery of Cosmeceuticals and Pharmaceuticals. *Applied Sciences*. 2020;10(5):1594.doi: 10.3390/app10051594
23. Dhapte-Pawar V, Kadam S, Saptarsi S, Kenjale PP. Nanocosmeceuticals: facets and aspects. *Future Science OA*. 2020;6(10):FSO613.doi:10.2144/fsoa-2019-0109.
24. Roberts R. *2021 Beauty Industry Trends & Cosmetics Marketing: Statistics and Strategies for Your Ecommerce Growth*. 2021.https://commonthreadco.com/blogs/coachs-corner/beauty-industry-cosmetics-marketing-ecommerce#statistics
25. Benson HAE. Skin Structure, Function, and Permeation. *Topical and Transdermal Drug Delivery*. 2011:1-22.doi:10.1002/9781118140505.ch1
26. Walters KA, Roberts MS. The structure and function of skin. *Dermatological and transdermal formulations*.1st ed. CRC Press; 2002:19-58.doi:10.1201/9780824743239
27. Barry BW. Novel mechanisms and devices to enable successful transdermal drug delivery. *Eur J Pharm Sci*. 2001;14(2):101-114.doi:10.1016/S0928-0987(01)00167-1
28. Godin B, Touitou E. Transdermal skin delivery: Predictions for humans from in vivo, ex vivo and animal models. *Advanced Drug Delivery Reviews*. 2007;59(11):1152-1161. doi:10.1016/j.addr.2007.07.004
29. Roohnikan M, Laszlo E, Babity S, Brambilla D. A Snapshot of Transdermal and Topical Drug Delivery Research in Canada. *Pharmaceutics*. 2019;11(6):256.doi:10.3390/pharmaceutics11060256
30. Arens EA, Zhang H. The skin's role in human thermoregulation and comfort. In: Pan N, Gibson P, eds. *Thermal and Moisture Transport in Fibrous Materials*, 1st ed. Woodhead Publishing Ltd; 2006:560-602. Accessed August 18 2021. https://escholarship.org/uc/item/3f4599hx
31. Roberts MS, Srikanth Cheruvu H, Mangion SE, et al. Topical drug delivery: history, percutaneous absorption, and product development. *Advanced Drug Delivery Reviews*. 2021:113929.doi:10.1016/j.addr.2021.113929
32. Montagna W. *The structure and function of skin*. 3rd ed.Elsevier; 2012. https://www.sciencedirect.com/book/9780125052634/the-structure-and-function-of-skin
33. Roberts MS, Mohammed Y, Pastore M, et al. Topical and cutaneous delivery using nanosystems. *J Control Release*. 2017;247:86-105.doi:10.1016/j.jconrel.2016.12.022
34. Ruela ALM, Perissinato AG, Lino MEdS, Mudrik PS, Pereira GR. Evaluation of skin absorption of drugs from topical and transdermal formulations. *Brazilian Journal of Pharmaceutical Sciences*. 2016;52(3):527-544.doi:10.1590/s1984-82502016000300018
35. Karadzovska D, Brooks JD, Monteiro-Riviere NA, Riviere JE. Predicting skin permeability from complex vehicles. *Advanced drug delivery reviews*. 2013;65(2):265-277. doi:10.1016/j.addr.2012.01.019
36. Notman R, Anwar J. Breaching the skin barrier—Insights from molecular simulation of model membranes. *Advanced drug delivery reviews*. 2013;65(2):237-250. doi:10.1016/j.addr.2012.02.011
37. Mathes SH, Ruffner H, Graf-Hausner U. The use of skin models in drug development. *Advanced drug delivery reviews*. 2014;69:81-102.doi:10.1016/j.addr.2013.12.006
38. N'Da DD. Prodrug strategies for enhancing the percutaneous absorption of drugs. *Molecules*. 2014;19(12):20780-20807.doi:10.3390/molecules191220780
39. Williams A. Structure and function of human skin. *Transdermal and topical drug delivery*. 1st ed. Pharmaceutical Press, London; 2003:1-25. Accessed November 1 2021. https://www.worldcat.org/title/transdermal-and-topical-drug-delivery-from-theory-to-clinical-practice/oclc/474778282
40. Benson HAE. Skin Structure, Function, and Permeation. In: Benson HAE, Watkinson AC, eds. *Transdermal and topical drug delivery : principles and practice*. Hoboken, N.J. : Wiley; 2012:1-22.doi:10.1002/9781118140505.ch1
41. Bäckman A, Ny A, Edlund M, et al. Epidermal Overexpression of Stratum Corneum Chymotryptic Enzyme in Mice: A Model for Chronic Itchy Dermatitis. *J Invest Dermatol*. 2002;118(3):444-449.doi:10.1046/j.0022-202x.2001.01684.x

42. Vasilopoulos Y, Cork MJ, Murphy R, et al. Genetic association between an AACC insertion in the 3'UTR of the stratum corneum chymotryptic enzyme gene and atopic dermatitis. *J Invest Dermatol*. 2004;123(1):62-66.doi:10.1111/j.0022-202X.2004.22708.x
43. Bouwstra JA, Honeywell-Nguyen PL, Gooris GS, Ponec M. Structure of the skin barrier and its modulation by vesicular formulations. *Prog Lipid Res*. 2003;42(1):1-36. doi:10.1016/S0163-7827(02)00028-0
44. Michaels A, Chandrasekaran S, Shaw J. Drug permeation through human skin: theory and in vitro experimental measurement. *AIChE J*. 1975;21(5):985-996. doi: 10.1002/aic.690210522
45. Jepps OG, Dancik Y, Anissimov YG, Roberts MS. Modeling the human skin barrier—Towards a better understanding of dermal absorption. *Advanced drug delivery reviews*. 2013;65(2):152-168.doi:10.1016/j.addr.2012.04.003
46. Anissimov YG, Jepps OG, Dancik Y, Roberts MS. Mathematical and pharmacokinetic modelling of epidermal and dermal transport processes. *Adv Drug Deliv Rev*. 2013;65(2):169-190.doi:10.1016/j.addr.2012.04.009
47. El Maghraby GM, Barry BW, Williams AC. Liposomes and skin: from drug delivery to model membranes. *Eur J Pharm Sci*. 2008;34(4-5):203-222.doi:10.1016/j.ejps.2008.05.002
48. Fibrich B, Lambrechts I, Lall N. Nanotechnology and Anti-Ageing Skin Care. *Natural Medicines*.1st ed. CRC Press; 2019:377-392. https://www.taylorfrancis.com/chapters/edit/10.1201/9781315187853-21/nanotechnology-anti-ageing-skin-care-fibrich-lambrechts-lall
49. Menon GK, Cleary GW, Lane ME. The structure and function of the stratum corneum. *Int J Pharm*. 2012;435(1):3-9.doi:10.1016/j.ijpharm.2012.06.005
50. Baroni A, Buommino E, De Gregorio V, Ruocco E, Ruocco V, Wolf R. Structure and function of the epidermis related to barrier properties. *Clin Dermatol*. 2012;30(3):257-262. doi:10.1016/j.clindermatol.2011.08.007
51. Abd E, Yousuf SA, Pastore M, et al. Skin models for the testing of transdermal drugs. *Clinical Pharmacology : Advances and Applications*. 2016:163-176. doi:10.2147/CPAA.S64788
52. Benson HAE. Skin Structure, Function, and Permeation. *Topical and Transdermal Drug Delivery*. John Wiley & Sons, Inc.; 2012:1-22.doi:10.1002/9781118140505.ch1
53. Scheuplein RJ. Mechanism of percutaneous absorption: II. Transient diffusion and the relative importance of various routes of skin penetration. *J Invest Dermatol*. 1967;48(1):79-88.doi:10.1038/jid.1967.11
54. Patzelt A, Lademann J. Drug delivery to hair follicles. *Expert opinion on drug delivery*. 2013;10(6):787-797.doi:10.1517/17425247.2013.776038
55. Ossadnik M, Richter H, Teichmann A, et al. Investigation of differences in follicular penetration of particle-and nonparticle-containing emulsions by laser scanning microscopy. *Laser physics*. 2006;16(5):747-750.doi:10.1134/S1054660X06050033
56. Pathan IB, Setty CM. Chemical penetration enhancers for transdermal drug delivery systems. *Tropical Journal of Pharmaceutical Research*. 2009;8(2):173-179. doi:10.4314/tjpr.v8i2.44527
57. Naik A, Kalia YN, Guy RH. Transdermal drug delivery: overcoming the skin's barrier function. *Pharm Sci Technolo Today*. 2000;3(9):318-326. doi:10.1016/s1461-5347(00)00295-9
58. Patel M, Bharadia P, Patel M. Skin penetration enhancement techniques–physical approaches. *Nature*. 2010;12(13):14. https://www.researchgate.net/publication/267382467_Skin_Penetration_Enhancement_Techniques_-_Physical_Approaches
59. Prausnitz MR, Langer R. Transdermal drug delivery. *Nat Biotechnol*. 2008;26(11):1261-1268.doi:10.1038/nbt.1504
60. Ramadon D, McCrudden MTC, Courtenay AJ, Donnelly RF. Enhancement strategies for transdermal drug delivery systems: current trends and applications. *Drug Delivery and Translational Research*. 2021;12(4):758-791.doi:10.1007/s13346-021-00909-6
61. Mitragotri S. Healing sound: the use of ultrasound in drug delivery and other therapeutic applications. *Nature Reviews Drug Discovery*. 2005;4(3):255-260. doi:10.1038/nrd1662
62. Dixit N, Bali V, Baboota S, Ahuja A, Ali J. Iontophoresis-an approach for controlled drug delivery: a review. *Current drug delivery*. 2007;4(1):1-10. doi:10.2174/156720181070401000

63. Benson HA, McIldowie M, Prow T. Magnetophoresis: skin penetration enhancement by a magnetic field. In: Dragicevic N, Maibach HI, eds. *Percutaneous Penetration Enhancers Physical Methods in Penetration Enhancement*. Springer; 2017:195-205. Accessed March 3, 2022.doi:10.1007/978-3-662-53273-7
64. Murthy SN, Sammeta SM, Bowers C. Magnetophoresis for enhancing transdermal drug delivery: mechanistic studies and patch design. *J Control Release*. 2010;148(2):197-203.doi:10.1016/j.jconrel.2010.08.015
65. Prausnitz MR. Microneedles for transdermal drug delivery. *Advanced drug delivery reviews*. 2004;56(5):581-587.doi:10.1016/j.addr.2003.10.023
66. Jhanker Y, Mbano MN, Ponto T, et al. Comparison of physical enhancement technologies in the skin permeation of methyl amino levulinic acid (mALA). *Int J Pharm*. 2021;610:121258.doi:10.1016/j.ijpharm.2021.121258
67. Kim B, Cho H-E, Moon SH, et al. Transdermal delivery systems in cosmetics. *Biomedical Dermatology*. 2020;4:1-12.doi:10.1186/s41702-020-0058-7
68. Karande P, Mitragotri S. Enhancement of transdermal drug delivery via synergistic action of chemicals. *Biochimica et Biophysica Acta (BBA) - Biomembranes*. 2009;1788(11):2362-2373.doi:10.1016/j.bbamem.2009.08.015
69. Yang Y, Kalluri H, Banga AK. Effects of chemical and physical enhancement techniques on transdermal delivery of cyanocobalamin (vitamin B12) in vitro. *Pharmaceutics*. 2011;3(3):474-484.doi:10.3390/pharmaceutics3030474
70. Moser K, Kriwet K, Naik A, Kalia YN, Guy RH. Passive skin penetration enhancement and its quantification in vitro. *Eur J Pharm Biopharm*. 2001;52(2):103-112. doi:10.1016/S0939-6411(01)00166-7
71. Lane ME. Skin penetration enhancers. *Int J Pharm*. 2013;447(1-2):12-21. doi: 10.1016/j.ijpharm.2013.02.040
72. Ahad A, Aqil M, Kohli K, et al. Chemical penetration enhancers: a patent review. *Expert Opin Ther Pat*. 2009;19(7):969-988.doi:10.1517/13543770902989983
73. Chen Y, Quan P, Liu X, Wang M, Fang L. Novel chemical permeation enhancers for transdermal drug delivery. *Asian Journal of Pharmaceutical Sciences*. 2014;9(2):51-64. doi:10.1016/j.ajps.2014.01.001
74. Barry B, Williams A. Penetration enhancers. *Adv Drug Deliv Rev*. 2003;56(5):603-618.doi:10.1016/j.addr.2003.10.025
75. Williams AC, Barry BW. Skin absorption enhancers. *Crit Rev Ther Drug Carrier Syst*. 1992;9(3-4):305-353.https://pubmed.ncbi.nlm.nih.gov/1458546/
76. Williams AC, Barry BW. Penetration enhancers. *Advanced drug delivery reviews*. 2012;64:128-137.doi:10.1016/j.addr.2012.09.032
77. *Percutaneous Penetration Enhancers Chemical Methods in Penetration Enhancement*. 1 ed. Springer, Berlin, Heidelberg; 2015.doi:10.1007/978-3-662-47039-8
78. Barry BW. Mode of action of penetration enhancers in human skin. *J Control Release*. 1987;6(1):85-97.doi:10.1016/0168-3659(87)90066-6
79. Brinkmann I, Müller-Goymann C. An attempt to clarify the influence of glycerol, propylene glycol, isopropyl myristate and a combination of propylene glycol and isopropyl myristate on human stratum corneum. *Die Pharmazie-An International Journal of Pharmaceutical Sciences*. 2005;60(3):215-220. https://www.ingentaconnect.com/content/govi/pharmaz/2005/00000060/00000003/art00012?crawler=true&mimetype=application/pdf
80. Barry B, Bennett S. Effect of penetration enhancers on the permeation of mannitol, hydrocortisone and progesterone through human skin. *J Pharm Pharmacol*. 1987;39(7):535-546.doi:10.1111/j.2042-7158.1987.tb03173.x.
81. Seki T, Sugibayashi K, Juni K, Morimoto Y. Percutaneous absorption enhancer applied to membrane permeation-controlled transdermal delivery of nicardipine hydrochloride. *Drug Des Deliv*.1989;4(1):69-75. https://pubmed.ncbi.nlm.nih.gov/2775447/
82. Osborne DW, Musakhanian J. Skin Penetration and Permeation Properties of Transcutol(R)-Neat or Diluted Mixtures. *AAPS PharmSciTech*. 2018;19(8):3512-3533. doi:10.1208/s12249-018-1196-8
83. Javadzadeh Y, Adibkia K, Hamishekar H. Transcutol®(diethylene glycol monoethyl ether): A potential penetration enhancer. *Percutaneous penetration enhancers chemical methods in penetration enhancement*. Springer; 2015:195-205. doi:10.1007/978-3-662-47039-8_12

84. Yousef SA, Mohammed YH, Namjoshi S, et al. Mechanistic Evaluation of Enhanced Curcumin Delivery through Human Skin In Vitro from Optimised Nanoemulsion Formulations Fabricated with Different Penetration Enhancers. *Pharmaceutics*. 2019;11(12):639. doi:10.3390/pharmaceutics11120639
85. Csizmazia E, Erős G, Berkesi O, Berkó S, Szabó-Révész P, Csányi E. Penetration enhancer effect of sucrose laurate and Transcutol on ibuprofen. *Journal of Drug Delivery Science and Technology*. 2011;21(5):411-415.doi:10.1016/S1773-2247(11)50066-8
86. Harrison JE, Watkinson AC, Green DM, Hadgraft J, Brain K. The Relative Effect of Azone® and Transcutol® on Permeant Diffusivity and Solubility in Human Stratum Corneum. *Pharm Res*. 1996;13(4):542-546.doi:10.1023/A:1016037803128
87. Nastiti CMRR, Ponto T, Mohammed Y, Roberts MS, Benson HAE. Novel Nanocarriers for Targeted Topical Skin Delivery of the Antioxidant Resveratrol. *Pharmaceutics*. 2020;12(2):108.doi:10.3390/pharmaceutics12020108.
88. López-Mesas M, Christoe J, Carrillo F, Crespi M. Supercritical fluid extraction with cosolvents of wool wax from wool scour wastes. *The Journal of Supercritical Fluids*. 2005;35(3):235-239.doi:10.1016/j.supflu.2005.01.008
89. Boncheva M, Damien F, Normand V. Molecular organization of the lipid matrix in intact Stratum corneum using ATR-FTIR spectroscopy. *Biochimica et Biophysica Acta (BBA) - Biomembranes*. 2008;1778(5):1344-1355.doi:10.1016/j.bbamem.2008.01.022
90. Coderch L, Fonollosa J, Martí M, Parra JL. Ceramides from wool wax. *Journal of the American Oil Chemists' Society*. 2004;81(9):897-898.doi:10.1007/s11746-004-0998-0
91. Carrer V, Guzmán B, Martí M, Alonso C, Coderch L. Lanolin-Based Synthetic Membranes as Percutaneous Absorption Models for Transdermal Drug Delivery. *Pharmaceutics*. 2018;10(3):73.doi:10.3390/pharmaceutics10030073
92. Schlossman ML, McCarthy JP. Lanolin and derivatives chemistry: relationship to allergic contact dermatitis. *Contact Dermatitis*.1979;5(2):65-72. doi:10.1111/j.1600-0536.1979.tb04801.x
93. Francoeur ML, Golden GM, Potts RO. Oleic acid: its effects on stratum corneum in relation to (trans) dermal drug delivery. *Pharm Res*. 1990;7(6):621-627. doi:10.1023/a:1015822312426
94. Goodman M, Barry BW. Lipid-protein-partitioning (LPP) theory of skin enhancer activity: finite dose technique. *Int J Pharm*. 1989;57(1):29-40. doi:10.1016/0378-5173(89)90260-3
95. Goodman M. *Differential scanning calorimetry and permeation studies of penetration enhancer and human skin interactions*. Dissertation. University of Bradford; 1986. https://ethos.bl.uk/OrderDetails.do?uin=uk.bl.ethos.374906
96. Abd E, Benson HAE, Mohammed YH, Roberts MS, Grice JE. Permeation Mechanism of Caffeine and Naproxen through in vitro Human Epidermis: Effect of Vehicles and Penetration Enhancers. *Skin Pharmacol Physiol*. 2019;32(3):132-141. doi:10.1159/000497225
97. Abd E, Namjoshi S, Mohammed YH, Roberts MS, Grice JE. Synergistic Skin Penetration Enhancer and Nanoemulsion Formulations Promote the Human Epidermal Permeation of Caffeine and Naproxen. *J Pharm Sci*. 2015:n/a-n/a.doi:10.1002/jps.24699
98. Sapra B, Jain S, Tiwary A. Percutaneous permeation enhancement by terpenes: mechanistic view. *The AAPS journal*. 2008;10(1):120-132.doi:10.1208/s12248-008-9012-0
99. Lim PFC, Liu XY, Chan SY. A Review on Terpenes as Skin Penetration Enhancers in Transdermal Drug Delivery. *Journal of Essential Oil Research*. 2009;21(5):423-428. doi:10.1080/10412905.2009.9700208
100. Williams AC, Barry BW. Terpenes and the Lipid–Protein–Partitioning Theory of Skin Penetration Enhancement. *Pharm Res*. 1991;8(1):17-24.doi:10.1023/A:1015813803205
101. Cornwell P, Barry B, Stoddart C, Bouwstra J. Wide-angle X-ray diffraction of human stratum corneum: effects of hydration and terpene enhancer treatment. *J Pharm Pharmacol*. 1994;46(12):938-950.https://academic.oup.com/jpp/article-pdf/46/12/938/36992824/j.2042-7158.1994.tb03248.x.pdf
102. Godwin DA, Michniak BB. Influence of drug lipophilicity on terpenes as transdermal penetration enhancers. *Drug Dev Ind Pharm*. 1999;25(8):905-915.doi:10.1081/ddc-100102251
103. El-Kattan AF, Asbill CS, Michniak BB. The effect of terpene enhancer lipophilicity on the percutaneous permeation of hydrocortisone formulated in HPMC gel systems. *Int J Pharm*. 2000;198(2):179-189.doi:10.1016/s0378-5173(00)00330-6

104. Shaker DS, Ishak RAH, Ghoneim A, Elhuoni MA. Nanoemulsion: A Review on Mechanisms for the Transdermal Delivery of Hydrophobic and Hydrophilic Drugs. *Sci Pharm*. 2019;87(3):17.doi:10.3390/scipharm87030017
105. Dipak KS. Engineering of Nanoemulsions for Drug Delivery. *Current Drug Delivery*. 2005;2(4):297-310.doi:10.2174/156720105774370267
106. Gupta A, Eral HB, Hatton TA, Doyle PS. Nanoemulsions: formation, properties and applications. *Soft matter*. 2016;12(11):2826-2841.doi:10.1039/C5SM02958A
107. Anton N, Vandamme TF. Nano-emulsions and micro-emulsions: clarifications of the critical differences. *Pharm Res*. 2011;28(5):978-985.doi:10.1007/s11095-010-0309-1
108. McClements DJ. Nanoemulsions versus microemulsions: terminology, differences, and similarities. *Soft matter*. 2012;8(6):1719-1729.doi:10.1039/C2SM06903B
109. Nastiti CMRR, Ponto T, Abd E, Grice JE, Benson HAE, Roberts MS. Topical nano and microemulsions for skin delivery. *Pharmaceutics*. 2017;9(4):37. doi:10.3390/pharmaceutics9040037
110. Djekic L, Primorac M. The influence of cosurfactants and oils on the formation of pharmaceutical microemulsions based on PEG-8 caprylic/capric glycerides. *Int J Pharm*. 2008;352(1-2):231-239.doi:10.1016/j.ijpharm.2007.10.041
111. Pavoni L, Perinelli DR, Bonacucina G, Cespi M, Palmieri GF. An Overview of Micro- and Nanoemulsions as Vehicles for Essential Oils: Formulation, Preparation and Stability. *Nanomaterials (Basel)*. 2020;10(1):135.doi:10.3390/nano10010135
112. Kouchak M, Handali S. Effects of various penetration enhancers on penetration of aminophylline through shed snake skin. *Jundishapur journal of natural pharmaceutical products*. 2014;9(1):24.doi:10.17795/jjnpp-12904
113. Scott RC. *Prediction of Percutaneous Penetration: Methods, Measurements, Modelling*. vol 2. IBC Technical Services; 1991.
https://books.google.com/books/about/Prediction_of_Percutaneous_Penetration.html?id=Qju2AAAAIAAJ
114. Breuer M. The interation between surfactants and keratinous tissues. *Journal of the Society of Cosmetic Scientists of Korea*. 1979;7(1):53-76. https://www.koreascience.or.kr/article/JAKO197911919650160.pdf
115. Lopes LB. Overcoming the cutaneous barrier with microemulsions. *Pharmaceutics*. 2014;6(1):52-77.doi:10.3390/pharmaceutics6010052
116. Scriven LE. Equilibrium bicontinuous structure. *Nature*. 1976;263(5573):123-125. doi:10.1038/263123a0
117. Schmidts T, Nocker P, Lavi G, Kuhlmann J, Czermak P, Runkel F. Development of an alternative, time and cost saving method of creating pseudoternary diagrams using the example of a microemulsion. *Colloids and Surfaces A: Physicochemical and Engineering Aspects*. 2009;340(1-3):187-192.doi:10.1016/j.colsurfa.2009.03.029
118. Berkman MS, Gulec K. Pseudo ternary phase diagrams: a practical approach for the area and centroid calculation of stable microemulsion regions. *Journal of the Faculty of Pharmacy of Istanbul University*. 2021;51(1):42-50. doi:10.26650/IstanbulJPharm.2020.0090
119. Santos P, Watkinson A, Hadgraft J, Lane M. Application of microemulsions in dermal and transdermal drug delivery. *Skin Pharmacol Physiol*. 2008;21(5):246-259. doi:10.1159/000140228.
120. Ita K. Progress in the use of microemulsions for transdermal and dermal drug delivery. *Pharm Dev Technol*. 2017;22(4):467.doi:10.3109/10837450.2016.1148722
121. Cavalcanti AL, Reis MY, Silva GC, et al. Microemulsion for topical application of pentoxifylline: in vitro release and in vivo evaluation. *Int J Pharm*. 2016;506(1-2):351-360. doi:10.1016/j.ijpharm.2016.04.065
122. Khater D, Nsairat H, Odeh F, et al. Design, Preparation, and Characterization of Effective Dermal and Transdermal Lipid Nanoparticles: A Review. *Cosmetics*. 2021;8(2):39. doi:10.3390/cosmetics8020039
123. Pardeike J, Hommoss A, Müller RH. Lipid nanoparticles (SLN, NLC) in cosmetic and pharmaceutical dermal products. *Int J Pharm*. 2009;366(1):170-184. doi:10.1016/j.ijpharm.2008.10.003
124. Yukuyama MN, Ghisleni DDM, Pinto TJA, Bou-Chacra NA. Nanoemulsion: process selection and application in cosmetics – a review. *Int J Cosmet Sci*. 2016;38(1):13-24. doi:10.1111/ics.12260
125. Solè I, Solans C, Maestro A, González C, Gutiérrez J. Study of nano-emulsion formation by dilution of microemulsions. *J Colloid Interface Sci*. 2012;376(1):133-139.

doi: 10.1016/0006-2944(75)90147-7
126. Podlogar F, Gasperlin M, Tomsic M, Jamnik A, Rogac MB. Structural characterisation of water-Tween 40/Imwitor 308-isopropyl myristate microemulsions using different experimental methods. *Int J Pharm*. 2004;276(1-2):115-128. doi:10.1016/j.ijpharm.2004.02.018
127. Danino D, Bernheim-Groswasser A, Talmon Y. Digital cryogenic transmission electron microscopy: an advanced tool for direct imaging of complex fluids. *Colloids and Surfaces A: Physicochemical and Engineering Aspects*. 2001;183:113-122.doi:10.1016/j.jcis.2012.02.063
128. Bhattacharya S, Stokes J, Kim M-W, Huang J. Percolation in an oil-continuous microemulsion. *Phys Rev Lett*. 1985;55(18):1884.doi:10.1103/PhysRevLett.55.1884
129. Acharya DP, Hartley PG. Progress in microemulsion characterization. *Current Opinion in Colloid & Interface Science*. 2012;17(5):274-280.doi:10.1016/j.cocis.2012.07.002
130. Kaur IP, Agrawal R. Nanotechnology: a new paradigm in cosmeceuticals. *Recent patents on drug delivery & formulation*. 2007;1(2):171-182. doi:10.2174/187221107780831888.
131. Tobin DJ. Introduction to skin aging. *Journal of Tissue Viability*. 2017;26(1):37-46. doi:10.1016/j.jtv.2016.03.002
132. Puizina-Ivic N. Skin aging. *Acta Dermatovenerologica Alpina Panonica Et Adriatica*. 2008;17(2):47.http://s3-eu-west-1.amazonaws.com/thejournalhub/10.15570/archive/acta-apa-08-2/1.pdf
133. Ramos-e-Silva M, Celem LR, Ramos-e-Silva S, Fucci-da-Costa AP. Anti-aging cosmetics: Facts and controversies. *Clin Dermatol*. 2013;31(6):750-758. doi:10.1016/j.clindermatol.2013.05.013
134. Makrantonaki E, Zouboulis CC. Characteristics and pathomechanisms of endogenously aged skin. *Dermatology*. 2007;214(4):352-360. doi:10.1159/000100890
135. Kohl E, Steinbauer J, Landthaler M, Szeimies RM. Skin ageing. *J Eur Acad Dermatol Venereol*. 2011;25(8):873-884.doi:10.1111/j.1468-3083.2010.03963.x
136. Naylor EC, Watson RE, Sherratt MJ. Molecular aspects of skin ageing. *Maturitas*. 2011;69(3):249-256.doi:10.1016/j.maturitas.2011.04.011
137. Hwang E, Park S-Y, Yin CS, Kim H-T, Kim YM, Yi TH. Antiaging effects of the mixture of Panax ginseng and Crataegus pinnatifida in human dermal fibroblasts and healthy human skin. *Journal of Ginseng Research*. 2017;41(1):69-77.doi: 10.1016/j.jgr.2016.01.001
138. Grove GL. Physiologic Changes in Older Skin. *Clin Geriatr Med*. 1989;5(1):115-125. doi:10.1016/S0749-0690(18)30699-2
139. Rawlings AV. Ethnic skin types: are there differences in skin structure and function?1. *Int J Cosmet Sci*. 2006;28(2):79-93.doi:10.1111/j.1467-2494.2006.00302.x
140. Kennedy C, Bastiaens MT, Willemze R, Bavinck JNB, Bajdik CD, Westendorp RG. Effect of smoking and sun on the aging skin. *J Invest Dermatol*. 2003;120(4):548-554.doi:10.1046/j.1523-1747.2003.12092.x
141. Friedman O. Changes associated with the aging face. *Facial Plast Surg Clin North Am*. 2005;13(3):371-380.doi:10.1016/j.fsc.2005.04.004
142. Contet-Audonneau JL, Jeanmaire C, Pauly G. A histological study of human wrinkle structures: comparison between sun-exposed areas of the face, with or without wrinkles, and sun-protected areas. *Br J Dermatol*. 1999;140(6):1038-1047. doi:10.1046/j.1365-2133.1999.02901.x
143. Nishiyama T, Amano S, Tsunenaga M, et al. The importance of laminin 5 in the dermal-epidermal basement membrane. *J Dermatol Sci*. 2000;24 Suppl 1:S51-59. doi:10.1016/s0923-1811(00)00142-0
144. Rousselle P, Keene DR, Ruggiero F, Champliaud M-F, Rest Mvd, Burgeson RE. Laminin 5 binds the NC-1 domain of type VII collagen. *The Journal of cell biology*. 1997;138(3):719-728.doi:10.1083/jcb.138.3.719
145. Champliaud M-F, Lunstrum GP, Rousselle P, Nishiyama T, Keene DR, Burgeson RE. Human amnion contains a novel laminin variant, laminin 7, which like laminin 6, covalently associates with laminin 5 to promote stable epithelial-stromal attachment. *The Journal of cell biology*. 1996;132(6):1189-1198.doi:10.1083/jcb.132.6.1189
146. Liu Y, Weng W, Gao R, Liu Y. New Insights for Cellular and Molecular Mechanisms of Aging and Aging-Related Diseases: Herbal Medicine as Potential Therapeutic Approach. *Oxid Med Cell Longev*. 2019;2019:4598167.doi:10.1155/2019/4598167

147. Lynch DB, Jeffery IB, O'Toole PW. The role of the microbiota in ageing: current state and perspectives. *WIREs Systems Biology and Medicine*. 2015;7(3):131-138. doi:10.1002/wsbm.1293
148. Shadyab AH, LaCroix AZ. Genetic factors associated with longevity: a review of recent findings. *Ageing research reviews*. 2015;19:1-7.doi:10.1016/j.arr.2014.10.005
149. Sergiev PV, Dontsova OA, Berezkin GV. Theories of aging: an ever-evolving field. *Acta Naturae*. 2015;7(1):9-18. https://www.ncbi.nlm.nih.gov/pmc/articles/PMC4410392/
150. Tan BL, Norhaizan ME, Liew W-P-P, Sulaiman Rahman H. Antioxidant and Oxidative Stress: A Mutual Interplay in Age-Related Diseases. *Front Pharmacol*. 2018;9(1162).doi:10.3389/fphar.2018.01162
151. Ghezzi P, Jaquet V, Marcucci F, Schmidt HHHW. The oxidative stress theory of disease: levels of evidence and epistemological aspects. *Br J Pharmacol*. 2017;174(12):1784-1796.doi:10.1111/bph.13544
152. Conti V, Izzo V, Corbi G, et al. Antioxidant Supplementation in the Treatment of Aging-Associated Diseases. *Front Pharmacol*. 2016;7(24):1-11.doi:10.3389/fphar.2016.00024
153. Franceschi C, Campisi J. J Gerontol A Biol Sci Med Sci 69 Suppl 1. S4-9; 2014. doi:10.1093/gerona/glu057.
154. Shanbhag S, Nayak A, Narayan R, Nayak UY. Anti-aging and sunscreens: paradigm shift in cosmetics. *Advanced pharmaceutical bulletin*. 2019;9(3):348.
doi: 10.15171/apb.2019.042.
155. Blasco MA. Mice with bad ends: mouse models for the study of telomeres and telomerase in cancer and aging. *EMBO J*. 2005;24(6):1095-1103. doi:10.1038/sj.emboj.7600598
156. Sarkar D, Fisher PB. Molecular mechanisms of aging-associated inflammation. *Cancer Lett*. 2006;236(1):13-23.doi:10.1016/j.canlet.2005.04.009
157. Kawahara K, Hohjoh H, Inazumi T, Tsuchiya S, Sugimoto Y. Prostaglandin E2-induced inflammation: Relevance of prostaglandin E receptors. *Biochim Biophys Acta*. 2015;1851(4):414-421.doi:10.1016/j.bbalip.2014.07.008
158. Tsuchida K, Kobayashi M. Oxidative stress in human facial skin observed by ultraweak photon emission imaging and its correlation with biophysical properties of skin. *Sci Rep*. 2020;10(1):9626.doi:10.1038/s41598-020-66723-1
159. Davalli P, Mitic T, Caporali A, Lauriola A, D'Arca D. ROS, cell senescence, and novel molecular mechanisms in aging and age-related diseases. *Oxid Med Cell Longev*. 2016;2016,
160. Rabe JH, Mamelak AJ, McElgunn PJ, Morison WL, Sauder DN. Photoaging: mechanisms and repair. *J Am Acad Dermatol*. 2006;55(1):1-19. doi:10.1016/j.jaad.2005.05.010
161. Gniadecka M, Wulf HC, Mortensen NN, Poulsen T. Photoprotection in vitiligo and normal skin. A quantitative assessment of the role of stratum corneum, viable epidermis and pigmentation. *Acta Derm Venereol*. 1996;76(6):429-432.doi:10.2340/0001555576429432
162. Haywood R, Wardman P, Sanders R, Linge C. Sunscreens inadequately protect against ultraviolet-A-induced free radicals in skin: implications for skin aging and melanoma? *J Invest Dermatol*. 2003;121(4):862-868.doi:10.1046/j.1523-1747.2003.12498.x
163. Levin AA, Sturzenbecker LJ, Kazmer S, et al. 9-cis retinoic acid stereoisomer binds and activates the nuclear receptor RXR alpha. *Nature*. 1992;355(6358):359-361. doi:10.1038/355359a0
164. Nasir A. Nanopharmaceuticals and Nanocosmeceuticals. *Cosmeceuticals and Cosmetic Practice*. 2013:45-54.doi:10.1002/9781118384824.ch5
165. Kligman LH. Effects of all-trans-retinoic acid on the dermis of hairless mice. *J Am Acad Dermatol*. 1986;15(4 Pt 2):779-785, 884-777.doi:10.1016/s0190-9622(86)70234-x
166. Weiss JS, Ellis CN, Headington JT, Voorhees JJ. Topical tretinoin in the treatment of aging skin. *J Am Acad Dermatol*. 1988;19(1 Pt 2):169-175.
doi:10.1016/s0190-9622(88)70161-9
167. Suzuki YJ, Aggarwal BB, Packer L. Alpha-lipoic acid is a potent inhibitor of NF-kappa B activation in human T cells. *Biochem Biophys Res Commun*. 1992;189(3):1709-1715. doi:10.1016/0006-291x(92)90275-p
168. Colven RM, Pinnell SR. Topical vitamin C in aging. *Clin Dermatol*. 1996;14(2):227-234.doi:10.1016/0738-081X(95)00158-C
169. Lin JY, Selim MA, Shea CR, et al. UV photoprotection by combination topical antioxidants vitamin C and vitamin E. *J Am Acad Dermatol*. 2003;48(6):866-874. doi:10.1067/mjd.2003.425

170. Farris PK. Topical vitamin C: a useful agent for treating photoaging and other dermatologic conditions. *Dermatol Surg*. 2005;31(7 Pt 2):814-817; discussion 818. doi:10.1111/j.1524-4725.2005.31725
171. Humbert PG, Haftek M, Creidi P, et al. Topical ascorbic acid on photoaged skin. Clinical, topographical and ultrastructural evaluation: double-blind study vs. placebo. *Exp Dermatol*. 2003;12(3):237-244.doi:10.1034/j.1600-0625.2003.00008.x
172. Mercken EM, Carboneau BA, Krzysik-Walker SM, de Cabo R. Of mice and men: The benefits of caloric restriction, exercise, and mimetics. *Ageing Research Reviews*. 2012;11(3):390-398.doi:10.1016/j.arr.2011.11.005
173. Reimers CD, Knapp G, Reimers AK. Does physical activity increase life expectancy? A review of the literature. *J Aging Res*. 2012;2012:243958.doi:10.1155/2012/243958
174. López-Otín C, Blasco MA, Partridge L, Serrano M, Kroemer G. The Hallmarks of Aging. *Cell*. 2013;153(6):1194-1217.doi:10.1016/j.cell.2013.05.039
175. Sallam N, Laher I. Exercise Modulates Oxidative Stress and Inflammation in Aging and Cardiovascular Diseases. *Oxid Med Cell Longev*. 2016;2016:7239639. doi:10.1155/2016/7239639
176. Ludlow AT, Zimmerman JB, Witkowski S, Hearn JW, Hatfield BD, Roth SM. Relationship between Physical Activity Level, Telomere Length, and Telomerase Activity. *Med Sci Sports Exerc*. 2008;40(10):1764-1771.doi:10.1249/MSS.0b013e31817c92aa
177. Puterman E, Lin J, Blackburn E, O'Donovan A, Adler N, Epel E. The Power of Exercise: Buffering the Effect of Chronic Stress on Telomere Length. *PLoS One*. 2010;5(5):e10837.doi:10.1371/journal.pone.0010837
178. Balan E, Decottignies A, Deldicque L. Physical Activity and Nutrition: Two Promising Strategies for Telomere Maintenance? *Nutrients*. 2018;10(12):1942.doi:10.3390/nu10121942
179. Hayat I, Ahmad A, Masud T, Ahmed A, Bashir S. Nutritional and Health Perspectives of Beans (Phaseolus vulgaris L.): An Overview. *Crit Rev Food Sci Nutr*. 2014;54(5):580-592. doi:10.1080/10408398.2011.596639
180. Thomas P, Wang Y-J, Zhong J-H, et al. Grape seed polyphenols and curcumin reduce genomic instability events in a transgenic mouse model for Alzheimer's disease. *Mutation Research/Fundamental and Molecular Mechanisms of Mutagenesis*. 2009;661(1):25-34. doi:10.1016/j.mrfmmm.2008.10.016
181. García-Calzón S, Zalba G, Ruiz-Canela M, et al. Dietary inflammatory index and telomere length in subjects with a high cardiovascular disease risk from the PREDIMED-NAVARRA study: cross-sectional and longitudinal analyses over 5 y. *The American Journal of Clinical Nutrition*. 2015;102(4):897-904.doi:10.3945/ajcn.115.116863
182. Emanuele E, Minoretti P, Altabas K, Gaeta E, Altabas V. Adiponectin expression in subcutaneous adipose tissue is reduced in women with cellulite. *Int J Dermatol*. 2011;50(4):412-416.doi:10.1111/j.1365-4632.2010.04713.x
183. Rao J, Gold MH, Goldman MP. A two-center, double-blinded, randomized trial testing the tolerability and efficacy of a novel therapeutic agent for cellulite reduction. *J Cosmet Dermatol*. 2005;4(2):93-102.doi:10.1111/j.1473-2165.2005.40208.x
184. Khan MH, Victor F, Rao B, Sadick NS. Treatment of cellulite: Part I. Pathophysiology. *J Am Acad Dermatol*. 2010;62(3):361-370; quiz 371-362.doi:10.1016/j.jaad.2009.10.042
185. Rossi AB, Vergnanini AL. Cellulite: a review. *J Eur Acad Dermatol Venereol*. 2000;14(4):251-262.doi:10.1046/j.1468-3083.2000.00016.x

Chapter 2. Skin delivery of Caffeine (CAF): Effect of Chemical Penetration Enhancers on Porcine Skin

2.1 Introduction

Caffeine (1,3,7-trimethylpurine-2,6-dione: CAF) is a methylxanthine alkaloid (Figure 2.1), naturally found in the seeds, leaves, and fruit of several plants such as *Coffea arabica,* L., *Camellia sinensis*, (L.) Kuntze, and *Ilex paraguariensis* (A.) St. Hil.

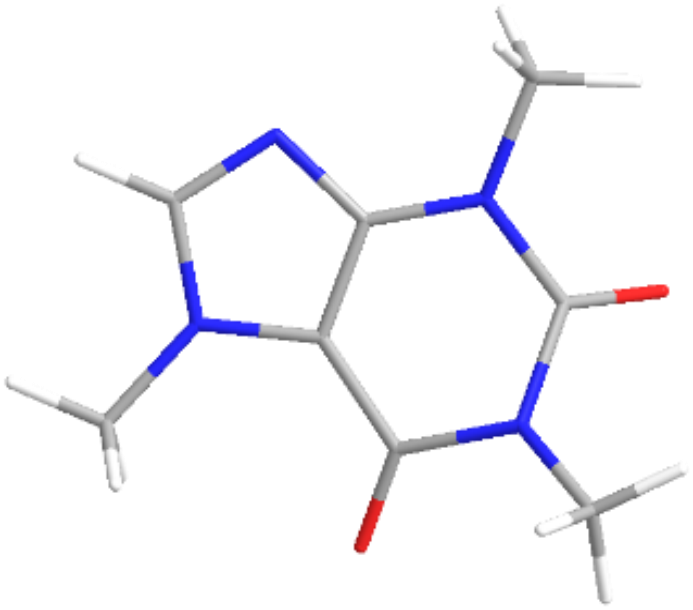

Figure 2.1 Structure of caffeine ($C_8H_{10}N_4O_2$: Carbon–grey, Hydrogen–white, Nitrogen–blue, Oxygen–red) (ChemDraw 16.0)

CAF has attracted interest due to its reported range of therapeutic effects both for topical and systemic drug delivery. This includes oral administration for the treatment of various types of cancers,[1-5] and action as a neuroprotective agent in vascular dementia.[6] A large prospective study was conducted to assess the relationship between coffee consumption (containing CAF) and cognitive decline in a community population of elderly people. The psychostimulant properties of CAF from a daily intake of coffee drinks appeared to reduce the decline in cognitive function for both verbal retrieval and visuospatial memory.[6] A range of positive effects on the skin and hair has been reported following oral administration of CAF, including skin

cancer chemoprevention due to its antioxidant properties by slowing skin photoageing and inhibiting UV-induced carcinogenesis.[7-9]

Following topical administration, CAF is reported to have localised effects on the skin and associated tissues. Topical CAF administration on hairless mouse skin enhanced the removal of DNA-damaged cells in keratinocytes by inhibiting the ATR/Chk1 pathway,[10] that promotes melanoma cancer.[11] Green coffee oil (GCO: *Coffea arabica,* L.) affected the synthesis of collagen, elastin, and glycosaminoglycans to improve the new formation of connective tissue in cultured keratinocytes.[12] The authors suggested that GCO could be a useful carrier vehicle in cosmetic formulations.

There is good evidence that CAF increases blood circulation to the scalp and stimulates hair follicle growth by inhibiting the action of the 5-α-reductase enzyme that is responsible for converting testosterone into dihydrotestosterone (DHT).[7,13] DHT is found in the prostate, skin and hair follicles. The actions of DHT, and the sensitivity of hair follicles to DHT, is what causes hair loss. CAF inhibits 5-α-reductase activity, resulting in a renewed growth phase of the hair. CAF also reduces muscle tension surrounding hair follicles to transfer nutrient supply via blood flow underlying the dermal papillae layer. In addition, CAF increases the microcirculation of blood vessels in the skin of the head, thereby contributing to nurturing hair bulbs. Thus, CAF works by multiple mechanisms to reduce hair loss.

CAF has also been shown to improve cellulite[14], a common condition characteried by the "cottage cheese" appearance of the skin and involving the microcirculatory and lymphatic systems.[15] For example, Lupi et al.[16] evaluated the effectiveness of anti-cellulite containing 7% of CAF solution (Elancyl® Chrono Active). After one month of treatment, there was a significant reduction of thigh circumference in more than 80% of treated participants and a 67.7% reduction in hip circumference.

Topical administration of CAF in anti-cellulite products acts to (i) prevent fatty cells accumulation in the skin (lipolysis),[16] (ii) facilitate lymphatic drainage, and also has other beneficial skin effects to (iii) prevent photoageing and photodamage in skin.[12,14,17] It is thought that the clinical efficacy of CAF in the management of cellulite is primarily through the actions of stimulating adipocyte lipolysis, inhibiting phosphodiesterase (PDE) and augmenting cyclic adenosine monophosphate (cAMP).[17] Herman and Herman[7] reviewed the role of CAF in

lipolysis and its potential cosmetic applications, as summarised below. Lipolysis is a breakdown of triglycerides stored in fat cells (adipocytes) by the lipoprotein lipase (LPL) enzyme, leading to fatty acids and glycerol. LPL is present on the fat cell membrane and is responsible for fat storage. In addition, lipase activity is controlled by catecholamines (adrenaline and noradrenaline) and hormones (insulin, adrenocorticotropin, glucagon). Insulin inhibits LPL, whilst adrenocorticotropin, adrenalin, noradrenalin and glucagon stimulate LPL. Decreasing cAMP levels further inhibits the lipolysis process, whereas increasing cAMP levels stimulates protein kinase A. Protein kinase A is responsible for regulating phosphorylation hormone-sensitive lipase (HSL). CAF stimulates lipolysis by inhibiting PDE activity and increasing cAMP levels in adipocytes. Conversion of cAMP to 5'-AMP (noncyclic) is related to PDE activity. The activation of HSL leads to triglycerides breaking down in the lipolysis process. CAF also facilitates lymphatic drainage by removing excess fat and toxins during the process of lipolysis.

CAF is frequently employed as a model hydrophilic active ingredient in skin penetration/permeation experiments; [18-22] therefore, there is a wealth of data on its skin penetration and the effect of formulation and other topical application methodologies.

The physicochemical properties of CAF are shown in Table 2.1.[23-25]

Table 2.1 Physicochemical properties of caffeine

Molecular weight (MW)	194.19 g/mol
Log P o/w	–0.07
pKa	14.0 at 25°C, 10.4 at 40°C
Solubility	1 in 46 of water, 1 in 1.5 of boiling water
Melting point	238°C
Solubility parameter	31 $MPa^{½}$

Table 2.2 provides a summary of representative studies of the skin permeation of CAF, with the inclusion criteria of restricting to the most appropriate skin models of human, pig, and piglet skin. It shows the range of formulations that have been investigated and includes studies of commercial products. Permeability parameters for evaluating CAF topical/transdermal delivery in IVPT included in the table are flux (Jss), permeability coefficient (Kp), cumulative amount (Q), and lag time.

Several approaches have been investigated in the development of topical CAF formulations. [26-33] For example, CAF was incorporated into deformable liposomes (DL), which were evaluated to determine the relative delivery into the skin appendages and the amount in

deeper skin layers associated with cellulitis and androgenetic alopecia.[34] The liposomes were composed of soybean phosphatidylcholine with propylene glycol (PG) incorporated to provide the flexibility required to allow the vesicles to squeeze between cells in the SC. CAF flux through the human skin epidermis was 1.94-fold for the liposome formulation compared to the CAF solution. Although this study provided a promising headline, liposomes can also bring disadvantages like leaking the core content to the external medium, impacting encapsulation efficiency. Drawbacks of this formulation approach were the relatively complicated fabrication procedure and the large volume of phospholipid needed to obtain high encapsulation of the hydrophilic CAF with a small proportion of unilamellar vesicles.

Micro-nanoemulsion formulations have properties that suggest they have the potential for successful skin delivery of CAF.[35-37] Micro-nanoemulsions made of oil, surfactant/co-surfactant and water, in defined ratios, form an isotropic, clear or transparent/translucent, single-phase system of nanosized droplets.[36,38] These formulations also offer simplicity of manufacturing and high stability. [35] Moreover, nanoemulsion fabrication is relatively production scalable and therefore practical for industrial development.[37,39]

Bonina et al.[33] investigated the effects of various penetration enhancers on testosterone (TST) and caffeine (CAF) penetration through excised human skin. Four enhancers were investigated, such as labrasol (LBS), labrafil (LBF), Transcutol (TSC) and propylene glycol dipelargonate (DPPG); whilst propylene glycol (PG) and liquid petrolatum (LP) as reference vehicles. The findings indicated that all enhancers significantly enhanced drug permeability. DPPG and LBF enhanced CAF flux relative to PG, while LBS and TSC increased the stratum corneum affinity for TST relative to LP. DPPG showed interaction with the lipid bilayers, and PG promoted DPPG penetrating stratum corneum and creating interaction sites in such a tissue.

In this current study, we selected nanoemulsions in the form of cream stabilised by emulsifiers via the hot emulsification method. The cream form provides good skin penetration/permeation of CAF within nano-sized. In addition, nano-cream formulations represent the most notable customer preference for cosmetic applications. Moreover, we chose formulation ingredients categorised as generally regarded as safe and effective (GRASE) to address the safety and irritancy profile of the semisolid nano-cream formulations.

Semisolid cream preparation was the most commonly chosen as common media, compared to other systems, because it is versatile and easily absorbed in the skin due to its water content and composition in fat. [40,41] Therefore, there is a strong relationship between rheology and sensory properties to meet customer acceptance. Skin feeling of a final cosmetic product, such as physical appearances (colour, odour, texture and consistency), spreading of creams, or leaving stickiness and greasiness upon application on the skin, plays an essential role in understanding customer expectations. Ideally, creams can be applied for widespread treatment areas. However, it will affect sensory parameters when creams are rubbed on the skin when the flow changes.[42,43]

The nano-creams were prepared in two different phases (oil and water) based on a blend of two non-ionic surfactants with a range of HLB values of 15. Finally, LAN, PG and TR were chosen due to their excellent solubilising capacity and skin penetration, enhancing the ability for the hydrophilic active ingredient and as they are primarily used in cosmetic products.

Table 2.2 Summary of *in vitro* penetration/permeation studies of topical/transdermal CAF formulations

Dosage forms	Formula details	Donor	Skin permeation evaluation		Ref
			Method	Results	
Biocellulose (99% water membrane) and gel	BC-CAF incorporated with glycerol and ethanol Gel-CAF incorporated with carbopol 940	12 mg BC-CAF; 400 mg of gel; 400 µL of CAF aqueous solution	Human abdominal skin R: PBS (pH 7.4)	*Flux J (µg/cm²/h) in 10 h* Gel: 4.41 ± 0.31 CAF aqueous solution: 7.53 ± 2.37 BC-CAF: 2.55 ± 0.82 *Q_{10} (µg/cm²)* Gel: 65.78 ± 8.95 CAF aqueous solution: 86 ± 23.85 BC-CAF: 33.52 ± 5.02 *Kp (cm/h)* Gel: $5.51 \times 10^{-4} \pm 3.92 \times 10^{-5}$ Aqueous solution: $9.42 \times 10^{-4} \pm 2.96 \times 10^{-4}$ BC-CAF: $3.19 \times 10^{-4} \pm 1.02 \times 10^{-4}$	30
Deformable liposome (DL)	Soybean phosphatidylcholine 1.5% Propylene glycol 0.3% Phenoxyethanol 0.1% PBS 70mL	160 µL of the liposome formulations	Human abdominal skin R: PBS (pH 7.4)	*Flux J (µg/cm²/h) in 24 h* DL-CAF: 1.68 ± 0.52 CL-CAF: 0.55 ± 0.15 CS: 1.08 ± 0.95 *Q_{24} (µg/cm²)* DL-CAF 1.68 ± 0.52 SC: 28.06 ± 12.33 Skin: 32.30 ± 11.71 Receptor: 40.26 ± 12.46 Total permeated: 100.62 ± 28.49	34
Gel	Three gel bases: Ethylene glycol, water, petrolatum, incorporated with carbopol 940	0.5-60 µg/cm²	Dermatomed abdominal skin (cadaver) (350 µm thick) R: normal saline (NaCl)	*Kp= 2.1-7.2 x 10⁴ cm/h* % absorbed (total)= 4.7-61.8	44

Dosage forms	Formula details	Donor	Skin permeation evaluation		Ref
			Method	Results	
Gel	Ethanol Propylene glycol (PG) Uniphen® P-23 (preservative) Gelling agent: carbopol® Ultrez-21	2.5 g of gel	Full thickness flank newborn pigskin R: PBS (pH 7.4)	Cumulative amount (µg) PG 15% > PG 30% > PG 7.5%	26
Gel	Glycerin Propylene glycol (PG) Dimethylenecopolyol (Dow Corning 193) Gelling agent: Carbopol® 934	300 mg of gel formulation	Dermatomed human abdominal skin (250-400µm thick) R: PBS (pH 7.4)	*Flux J (µg/cm²/h) in 6 h* 1 mg/cm²: Gel 1% of CAF: 0.252 ± 0.108 Gel 3%: 0.306 ± 0.21 Gel 5%: 0.552 ± 0.03 *Q_6 (µg)* 1 mg/cm²: Gel 1% of CAF: 3.52 ± 1.31 Gel 3%: 4.18 ± 1.35 Gel 5%: 6.88 ± 0.53 *Amount CAF deposited (µg)*: 1 mg/cm²: Gel 1% of CAF: 31.4 Gel 3%: 94.2 Gel 5%: 157 Lagtime (h) Amount of gel deposited Gel 1% of CAF: 2 Gel 3%: 1.97 Gel 5%: 2.07	27

Dosage forms	Formula details	Donor	Skin permeation evaluation		Ref
			Method	Results	
ME Emulsion Gel	ME: lipids (PEG-8 caprylic/capric glycerides; polyglycerol-6 dioleate; isostearyl isostearate; diisopropyl adipate; S/Co and water E: lipids (PEG-6 stearate PEG-32 stearate; isostearyl isostearate; diisopropyl adipate); S/Co, xanthan gum, ultrez®10 and water Gel: lipids (hydroxypropyl guar); S/Co, ultrez®10 and water	1 g of formulation containing 8 mg CAF	Dermatomed pigskin (400µm thick) R: PBS (pH 7.4)	<u>Without hypodermis</u> *Flux J (µg/cm²/h) in 24 h* ME: 28.8 ± 0.2 E: 15.6 ± 0.8 Gel: 17.11 ± 0.6 Control: 14.1 ± 0.9 *Lag time (h)* ME: 1.31 ± 0.18 E: 2.78 ± 0.26 Gel: 2.36 ± 0.20 Control: 1.30 ± 0.01 *Kp (cm/h)* ME: 3.59×10^{-3} E: 1.95×10^{-3} Gel: 2.14×10^{-3} Control: 1.09×10^{-4} <u>With hypodermis</u> *Flux J (µg/cm²/h) in 24 h* ME: 509 ± 10 E: 497 ± 35 Gel: 437 ± 0.13 *Lag time (h)* ME: 5.09 ± 0.10 E: 4.97 ± 0.35 Gel: 5.37 ± 0.13 *Kp (cm/s)* ME: 2.62×10^{-3} E: 1.55×10^{-3} Gel: 1.63×10^{-3}	45

Dosage forms	Formula details	Donor	Skin permeation evaluation		Ref
			Method	Results	
ME	Oil: Labrafil M 1944 CS (oleoyl polyoxyl-6 glycerides) S: Cremophor EL (polyoxyl 35 castor oil) Co: Tetraglycol Water: PBS	0.1 g formulation containing 1 mg of CAF	Full-thickness newborn pigskin R: PBS (pH 7.4)	*Flux J (µg/cm²/h) in 24 h* ME4: 16.08 ± 3.52 *Q_{24} (µg/cm²)* ME4: 374.18 ± 27.70 *Skin retention (µg/g)* ME4: 177.28 ± 14.24	46
ME	W/O ME20: Oil: Isopropyl palmitate S: Labrasol® (PEG-8 caprylic/capric triglycerine), glyceryl oleate Co: propylene carbonate Water ME20 gel: Amorphous silica	0.5 g of formulation	Full-thickness porcine ear skin R: PBS (pH 7.4)	Pig/frozen-thawed *Kp (cm/h) in 12 h* ME20= 3.7 ± 0.8 ME20 gel= 3.3 ± 0.8 *Q_{24} (µg/cm²)* ME20= 778.1 ± 141.8 ME20 gel = 706.1 ± 144.9	9
ME	Penetration enhancers Oil: Eucalyptol or oleic acid (OA) S: Volpo-N10® Co: Ethanol Water	1 mL of formulation	Full-thickness human abdominal skin R: PBS (pH 7.4)	*Flux J (µg/cm²/h) in 24 h* E1: 263.6 ± 1.2 E2: 267.7 ± 24.0 O1: 118.8 ± 57.3 O2: 136.4 ± 95.2 *Control* (CAF) C1: 2.2 ± 0.8 C2: 25.6±3.1 C3: 2.5± 0.7 C4: not identified	32

Dosage forms	Formula details	Donor	Skin permeation evaluation		Ref
			Method	Results	
NE	Oil: Caprylic/capric triglycerine S: Oleth-3, Oleth-20 Water	150 µL	Human abdominal skin R: PBS (pH 7.4)	*Kp (cm/h) in 24 h* F3: 0.00005016 CAF sol: 0.0024	47
NLC	Lipids: Miglyol 812 (caprylic/ capric triglyceride), Precifac® ATO (palmityl palmitate) Surfactant: polysorbate 60	300 µL of formulation	Porcine ear skin R: HEPES buffer (zwitterionic sulfonic acid buffering agent)	CAF permeation in 8 h: NLC-CS: 2.5 x 10^7 µg/cm^2 CS extract: 2.0 x 10^7 µg/cm^2	48
Emulsion	O: Vaseline oil, cetearyl octanoate S: cetyl dimethicone copolyol, synperonic PE/F127® (poloxamer 407) Water, MgSO4.7H2O	1.25%; 260 mg/cm^2	Human abdominal skin R: PBS (pH 7.4)	*Kp (cm/h) in 24 h* O/W: 6.02 ± 0.16 x 10^4 W/O/W: 2.38 ± 0.2 x 10^4 Lag time (h) O/W: 16 ± 2 W/O/W: 18 ± 2 *Q_{24} absorbed (%)* O/W: 3.21 ± 0.18 W/O/W: 1.25 ± 0.17	49
Emulsion	Pickering emulsion (PE): Hydrophobic silica HDK H20, cyclomethicones DC®245, preservative, water Classical emulsion (CE): Abil® EM97 (cyclopentasiloxane), Abil® Wax 9810 (alkyl methicone), cyclomethicones DC®245, preservative, water	1 g of emulsion	Full thickness flank pigskin R: 0.9% NaCl aqueous solution	*Flux J (µg/cm^2/h) in 24 h* PE: 25 ± 4 CE: 9.7 ± 1.4 *Kp (cm/h) in 24 h* PE: 0.0030 ± 0.0005 CE: 0.0010 ± 0.0002 *Lag time (h)* PE: 0.5 ± 0.1 CE: 0.92 ± 0.08 *Q_{24} (µg/cm^2)* PE: 500 ± 60 CE: 223 ± 25	31

Emulsion	O/W: PEG-24 glyceryl stearate, glyceryl stearate, octyl stearate, kathon CG (preservative), cetylstearylic alcohol, paramethyl, glycerine, water	100 mg of emulsion	Human abdominal skin R: saline	*Flux J (µg/cm²/h) in 12 h* CAF: 0.2-1.6 *Kp (cm/h) in 12 h* CAF: Kp= 1.5-2.9 x 10^3 Lag time (h) CAF: 0.70-1.63	50
ME	O: Isopropyl myristate S: Labrasol (PEG-8 caprylic/capric triglycerine) CoS: Cremophor EL (polyoxyl 35 castor oil) Water	150 µL of formulation	Dermatomed abdominal porcine skin (500 µm thick) R: PBS (pH 7.4)	*Flux J (µg/cm²/h) in 24 h* ME: 5.11-11.63 Q_{24} *(µg/cm²)* ME: 91.79-237.79	51

Dosage forms	Formula details	Donor	Skin permeation evaluation		Ref
			Method	Results	
O/W emulsion W/O emulsion Hydrogel Solution	O/W emulsion: water, silicon oil, glycerin, almond oil, sorbitan tristearate, PEG-40 stearate, carbomer 950, triethanolamine, imidazolidinyl urea, methylparaben W/O emulsion: water, silicon oil, glycerin, almond oil, methyl glucose dioleate, cetyl dimethicone copolyol, imidazolidinyl urea Solution: water, ethanol, glycerine, almond oil, methyl glucose dioleate, imidazolidinyl urea Hydrogel: water, ethanol, carbomer 950, triethanolamine, imidazolidinyl urea, methylparaben	10mg/cm^2	Human abdominal skin (300-400µm thick) R: PBS containing 0.25% Tween 80	*Skin penetration rates(J) (µg/cm^2/h) in 24 h* O/W: 57x 10^4 ± 22 x 10^4 W/O: 84 x 10^4 ± 26.5 x 10^4 Hydrogel: 76 x 10^4 ± 25.6 x 10^4 Solution: 63.6 x 10^4 ± 32.9 x 10^4 *Cumulative amount (µg/cm^2) in 24 h* SC: O/W: 34 x 10^4 ± 15 x 10^4 W/O: 61 x 10^4 ± 30 x 10^4 Hydrogel: 54 x 10^4 ± 47 x 10^4 Solution: 36 x 10^4 ± 14 x 10^4 Epidermis: O/W: 107 x 10^4 ± 28 x 10^4 W/O: 164 x 10^4 ± 58 x 10^4 Hydrogel: 151 x 10^4 ± 37 x 10^4 Solution: 106 x 10^4 ± 21 x 10^4 Below epidermis: O/W: 1384 x 10^4 ± 519 x 10^4 W/O: 2033 x 10^4 ± 638 x 10^4 Hydrogel: 1832 x 10^4 ± 614 x 10^4 Solution: 1549 x 10^4 ± 796 x 10^4 Dermis/membrane: O/W: 18 x 10^4 ± 7 x 10^4 W/O: 24 x 10^4 ± 9 x 10^4 Hydrogel: 15 ± 6 x 10^4 Solution: 22 ± 9 x 10^4 % permeation: 15-20	29

Dosage forms	Formula details	Donor	Skin permeation evaluation		Ref
			Method	Results	
ME	O/W: Tween®21, isononyl isononanoate, water W/O: Tween®21, Span®20, isononyl isononanoate, water Bicontinuous: Tween®21, Span®20, isononyl isononanoate, water	1 g of formulation	Full thickness pigskin R: 0.9% NaCl aqueous solution	*Flux J (µg/cm²/h) in 24 h* O/W: 99 ± 14 W/O: 35 ± 10 Bicontinuous: 43 ± 5 Control: 32 ± 10 *Kp (cm/h) in 24 h* O/W: 0.012 ± 0.002 W/O: 0.004 ± 0.001 Bicontinuous: 0.0053 ± 0.0006 Control: 0.004 ± 0.001 *Lag time (min)* O/W: 35 ± 8 W/O: 52 ± 12 Bicontinuous: 48 ± 7 Control: 57 ± 9 *Q_{24} (µg/cm²)* O/W: 1538 W/O: 717 Bicontinuous: 1096 Control: 717	52

Dosage forms	Formula details	Donor	Skin permeation evaluation		Ref
			Method	Results	
Ointment	Four ointment bases [The new German Pharmacopoeia (DAB. 7)] Vaseline, aqueous woolwax alcohol, aqueous hydrophilic, polyethylene glycol	30 mg of ointment	Human skin R: saltwater solution	*Q in 1.67h (µg/cm²)* SC: 0.632-2.182 Epidermis: 0.137-0.508 Dermis: 0.056-0.667	53
Suspension	Vehicles: Labrasol® (LBS) (PEG-8 caprylic/capric triglycerine), Labrafil® (LBF) (glycolysed ethoxylated glycerides), Transcutol® (TSC) (diethylene glycol monoethyl ether), DPPG® (propylene glycol dipelargonate), propylene glycol (PG)	100 µL of formulation	Human breast skin R: saline	*Flux J (µg/cm²/h) in 24 h* PG: 0.698 ± 0.099 Water: 0.724 ± 0.041 TSC: 0.635 ± 0.197 LBS: 0.277 ± 0.057 LBF: 1.162 ± 0.085 DPPG: 2.278 ± 0.353 PG-DPPG: 2.193 ± 0.174 *Kp (cm/h) in 24 h* PG: 0.059 ± 0.033 Water: 0.048 ± 0.033 TSC: 0.032 ± 0.024 LBS: 0.034 ± 0.024 LBF: 0.049 ± 0.048 DPPG: 0.055 ± 0.019 PG-DPPG: 0.062 ± 0.024	33

Notes: R= receptor fluid; ME=microemulsion; NE=nanoemulsion; O= oil phase; S= surfactant; CoS= cosurfactant; PBS= phosphate buffer solution; Q=cumulative amount; ER= enhancement ratio; O/W= oil in water; W/O= water in oil

We adopted a semi-practical Quality by Design (QbD) framework for designing our CAF semisolid creams based nanoemulsion systems to understand the physicochemical properties of topical formulation ingredients and their vehicles to optimise the physical, chemical and skin delivery characteristics of the product. The formulation components, such as oils, surfactants, cosurfactants and other vehicles, may act as penetration enhancers and affect skin permeability. The International Conference on Harmonisation of Technical Requirements for Registration of Pharmaceuticals for Human Use (ICH) introduced Pharmaceutical QbD guidelines to guide quality management during drug development and production. Comprehensive implementation of Pharmaceutical QbD includes defining the quality target product profile (QTPP) and critical quality attributes (CQAs) of a drug product. QbD also encourages using tools such as the design of experiment (DOE), establishment of a control strategy, continual improvement and innovation throughout the product life cycle and accomplishment of risk assessment to identify critical material attributes (CMAs) and critical process parameters (CPPs).[54,55] Here, we defined a QTPP and identified several CQAs for topical nano-cream formulations that included good safety and compatibility profile, low skin irritancy, and adequate CAF solubility in water lipid-soluble, physically and chemically stable during storage, pH skin and with desired globule size.

In this current study, we developed nanoemulsions in the form of creams stabilised by emulsifiers via the hot emulsification method combined with energy input and evaluated their properties including skin penetration/permeation of CAF within nano-sized.

2.1.1 Objectives of the study

The overall objective of the present study was to prepare a CAF-loaded nanoemulsion based semisolid using the QbD approach and formulate them as a suitable cosmeceutical cream for enhanced anticellulite and skin permeability in cellulite treatment. A desired future outcome was to facilitate better skin rejuvenation, particularly improvement in cellulite appearance.

The specific objectives of the study were:

1. To develop and validate an HPLC assay for CAF determination and extraction from skin tissues.
2. To develop semisolid nano-cream formulations fabricated with different chemical penetration enhancers (CPEs) for skin delivery of CAF.

3. To characterise the physical properties of the CAF nano-cream formulations.
4. To assess the effects of various CPEs on penetration/permeation of CAF into and through the skin.

2.2 Experimental design

2.2.1 Materials

CAF of analytical grade (CAS# 58-08-2 (C0750) with 99% purity level), isopropyl myristate (IPM;CAS# 110-27-0), and butylated hydroxytoluene (BHT;CAS# B-1378) were purchased from Sigma-Aldrich (North Ryde, NSW, Australia). Cetearyl alcohol (stearyl alcohol and cetyl alcohol) (stearyl alcohol: CAS# 112-92-5; cetyl alcohol: CAS# 36653-82-4), ceteareth-20 (CAS# 68439-49-6), and dimethicone 350 CST (CAS# 9006-65-9) were purchased from New Directions Laboratory (Marrickville, NSW, Australia). Lanolin USP anhydrous (CAS# 8006-54-0) was purchased from PCCA (Matraville, NSW, Australia). Extra virgin olive oil (CAS# 8001-25-0) and optiphen™ plus (phenoxyethanol, caprylyl glycol and sorbic acid) (phenoxyethanol: CAS# 122-99-6; caprylyl glycol: CAS# 1117-86-8; sorbic acid: CAS# 110-44-1) were purchased from Range Products (Welshpool, WA, Australia). DL-alpha-tocopheryl acetate (CAS# 7695-91-2) was purchased from Australian wholesale oils (Rydalmere, NSW, Australia). Triethanolamine (CAS# 102-71-6) and ethylene diamine tetra-acetic acid (EDTA) (CAS# 139-33-3.) were purchased from BDH Laboratory Supplies (Poole, Dorset, UK) distributed by Merck Pty Ltd. (Kilsyth, Victoria, Australia). Carbopol® 940 (CAS# 9003-01-4) was a gift from Lubrizol International Inc. (Silverwater, NSW, Australia). Propylene glycol BP (CAS# 57-55-6) was purchased from PharmAust Manufacturing (Malaga, WA, Australia). Transcutol® P (diethylene glycol monoethyl ether-CAS# 111-90-0) were kind gifts from Gattefossé (Saint-Priest, France). Veet™ hair removal cream (containing potassium thioglycolate) was purchased from Reckitt Benckiser Pty Ltd. (Sydney, NSW, Australia) Methanol HPLC grade and hexane was from Fisher Chemical (USA), deionised water-passed through a Milli-Q RC apparatus (Millipore Corporation, Bedford, MA, USA). PBS (pH 7.4) (phosphate-buffered saline solution) was prepared by dissolving 8.0 g NaCl, 0.2 g KCl, 1.44 g Na2HPO4, and 0.24 g KH2PO4 into 1-liter deionised water and adjusting for pH 7.4 with 0.1 N potassium hydroxide. Potassium chloride and sodium chloride were purchased from Chem-Supply Australia Pty Ltd. Potassium dihydrogen orthophosphate was purchased from Thermo

Fisher Scientific (Scoresby, Australia). Di-sodium hydrogen orthophosphate anhydrous was purchased from Merck Pty Ltd. (Bayswater, VIC, Australia). Ultra cellulite cream (containing CAF 2% with shea butter cream base) was purchased from Green Organics (LOT #CO91633) (Salt Lake City, UT, USA).

2.2.2 HPLC analysis method validation

An HPLC method was developed to analyse CAF in pharmaceutical formulations and extraction of CAF from skin tissues.

The Agilent™ 1200 series HPLC system used consisted of:

1. Automated injection system/autosampler (Agilent™ G1329A, Serial No. DE64765738)
2. Binary pump (Agilent™ G1312A, serial no. DE63058944)
3. Solvent degasser (Agilent™ G1379B, serial no.JP73107188)
4. Multi-wavelength (MWD) detector (Agilent™ G1365B, serial no. DE63055930)
5. Chemstation Rev B.04.03-SP1 software (Agilent Technologies Inc., Waldbronn, Germany)

The HPLC system conditions were adapted from Naegele[56], with some modifications as outlined in Table 2.3

Table 2.3 HPLC instrument system set-up

System set up	Description
Stationary phase	Phenomenex® C18 5 µm column, 150 mm x 4.6 mm
Security guard cartridge	Phenomenex® C18, 4 x 3 mm
Mobile phase	Isocratic methanol: water = 30:70
Flow rate	1 mL/min
CAF detection	λmax = 272 nm
Retention time	3.4 ± 0.1 min
Total analysis time	6 min

2.2.2.1 Linearity

Linearity was assessed by a series of CAF concentrations (20, 10, 1, 0.5 and 0.025 µg/mL) with serial dilution. A stock solution of 500 µg/mL was made by dissolving 25 mg of CAF in 50 mL of a mixture of methanol (MeOH) and PBS (pH 7.4) (50:50). Linearity was calculated by the R-squared value.

2.2.2.2 System suitability test

Precision

CAF solutions at three concentrations (20, 1, 0.025 µg/mL) were analysed in six replicates for each concentration. Relative standard deviation (RSD) values were calculated for all concentrations. The acceptable RSD was < 5%.[57]

Sensitivity

The blank solvent, a mixture of MeOH: PBS (50:50), was injected six times with an analysis time of 6 min for each injection. The noise to peak ratio was calculated by dividing the standard deviation of the blank with the slope of the peak height of the calibration curve. The limit of detection (LOD) and limit of quantification (LOQ) was determined as three times and ten times the baseline noise level in the assay, respectively. LOD and LOQ were estimated using the following equations:

$$LOD = 3x \frac{average\ SD\ of\ noises}{slope\ of\ peak\ heights\ vs\ standard\ concentration} \quad (1)$$

$$LOQ = 10x \frac{average\ SD\ of\ noises}{slope\ of\ peak\ heights\ vs\ standard\ concentration} \quad (2)$$

Accuracy

A mass balance study of CAF extraction from the piglet skin was carried out to assess the assay's accuracy and validate the IVPT protocol. The purpose of this experiment was the recovery of CAF skin extraction. Briefly, a pre-weighed section of skin tissue was soaked in 5 mL of 20,000 µg/mL CAF in PBS (pH 7.4) solution in a water bath (Clifton, NE2-22D, Nickel-Electro Ltd., North Somerset, England), and stirred by magnetic stirring at 600 rpm/min at 35°C. After 8h immersion, the skin surface was touched dry with Kimwipes® (Kimtech Science, Kimberly-Clark Professional, Milsons Point, Australia). The skin was then sectioned prior to the CAF extraction using a solvent extractor (a mixture of PBS (pH 7.4) and MeOH). The extraction was stirred for 2h at ambient temperature. The CAF in the remaining donor, wash, and skin extraction was determined using the HPLC assay described above.

2.2.3 CAF-loaded nano-cream formulations development

Eight CAF-loaded nano-cream formulations were prepared as per the compositions outlined in Table 2.4. CAF nano-creams were prepared by a hot emulsification process based on Wojciechowska et al.[58] with some modifications. The aqueous and oily phases were heated separately until reaching 70°C. All oil-soluble ingredients (phase A) were melted at 70°C, whereas all aqueous-soluble ingredients (phase B), including CAF 2% (w/w) concentration, were dissolved in water at 70°C. Subsequently, phase A was added to phase B, stirred with a homogeniser (Heildoph, DIAX 900, Germany) at 8000 rpm (speed no. 1) for 15 min to form an emulsion, then continuously stirred until the temperature reduced to 50°C. Optiphen plus® (preservative) and DL-alpha-tocopheryl acetate were then added with homogenisation at 8000 rpm for 15 min to obtain a smooth and uniform consistency. Finally, the drop-wise addition of triethanolamine was adjusted to reach the pH suitable for skin application at ~5.0 (MColorpHast, Darmstadt, Germany). The emulsion was allowed to cool down to room temperature. All processes were conducted at room temperature. All CAF creams were stored at room temperature until time of further physical and chemical evaluations.

2.2.4 Physical evaluation of topical creams

As detailed below, CAF creams were physically characterised in appearance (visually organoleptic), pH in cream and pH in the aqueous phase separation, globule size, and rheological properties.

2.2.4.1 Organoleptic characteristics

After preparation, all CAF nano-cream formulations were tested for appearance, colour, consistency, homogeneity, phase separation, and texture at room temperature. Homogeneity and texture were tested by pressing a small quantity of the formulated cream between the thumb and index finger. The consistency of the formulations and the presence of coarse particles were used to evaluate the homogeneity and texture of the formulations. These characteristics were assessed by visual observation.[59,60]

2.2.4.2 pH measurement

The pH of each cream was tested immediately after preparation with pH test strips at ~5.0 (McolorpHast, Darmstadt, Germany). The pH of the cream was further determined accurately

using a calibrated benchtop pH meter (HI 8519 N; Hanna Instruments, Woonsocket, RI, USA). Similarly, after cooling down, the creams were separated using high-speed centrifugation (model: Optima XE-100; rotor type: 70.1 Ti; Beckman Coulter Inc., CA, USA) at 55,000 rpm for 4h, then the separated aqueous phase was measured using a calibrated pH meter.

Table 2.4 Composition and formula CAF topical creams (all as % w/w)

INCI Name	Formula							
	LAN	**PG5**	**PG10**	**TR5**	**TR10**	**CA**	**CB**	**CC**
Phase A								
Cetearyl alcohol	3	3	3	3	3	3	3	3
IPM	1	1	1	1	1	1	1	1
Lanolin anhydrous	2	-	-	-	-	2	2	2
Dimethicone 350 CST	1	1	1	1	1	1	1	1
BHT	0.05	0.05	0.05	0.05	0.05	0.05	0.05	0.05
Extra virgin olive oil	3	3	3	3	3	3	3	3
Ceteareth-20	2	2	2	2	2	2	2	2
Phase B								
Propylene glycol	-	5	10	-	-	5	-	5
Carbopol®-940	0.15	0.15	0.15	0.15	0.15	0.15	0.15	0.15
EDTA	0.1	0.1	0.1	0.1	0.1	0.1	0.1	0.1
CAF	2	2	2	2	2	2	2	2
Transcutol® P	-	-	-	5	10	-	5	5
Others								
Optiphen plus®	0.75	0.75	0.75	0.75	0.75	0.75	0.75	0.75
DL-alpha-tocopheryl acetate	0.5	0.5	0.5	0.5	0.5	0.5	0.5	0.5
TEA	qs	qs	qs	qs	qs	qs	qs	qs
Aqueous ad	100	100	100	100	100	100	100	100

INCI Name= International Nomenclature of Cosmetic Ingredient; ad=up to; qs= quantum satis (quantum sufficit / as much as is sufficient); CST= centistokes; IPM= isopropyl myristate; BHT= butylated hydroxytoluene; EDTA= ethylenediaminetetra-acetic acid; CAF= caffeine; TEA= triethanolamine; CPE= chemical penetration enhancer.

Cream base containing CAF with the addition of CPE: LAN= lanolin; PG5= propylene glycol 5%; PG10= propylene glycol 10%; TR5= transcutol 5%; TR10= transcutol 10%; CA= combination A-lanolin propylene glycol 5%; CB= combination B-lanolin transcutol 5%; CC= combination C-lanolin transcutol propylene glycol 5%.

2.2.4.3 Globule size

The globule size distribution of the CAF-loaded nano-cream formulation was determined by photon correlation spectroscopy (PCS) using a Zetasizer Nano™ ZSP (Malvern, UK) following 100 times dilution with deionised water to avoid multiple scattering.[61]

2.2.4.4 CAF in the aqueous phase of the creams

The distribution of solubilised CAF in the aqueous phase was determined by a phase separation study using ultra-centrifugation (Optima XE-100, type 70.1 Ti rotor, Beckman Coulter Inc., CA, USA) at 55,000 rpm for 4h. The saturation solubility of CAF was evaluated by adding an excess amount of CAF to each of the separated aqueous phases, then subsequently stirred at 1000 rpm/min for 24h at room temperature and then centrifuged at 15rcf (~ 12.7 rpm) for 10 min. The supernatant was diluted with PBS (pH 7.4) solution followed by HPLC analysis. The amount of CAF in the separated aqueous phase was determined by HPLC analysis.

2.2.4.5 Viscosity and rheological properties

All rheological tests were performed with an AR-G2 rheometer (TA Instruments®, New Castle, DE, USA) equipped with a Peltier stage for controlling temperature and fitted with parallel plate geometry (d= 40mm). A Peltier stage and geometry were covered with adhesive-backed 180 grit sandpaper to avoid wall slippage and prevent erroneous measurement with poor reproducibility.[62] The sample volume of 1000 µL was loaded on the Peltier stage and the geometry was set at 500 µm height. Any excess amount of sample that protruded beyond the geometry area was carefully removed. A pre-shear of the sample was performed at the shear rate of 1 s^{-1} for 1 min, followed by 2 min of equilibration without any shear. The fresh nano-cream formulations were analysed by employing the steady-state flow sweep and oscillatory amplitude sweep tests. Measurements were made in triplicate and at 32°C (physiological condition).

<u>Shear stress flow sweep</u>

The flow sweep test was performed to measure the apparent viscosity as a function of shear stress. The shear stress was set to increase logarithmically from 0.1 to 1000 Pa with measurements made at 10 points per decade in log mode.

Shear strain amplitude sweep

The amplitude sweep experiment was performed at 1 Hz, varying the strain amplitude from 0.01 to 1000%. An elastic or storage modulus (G′) and a viscous or loss modulus (G″) were plotted on a logarithmic scale.

2.2.5 *In vitro* penetration/permeation test (IVPT)

2.2.5.1 Skin source and preparation

Piglet skin is a good model for human skin surrogates because of physiological and anatomical similarities.[63-65] Stillborn piglets were collected from routine vet visits to a local pig farm and made available within 24h. No ethical approval was required. Full-thickness skin was obtained from the piglet body and extraneous fat tissues were carefully removed by a surgical scalpel blade (no. 21). Hairs were removed using Veet® depilatory cream (Reckitt Benckiser Pty Ltd., NSW, Australia) applied for 10 min, followed by gentle scraping with a curved spatula. This method had been previously validated on pig skin by our group.[63] The skin was then rinsed thoroughly with PBS at pH 7.4 to remove any further cream, dried, wrapped in aluminium foil, packed in a polyethylene bag, and stored at -20°C until use.

2.2.5.2 IVPT experimental design

Experimental setup

For each experiment, three different piglet skin donors were used to provide 6-9 replications. Full-thickness excised skin was defrosted at room temperature immediately before each experiment and cut into suitable sized circles for mounting in the Franz cells. Skin thickness was measured by a digital vernier calliper (Model K11100, Kincrome Australia Pty Ltd., Scoresby, Australia). The skin was mounted between the donor and receptor compartments of a vertical Franz diffusion cell with the stratum corneum (SC) side facing the donor and clamped (Figure 2.2). Skin barrier integrity testing was conducted by measuring the electrical resistance using a digital multimeter (UNI-T®, UT58 series, Opava-Předměstí, Česko). In brief, PBS solution was placed in the donor and receptor compartments and allowed to equilibrate in the water bath at 35°C for 20 min. One probe of the multimeter was inserted via the arm into receptor fluid, and the other was applied to the donor solution. Skin was included that had resistance between 1 MΩ and 50 kΩ.[66] The PBS solutions in the donor compartment was discarded and the skin surface was dried by delicately wiping with tissue (Kimtech Science

Kimwipes®, Kimberly-Clark Professional, Milsons Point, Australia). A magnetic stirrer was added to the receptor compartment and continuously stirred at 600 rpm/min. The cells were maintained in a water bath system at 35°C to provide a skin surface temperature of 32°C.[67] Two hundred milligrams of nano-cream formulations, marketed CAF product or CAF in aqueous solution (control) was applied to the donor compartment and sealed with parafilm M® Laboratory Film (Greenwich, Connecticut, USA). Samples (total receptor fluid volume) were withdrawn from the receptor compartment at six-time points (0.5, 1, 2, 4, 6, and 8h) and immediately replaced by fresh pre-warmed receptor solution (total replacement). The experimental protocol is summarised in Table 2.5. Receptor samples (500 µL) were placed in an eppendorf vial, 500 µL MeOH added, vortex mixed at 600 rpm for 5 min, then centrifuged at 15,000 rcf for 10 min at 25°C, prior to HPLC analysis for CAF content.

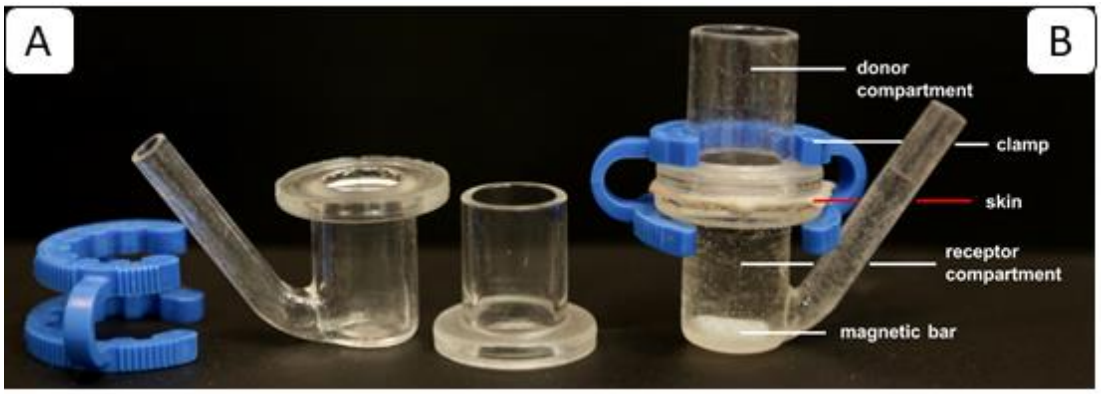

Figure 2.2 Franz diffusion cell set up: (A) disassembled (B) assembled cell

Skin distribution study

After completing the 8h experiment, the remaining cream in the donor compartment was transferred to a volumetric flask and made up to 20.0 mL with PBS. 0.5 mL taken from the first volumetric flask was diluted to 20.0 mL with PBS in the second volumetric flask. At the final, CAF was separated from the remaining oil phase by adding 1.0 mL hexane (HXN) with equal volume. Glass Pasteur pipettes removed CAF from the bottom line of two immiscible liquids. HPLC then determined the concentration of CAF in the remaining donor.

A tape stripping process was conducted to assess the amount of CAF on the SC. After transferring the remaining cream from the donor, the skin was washed to remove any remaining formulation (washing fluid retained and then combined with mass balance calculation). The skin surface was gently dried with Kimwipes® and treated to separate the SC and remaining skin tissue E+D+F (epidermis/dermis/follicle). To obtain the drug in SC, D-

Squame® adhesive tapes with a diameter of 22 mm (CuDerm, Dallas, TX, USA) were applied on the skin surface with a D-Squame disc® applicator based on the method of Davies et al. with modification.[68] A total of 10 tape strips were used; the first two strips were assumed to include unabsorbed CAF, and the remaining 8 tapes absorbed into the SC. The tapes were soaked in 2 mL of PBS: MeOH 50:50 mixture, vortex mixed for 5 min, and the soaking solution then centrifuged at 15,000 rcf for 10 min at room temperature. The remaining skin was cut into pieces and weighed. CAF was extracted by soaking in a solution mixture (PBS: MeOH = 50:50) with the aid of magnetic stirring (600 rpm/min) for 2h at ambient temperature. The supernatant fluid was collected, centrifuged to precipitate any fatty tissue and CAF content analysed by HPLC.

Table 2.5 Experimental setup conditions of *in vitro* penetration/permeation study

System set up	Description
Membrane type	Full-thickness of newborn piglet skin
Skin surface diameter	1.2-1.3 cm^2
Volume receptor	3-3.5 mL
Receptor fluid	PBS (pH 7.4) : MeOH = 50:50
Initial dose donor	200 mg cream base contained 4 mg of CAF or either 2% CAF in aqueous solution
Water-bath temperature	35°C (equal to the body skin temperature of 32°C)
Stirring flow rate	600 rpm
Duration of incubation	8 hours
Sampling time-points	0.5, 1, 2, 4, 6, 8 hours
Sampling type	Total volume replacement

2.2.6 Stability

The stability of CAF creams was determined over 4 months of storage at room temperature (± 60% relative humidity) to indicate the stability of CAF in the nano-cream formulations. Physical appearance and the CAF content were determined after storage at 22-25°C in cream containers.

2.2.7 Data analysis

CAF in receptor solution was plotted as the cumulative amount of CAF permeated through the skin (µg/cm^2) versus time (h) for all applied formulations. This data was used to determine the permeability parameters as outlined below:

Steady-state flux

Flux is defined as the diffusion rate or transport of a substance across a permeable membrane. After drug permeation has reached a steady-state, the steady-state flux (*Jss*) (µg/cm^2/h) was calculated using the following equation:

$$Jss = \frac{dQ}{dt} = \frac{DAKC}{h} \quad (3)$$

Q cumulative amount *(*µg/cm^2)
D diffusion coefficient of permeant in the skin
A diffusional area
K partition coefficient between SC and the vehicle
C applied concentration of permeant
h diffusional path length

Permeability coefficient

The permeability coefficient through the membrane *(Kp) (cm/h)* was determined according to the following equation:

$$Kp = \frac{Jss.H}{Co} \quad (4)$$

H thickness of membrane *(cm)*
Co initial drug concentration *(µg)*

Lag time

Lag time is the initial time of CAF permeated to the skin. Lag time (*t*) is calculated based on the linear portion of graph of the cumulative amount/area vs time (y=0) as:

$$Lag\ time = \frac{-(intercept\ of\ the\ graph)}{slope} \quad (5)$$

Enhancement ration (ER)

This factor was calculated to find the relative enhancement in the flux of formulations in respect to the reference enhancement ratio. The enhancement ratio was estimated according to the following equation:

$$ER = \frac{Jss\ formulation}{Jss\ reference} \quad (6)$$

Total mass balance was the accumulation of CAF remaining in donor solution, CAF passed through the receptor, CAF obtained from tapes stripping and CAF recovered from skin tissue extraction.

2.2.8 Statistical analysis

All experiments were carried out in triplicate. The data are expressed as mean ± SD (non-biological related measurements) and mean ± SEM (biologically related measurements). All data were analysed using GraphPad Prism™ 9 software (Graphpad Software Inc., CA, USA), using two-way ANOVA with Tukey post hoc test. Data were considered to be statistically significant if $p < 0.05$.

2.3 Results

2.3.1 HPLC analytical method

The HPLC method provided a single CAF peak for the stock solution and good separation from any skin sample-related peaks. The CAF peak retention time was 3.4 ± 0.1 min in a total analysis time of 6.0 min (Figure 2.3), with no interference from any other peaks regardless of sample origin.

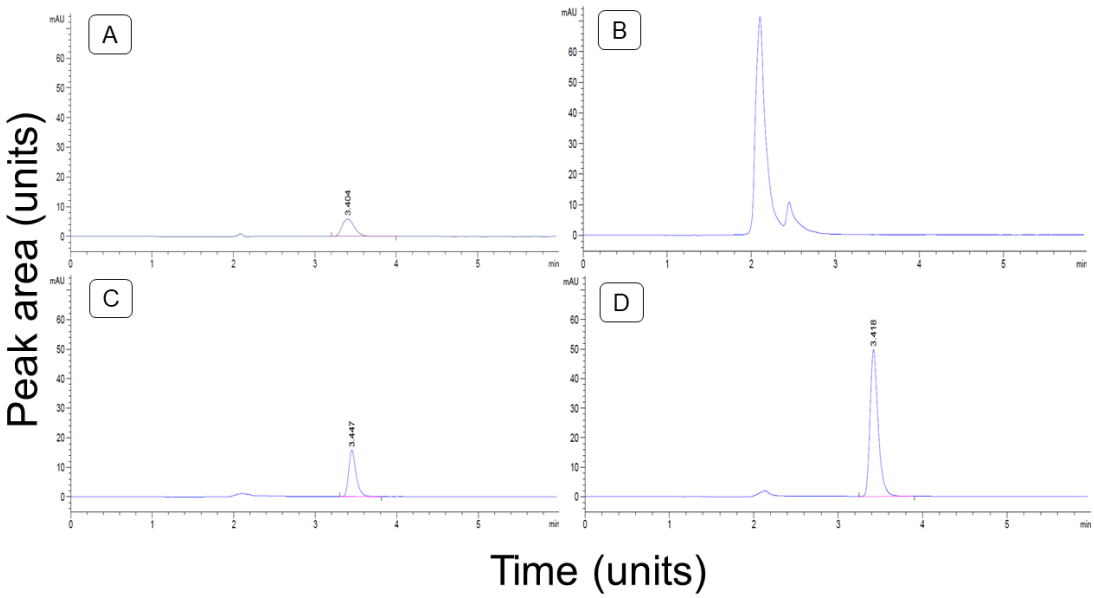

Figure 2.3 HPLC chromatograms (peak area versus time) of (A) 1 µg/mL CAF solution as prepared for the calibration curve; (B) LAN formulation matrix without CAF; (C) LAN formulation matrix with CAF incorporated; (D) Skin extract following administration of LAN formulation with CAF incorporated in IVPT experiment.

This analytical method validated linearity and range and system suitability testing (precision, sensitivity and accuracy).

Linearity

The analytical calibration curve constructed for CAF was linear in the range 0.025-20 µg/mL (R^2= 0.9999: Figure 2.4).

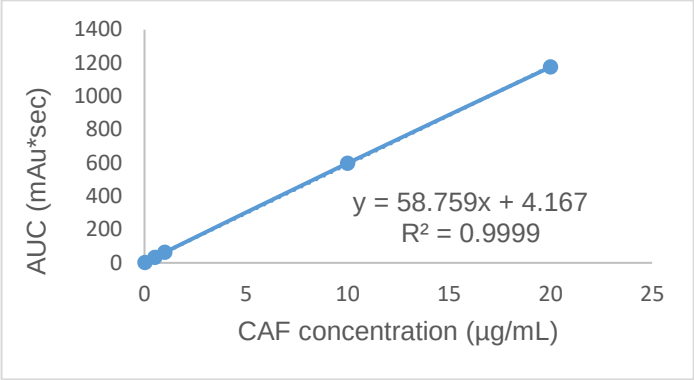

Figure 2.4 Representative of CAF calibration curve

Sensitivity

The LOD and LOQ for determination of CAF, calculated by injecting samples and blank solution six times, were 6.5 ng/mL and 21.6 ng/mL, respectively.

Assay precision

The coefficient of variation precision parameters calculated from the RSD (*n* = *6*) is presented in Table 2.6. The acceptability criterion of precision repeatability has been fulfilled with RSD. < 5% in the high, medium, and low concentrations.

Table 2.6 Precision of CAF assay (mean ± SD; *n*=6)

	CAF concentration		
Concentration (µg/mL)	0.025	1	20
RSD (%)	0.43	0.42	0.32

Table 2.7 Mass balance study of CAF skin extraction (mean ± SD; *n*=3)

Initial donor (µg)	Distribution of CAF (µg)			Total distribution (µg)	Recovery (%)
	Remaining donor	Wash	Skin extraction		
103033.67 ± 5.38	94955.71 ± 778.76	1746.91 ± 201.59	3760.57 ± 0.97	100463.19 ± 838.92	97.51 ± 0.81

Accuracy

Results for CAF recovery from the skin tissue are shown in Table 2.7. The mass balance recovery of CAF was the percentage of CAF recovered (adding the amount of CAF recovered

in the remaining donor, wash liquid and skin extraction liquid) divided by CAF added in the initial donor. The percent recovery of CAF was 97.51 ± 0.81 %.

2.3.2 CAF-loaded nano-cream formulations

All nano-cream formulations were successfully formulated based on the oily and aqueous phases using a hot emulsification process and a combination of the homogenizer. CAF-loaded nano-cream formulations showed stable systems with a suitable consistency for topical application. All nano-cream formulations containing CAF that were fabricated were white pearl opaque and their physical characteristics are described in section 2.3.3.

2.3.3 Physical characteristics of CAF nano-cream formulations

2.3.3.1 Organoleptic and other characterisations

Visually, all nano-cream formulations had a gleaming and lustrous tone of white pearl. In comparison, the marketed 2% CAF cream was opaque ivory-goldish. At ambient temperature, they were homogenous, smooth in texture, easily washable and did not form a greasy film on the skin upon application. All creams were easily spreadable on the skin. There was no phase separation in any nano-cream formulations when observed immediately after manufacturing nor during long-term storage (4 months) at room temperature. The globule size ranged from 297.40 ± 5.60 to 470.73 ± 48.29 nm (Table 2.8). The globule size of LAN was slightly larger than that of TR5 (Table 2.8). The pH of all nano-cream formulations was less than 6, bringing them close to the pH range of the skin. Whilst the aqueous phase pH was in the range of 5.55 to 5.98 (Table 2.8).

The physical appearance, pH, globule size of CAF nano-cream formulations measured prior to IVPT is displayed in Table 2.8.

2.3.3.2 Solubility of CAF in nano-cream formulations

Table 2.9 shows the thermodynamic activity of CAF in the cream products. The initial degree of saturation of CAF in the aqueous phase was lowest for PG10 and highest was LAN. The amount of CAF in the aqueous phase was similar across all the formulations, ranging from 18.59 ± 0.03 to 20.54 ± 0.02 (Table 2.9).

Table 2.8 Physical characteristics of CAF creams (mean ± SD; *n* = 3)

Formula	Physicochemical evaluation								
	Appearance	Colour	Consistency	Homogeneity	Phase separation	Texture	pH		Globule size (nm)
							cream	aqueous phase	
Marketed CAF	Opaque	Ivory-goldish	Excellent	Homogenous	No	Smooth	6.84 ± 0.02	6.81 ± 0.01	> 1000
LAN	Opaque	White pearl	Excellent	Homogenous	No	Smooth	5.64 ± 0.01	5.55 ± 0.01	425.00 ± 5.37
PG5	Opaque	White pearl	Excellent	Homogenous	No	Smooth	5.36 ± 0.02	5.57 ± 0.01	461.00 ± 4.91
PG10	Opaque	White pearl	Excellent	Homogenous	No	Smooth	5.59 ± 0.01	5.75 ± 0.01	470.73 ± 48.29
TR5	Opaque	White pearl	Excellent	Homogenous	No	Smooth	5.71 ± 0.02	5.65 ± 0.02	297.40 ± 5.60
TR10	Opaque	White pearl	Excellent	Homogenous	No	Smooth	5.85 ± 0.03	5.79 ± 0.01	380.10 ± 4.70
CA	Opaque	White pearl	Excellent	Homogenous	No	Smooth	5.66 ± 0.01	5.59 ± 0.01	331.60 ± 15.00
CB	Opaque	White pearl	Excellent	Homogenous	No	Smooth	5.61 ± 0.02	5.67 ± 0.01	332.03 ± 30.65
CC	Opaque	White pearl	Excellent	Homogenous	No	Smooth	5.91 ± 0.01	5.98 ± 0.01	350.73 ± 0.46

Marketed CAF: commercial topical containing the same amount (2%) of CAF

Table 2.9 Solubility of CAF observed in eight nano-cream formulations (mean ± SD; *n* = 3)

Parameter	LAN	PG5	PG10	TR5	TR10	CA	CB	CC
Amount of CAF in the aqueous phase (mg/g)	20.54 ± 0.37	20.25 ± 0.07	18.75 ± 0.04	18.96 ± 0.02	18.53 ± 0.02	20.13 ± 0.04	18.59 ± 0.03	18.65 ± 0.03
Saturation solubility of CAF in the aqueous phase (mg/g)	23.00 ± 0.01	23.81 ± 0.02	25.47± 0.04	21.99 ± 0.04	21.15 ± 0.07	23.87 ± 0.12	23.22 ± 0.03	24.82 ± 0.03
Initial degree of saturation	0.89	0.85	0.74	0.86	0.88	0.84	0.80	0.75

2.3.3.3 Viscosity and rheological properties

Shear stress flow sweep rheograms (Figure 2.5) show the viscosity profiles observed for the CAF nano-cream formulations under controlled steady-state incremental shear stress mode conditions at 32°C. All rheogram profiles exhibited low shear plateau, shear-thinning behaviour (pseudoplastic flow above the yield stress) and high-shear viscosity regions. As the shear stress approached zero, viscosity showed a plateau. The zero shear viscosity value was determined by extrapolating the low-shear plateau to zero shear stress (Table 2.10). As the stress increased toward critical stress (referred to as yield stress), the viscosity started to reduce by several orders of magnitude, where shear-thinning arose from an irreversible breakdown or an alteration of the semisolid microstructure. The observation was carried out in triplicate. The semisolid started to flow above the critical stress. The marketed CAF curve showed the highest zero shear viscosity (144601 ± 17612 Pa.s), whilst TR5 formulation showed the lowest (4997 ± 760 Pa.s) (Table 2.10, Figure 2.5). Furthermore, the marketed CAF also showed the highest yield stress (92.35 Pa), whereas TR5, CA and CC nano-cream formulations showed comparable yield stress of 4 Pa (Table 2.10, Figure 2.5).

Figure 2.6 shows the dynamic modulus curves of all creams analysed through an oscillatory rheological test. At low strain amplitudes, the elastic (G′) and the viscous (G″) modulus formed a constant plateau region known as the linear viscoelastic (LVR) range. The LVR region indicates the range in which the test can be carried out without destroying the structure of the cream itself. The values of G′ and G″ in the LVR region indicated the viscoelastic character of the creams. Practically, G′ values in the LVR region represent the stiffness of the product. For all creams analysed, G′ was higher than G″ in the LVR, revealing a dominating elastic character of the products at the low strain range; thus, the products have a solid structure. The difference between the plateau G′ and G″ (crossover) for the marketed product was substantially lower than one decade compared to the gap observed in the remaining creams approximating less than one decade (less than ten times). The marketed product showed high viscosity and elastic modulus (G′). These attributions showed the product was significantly stiffer than other nano-cream formulations. The flow index value of the marketed product was smaller (less than 1), indicating that the marketed product may exhibit brittle breakdown and cohesive resistance to spreading onto the skin surface during application.

As the controlled strain is continuously ramped, it deviates from the LVR region at a specific strain or stress value, called the limiting value of LVR. The linearity limit, calculated using the strain as a percentage, is also referred to as the yield point beyond which the structure undergoes irreversible deformation. After that, the structure began to collapse drastically, and a transition from G′ > G″ to G″ > G′ occurred. The crossover point of G′ and G″ during this transition process is called the flow point (G′ = G″), beyond which the product behaved as a viscoelastic liquid. In the region between the yield point and flow point, G′ > G″ (yield zone), the initial structural strength of the LVR region decreased (Table 2.10). However, the sample still predominantly displayed the properties of elastic solid matter (Figure 2.6).

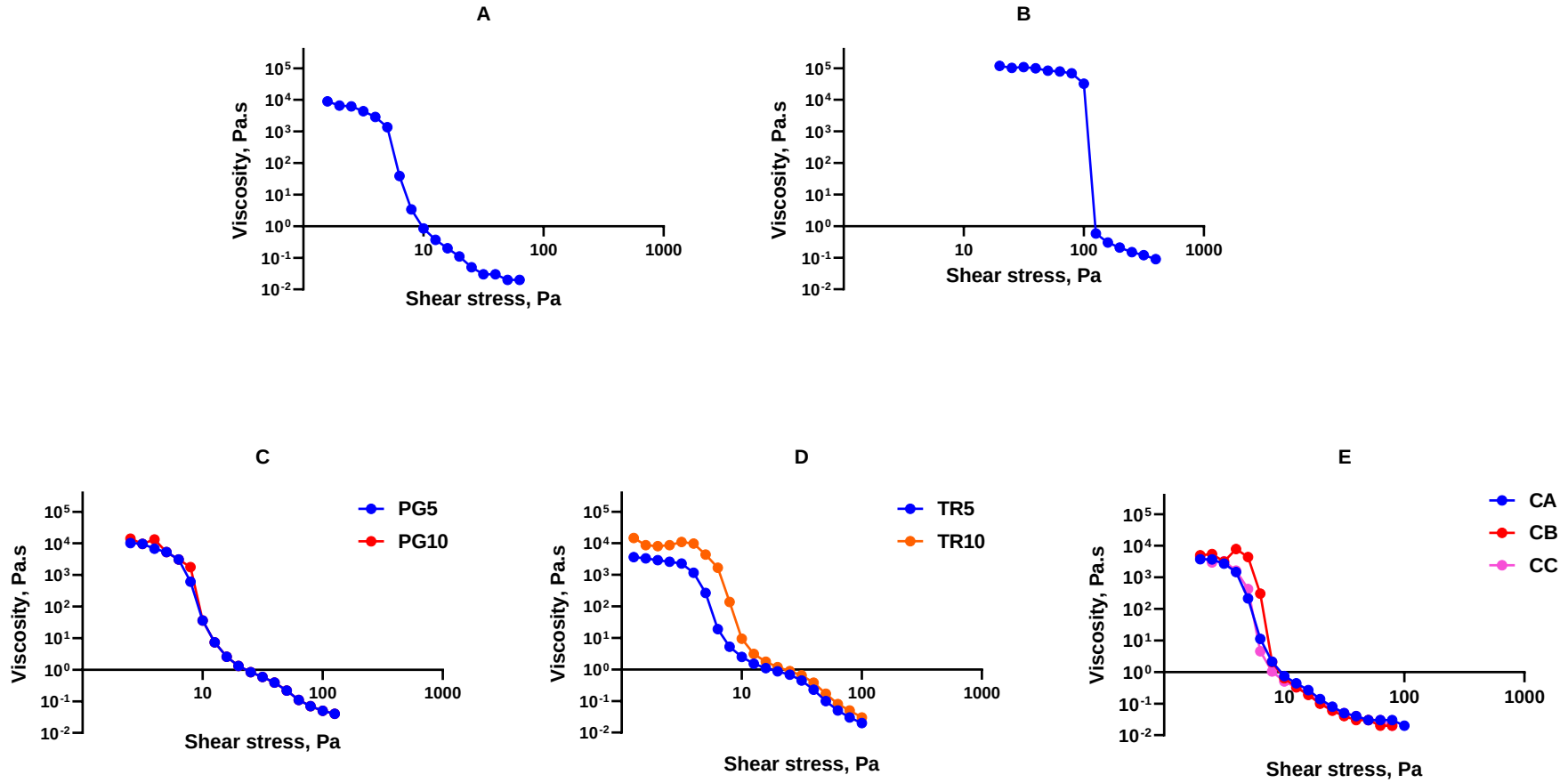

Figure 2.5 Viscosity flow sweep rheograms in CAF nano-cream formulations. (A) LAN; (B) Marketed; (C) PG5 and PG10; (D) TR5 and TR10; (E) CA, CB and CC nano-cream formulations

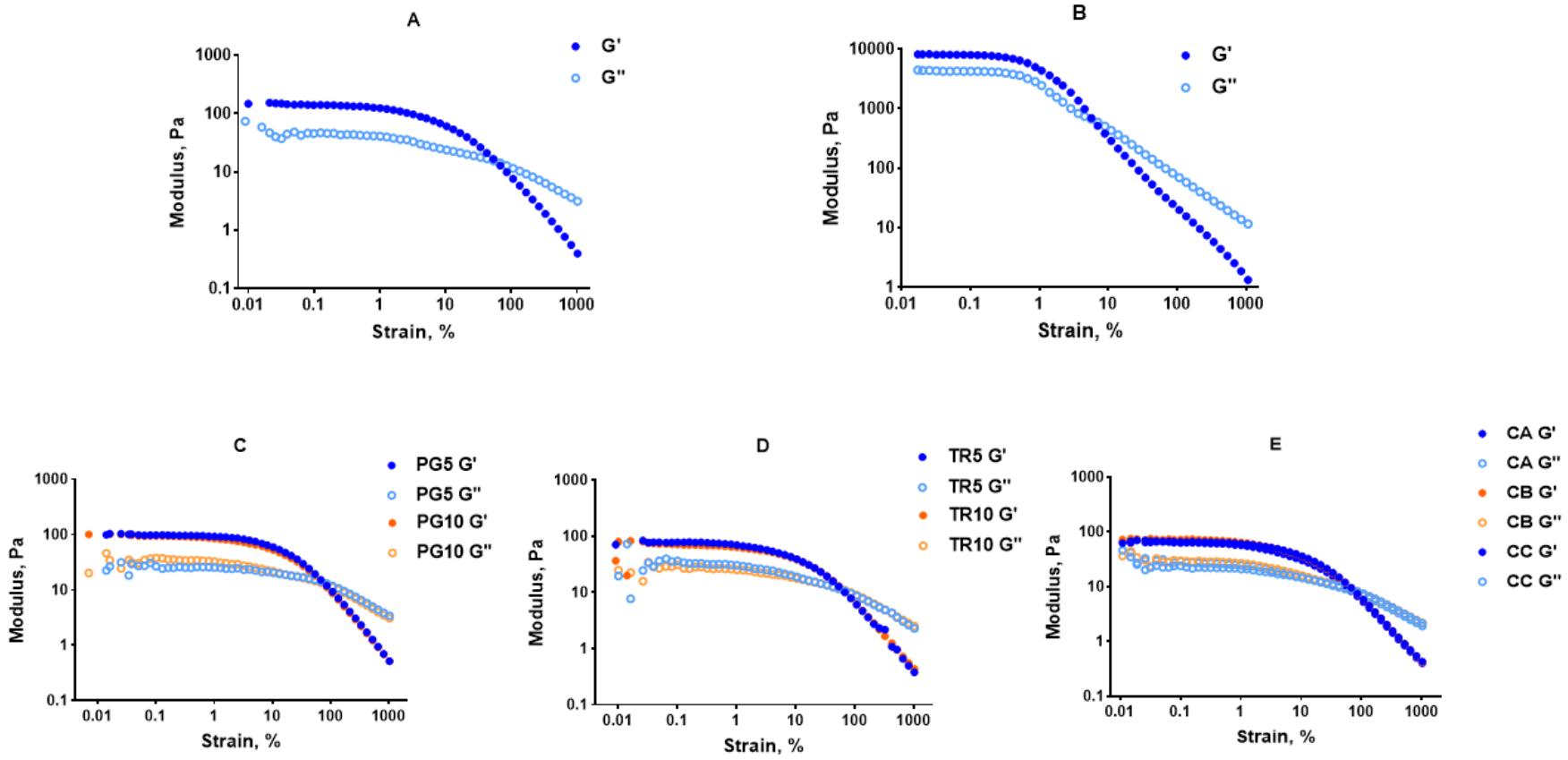

Figure 2.6 Elastic modulus (G′) and the viscous modulus (G″) curves with percent strain of CAF nano-cream formulations. (A) LAN; (B) Marketed; (C) PG5 and PG10; (D) TR5 and TR10; (E) CA, CB and CC nano-cream formulations

Table 2.10 Rheological properties of CAF creams derived through controlled shear stress flow sweep

Sample	Rotational rheology parameters		Oscillatory rheology parameters				
	Zero shear viscosity	Yield stress	Plateau G′	Yield stress	Yield point strain	Flow point strain	Flow transition index
	η_0 (Pa.s)	σ_0 (Pa)	(G'_P) (Pa)	σ_0 (Pa)	%	%	n
Marketed	144601 ± 17612	92.35 ± 11.82	8057 ± 664	52.69 ± 1.68	0.16 ± 0.00	6.17 ± 0.40	39.78 ± 2.61
LAN	8814 ± 1050	4.84 ± 0.10	138.82 ± 9.90	7.03 ± 0.48	0.49 ± 0.01	59.52 ± 2.32	122.11 ± 6.34
PG5	17721 ± 2401	7.06 ± 0.68	95.77 ± 6.67	8.39 ± 0.36	1.26 ± 0.29	74.73 ± 4.84	62.10 ± 18.10
PG10	13219 ± 1633	6.81 ± 0.25	93.08 ± 7.16	7.56 ± 0.51	0.59 ± 0.07	76.60 ± 0.00	131.78 ± 16.01
TR5	4997 ± 760	3.96 ± 0.36	77.35 ± 4.43	5.27 ± 0.56	0.50 ± 0.11	63.27 ± 4.35	131.20 ± 38.80
TR10	12021 ± 1289	5.50 ± 0.81	68.05 ± 8.08	5.30 ± 0.86	0.58 ± 0.08	62.13 ± 2.70	108.13 ± 11.41
CA	6227 ± 254	4.08 ± 0.43	66.68 ± 7.26	4.80 ± 0.26	0.63 ± 0.00	73.10 ± 1.75	116.03 ± 2.78
CB	9026 ± 1107	5.49 ± 0.68	72.00 ± 8.81	4.61 ± 0.28	0.46 ± 0.06	72.37 ± 3.06	159.00 ± 20.20
CC	7311 ± 480	4.06 ± 0.62	61.51 ± 5.72	4.03 ± 0.30	0.50 ± 0.01	69.33 ± 4.91	139.57 ± 9.13

2.3.4 *In vitro* penetration/permeation study

CAF was detected in all skin regions (SC and E+D+F) and permeated through the skin to the receptor fluid following topical administration of all nano-cream formulations, the CAF marketed formulation, or CAF in aqueous solution (control).

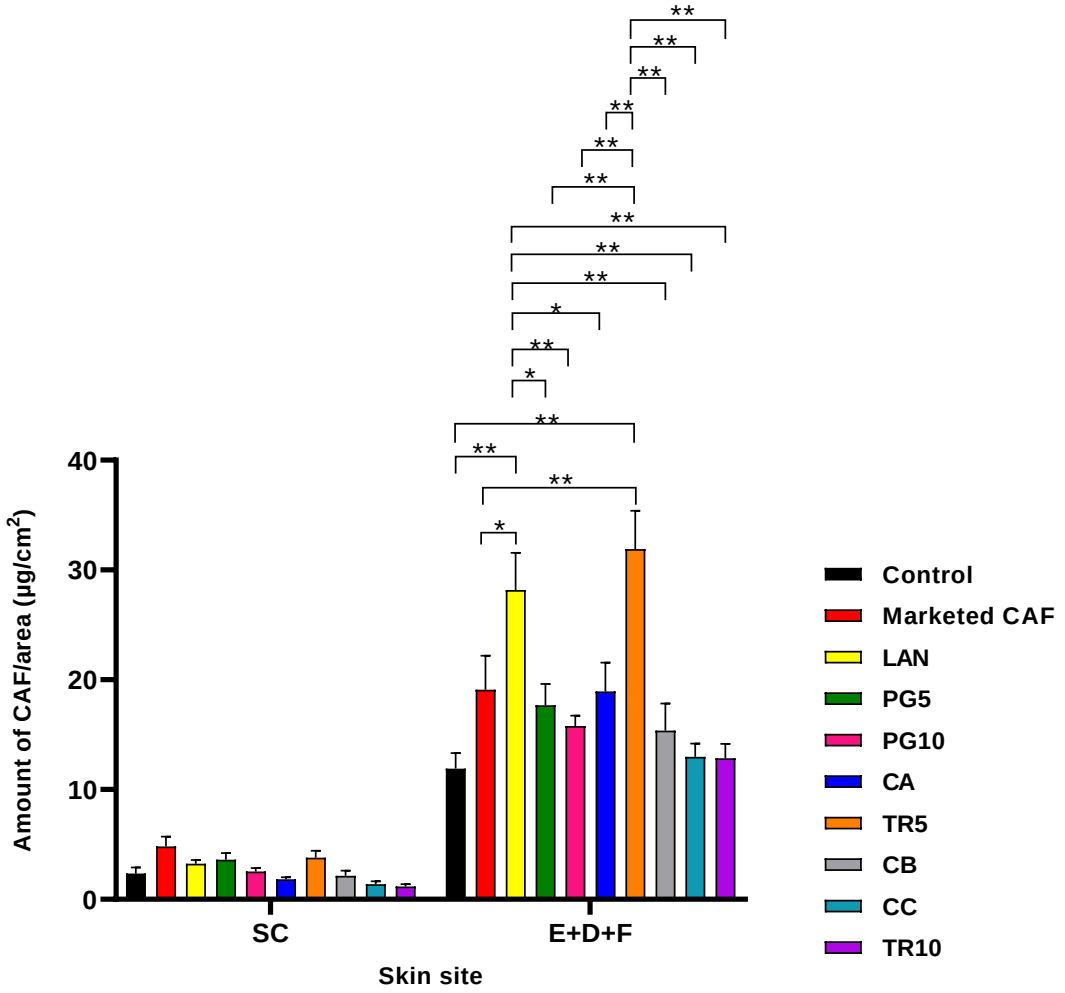

Figure 2.7 Skin penetration profile of nano-cream formulations compared to marketed topical product and CAF in aqueous control: the distribution of CAF in the SC and E+D+F; (mean ± SEM; *n* = 8-9; **p* < 0.01, ***p* < 0.0001). SC= stratum corneum; E+D+F = epidermis, dermis and follicles

Figure 2.7 and Table 2.12 present the amount of CAF per area of each skin tissue at 8h following administration of each CAF formulation. There was no statistically significant difference in CAF penetration into the SC between the applied formulations, the marketed CAF topical product, and the CAF aqueous control solution. However, there was a statistically significant difference in the amount of CAF that penetrated to the deeper skin (E+D+F) regions from the range of applied CAF formulations (28.18 ± 3.39; 19.10 ± 3.10; 11.90 ± 1.43 µg/cm^2 respectively; **p* < 0.01, ***p* < 0.0001) (Table 2.11 and 2.12). The marketed CAF cream product

and CAF nano-cream formulations containing TR5 and PG5 showed the highest penetration of CAF in the SC (3.78 ± 0.64; 3.61 ± 0.61 µg/cm^{2,} respectively), although the difference in the SC was not statistically significant (Figure 2.7, Table 2.11 and Table 2.12). In the combined area of epidermis, dermis and follicles (E+D+F), the CAF distribution of LAN and TR5 nano-cream formulations were similar results (28.18 ± 3.39; 31.91 ± 3.49 µg/cm^{2,} respectively; Table 2.12). Both formulations showed significant differences in CAF in aqueous control (***p* < 0.0001; Table 2.11). Overall, there were a 2.3-fold increase in CAF in both SC and (E+D+F) regions for LAN compared to CAF in aqueous control.

Table 2.11 Summary of statistical significance (p-values) in the distribution of CAF in the epidermis-dermis-follicle (E+D+F) region

Formula	P-value									
	Control: CAF in aqueous	**Marketed CAF**	**LAN**	**PG5**	**PG10**	**TR5**	**TR10**	**CA**	**CB**	**CC**
Control: CAF in aqueous	x	0.0936 (ns)	<0.0001	0.3358 (ns)	0.8439 (ns)	<0.0001	>0.9999 (ns)	0.1096 (ns)	0.9128 (ns)	>0.9999 (ns)
Marketed CAF	x	x	0.0089	0.9999 (ns)	0.9336 (ns)	<0.0001 (ns)	0.2353 (ns)	>0.9999 (ns)	0.8744 (ns)	0.26 (ns)
LAN	0.001	<0.0001	x	0.001	<0.0001	0.8726 (ns)	<0.0001	0.0072	<0.0001	<0.0001
PG5	x	x	x	x	0.9986 (ns)	<0.0001	0.6017 (ns)	>0.9999 (ns)	0.9942 (ns)	0.6361 (ns)
PG10	x	x	x	x	x	x	x	x	>0.9999 (ns)	0.9774 (ns)
TR5	x	x	x	x	x	x	<0.0001	x	<0.0001	<0.0001
TR10	x	x	x	x	x	x	x	x	x	x
CA	x	x	x	x	x	<0.0001	0.2664 (ns)	x	0.8994 (ns)	0.2931 (ns)
CB	x	x	x	x	x	x	0.9891 (ns)	x	x	0.9923 (ns)
CC	x	x	x	x	x	x	>0.9999 (ns)	x	x	x

Notes: ns= not statistically significant

Table 2.12 Skin distribution of CAF from nano-cream formulations, marketed product and aqueous solution control (mean ± SEM; *n* = 8-9)

Formula	CAF distribution in the skin (µg/cm^2)		ER
	SC	E+D+F	
Control: CAF in aqueous	2.34 ± 0.55	11.90 ± 1.43	1.00
Marketed CAF	4.81 ± 0.90	19.10 ± 3.10	1.68
LAN	3.23 ± 0.35	28.18 ± 3.39	2.30
PG5	3.61 ± 0.61	17.69 ± 1.94	1.49
PG10	2.53 ± 0.31	15.78 ± 0.95	1.28
TR5	3.78 ± 0.64	31.91 ± 3.49	2.51
TR10	1.17 ± 0.22	12.86 ± 1.30	0.98
CA	1.83 ± 0.18	18.95 ± 2.61	1.46
CB	2.15 ± 0.47	15.38 ± 2.45	1.23
CC	1.38 ± 0.25	12.98 ± 1.21	1.01

ER = enhancement ratio, was a ratio of the mean total amount of CAF deposited in the skin (SC and E+D+F) from formulated creams/CAF in aqueous control

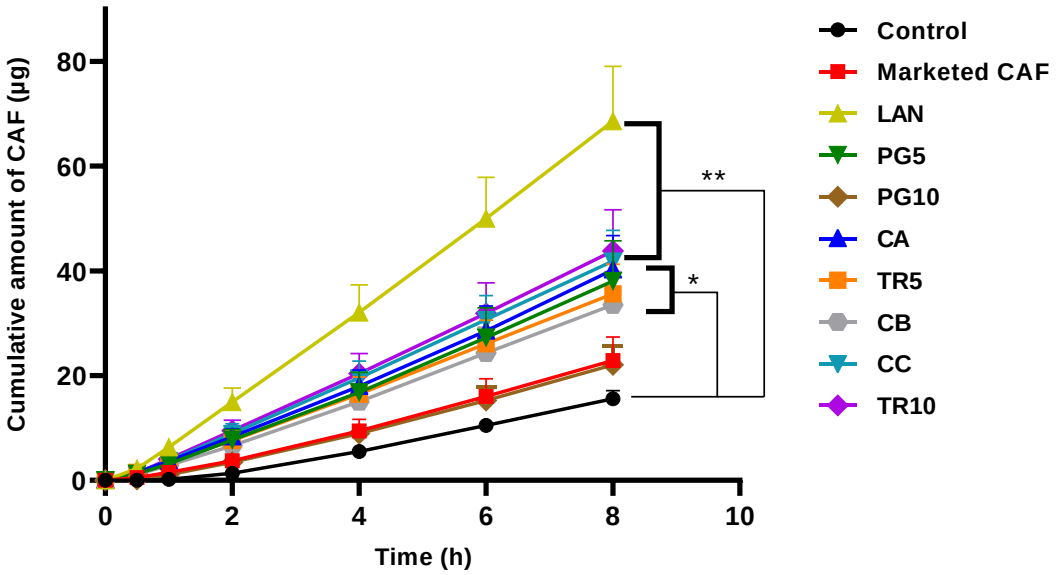

Figure 2.8 Cumulative amount of CAF penetrated in receptor solution over 8h from all formulated topical creams (mean ± SEM; *n* = 8-9, **p* < 0.05, ***p* < 0.0001)

Figure 2.8 illustrates the permeation profile of CAF of all formulated nano-creams, marketed CAF product, and CAF in aqueous control. The addition of LAN in the CAF nano-cream formulation showed the highest permeation of CAF through the skin (68.63 ± 11.59 µg respectively; $p < 0.0001$) followed by the TR10 and CC nano-cream formulations (43.80 ± 7.89; 41.87 ± 5.88 µg; $p < 0.0001$), respectively (Figure 2.8, Table 2.13 and Table 2.14). The cumulative amount of CAF permeated over 8h (Figure 2.8) was significantly higher for the PG5, TR5, CA and CB nano-cream formulations (38.08 ± 7.66; 35.63 ± 5.64; 40.20 ± 6.54 and

33.53 ± 6.35 µg, respectively); (Table 2.13 and Table 2.14) than from CAF in aqueous control (15.57 ± 1.57 µg) (Table 2.13).

There was no significant difference in the cumulative amount of CAF permeated through the skin over 8h (Figure 2.8 and Table 2.14) for the PG10 nano-cream formulation, compared to CAF in aqueous control. However, there was a 1.28-fold increase in the amount of CAF in both SC and epidermal-dermal-follicular regions from the PG10 formulation (Table 2.12).

The summary of experimental data of CAF skin permeation is presented in Table 2.13. The LAN nano-cream formulation showed high CAF flux and had a short lag time than CAF in aqueous control and marketed CAF topical product. Additionally, LAN in nano-cream formulation enhanced the CAF skin permeation by approximately 3.49 fold.

Table 2.13 shows the steady-state flux of CAF was 8.829 ± 1.472 µg/cm^2/h from the LAN nano-cream formulation, whilst the flux of control CAF solution was 2.533 ± 0.480 µg/cm^2/h. CAF in the LAN nano-cream formulation permeated three and a half times faster than the control CAF aqueous solution. CAF lag time from the LAN nano-cream formulation was three times shorter than CAF in aqueous control lag time. The enhancement ratio was similar for the PG5, CA, TR5, TR10 and CC nano-cream formulations, with the entire ratio being approximately two. Lag time for the PG5, CA, TR5, TR10 and CC nano-cream formulations was half the lag time of control CAF in aqueous solution (Table 2.13).

Overall, nanoformulations in the form of cream fabricated with different CPEs for skin delivery of CAF had shown a significant difference in cumulative amount permeated through the skin over 8h. The LAN nano-cream formulation appeared to be a promising topical formulation of CAF with good skin penetration and permeation characteristics. LAN enhanced the penetration and permeation of CAF acted as CPE was considered for further investigation in the preclinical efficacy *in vivo* study.

Table 2.13 Summary of experimental data for CAF skin penetration/permeation parameters in nano-cream formulations (mean ± SEM; *n* = 8-9)

Formula	Cumulative amount (µg)	Steady-state flux (*Jss*; µg/cm^2/h)	Permeability coefficient (Kp; cm/h)	Lag time (min)	ER
Control: CAF in aqueous	15.57 ± 1.57	2.533 ± 0.480	0.001 ± 0.001	53.22 ± 3.42	1.00
Marketed CAF	22.88 ± 4.50	2.827 ± 0.555	0.001 ± 0.001	44.88 ± 5.46	1.12
LAN	68.63 ± 11.59	8.829 ± 1.472	0.002 ± 0.001	21.78 ± 3.66	3.49
PG5	38.08 ± 7.66	4.960 ± 0.004	0.001 ± 0.001	28.14 ± 5.22	1.96
PG10	22.06 ± 3.55	2.920 ± 0.465	0.001 ± 0.001	45.84 ± 3.78	1.15
TR5	35.63 ± 5.64	4.556 ± 0.659	1.650 ± 0.292	34.50 ± 6.24	1.80
TR10	43.80 ± 7.89	5.191 ± 1.036	2.312 ± 0.565	23.22 ± 4.32	2.05
CA	40.20 ± 6.54	5.055 ± 0.870	0.001 ± 0.001	21.78 ± 3.06	1.99
CB	33.53 ± 6.35	5.539 ± 0.715	2.348 ± 0.521	16.50 ± 2.52	2.19
CC	41.87 ± 5.88	5.417 ± 0.748	2.146 ± 0.488	21.90 ± 5.46	2.14

ER= enhancement ratio was calculated based on the ratio of mean values of *Jss* of the formulations to CAF in an aqueous solution

Table 2.14 Summary of p-value in the cumulative amount of CAF of all formulated creams after 8h permeation through the skin

Formula	P-value									
	Control: CAF in aqueous	**Marketed CAF**	**LAN**	**PG5**	**PG10**	**TR5**	**TR10**	**CA**	**CB**	**CC**
Control: CAF in aqueous	x	0.9215 (ns)	<0.0001	0.001	0.9621 (ns)	0.0044	<0.0001	0.0003	0.0251	<0.0001
Marketed CAF	x	x	<0.0001	0.047	>0.9999 (ns)	0.1512 (ns)	0.0003	0.0172	0.4299 (ns)	0.0029
LAN	x	x	x	<0.0001	<0.0001	<0.0001	<0.0001	<0.0001	<0.0001	<0.0001
PG5	x	x	x	x	0.02575	>0.9999 (ns)	0.9716 (ns)	>0.9999 (ns)	0.9942 (ns)	0.6361 (ns)
PG10	x	x	x	x	x	0.0966 (ns)	0.0001	0.0096	>0.9999 (ns)	0.0015
TR5	x	x	x	x	x	x	<0.0001	x	<0.0001	<0.0001
TR10	x	x	x	x	x	x	x	x	x	x
CA	x	x	x	x	x	0.9955	0.2664 (ns)	x	0.9493 (ns)	>0.9999 (ns)
CB	x	x	x	x	x	x	0.485 (ns)	x	x	0.792 (ns)
CC	x	x	x	x	x	x	>0.9999 (ns)	x	x	x

Notes: ns= no significant

Table 2.15 Mass balance of *in vitro* penetration/permeation study of CAF into and through the skin (mean ± SEM; *n* = 8-9)

Formula	IA (µg)	CAF distribution (µg)				Total of CAF distribution (µg)	Recovery (%)
		RA	SC	E+D+F	R		
Control: CAF in aqueous	4450.05 ± 13.26	4184.62 ± 30.84	2.34 ± 0.55	11.90 ± 1.43	25.12 ± 4.69	4230.75 ± 26.93	95.08 ± 0.76
Marketed CAF	4387.02 ± 22.04	4249.97 ± 88.51	4.81 ± 0.90	19.10 ± 3.10	30.52 ± 7.66	4303.51 ± 87.28	98.97 ± 1.73
LAN	4192.48 ± 14.26	4180.89 ± 40.75	3.23 ± 0.35	28.18 ± 3.39	82.47 ± 13.94	4294.77 ± 28.89	102.44 ± 0.63
PG5	4409.64 ± 19.73	4169.12 ± 34.02	3.61 ± 0.61	17.69 ± 1.94	49.00 ± 8.79	4235.15 ± 26.98	96.05 ± 0.57
PG10	4531.77 ± 19.88	4404.12 ± 22.64	2.53 ± 0.31	15.78 ± 0.95	25.91 ± 4.00	4447.64 ± 23.31	98.14 ± 0.26
TR5	4424.93 ± 3.61	4235.63 ± 35.49	3.78 ± 0.64	31.91 ± 3.49	43.18 ± 6.76	4312.58 ± 29.65	97.46 ± 0.67
TR10	4450.85 ± 3.08	4331.63 ± 27.73	1.17 ± 0.22	12.86 ± 1.30	48.80 ± 10.26	4393.30 ± 29.65	98.71 ± 0.65
CA	4436.73 ± 4.00	4381.76 ± 21.66	1.83 ± 0.18	18.95 ± 2.61	47.15 ± 8.54	4448.69 ± 25.38	100.27 ± 0.55
CB	4376.08 ± 4.66	4246.90 ± 40.88	2.15 ± 0.47	15.38 ± 2.45	51.77 ± 6.89	4314.50 ± 34.08	98.59 ± 0.79
CC	4481.46 ± 3.57	4380.43 ± 14.91	1.38 ± 0.25	12.98 ± 1.21	51.23 ± 7.88	4445.66 ± 9.72	99.20 ± 0.24

IA= initial amount of CAF in the donor compartment; RA= remaining amount of CAF in the donor compartment; SC= amount of CAF in the stratum corneum; E+D+F= amount of CAF in epidermis, dermis and follicles; R= amount of CAF in the receptor compartment

Table 2.15 presents the mass balance of in vitro penetration/permeation of CAF into and through the skin. The recovery results, based on CAF recovered from receptor solution, tape stripping, donor solution and skin extraction at 8h. Mass balance recovery of CAF from all nano-cream formulations and CAF in aqueous control was in the range of 95.08 ± 0.76% to 102.44 ± 0.63%.

2.3.5 Stability of CAF creams during storage

We observed that CAF nano-cream formulations showed adequate physical stability (globule size and pH cream) over 4 months (Table 2.16). All developed nano-creams stored at 22-25°C without protection from light were stable for the entire 4 months and showed excellent physical characteristics for skin application without any alteration in colour. In addition, all 2% nano-cream formulations remained stable with the CAF potency of 99.99-100.00% during 4-months storage (Figure 2.9).

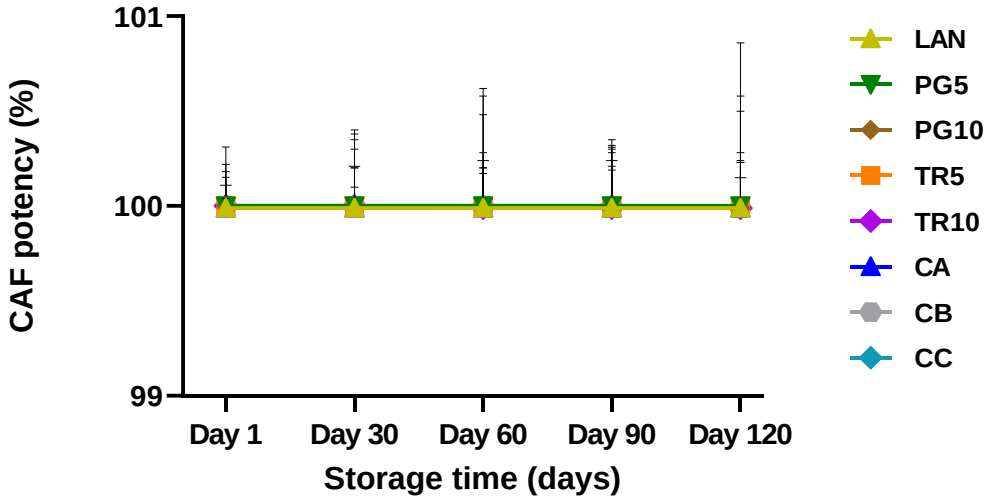

Figure 2.9 Percentage of CAF remaining after 120 days (4 months) storage of nano-cream formulations at room temperature and exposure to light

Table 2.16 CAF nano-cream formulations physical stability during 4-months storage (mean ± SD; *n* = 3) at 22-25°C

Formula	pH cream				Globule size (nm)			
	M1	M2	M3	M4	M1	M2	M3	M4
LAN	5.51 ± 0.01	5.50 ± 0.01	5.57 ± 0.01	5.50 ± 0.01	425.50 ± 4.59	423.07 ± 23.70	421.47 ± 2.22	423.10 ± 6.58
PG5	5.38 ± 0.01	5.41 ± 0.01	5.46 ± 0.01	5.43 ± 0.02	470.10 ± 3.40	475.53 ± 12.11	466.67 ± 20.79	470.57 ± 24.98
PG10	5.58 ± 0.01	5.56 ± 0.01	5.59 ± 0.01	5.58 ± 0.01	467.37 ± 35.77	478.50 ± 38.83	466.67 ± 6.93	472.33 ± 12.99
TR5	5.66 ± 0.01	5.66 ± 0.06	5.68 ± 0.02	5.67 ± 0.01	296.40 ± 10.35	292.00 ± 8.28	290.37 ± 8.72	290.20 ± 14.01
TR10	5.95 ± 0.01	5.91 ± 0.01	5.96 ± 0.02	5.95 ± 0.01	375.70 ± 4.09	381.37 ± 5.77	377.27 ± 6.01	380.83 ± 13.16
CA	5.63 ± 0.02	5.67 ± 0.02	5.70 ± 0.01	5.59 ± 0.01	350.57 ± 11.64	341.73 ± 12.31	350.33 ± 7.44	350.33 ± 7.93
CB	5.63 ± 0.01	5.64 ± 0.01	5.63 ± 0.03	5.62 ± 0.01	340.60 ± 4.16	331.80 ± 1.77	333.93 ± 12.04	340.87 ± 7.98
CC	5.94 ± 0.02	5.97 ± 0.02	5.98 ± 0.02	5.92 ± 0.01	356.23 ± 5.42	345.47 ± 9.91	344.23 ± 1.79	344.93 ± 8.66

Notes: M1= 1st month; M2= 2nd month; M3= 3rd month and M4= 4th month

2.4 Discussion

Pharmaceutical QbD is a modern approach to ensure the quality of pharmaceutical products and improve sensorial properties on the skin. Implementing the concept of QbD to topical dermatological dosage forms is in the initial stages. QbD principles were applied and materials were chosen based on their physicochemical properties and safety profile. The preparation of CAF nano-cream formulations typically involved homogenisation of the oily phase and aqueous phase along with the active ingredient to form oil-in-water (O/W) creams at 70°C. Three process parameters, including the temperature of oil/water phases, homogenisation speed and emulsification time, were identified as CPP.

A TPP was generated and set; simple fabrication produced nanoemulsion-based semisolid systems containing CAF. All nano-cream formulations had good homogeneity and spreadability, smooth texture, and excellent skin consistency (attractive appearance). The CAF nano-cream formulations were stable (physically and chemically). When incorporated with penetration-enhancing chemicals, they provided CAF effectively (reasonable amounts of CAF penetrate/permeate into and through the skin). The nano-cream formulations met the TPP regarding feasibility and scalability of fabrication, rheology properties and skin target for anticellulite in the epidermis and dermis regions. In addition, a suitable HPLC assay method, including skin extraction and quantification of CAF was developed and validated. The HPLC analytical method for CAF provided a suitable system including linearity, sensitivity, precision and accuracy for mass balance purposes (recovery > 95%) in all *in vitro* penetration/permeation studies. These criteria were performed to meet the requirement of the QTPP framework for assessing a successful formulation strategy.[54,55] The mechanism of penetration enhancement of these systems included thermodynamic driving force, drug solubility-partitioning in the SC, intercellular lipid fluidisation and SC hydration.

We examined the effect of these formulations on CQAs, including CAF solubility in nano-cream formulations, pH in creams and in the aqueous phase separation, and desired globule size. All systems generated globule sizes in the ~330-470 nm range (Table 2.8). It is noteworthy that globule size plays an essential role in releasing the drug from the formulation.[69,70] Badran et al.[71] reported increasing the drug release of meloxicam from formulation due to smaller

globule sizes offered a large surface area. Our group also demonstrated that a reduction in globule size in vesicle formulations enhanced the penetration of deeper skin layers.[72]

We noted that the pH of all CAF nano-cream formulations was in the range of 5.36-5.91 and the aqueous phase pH separated from nano-cream formulations was in the range of 5.55 to 5.98 (Table 2.8). The aqueous phase pH indicates the ratio of the ionised and unionised fraction of active ingredients and their behaviour in the vehicle.[69,73] It is more likely that the ionised and unionised active ingredient ratio in all the aqueous phases was comparable to all nano-cream formulations. CAF is a hydrophilic active ingredient primarily dissolved in the aqueous phase. Sharma et al.[73] reported that unionised-to-ionised ratios of metronidazole in all the aqueous phases were more likely to be similar to all topical creams. Caffeine and metronidazole are water-soluble drugs. It was assumed that the amount of metronidazole in the aqueous layer might influence drug permeation across the skin. Therefore, it was decided to split the aqueous phase and quantify the amount of drug dissolved in the aqueous.[73]

We also observed the rheological evaluation for all nano-creams. The shear sweep test provides insights into the various rheological phases a semisolid product goes through, from where the product is in a container (static state) to when applied to the skin (high-flow state). It is accepted that increasing yield stress values shows solid-like behaviour; therefore, it is required to apply high energy stress to deform a solid to liquid-like behaviour.[74] Table 2.10 shows that the marketed CAF had the highest yield stress (σ_0) of ~52.69 Pa. The CC formulation had the lowest yield stress of ~4.03 Pa. The value of σ_0 demonstrates the energy needed to spread the product. Higher σ_0 values represent that the materials can withstand container movement during manufacturing, packaging and transportation. Too high may lead to a significant, cohesive resistance during application on the skin.[75] Yao's group described three different body lotions (A-C).[76] One of the tests, the applicability test, assessed the lotions spread into the skin without feeling greasy and sticky. They found lotion C had a higher yield stress value than lotion A and lotion B. At high stress, the highest viscosity was lotion C > lotion B > lotion A. Lotion A was reported to have the best ease of applicability (lower yield stress and lower viscosity at high shear).

Adapting from Yao's study, it can be interpreted that our novel nano-cream formulations have the best ease of applicability to the following rank order: TR5 > CC > CA > LAN > CB > TR10

> PG 10 > PG5. The marketed CAF cream had the worse applicability because it had higher yield stress and higher viscosity at high shear. Both yield stress and high-shear viscosity can be correlated with the product applicability. Yield stress is indicative of the resistance the product may exhibit at the initiation of product application, where the structure needs to deform and flow. High-shear viscosity can indicate product film thickness and applicability when a product has already been sheared and spread onto the skin site. The yield stress does not affect the IVPT profile of CAF from the nano-cream formulations.[73] However, viscosity also plays a vital role in improving spreadability, easing the application, and prolonging product retention in the skin. Yamamoto et al.[77] also reported that rheological properties influence human sensory feeling. Measuring rheological properties of semisolid preparations, typically the "soft matter" of nanostructures and microstructures, helps provide valuable sensory attributes and consumer evaluation information.[77,78]

G′ represents the elastic response of the material.[73] In the current study, G′ function curves of all nano-cream formulations, except the marketed cream, dropped continuously after leaving the LVR region, indicating a gradual breakdown of the superstructure. In contrast, the curve of the marketed product showed a sharp downturn at the limit of the LVR region, exhibiting brittle fracturing behaviour where the marketed sample was under shear did not break homogeneously.[75]

Our study observed the effect of the addition of penetration enhancers in semisolid systems compared to CAF in aqueous control and marketed CAF topical product. Nano-cream formulations containing various types of penetration enhancers significantly increased penetration and retention of CAF for all formulated nano-creams (Figure 2.7 and Figure 2.8). Penetration enhancers-containing fatty acids, esters, alcohols and ether alcohols incorporated formulas were of interest in this study as they offer advantages in terms of excellent penetrating capacity for passive skin transport.[79-82]

Previous studies had investigated the penetration/permeation of CAF with different dosage forms for topical/transdermal delivery. For example, Abd et al.[34] prepared CAF-loaded deformable liposomes that showed topical liposomes enhanced the skin delivery of CAF. Although liposomes give the advantage of providing bilayer fluidity, they are also prone to leaking from the core content to the external medium; consequently, the encapsulated drugs

are out of the vesicles and less flexible to enter SC.[83,84] Accumulation of liposome and adhesion on the SC should be taken into consideration due to the drawback of this formulation.[85]

Another study was conducted by Bolzinger et al.[28] to examine three different dosage forms for CAF transport. The three dosages forms were oil-in-water (O/W) microemulsion with alcohol-free, a conventional emulsion in O/W type, and an aqueous gel. The *in vitro* experiments were carried out using hypodermis pig skins. The results showed 23% of CAF from O/W microemulsion reached the hypodermis within 24h of diffusion. It was 1.3-fold larger than conventional emulsion and gel forms. Furthermore, microemulsion forms stored 50% of CAF in the hypodermis and the remaining amount of CAF passed through the receptor.

We designed our QTPP for cellulite treatment based on supporting evidence-based practice. Eight nano-cream formulations (LAN, PG5, PG10, TR5, TR10, CA, CB, CC) were designed to include a single or combination of CPEs (lanolin, propylene glycol, transcutol® P) with 2% CAF. All nano-cream formulations were successfully fabricated using a low-energy method to meet one of the critical attributes of our formulation method.

LAN, PG and TR have been widely applied as vehicles in formulations for topical and transdermal delivery.[21,27,86-89] All components are categorised as GRAS by the U.S. FDA.[90-92] PG is a well-known penetration enhancer used in skin preparation as a “carrier-solvent” (solvent/co-solvent) to enhance drug permeation topical transdermal formulations [93-95]. We observed the effects of the addition PG5 and PG10; the steady-state fluxes were 4.960 ± 0.004 and 2.920 ± 0.465 μg/cm^2/h, indicating a higher concentration of penetration enhancers did not give a higher flux (Table 2.13). Whilst, we also found that the concentration of PG was higher, the chances of lagtime were longer (Table 2.13). Amnuaikit et al. [88] reported that PG in different concentrations influenced CAF skin permeation. They found that the gel dosage form contained PG 15% was the highest amount of CAF permeated through the skin, following PG 30% and PG 7.5%.

Interestingly, our study also found that cream dosage forms incorporated with PG5 had a higher amount of CAF permeating through the skin than PG10 (Table 2.13). A high concentration of PG may interfere with the skin permeation of the active compound,[88] resulting in the fluxes result. This has been previously shown by Abd et al.[34], who investigated the

influence of adding an edge activator, PG. They incorporated CAF with DL with or without the addition of an edge activator. The findings found that DL-CAF flux was 1.94-folds higher than the control solution.

Furthermore, the CAF flux from DL was 1.56- and 3.05-folds higher than control and conventional liposome with CAF (CL-CAF), whilst the lowest flux was seen for CL-CAF. Thus, the presence of PG facilitated liposomes to squeeze flexibly between corneocytes of the SC to get through deeper layers of the skin. Obtaining small unilamellar vesicles with bilayer fluidity gives the capacity to permeate fully through the SC. It could alter the thermodynamic activity of drugs into the skin and disturb SC lipid bilayer structures.[96,97]

TR is high purity of diethylene glycol monoethyl ether (DEGEE), which was selected as a skin permeation enhancer to aid in penetrating skin transport without compromising skin integrity.[79,98-100] TR has impressed as an excellent and safe hydroalcoholic solubiliser in the cosmetic industry.[79,101] Haq et al. [102] examined the effect of 5% TR on thymoquinone flux enhancement in human cadaver skin. Their findings revealed that TR provides adequate thymoquinone flux and helps form a reservoir in the lipid-rich regions of the stratum corneum. Our study investigated the effects of TR5 and TR10 nano-cream formulations on the diffusivity of a hydrophilic model permeant (CAF) applied under infinite dose conditions to porcine skin. Our results of CAF flux (μg/cm^2/h) in TR5 (4.556 ± 0.659) and TR10 nano-cream formulations (5.191 ± 1.036) showed that the concentration of TR did not relate to the flux achieved (Table 2.13).

The amount of CAF that penetrated in the SC at the end of the 8h experiment, from all diffusion studies, is illustrated in Figure 2.7. It was observed that the addition of CPEs did not enhance CAF diffusion significantly ($p > 0.05$) for all nano-cream formulations compared to control CAF aqueous solution and marketed CAF. However, the addition of CPEs (LAN and TR5) incorporated into semisolid systems significantly enhanced CAF diffusion in E+D+F (Figure 2.7*;* $p < 0.01$, $p < 0.0001$, respectively). Although the myth of allergy from LAN has been debated for decades, there is little concrete scientific evidence [103,104]. LAN contains cholesterol, ceramides, free fatty acids, vital SC lipids.[105-107] It has been proved that LAN in combination with synthetic membranes can provide lipidic components similar to the lipidic matrix of the SC.[81] Comparison between LAN and other CPE (PG5, PG10, CA, CB, CC, TR10)

formulations, alone or in combination, has shown a significant difference ($p < 0.01$, Figure 2.7) in enhanced CAF diffusion in the epidermal-dermal-follicle region. LAN has shown high flux and short lag time. Moreover, LAN formulation demonstrated approximately a 3.49-fold enhanced CAF skin permeation (Table 2.13).

Figure 2.8 illustrates the permeation profile of CAF of all formulated nano-creams, marketed CAF product and CAF in aqueous control. At the end of 8h, there was a significant difference in the CAF cumulative amount of all nano-cream formulations permeated through the skin, except for PG10. Additionally, LAN in nano-cream formulation showed the highest permeation of CAF through the skin ($p < 0.0001$). In contrast, Joshita et al. [108] showed the gel dosage form had the highest CAF penetration followed by cream and ointment. LAN was selected as one of the CPEs, consisting of 33 hydroxyl and polyhydroxy esters of sterols and 36 free fatty acids [109]. It has a water-holding capacity, [110] thus helping improve stability.[103] LAN can also increase the permeability of the active compound through the skin due to LAN chemical properties similar to human sebum. [110] Flockhart et al. [111] reported that nanoemulsions derived from LAN (Medilan®) were able to be potential drug delivery vehicles. LAN-containing nanoemulsions were called lanosomes. It was composed of 5 parts Laneth 20; 25 parts lanolin (Medilan®); 70 parts water and produced globule size in 50-150 nm.

The marketed CAFcontaining shea butter base and other ingredients were more likely similar to our developed nano-creams. The marketed product also contained the same concentration of 2% of CAF. The flux result was 2.827 ± 0.555 µg/cm^2/h compared with CAF control solution (2.533 ± 0.480 µg/cm^2/h) (Table 2.13). The physical appearance of the marketed product was very thick feeling and had higher consistency. It is presumed higher viscosity can affect the permeation flux.

Inclusion of penetration enhancers increased CAF penetration to the deeper skin target site (E+D+F) compared to CAF in aqueous control (Table 2.12), with following order of penetration TR5 > LAN > Marketed > CA-LPG5 > PG5 > PG10 > CB > CC > TR10 in the CAF nano-cream formulations, although the TR5 and LAN nano-cream formulations had significantly greater CAF penetration ($p < 0.0001$: Figure 2.7). LAN and TR5 nano-cream formulations enhanced the CAF skin penetration by approximately 2.5-fold (Table 2.12). There was no significant difference in CAF penetration to the SC across semisolid nano-cream formulations (Figure

2.7). Interestingly, penetration enhancers resulted in greater deep tissue penetration than SC deposition in all cases. CPEs can facilitate CAF diffusion within skin tissues. We considered how the nanoemulsions incorporated with penetration enhancers promoted skin penetration. Many possible mechanisms of skin penetration enhancement give synergetic effects. First, enhanced solubility of CAF in the applied vehicles, as seen in Table 2.9. In this case, we measured the amount of CAF in the aqueous phase. Furthermore, combination surfactants, oils and penetration enhancers may disrupt the intercellular SC lipids by fluidisation of the SC.[112,113] Lastly; penetration enhancers may improve partitioning between the skin and the formulation (TA < 1) (Table 2.9). Overall, the data suggest incorporating skin penetration enhancers increased release from nano-cream formulations to SC and improved partitioning from SC into epidermal tissues and diffusion within skin tissue.

In this chapter, we have successfully developed nanoemulsion-based semisolid systems for skin delivery of CAF. We also demonstrated that all nano-cream formulations met the QTPP criteria and fulfilled the CQA of a topical product. In this study, all nano-cream formulations achieved sustained delivery of CAF into and through the skin over 8h. The greatest flux was seen for the addition of LAN in CAF nano-cream formulation. The LAN nano-cream formulation presented the best capability to enhance CAF permeation through the skin. To improve the confidence level in the treatment of cellulite, *in vitro* results do not always guarantee *in vivo* efficacy; therefore, the LAN nano-cream formulation was chosen to facilitate skin delivery of CAF and potentially exert an anticellulite effect in the human preclinical study (see Chapter 4).

2.5 References

1. Sarkaria JN, Busby EC, Tibbetts RS, et al. Inhibition of ATM and ATR kinase activities by the radiosensitizing agent, caffeine. *Cancer Res*. 1999;59(17):4375-4382. https://aacrjournals.org/cancerres/article/59/17/4375/505493
2. Sabisz M, Skladanowski A. Modulation of cellular response to anticancer treatment by caffeine: inhibition of cell cycle checkpoints, DNA repair and more. *Curr Pharm Biotechnol*. 2008;9(4):325-336.doi:10.2174/138920108785161497
3. Hayashi K, Tsuchiya H, Yamamoto N, et al. Impact of serum caffeine monitoring on adverse effects and chemotherapeutic responses to caffeine-potentiated chemotherapy for osteosarcoma. *J Orthop Sci*. 2009;14(3):253-258.doi:10.1007/s00776-009-1336-9
4. Wehner MR, Linos E. One More Reason to Continue Drinking Coffee-It May Be Good for Your Skin. *JAMA dermatology*. 2018;154(12):1385-1386. doi:10.1001/jamadermatol.2018.3300
5. Song F, Qureshi AA, Han J. Increased caffeine intake is associated with reduced risk of basal cell carcinoma of the skin. *Cancer Res*. 2012;72(13):3282-3289.doi:10.1158/0008-5472.Can-11-3511
6. Ritchie K, Carrière I, De Mendonca A, et al. The neuroprotective effects of caffeine: a prospective population study (the Three City Study). *Neurology*. 2007;69(6):536-545.

7. Herman A, Herman AP. Caffeine's mechanisms of action and its cosmetic use. *Skin Pharmacol Physiol*. 2013;26(1):8-14.doi:10.1159/000343174
8. A Aljuffali I, Hsu C-Y, Lin Y-K, Fang J-Y. Cutaneous delivery of natural antioxidants: the enhancement approaches. *Curr Pharm Des*. 2015;21(20):2745-2757. doi:10.2174/1381612821666150428125428
9. Sintov AC, Greenberg I. Comparative percutaneous permeation study using caffeine-loaded microemulsion showing low reliability of the frozen/thawed skin models. *Int J Pharm*. 2014;471(1-2):516-524.doi:10.1016/j.ijpharm.2014.05.040
10. Lu YP, Lou YR, Peng QY, Xie JG, Nghiem P, Conney AH. Effect of caffeine on the ATR/Chk1 pathway in the epidermis of UVB-irradiated mice. *Cancer Res*. 2008;68(7):2523-2529. doi:10.1158/0008-5472.Can-07-5955
11. Melero A, Guillot A, Carneiro C, et al. Caffeine analysis and extraction from a topical cream intended for UV-skin protection. *Journal of Dispersion Science and Technology*. 2020:1-7.doi: 10.1080/01932691.2020.1838919
12. Del Carmen Velazquez Pereda M, de Campos Dieamant G, Eberlin S, et al. Effect of green Coffea arabica L. seed oil on extracellular matrix components and water-channel expression in in vitro and ex vivo human skin models. *J Cosmet Dermatol*. 2009;8(1):56-62. doi 10.1111/j.1473-2165.2009.00425.x
13. Fischer T, Hipler U, Elsner P. Effect of caffeine and testosterone on the proliferation of human hair follicles in vitro. *Int J Dermatol*. 2007;46(1):27-35. doi:10.1111/j.1365-4632.2007.03119.x
14. Velasco MVR, Tano CTN, Machado-Santelli GM, Consiglieri VO, Kaneko TM, Baby AR. Effects of caffeine and siloxanetriol alginate caffeine, as anticellulite agents, on fatty tissue: histological evaluation. *J Cosmet Dermatol*. 2008;7(1):23-29. doi:10.1111/j.1473-2165.2008.00357.x
15. Rawlings AV. Cellulite and its treatment. *Int J Cosmet Sci*. 2006;28(3):175-190. doi:10.1111/j.1467-2494.2006.00318.x
16. Lupi O, Semenovitch IJ, Treu C, Bottino D, Bouskela E. Evaluation of the effects of caffeine in the microcirculation and edema on thighs and buttocks using the orthogonal polarization spectral imaging and clinical parameters. *J Cosmet Dermatol*. 2007;6(2):102-107. doi:10.1111/j.1473-2165.2007.00304.x
17. Luo L, Lane ME. Topical and transdermal delivery of caffeine. *Int J Pharm*. 2015;490(1):155-164.doi:10.1016/j.ijpharm.2015.05.050
18. Kim C, Shim J, Han S, Chang I. The skin-permeation-enhancing effect of phosphatidylcholine: caffeine as a model active ingredient. *Journal of cosmetic science*. 2002;53(6):363-374.https://pubmed.ncbi.nlm.nih.gov/12512013/
19. Trauer S, Patzelt A, Otberg N, et al. Permeation of topically applied caffeine through human skin--a comparison of in vivo and in vitro data. *Br J Clin Pharmacol*. 2009;68(2):181-186.doi:10.1111/j.1365-2125.2009.03463.x
20. Heard CM, Johnson S, Moss G, Thomas CP. In vitro transdermal delivery of caffeine, theobromine, theophylline and catechin from extract of Guarana, Paullinia Cupana. *Int J Pharm*. 2006;317(1):26-31.doi:10.1016/j.ijpharm.2006.02.042
21. Shakeel F, Ramadan W. Transdermal delivery of anticancer drug caffeine from water-in-oil nanoemulsions. *Colloids and Surfaces B: Biointerfaces*. 2010;75(1):356-362. doi:10.1016/j.colsurfb.2009.09.010
22. Trauer S, Lademann J, Knorr F, et al. Development of an in vitro modified skin absorption test for the investigation of the follicular penetration pathway of caffeine. *Skin Pharmacol Physiol*. 2010;23(6):320-327.
23. Moffat AC, Osselton MD, Widdop B, Watts J. *Clarke's analysis of drugs and poisons*. vol 3. Pharmaceutical press London; 2011. Accessed April 15,2021. https://www.pharmpress.com/product/9780853697114/clarkes-analysis-of-drugs-and-poisons
24. Bustamante P, Navarro J, Romero S, Escalera B. Thermodynamic Origin of the Solubility Profile of Drugs Showing one or two Maxima Against the Polarity of Aqueous and Nonaqueous Mixtures: Niflumic Acid and Caffeine. *J Pharm Sci*. 2002;91(3):874-883. doi:10.1002/jps.10076
25. Dias M, Farinha A, Faustino E, Hadgraft J, Pais J, Toscano C. Topical delivery of caffeine from some commercial formulations. *International Journal of Pharmaceutics*. 1999;182(1):41-47.doi:10.1016/s0378-5173(99)00067-8

26. Amnualkit T, Ingkatawornwong S, Maneenuan D, Worachotekamjorn K. Caffeine Topical Gel Formulation. *Isan Journal of Pharmaceutical Sciences*.2008;4(1):1-9 doi:10.14456/ijps.2008.2
27. Mustapha RB, Lafforgue C, Fenina N, Marty J. Influence of drug concentration on the diffusion parameters of caffeine. *Indian J Pharmacol*. 2011;43(2):157.
28. Bolzinger M-A, Briançon S, Pelletier J, Fessi H, Chevalier Y. Percutaneous release of caffeine from microemulsion, emulsion and gel dosage forms. *Eur J Pharm Biopharm*. 2008;68(2):446-451.doi:10.4103/0253-7613.77351
29. Dreher F, Fouchard F, Patouillet C, Andrian M, Simonnet JT, Benech-Kieffer F. Comparison of Cutaneous Bioavailability of Cosmetic Preparations Containing Caffeine or α-Tocopherol Applied on Human Skin Models or Human Skin ex vivo at Finite Doses. *Skin Pharmacol Physiol*. 2002;15(suppl 1)(Suppl. 1):40-58.doi:10.1159/000066680
30. Silva NHCS, Drumond I, Almeida IF, et al. Topical caffeine delivery using biocellulose membranes: a potential innovative system for cellulite treatment. *Cellulose*. 2014;21(1):665-674.doi:10.1007/s10570-013-0114-1
31. Frelichowska J, Bolzinger MA, Valour JP, Mouaziz H, Pelletier J, Chevalier Y. Pickering w/o emulsions: drug release and topical delivery. *Int J Pharm*. 2009;368(1-2):7-15. doi:10.1016/j.ijpharm.2008.09.057
32. Abd E, Namjoshi S, Mohammed YH, Roberts MS, Grice JE. Synergistic Skin Penetration Enhancer and Nanoemulsion Formulations Promote the Human Epidermal Permeation of Caffeine and Naproxen. *J Pharm Sci*. 2015:n/a-n/a.doi:10.1002/jps.24699
33. Bonina FP, Carelli V, Di Colo G, Montenegro L, Nannipieri E. Vehicle effects on in vitro skin permeation of and stratum corneum affinity for model drugs caffeine and testosterone. *Int J Pharm*. 1993;100(1):41-47.doi:10.1016/0378-5173(93)90073-O
34. Abd E, Gomes J, Sales CC, et al. Deformable liposomes as enhancer of caffeine penetration through human skin in a Franz diffusion cell test. *Int J Cosmet Sci*. 2021;43(1):1-10.doi:https://doi.org/10.1111/ics.12659
35. Nastiti CMRR, Ponto T, Abd E, Grice JE, Benson HAE, Roberts MS. Topical nano and microemulsions for skin delivery. *Pharmaceutics*. 2017;9(4):37. doi:10.3390/pharmaceutics9040037
36. Shaker DS, Ishak RAH, Ghoneim A, Elhuoni MA. Nanoemulsion: A Review on Mechanisms for the Transdermal Delivery of Hydrophobic and Hydrophilic Drugs. *Sci Pharm*. 2019;87(3):17.doi:10.3390/scipharm87030017
37. Yukuyama MN, Ghisleni DDM, Pinto TJA, Bou-Chacra NA. Nanoemulsion: process selection and application in cosmetics – a review. *Int J Cosmet Sci*. 2016;38(1):13-24. doi:10.1111/ics.12260
38. Chime S, Kenechukwu F, Attama A. Nanoemulsions—advances in formulation, characterization and applications in drug delivery.In: Sezer AD. *Application of Nanotechnology in Drug Delivery*. 1st ed. chapter 3. Intech Open;2014.Accessed December 30, 2021. doi: 10.5772/58673
39. Azmi NAN, Elgharbawy AA, Motlagh SR, Samsudin N, Salleh HM. Nanoemulsions: factory for food, pharmaceutical and cosmetics. *Processes*. 2019;7(9):617. doi: https://doi.org/10.3390/pr7090617
40. Knowlton JL. Emulsion theory. In: Butler H, ed. *Poucher's Perfumes, Cosmetics and Soaps*. Springer Netherlands; 2000:601-623.doi:10.1007/978-94-017-2734-1_19
41. Otto A, Du Plessis J, Wiechers JW. Formulation effects of topical emulsions on transdermal and dermal delivery. *Int J Cosmet Sci*. 2009;31(1):1-19. doi:10.1111/j.1468-2494.2008.00467.x
42. Lee Y-J, Baik S-J, Lee H-W, et al. A Study on the Correlation of the Skin Feeling with Rheological Parameters and Other Physical Properties. *Journal of the Society of Cosmetic Scientists of Korea*. 2004;30(2):141-145. https://www.koreascience.or.kr/article/JAKO200411923001598.page
43. Fabbron-Appas CT, Pandey P, Parekh HS, et al. Impact of different emollient esters on body emulsions: Sensory, physicochemical, and biometrological characterization. *Journal of Sensory Studies*. 2021;36(4):e12660. doi:10.1111/joss.12660
44. Bronaugh RL, Franz TJ. Vehicle effects on percutaneous absorption: in vivo and in vitro comparisons with human skin. *Br J Dermatol*. 1986;115(1):1-11. doi:10.1111/j.1365-2133.1986.tb06214.x

45. Bolzinger MA, Briancon S, Pelletier J, Fessi H, Chevalier Y. Percutaneous release of caffeine from microemulsion, emulsion and gel dosage forms. *Eur J Pharm Biopharm*. 2008;68(2):446-451.doi:10.1016/j.ejpb.2007.10.018
46. Ma H, Yu M, Lei M, Tan F, Li N. A novel topical targeting system of caffeine microemulsion for inhibiting UVB-induced skin tumor: characterization, optimization, and evaluation. *AAPS PharmSciTech*. 2015;16(4):905-913.doi:10.1208/s12249-014-0278-5
47. Freire TB, Dario MF, Mendes OG, et al. Nanoemulsion containing caffeine for cellulite treatment: characterization and in vitro evaluation. *Brazilian Journal of Pharmaceutical Sciences*. 2019;55:e18236.doi:10.1590/s2175-97902019000218236
48. Rodrigues F, Alves AC, Nunes C, et al. Permeation of topically applied caffeine from a food by-product in cosmetic formulations: Is nanoscale in vitro approach an option? *Int J Pharm*. 2016;513(1-2):496-503.doi:10.1016/j.ijpharm.2016.09.059
49. Doucet O, Ferrero L, Garcia N, Zastrow L. O/W emulsion and W/O/W multiple emulsion: physical characterization and skin pharmacokinetic comparison in the delivery process of caffeine. *Int J Cosmet Sci*. 1998;20(5):283-295. doi:10.1046/j.1467-2494.1998.181621.x
50. Bonina F, Bader S, Montenegro L, Scrofani C, Visca M. Three phase emulsions for controlled delivery in the cosmetic field. *Int J Cosmet Sci*. 1992;14(2):65-74. doi:10.1111/j.1467-2494.1992.tb00040.x
51. Zhang J, Michniak-Kohn B. Investigation of microemulsion microstructures and their relationship to transdermal permeation of model drugs: ketoprofen, lidocaine, and caffeine. *Int J Pharm*. 2011;421(1):34-44.doi:10.1016/j.ijpharm.2011.09.014
52. Naoui W, Bolzinger M-A, Fenet B, et al. Microemulsion Microstructure Influences the Skin Delivery of an Hydrophilic Drug. *Pharm Res*. 2011;28(7):1683-1695.doi:10.1007/s11095-011-0404-y
53. Zesch A, Schaefer H, Stüttgen G. The quantitative distribution of percutaneously applied caffeine in the human skin. *Arch Dermatol Res*. 1979;266(3):277-283. doi:10.1007/bf00418573
54. ICH Expert Working Group Harmonised Tripartite Guideline: Quality Risk Management Q8(R2). 2009. Accessed December 08, 2021. https://database.ich.org/sites/default/files/Q8_R2_Guideline.pdf
55. ICH Expert Working Group Harmonised Tripartite Guideline: Pharmaceutical Development Q9. 2005. Accessed December 08, 2021. https://database.ich.org/sites/default/files/Q9_Guideline.pdf
56. Naegele E. Determination of Caffeine in Coffee Products According to DIN 20481. *Agilent Technologies Application Note, publication number*. 2016. Accessed April 04, 2021. https://www.agilent.com/cs/library/applications/5991-2851EN.pdf
57. Namjoshi S, Caccetta R, Edwards J, Benson HA. Liquid chromatography assay for 5-aminolevulinic acid: application to in vitro assessment of skin penetration via Dermaportation. *J Chromatogr B Analyt Technol Biomed Life Sci*. 2007;852(1-2):49-55. doi:10.1016/j.jchromb.2006.12.040
58. Wojciechowska K, Zun M, Dwornicka D, Swiader K, Kasperek R, Poleszak E. Physical properties and caffeine release from creams prepared with different oils. *Current Issues in Pharmacy and Medical Sciences*. 2014;27(4):224-228. https://sciendo.com/pdf/10.1515/cipms-2015-0020
59. Chen MX, Alexander KS, Baki G. Formulation and Evaluation of Antibacterial Creams and Gels Containing Metal Ions for Topical Application. *Journal of Pharmaceutics*. 2016;2016:5754349.doi:10.1155/2016/5754349
60. Bolla PK, Clark BA, Juluri A, Cheruvu HS, Renukuntla J. Evaluation of Formulation Parameters on Permeation of Ibuprofen from Topical Formulations Using Strat-M® Membrane. *Pharmaceutics*. 2020;12(2):151.doi:10.3390/pharmaceutics12020151
61. Calderó G, García-Celma MJ, Solans C. Formation of polymeric nano-emulsions by a low-energy method and their use for nanoparticle preparation. *J Colloid Interface Sci*. 2011;353(2):406-411.doi:10.1016/j.jcis.2010.09.073
62. Carotenuto C, Minale M. On the use of rough geometries in rheometry. *Journal of Non-Newtonian Fluid Mechanics*. 2013;198:39-47.doi:10.1016/j.jnnfm.2013.04.004
63. Nastiti CM, Mohammed Y, Telaprolu KC, et al. Evaluation of quantum dot skin penetration in porcine skin: Effect of age and anatomical site of topical application. *Skin Pharmacol Physiol*. 2019;32(4):182-191.doi:10.1159/000499435

64. Simon GA, Maibach HI. The Pig as an Experimental Animal Model of Percutaneous Permeation in Man: Qualitative and Quantitative Observations – An Overview. *Skin Pharmacol Physiol*. 2000;13(5):229-234.doi:10.1159/000029928
65. Barbero AM, Frasch HF. Pig and guinea pig skin as surrogates for human in vitro penetration studies: a quantitative review. *Toxicol In Vitro*. 2009;23(1):1-13. doi:10.1016/j.tiv.2008.10.008
66. Davies DJ, Ward RJ, Heylings JR. Multi-species assessment of electrical resistance as a skin integrity marker for in vitro percutaneous absorption studies. *Toxicol In Vitro*. 2004;18(3):351-358.doi:10.1016/j.tiv.2003.10.004
67. Zhang Q, Grice JE, Li P, Jepps OG, Wang G-J, Roberts MS. Skin solubility determines maximum transepidermal flux for similar size molecules. *Pharm Res*. 2009;26(8):1974-1985.
68. Davies DJ, Heylings JR, McCarthy TJ, Correa CM. Development of an in vitro model for studying the penetration of chemicals through compromised skin. *Toxicol In Vitro*. 2015;29(1):176-181.doi:10.1016/j.tiv.2014.09.012
69. Abd E, Benson HAE, Mohammed YH, Roberts MS, Grice JE. Permeation Mechanism of Caffeine and Naproxen through in vitro Human Epidermis: Effect of Vehicles and Penetration Enhancers. *Skin Pharmacol Physiol*. 2019;32(3):132-141. doi:10.1159/000497225
70. Anton N, Gayet P, Benoit J-P, Saulnier P. Nano-emulsions and nanocapsules by the PIT method: An investigation on the role of the temperature cycling on the emulsion phase inversion. *Int J Pharm*. 2007;344(1):44-52.doi:10.1016/j.ijpharm.2007.04.027
71. Badran MM, Taha EI, Tayel MM, Al-Suwayeh SA. Ultra-fine self nanoemulsifying drug delivery system for transdermal delivery of meloxicam: Dependency on the type of surfactants. *J Mol Liq*. 2014;190:16-22.doi:10.1016/j.molliq.2013.10.015
72. Abd E, Roberts MS, Grice JE. A Comparison of the Penetration and Permeation of Caffeine into and through Human Epidermis after Application in Various Vesicle Formulations. *Skin Pharmacol Physiol*. 2016;29(1):24-30.doi:10.1159/000441040
73. Sharma PK, Panda A, Parajuli S, et al. Effect of surfactant on quality and performance attributes of topical semisolids. *Int J Pharm*. 2021;596:120210. doi:0.1016/j.ijpharm.2021.120210
74. Barnes HA. The yield stress—a review or 'παντα ρει'—everything flows? *Journal of Non-Newtonian Fluid Mechanics*. 1999;81(1):133-178.doi:10.1016/S0377-0257(98)00094-9
75. Dabbaghi M, Namjoshi S, Panchal B, et al. Viscoelastic and Deformation Characteristics of Structurally Different Commercial Topical Systems. *Pharmaceutics*. 2021;13(9):1351.doi:10.3390/pharmaceutics13091351
76. Yao ML, Patel JC. Rheological Characterization of Body Lotions. *Applied Rheology*. 2001;11(2):83-88.doi:10.1515/arh-2001-0005
77. Yamamoto Y, Fukami T, Koide T, et al. Comparative pharmaceutical evaluation of brand and generic clobetasone butyrate ointments. *Int J Pharm*. 2014;463(1):62-67. doi:10.1016/j.ijpharm.2013.12.054
78. Stokes JR, Frith WJ. Rheology of gelling and yielding soft matter systems. *Soft Matter*. 2008;4(6):1133-1140.doi:10.1039/B719677F
79. Osborne DW, Musakhanian J. Skin Penetration and Permeation Properties of Transcutol(R)-Neat or Diluted Mixtures. *AAPS PharmSciTech*. 2018;19(8):3512-3533. doi:10.1208/s12249-018-1196-8
80. Barry BW. Mode of action of penetration enhancers in human skin. *J Control Release*. 1987;6(1):85-97.doi:10.1016/0168-3659(87)90066-6
81. Carrer V, Guzmán B, Martí M, Alonso C, Coderch L. Lanolin-Based Synthetic Membranes as Percutaneous Absorption Models for Transdermal Drug Delivery. *Pharmaceutics*. 2018;10(3):73.doi:10.3390/pharmaceutics10030073
82. Dixit S. Lanolin for Silky, Soft, Smooth Skin. *Chemical-Weekly-Bombay*. 2001;47(10):153-156.
https://www.academia.edu/31299535/Lanolin_for_Silky_Soft_Smooth_Skin
83. Touitou E, Dayan N, Bergelson L, Godin B, Eliaz M. Ethosomes—novel vesicular carriers for enhanced delivery: characterization and skin penetration properties. *J Control Release*. 2000;65(3):403-418.doi:10.1016/s0168-3659(99)00222-9
84. Cevc G. Lipid vesicles and other colloids as drug carriers on the skin. *Advanced drug delivery reviews*. 2004;56(5):675-711.doi:10.1016/j.addr.2003.10.028

85. Ashtikar M, Nagarsekar K, Fahr A. Transdermal delivery from liposomal formulations–Evolution of the technology over the last three decades. *J Control Release*. 2016;242:126-140.doi:10.1016/j.jconrel.2016.09.008
86. Jacob SE, Matiz C, Herro EM. Compositae-associated allergic contact dermatitis from bisabolol. *Dermatitis*. 2011;22(2):102-105.doi:10.2310/6620.2011.10118
87. Gilliet M, Conrad C, Geiges M, et al. Psoriasis triggered by toll-like receptor 7 agonist imiquimod in the presence of dermal plasmacytoid dendritic cell precursors. *Arch Dermatol*. 2004;140(12):1490-1495.doi:10.1001/archderm.140.12.1490
88. Amnuaikit T, Maneenuan D, Boonme P. Evaluation of caffeine gels on physicochemical characteristics and in vivo efficacy in reducing puffy eyes. *J App Pharm Sci*. 2011;1(2):56-59.
http://www.beauty-review.nl/wp-content/uploads/2015/03/Evaluation-of-Caffeine-Gels-on-Physicochemical-Characteristics-and-In-Vivo-Efficacy-in-Reducing-Puffy-Eyes.pdf
89. Touitou E, Levi-Schaffer F, Dayan N, Alhaique F, Riccieri F. Modulation of caffeine skin delivery by carrier design: liposomes versus permeation enhancers. *Int J Pharm*. 1994;103(2):131-136.doi:10.1016/0378-5173(94)90093-0
90. Johnson W, Jr. Final report on the safety assessment of PEG-25 propylene glycol stearate, PEG-75 propylene glycol stearate, PEG-120 propylene glycol stearate, PEG-10 propylene glycol, PEG-8 propylene glycol cocoate, and PEG-55 propylene glycol oleate. *Int J Toxicol*. 2001;20 Suppl 4:13-26.doi:10.1080/10915810152902556
91. Srivastava S, Mishra S, Dewangan J, et al. Safety assessment of the pharmacological excipient, diethylene glycol monoethyl ether (DEGEE), using in vitro and in vivo systems. *DARU Journal of Pharmaceutical Sciences*. 2019;27(1):219-231.
doi:10.1007/s40199-019-00264-5
92. Elder R. Final report of the safety assessment for acetylated lanolin alcohol and related compounds. *J Environ Pathol Toxicol*. 1980;4(4):63-92.
https://www.cir-safety.org/sites/default/files/115_buff3g_suppl.pdf
93. Barrett CW, Hadgraft JW, Caron GA, Sarkany I. The effect of particle size and vehicle on the percutaneous absorption of fluocinolone acetonide. *Br J Dermatol*. 1965;77(11):576-578.doi:10.1111/j.1365-2133.1965.tb14578.x
94. Nicolazzo JA, Morgan TM, Reed BL, Finnin BC. Synergistic enhancement of testosterone transdermal delivery. *J Control Release*. 2005;103(3):577-585. doi:10.1016/j.jconrel.2004.12.007
95. Hoelgaard A, Møllgaard B. Dermal drug delivery — Improvement by choice of vehicle or drug derivative. *J Control Release*. 1985;2:111-120.doi:10.1016/0168-3659(85)90037-9
96. Abdulbaqi IM, Darwis Y, Khan NAK, Abou Assi R, Khan AA. Ethosomal nanocarriers: the impact of constituents and formulation techniques on ethosomal properties, in vivo studies, and clinical trials. *International journal of nanomedicine*. 2016;11:2279-2304.
doi:10.2147/IJN.S105016
97. Ahad A, Aqil M, Kohli K, Sultana Y, Mujeeb M. Enhanced transdermal delivery of an anti-hypertensive agent via nanoethosomes: statistical optimization, characterization and pharmacokinetic assessment. *Int J Pharm*. 2013;443(1-2):26-38.
doi:10.1016/j.ijpharm.2013.01.011
98. Csizmazia E, Erős G, Berkesi O, Berkó S, Szabó-Révész P, Csányi E. Penetration enhancer effect of sucrose laurate and Transcutol on ibuprofen. *Journal of Drug Delivery Science and Technology*. 2011;21(5):411-415.doi:10.1016/S1773-2247(11)50066-8
99. Harrison JE, Watkinson AC, Green DM, Hadgraft J, Brain K. The relative effect of Azone® and Transcutol® on permeant diffusivity and solubility in human stratum corneum. *Pharmaceutical research*. 1996;13(4):542-546.doi:10.1023/a:1016037803128
100. Dragicevic N, Maibach HI. *Percutaneous penetration enhancers chemical methods in penetration enhancement: nanocarriers*. 1st ed. Springer; 2016. Accessed May 06, 2021. https://link.springer.com/content/pdf/10.1007%2F978-3-662-47862-2.pdf
101. Yousef SA, Mohammed YH, Namjoshi S, et al. Mechanistic Evaluation of Enhanced Curcumin Delivery through Human Skin In Vitro from Optimised Nanoemulsion Formulations Fabricated with Different Penetration Enhancers. *Pharmaceutics*. 2019;11(12):639. doi:10.3390/pharmaceutics11120639
102. Haq A, Michniak-Kohn B. Effects of solvents and penetration enhancers on transdermal delivery of thymoquinone: permeability and skin deposition study. *Drug Delivery*. 2018;25(1):1943-1949.doi:10.1080/10717544.2018.1523256

103. Lee B, Warshaw E. Lanolin allergy: history, epidemiology, responsible allergens, and management. *Dermatitis*. 2008;19(2):63-72.doi:10.2310/6620.2008.07060
104. Kligman AM. The myth of lanolin allergy. *Contact Dermatitis*. 1998;39(3):103-107. doi:10.1111/j.1600-0536.1998.tb05856.x
105. López-Mesas M, Christoe J, Carrillo F, Crespi M. Supercritical fluid extraction with cosolvents of wool wax from wool scour wastes. *The Journal of Supercritical Fluids*. 2005;35(3):235-239.doi:10.1016/j.supflu.2005.01.008
106. Boncheva M, Damien F, Normand V. Molecular organization of the lipid matrix in intact Stratum corneum using ATR-FTIR spectroscopy. *Biochimica et Biophysica Acta (BBA) - Biomembranes*. 2008;1778(5):1344-1355.doi:10.1016/j.bbamem.2008.01.022
107. Coderch L, Fonollosa J, Martí M, Parra JL. Ceramides from wool wax. *Journal of the American Oil Chemists' Society*. 2004;81(9):897-898.doi:10.1007/s11746-004-0998-0
108. Djajadisastra J, Sutriyo H. Percutane transport profile of caffeine and aminophillin as anticellulite and the influences of other substances on in vitro penetration.*International Journal of Pharmacy and Pharmaceutical Sciences*. 2014;6(5):532-538. https://innovareacademics.in/journal/ijpps/Vol6Issue5/9436.pdf
109. Sengupta A, Behera J. Comprehensive view on chemistry, manufacturing & applications of lanolin extracted from wool pretreatment. *American Journal of Engineering Research*. 2014;3(7):33-43.https://ajer.org/papers/v3(7)/F0373343.pdf
110. Sagiri SS, Behera B, Pal K, Basak P. Lanolin-based organogels as a matrix for topical drug delivery. *Journal of applied polymer science*. 2013;128(6):3831-3839. doi:10.1002/app.38590
111. Flockhart IR, Steel I, Kitchen G. Nanoemulsions derived from lanolin show promising drug delivery properties. *J Pharm Pharmacol*. 1998;50(S9):141-141. doi:10.1111/j.2042-7158.1998.tb02341.x
112. Williams AC, Barry BW. Skin absorption enhancers. *Crit Rev Ther Drug Carrier Syst*. 1992;9(3-4):305-353. https://pubmed.ncbi.nlm.nih.gov/1458546/
113. Barry B, Williams A. Penetration enhancers. *Adv Drug Deliv Rev*. 2003;56(5):603-618.doi:10.1016/j.addr.2003.10.025

Chapter 3. The Reliability of a Standardised Tool for Evaluating Severity of Cellulite in the Female Posterior Thigh

(Submitted / Under review)

Ponto T, Benson HAE and Wright A. The Reliability of a Standardised Tool for Evaluating Severity of Cellulite in the Female Posterior Thigh.

Submitted (22 February 2022) in the Journal of Cosmetic Dermatology (JCD-09-2021-1339).

Abstract

Background: Numerous products and minimally-invasive procedures are available to reduce cellulite. However, there are a limited number of tools to evaluate the effects of these interventions and some are relatively complex to implement. ***Objectives:*** This study evaluated the reliability of a standardised grading system for scoring the overall severity of cellulite on the posterior thigh. The study evaluated inter-rater and intra-rater (test/retest) reliability of the method and engaged in an iterative process to develop a reliable method to evaluate changes in the appearance of cellulite. ***Methods:*** There were two stages in the validation process. The first stage was an open process without evaluator training. The second stage was a more controlled process with training given and moderator involvement to review grade selections. In the first stage, inter-rater reliability was examined across five evaluators who were asked to evaluate 24 photographs (right thighs) based on a cellulite graded severity chart. During the second stage, the same photographs were examined by paired evaluators who had received additional training. Scores were independently moderated by a third person. The inter-rater reliability and intra-rater reliability over a 4-week interval were evaluated using intraclass correlation coefficients (ICCs). ***Results:*** 24 female participants (18–51 years, mean 31.68±9.03 years) with a mean BMI of 29.04±6.52 participated in the trial. Five female evaluators completed the initial evaluations. In stage 1, the inter-rater reliability ($ICC_{2,5}$) was 0.838 (95%CI:0.700–0.922) and test/retest $ICC_{3,1}$ values ranged from 0.360–0.990. In stage 2, the inter-rater reliability for 2 evaluators improved to 0.978 (95%CI: 0.948–0.991), and the

test/retest reliability of the moderated scoring method improved to 0.993 (95%CI: 0.983–0.997). ***Conclusions:*** The iterative process developed a simple and reliable method of rating cellulite severity, with excellent inter-and intra-rater reliability, based on evaluating images of cellulite against a standard set of graded severity images. A reliable method of assessing cellulite severity is essential for undertaking future clinical trials to evaluate cellulite treatments.

3.1 Introduction

Cellulite is a common problem for women and affects 80–90% of postpubertal females.[1-3] Cellulite mainly appears on the buttocks and the thighs.[1,4] Ginoide Hydrolipodystrophy (GHLD) is the medical term for cellulite, a metabolic disorder of the dermo-epidermal junction associated with an increase in the size and number of adipocytes.[5] The adipose tissue bulges into the dermis and leads to a skin appearance that is often described as "orange peel" or "cottage-cheese like".[6] Currently, there are numerous commercial topical anti-cellulite treatments and minimally-invasive procedures that are used to reduce the appearance of cellulite.[3,7,8] To evaluate the clinical effectiveness of these treatments, a reliable assessment tool is required.

In previous studies, Byun et al.[6] and de Godoy et al.[9] assessed cellulite treatment with different techniques but they did not include detailed descriptions of their assessment methods or provide information on the reliability of their measurement processes. Several assessment systems, for example, the Hexsel cellulite severity scale (CSS)[10] and the Nurnberger-Muller scale[11] to measure cellulite have been developed. Although some of these standardised photonumeric scales were reproducible,[12] the methods have often been relatively complex and difficult or time-consuming to implement practically.[10,12,13] Hexsel et al.[10] assessed the reliability of the CSS in evaluating cellulite of the buttock and thigh regions. They demonstrated good to excellent inter-rater evaluation of different item scores and good to excellent test-retest reliability for a single experienced assessor. De La Casa Almeida et al.[14] assessed the reliability of the CSS in evaluating cellulite of the entire buttock and thigh region and also demonstrated excellent inter-rater and intra-rater reliability. Bielfeldt et al.[15] used standardised images to assess cellulite on the anterior thigh but they did not provide information about the reliability of their assessment process. The primary limitation of the CSS is that it requires very experienced evaluators to rate several different aspects of the cellulite appearance rather

than providing a simple overall score of severity. Other evaluation scales, such as the Global Aesthetic Improvement Scale (GAIS) were not designed for assessing treatment of cellulite but this tool has also been used to evaluate changes of cellulite in clinical trials.[12,16-18] There is a need to develop a simple, easily implemented scoring system to specifically evaluate the severity of cellulite. This would provide a single, clear outcome variable to assess in clinical trials. When using any method to assess and grade visual images it is very important to establish the reliability of the measurements obtained. Reliability can be defined as the extent to which measurements can be replicated[19] and it is important to ensure that assessment processes are reliable before they can be used in longitudinal studies to evaluate treatments. Assessment of reliability has been applied to other visual (photographic) assessment processes. For example, Day et al.[20] conducted a validation study on the Wrinkle Severity Rating Scale (WSRS). Five evaluators were asked to rate 30 photographic images of nasolabial folds using the 5-grade WSRS (1–5). The assessment was repeated two weeks later. Inter-rater agreement ranged from 67.7% to 72.3% and intra-rater agreement ranged from 68.7% to 72.7%, suggesting moderate to good levels of agreement.

Shoshani et al.[21] evaluated the reliability of the Modified Fitzpatrick Wrinkle Scale (MFWS). The validation process involved a two-stage process. In the first stage, nine trained assessors (either dermatologists or plastic surgeons) used a set of 4 reference photographs to grade 40 volunteer's photographs in 2 hours following training. Following the second session, after 12 to 16 days, the 5 assessors who achieved the highest intra- and inter-rater reliability were chosen to carry on with the second stage. In the second stage, each assessor rated a set of 100 photographs, using the MFWS. A follow-up assessment was also carried out after 12 to 16 days. Inter-rater reliability ranged from 0.65 to 0.74 and intra-rater agreement ranged from 0.71 to 0.79, again suggesting moderate to good levels of agreement.

Flynn et al.[22] evaluated 50– upper face photographs from a total of 359 subjects both men and women, using four, 5–point rating scales based on computerised photonumerical images. Twelve evaluators rated the photographs in two separate rating cycles and their scores were analysed to assess inter-and intra-rater reliability. Inter-rater reliability was substantial (>0.60) and intra-rater was high (>0.70) for all wrinkles scales.

Establishing the reliability of any visual assessment scale is important to confirm the utility of that scale in the research or clinical setting. The aim of the present study was therefore to evaluate the reliability of a simplified process to assess the global severity of cellulite on the female posterior thigh, using reference photographs.

3.2 Experimental design

3.2.1 Materials and Methods

3.2.1.1 Participants

This two-stage reliability study recruited healthy females aged from 18 to 55 years, with a BMI > 22 to encompass the normal, overweight and obese ranges, consecutively enrolled from September 2019 to March 2020. All participants presented with at least mild cellulite. We excluded participants who had used anti-cellulite treatment in the past 3 months or had major surgery in the past year, including liposuction or had any scarring of the skin tissues in the upper thigh area. This study was approved by the Ethics Committee of Curtin University (HSE2019–0521). Informed consent was obtained from all participants.

3.2.1.2 Evaluators

Each image was evaluated by five evaluators. The evaluators were all female, held postgraduate qualifications, and had a background in research. Participants expressed a preference for their images to be reviewed by female evaluators. In the initial stage evaluators received written instructions on the process to be followed. In stage 2 more detailed training was carried out with a discussion of images that were more difficult to evaluate.

3.2.1.3 Photographic images

All assessments were carried out in our clinical trial laboratory (~ 4.0 x 4.0 m). The back wall was covered by an adjustable background on a tripod stand and a black matte fabric backdrop, mounted alongside the background. The floor was neutral grey. The participant was illuminated with a high-quality LED light and ambient temperature was controlled in the range of 22–25 °C.

The camera used was a Canon EOS 550D (Rebel T2i / Kiss X4 Digital) (serial no. 2432309240, made in Japan) with a 55-mm lens. The camera was set to AF (autofocus). Essential settings included the aperture size set to F5.6, 1/35 (focal length), and the ISO

(sensitivity to light) set to 800. The shutter speed was set between 1/80 or 1/100 seconds for participants depending on whether they had darker or lighter skin tones. The camera was mounted on a tripod and was placed at a height of 80 cms, 60 cm away from the participant's location.

We placed a 19-inch classic LED ring light (LUVO, Australia) emitting 4,800 lumens to illuminate the participant's posterior thighs. The LED ring light has an adaptable pan head, which can be used to personalise and customise lighting at different heights and angles. It included interchangeable white and yellow filter/diffusers and provided a daylight level of lighting by adjusting the brightness control, which helped to soften the light, reducing glare and harsh shadows. The interval of illumination was adjusted based on the skin tone of each participant and standardised for each photographic session for that participant. By adjusting the interval of illumination it was possible to ensure that the images were not underexposed or overexposed. For example, overexposed images may mask the appearance of cellulite so it is important to ensure that all are appropriately illuminated.

Participants wore a standard black thong and stood on two medical footstools facing the back wall of the laboratory with their arms crossed over their chest. The position of the footstools was marked using tape to ensure that the participant's legs were evenly spread with their feet 55 cms apart.

Images were analysed using Adobe Photoshop Lightroom CC version 10.1 software (Adobe Inc, San Jose, California, USA) and printed on A5 size (5 x 7 inches) glossy photographic paper (Kodak®, Rochester, USA).

During each photography session, the participant's position and lighting conditions were standardised and they were always photographed from the same position and by the same investigator.

3.2.1.4 Cellulite grading

Nine standard photographs (score 0 to 8) were selected as representative of a range of cellulite presentations and presented in order of severity to provide a grading scale chart (Figure 1). Dupont et al.[23] initially developed the scale chart. The standards were selected on their ability to adequately portray a range of cellulite appearances and to be easily reprintable. Permission

was obtained from the authors and we used the standard set of 9 images as the basis for grading cellulite severity in our study participants.[23]

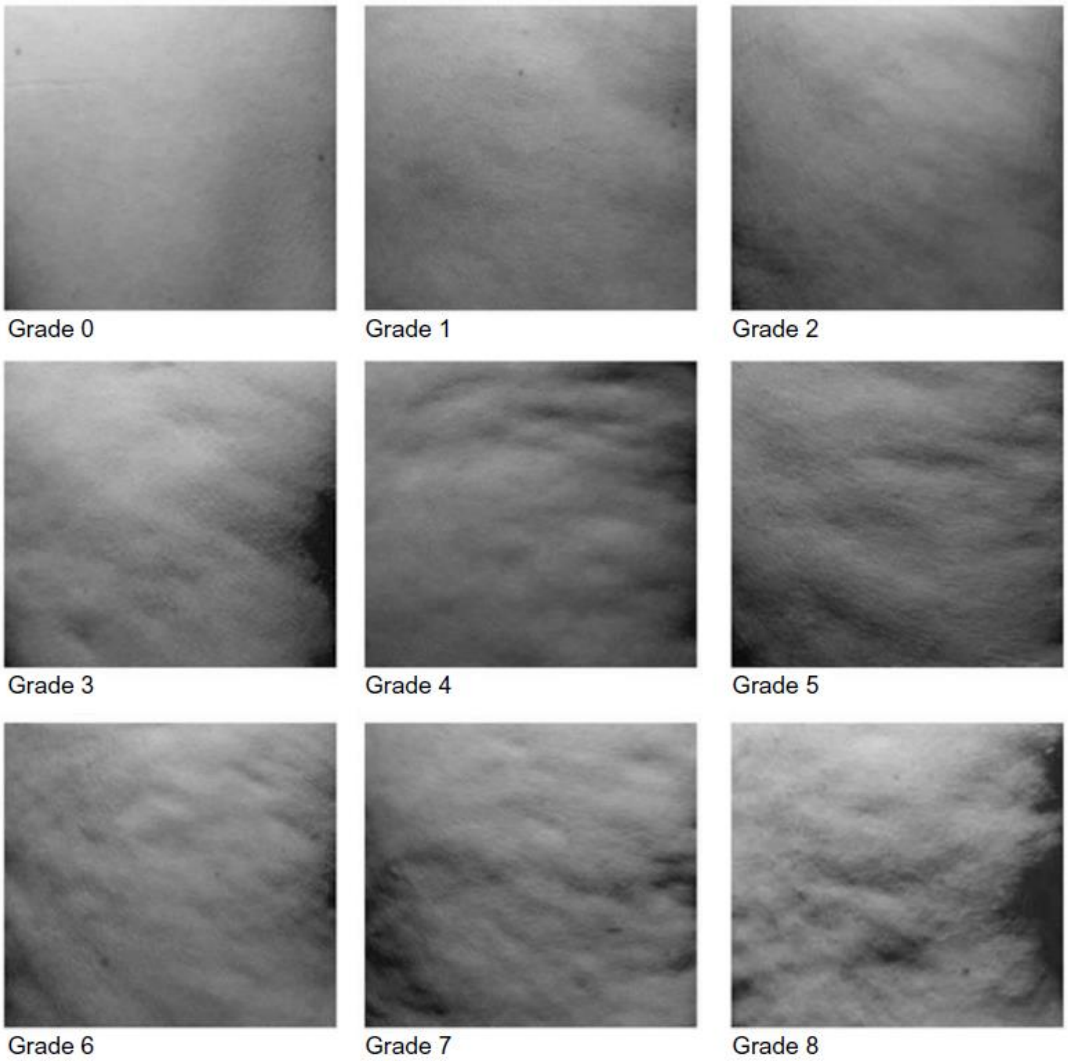

Figure 1. A representation of a grading scale chart for cellulite appearance. The grade goes from 0 to 8 (no intensity and maximum intensity). The figure is reproduced from Dupont et al.[23] with permission

We established a standardised protocol (Table 1) for evaluators to follow to grade images of the cellulite appearance of the posterior thigh relative to a chart based on the 9 standardised images. Evaluators were asked to follow the steps outlined in this protocol and provide a score for the cellulite appearance on the posterior thigh of each participant.

Table 1. Guideline to grade the cellulite appearance

Instructions
1. Review the grading system before viewing the photographs. There are three rows of images depicting cellulite on the upper thighs. The severity of the cellulite images increases from left to right.
2. Turn over the first photograph and note the code of the photograph. Review the photograph and focus on the most severe area of cellulite on the posterior thigh in the assigned area.
3. Compare the cellulite appearance on the photograph to the images on the cellulite grading chart. Based on the appearance of the most severe cellulite area decide which row of images on the grading chart is closest.
4. Next, compare the photograph with the 3-graded images within the chosen row and decide which is most comparable.
5. If there is any doubt between the two grades, select the higher grade.
6. Write down the chosen cellulite grade.
7. Repeat steps 1 – 6 for each photograph, viewing only one photograph at a time.

3.2.1.5 Evaluation of reliability stage 1

In order to evaluate the inherent reliability of the grading process outlined in Table 1 reliability was assessed in an open process with untrained evaluators. The aim was to assess the internal consistency amongst evaluators (inter-rater reliability) and consistency of evaluators in repeated tests (intra-rater reliability). Evaluators were provided with the written instructions outlined in Table 1 but no additional training was provided. The five evaluators were asked to grade one set of photographs of the 24 participants using the severity grading scale chart. Each photograph was evaluated by all evaluators on two occasions, 4 weeks apart. On all occasions, the photographs were presented in a random order for each of the evaluators.

3.2.1.6 Evaluation of reliability stage 2

In this phase, the evaluation process was carried out in a more controlled manner. A pair of evaluators received more detailed training and had additional practice with the scoring process, including discussion of difficult to evaluate images. In addition, a third party acted as a moderator when the 2 evaluators produced non-identical grades. The moderator was required to follow the same steps in the evaluation process and was required to nominate a specific grade rather than simply taking an average of the evaluator scores. Thus, the moderator provided a corrected agreement in the grading process to establish a set of final grades for all of the images. The scoring and moderation process was also repeated after 4 weeks on the same set of images, presented in random order.

3.2.1.7 Statistical analysis

Data were analysed using SPSS® version 26.0 software (SPSS Inc, Chicago, Illinois, USA). Inter-rater reliability and test/re-test reliability were determined by comparing photograph grades amongst evaluators and repeated evaluations. Reliability was assessed using Intraclass Correlation Coefficients (ICC) assessing absolute agreement, based on a two-way random-effects model for inter-rater reliability and two-way mixed-effects model for intra-rater, test/retest reliability. The level of agreement based on the ICC score was rated as poor (0.5), moderate (≥0.50 to <0.75), good (≥0.75to <0.90), or excellent (≥0.90).[19]

3.3 Results

Twenty-four female participants completed the trial from a recruitment cohort of 27. Three participants withdrew due to study commitments and family issues. The age range was from 18–51 years (mean age 31.68 ± 9.03) and the mean BMI was 29.04 (± 6.52). The 5 female evaluators had a mean age of 46 ± 13.13 years.

In stage 1, the inter-rater reliability ($ICC_{2,5}$) for the absolute agreement was 0.838 (95% CI: 0.700–0.922) (Table 2), indicating good reliability, and the intra-rater test/retest $ICC_{3,1}$ values ranged from 0.360–0.990 (Table 3) indicating that intra-rater reliability ranged from poor to excellent depending on the evaluator.

Table 2 Inter-rater reliability analysis (Intraclass correlation coefficient-ICC) (*n= 24*)

	Mean ± SD	**Right**
		ICC value
Evaluator 1	2.92 ± 2.586	
Evaluator 2	2.12 ± 1.262	0.838
Evaluator 3	3.83 ± 2.548	(95% CI: 0.700–0.922)
Evaluator 4	3.71 ± 2.116	*P* value < 0.001
Evaluator 5	3.96 ± 1.922	

Statistical significance *P*-value < 0.05

Table 3 Test-retest reliability analysis (*n= 24*)

		Right	95% CI
Evaluator 1	ICC	0.360	(-0.455–0.721)
	P-value	< 0.1	
Evaluator 2	ICC	0.818	(0.052–0.944)
	P-value	< 0.001	
Evaluator 3	ICC	0.986	(0.969–0.994)
	P-value	< 0.001	
Evaluator 4	ICC	0.990	(0.977–0.996)
	P-value	< 0.001	
Evaluator 5	ICC	0.931	(0.842–0.970)
	P-value	< 0.001	

Statistical significance *P*-value < 0.05

In stage two (following further training), the inter-rater reliability for two evaluators improved to $ICC_{2,2}$ 0.978 (95% CI: 0.948–0.991) (Table 4) indicating excellent consistency of assessment. The intra-rater reliability of the first evaluator was $ICC_{3,1}$ 0.992 (95% CI: 0.982–0.997) and for the second evaluator it was $ICC_{3,1}$ 0.962 (95% CI: 0.912–0.984). Inclusion of the moderator resulted in test/retest reliability of $ICC_{3,1}$ 0.993 (95% CI: 0.983–0.997) indicating excellent reliability, clearly demonstrating that the reliability of the assessment method was further improved by using the moderation approach.

Table 4. Results of the inter-rater reliability analysis (*n= 24*)

	Right	
Evaluator 1 (Mean ± SD)	ICC 0.978	Evaluator 2 (Mean ± SD)
3.83 ± 2.036	*P*-value < 0.001	4.04 ± 2.116

Statistical significance *P*-value < 0.05

3.4 Discussion

This study describes a simple standardised process for assessing the severity of cellulite on the posterior thigh. We evaluated the reliability of grading cellulite images against a set of standardised, graded images using a standardised protocol. The reliability of the scores obtained was evaluated in two stages. In stage 1 all of the evaluators were untrained and the assessment was carried out in a fairly open process to determine the inherent reliability of the assessment protocol. Under these conditions, there was considerable variation between evaluators and although the overall inter-rater reliability was good there was considerable variation in the intra-rater test/re-test reliability. In stage 2 the evaluators received further training by evaluating additional images and by reviewing and discussing images that were considered to be difficult to rate. In addition, a third reviewer acted as a moderator to assign a final score for images in which the primary evaluators did not agree. Using this process, we were able to demonstrate excellent inter-rater reliability and excellent intra-rater test/re-test reliability, thereby improving the value of the grading system as a measure for use in clinical trials. The protocol provides a single measure of overall cellulite severity and it was clear that providing additional evaluator training and including a moderator in the process substantially improved the reliability of the scoring system. It is important to note that ICC ≥ 0.7 is considered to indicate acceptable reliability.[12]

In a previous study, Longhitano et al.[24] assessed cellulite and skin laxity in the area above the knee on both anterior thighs. The knee cellulite severity score (KCSS) was adapted and then modified from the Cellulite Severity Scale (CSS).[10,11] The KCSS evaluated three key cellulite morphological features (number of depressions, depth of depressions, and presence of laxity) and graded each feature from 0 to 3, producing a classification of no lesions (0), mild (1–3), moderate (4–6) and severe (7–9). The classification-standardised cellulite images were scored according to four grades (zero grade, first grade, second grade and third grade). The data showed good to excellent intra-rater reliability results (ICC), 0.91–0.97 (left side) and 0.96–0.98 (right side) among three evaluators. The present study demonstrated similar levels of intra-rater reliability with a further improvement in reliability ($ICC_{3,1}$ 0.993) when we implemented the moderation method.

Cohen et al.[12] also reported inter-rater and intra-rater reliability values when six clinicians evaluated a change in cellulite severity on the buttocks of adult females. The inter-rater ICC was 0.86 (95% CI: 0.78–0.88) and the range of intra-rater ICCs was 0.80 (95% CI: 0.63–0.89) to 0.89 (95% CI: 0.83–0.93) for both buttocks. These values are comparable to the current stage 1 study although the addition of training and moderation in our study resulted in a further improvement in reliability.

The present study demonstrates that by using a simple rating of overall cellulite severity it is possible to develop a reliable evaluation process. Providing training for the evaluators improve the reliability of the image grading system, and that reliability can be further enhanced by including a moderator to assign a final image grade when two evaluators have assigned different grades for an image.

The present study has not assessed all of the measurement parameters that would be required to establish the cellulite severity score as an outcome measure for future clinical trials. Further research is required to assess the sensitivity of this procedure in assessing clinical change and determining the minimal clinically important difference for this measure. An understanding of these parameters will add to the utility of the cellulite severity measure.

3.5 Conclusion

A standardised method for scoring images of cellulite against a set of graded images of cellulite severity demonstrated moderate inter-rater reliability using minimally trained evaluators. With

the addition of further training inter-rater reliability improved, and with the addition of a moderation process, intra-rater test/retest reliability was excellent. The process of providing a singular grading of overall cellulite severity and using trained evaluators and a moderator to evaluate severity provides a very reliable outcome measure for future clinical trials. The inclusion of a moderator is a strategy that could be adapted for assessing visual changes in other skin conditions.

3.6 Acknowledgements

We acknowledge funding from the Australian Government Research Training Program Scholarship. We thank all of the evaluators for their help in evaluating the photographs, and the study participants for their time and cooperation.

3.7 References

1. Zerini I, Sisti A, Cuomo R, et al. Cellulite treatment: a comprehensive literature review. *J Cosmet Dermatol*. 2015;14(3):224-240.doi:10.1111/jocd.12154
2. Janda K, Tomikowska A. Cellulite–causes, prevention, treatment. *Pomeranian Journal of Life Sciences*. 2014;60(1):29-38. https://pubmed.ncbi.nlm.nih.gov/25518090/
3. Luebberding S, Krueger N, Sadick NS. Cellulite: an evidence-based review. *Am J Clin Dermatol*. 2015;16(4):243-256.doi:10.1007/s40257-015-0129-5
4. Herman A, Herman AP. Caffeine's mechanisms of action and its cosmetic use. *Skin Pharmacol Physiol*. 2013;26(1):8-14.doi:10.1159/000343174
5. Freire TB, Dario MF, Mendes OG, et al. Nanoemulsion containing caffeine for cellulite treatment: characterization and in vitro evaluation. *Brazilian Journal of Pharmaceutical Sciences*. 2019;55:e18236.doi:10.1590/s2175-97902019000218236
6. Byun S-Y, Kwon S-H, Heo S-H, Shim J-S, Du M-H, Na J-I. Efficacy of Slimming Cream Containing 3.5% Water-Soluble Caffeine and Xanthenes for the Treatment of Cellulite: Clinical Study and Literature Review. *Annals of dermatology*. 2015;27(3):243-249. doi:10.5021/ad.2015.27.3.243
7. Bazela K, Debowska R, Tyszczuk B, Rogiewicz K, Eris I. Noninvasive Techniques for Anti-cellulite Product Efficacy Evaluation. *Cosmetics and toiletries*. 2011;126(5),
8. Dias M, Farinha A, Faustino E, Hadgraft J, Pais J, Toscano C. Topical delivery of caffeine from some commercial formulations. *Int J Pharm*. 1999;182(1):41-47. doi:10.1016/S0378-5173(99)00067-8
9. de Godoy JM, Groggia MY, Ferro Laks L, Guerreiro de Godoy Mde F. Intensive treatment of cellulite based on physiopathological principles. *Dermatol Res Pract*. 2012;2012:834280.doi:10.1155/2012/834280
10. Hexsel D, Dal'forno T, Hexsel C. A validated photonumeric cellulite severity scale. *J Eur Acad Dermatol Venereol*. 2009;23(5):523-528. doi:10.1111/j.1468-3083.2009.03101.x
11. Nürnberger F, Müller G. So-called cellulite: an invented disease. *The Journal of Dermatologic Surgery and Oncology*. 1978;4(3):221-229.
doi: 10.1111/j.1524-4725.1978.tb00416.x
12. Cohen JL, Sadick NS, Kirby MT, et al. Development and Validation Clinician and Patient Reported Photonumeric Scales to Assess Buttocks Cellulite Severity. *Dermatol Surg*. 2020;46(12):1628. doi:10.1097/DSS.0000000000002756
13. Robinson DM, Kaminer MS. Cellulite: a review of pathogenesis-directed therapy. 2017:179-184.doi:10.12788/j.sder.2017.031.
14. De La Casa Almeida M, Suarez Serrano C, Jiménez Rejano JJ, Chillón Martínez R, Medrano Sánchez EM, Rebollo Roldán J. Intra- and inter-observer reliability of the application

of the cellulite severity scale to a Spanish female population. *J Eur Acad Dermatol Venereol*. 2013;27(6):694-698.doi:10.1111/j.1468-3083.2012.04536.x
15. Bielfeldt S, Buttgereit P, Brandt M, Springmann G, Wilhelm KP. Non-invasive evaluation techniques to quantify the efficacy of cosmetic anti-cellulite products. *Skin Res Technol*. 2008;14(3):336-346.doi:10.1111/j.1600-0846.2008.00300.x
16. Kaminer MS, Coleman III WP, Weiss RA, Robinson DM, Coleman IV WP, Hornfeldt C. Multicenter pivotal study of vacuum-assisted precise tissue release for the treatment of cellulite. *Dermatol Surg*. 2015;41(3):336-347.doi:10.12788/j.sder.2017.031
17. Petti C, Stoneburner J, McLaughlin L. Laser cellulite treatment and laser-assisted lipoplasty of the thighs and buttocks: Combined modalities for single stage contouring of the lower body. *Lasers Surg Med*. 2016;48(1):14-22.doi:10.1002/lsm.22437
18. Sadick NS, Goldman MP, Liu G, et al. Collagenase clostridium histolyticum for the treatment of edematous fibrosclerotic panniculopathy (cellulite): a randomized trial. *Dermatol Surg*. 2019;45(8):1047.doi:10.1097/DSS.0000000000001803
19. Koo TK, Li MY. A guideline of selecting and reporting intraclass correlation coefficients for reliability research. *J Chiropr Med*. 2016;15(2):155-163. doi:10.1016/j.jcm.2016.02.012
20. Day DJ, Littler CM, Swift RW, Gottlieb S. The wrinkle severity rating scale. *Am J Clin Dermatol*. 2004;5(1):49-52.doi:10.2165/00128071-200405010-00007
21. Shoshani D, Markovitz E, Monstrey SJ, Narins DJ. The modified Fitzpatrick Wrinkle Scale: a clinical validated measurement tool for nasolabial wrinkle severity assessment. *Dermatol Surg*. 2008;34 Suppl 1:S85-91; discussion S91. doi:10.1111/j.1524-4725.2008.34248.x
22. Flynn TC, Carruthers A, Carruthers J, et al. Validated Assessment Scales for the Upper Face. *Dermatol Surg*. 2012;38(2 Spec No.):309-319. doi:10.1111/j.1524-4725.2011.02248.x
23. Dupont E, Journet M, Oula ML, et al. An integral topical gel for cellulite reduction: results from a double-blind, randomized, placebo-controlled evaluation of efficacy. *Clin Cosmet Investig Dermatol*. 2014;7:73-88. doi:10.2147/ccid.S53580
24. Longhitano S, Galadari H, Cascini S, et al. A validated photonumeric cellulite severity scale for the area above the knees: the knee cellulite severity score. *J Eur Acad Dermatol Venereol*. 2020;34(9):2152-2155.doi:10.1111/jdv.16269

Chapter 4. Targeted Topical Delivery of Caffeine (CAF) in the Management of Cellulite

4.1 Introduction

Chapter 2 reported the successful development of several novel nanoemulsion-based semisolid systems (creams) for CAF skin delivery. In addition, we demonstrated that cream formulations can enhance the penetration/permeation of CAF into and through the skin. Prior to examining the efficacy of our CAF cream for cellulite reduction in healthy women, we validated a simple and reliable tool for evaluating cellulite on the posterior thigh in clinical and experimental settings (Cellulite Severity Scale - Chapter 3). The optimised 2% CAF nano-cream formulation containing LAN was selected because it has shown good skin permeation in our in vitro experiments.

4.1.1 Treatment of cellulite

In recent years, many topical products and minimally invasive procedures have been developed to help treat and minimise the appearance of cellulite. Therefore, cellulite treatments can be divided into two main therapeutic categories; minimally invasive procedures and pharmacological agents.

4.1.1.1 Minimally-invasive procedures

Several non-surgical methods have been developed to overcome the dimpled or irregular skin appearance known as cellulite. Most of the procedures use various devices to target the fibrous septae, collagenous structures linking muscle to the overlying skin. Cellulite is an abnormal condition in which the septae form a honeycomb structure, which allows fat layers through to the region underlying the skin.[1,2]

There are several minimally–invasive procedures that have been employed to treat cellulite: physical methods,[3-5] energy-based devices,[3,5] and injectable biologic agents.[5]

Physical methods

***Endermologie (lipomassage)*:** An electrically powered handheld massage machine that uses positive pressure from two revolving rollers and negative pressure from a vacuum chamber.[4,6,7] As the machine is moved over the affected area of skin, folds of skin (protected by a nylon

cover) are sucked into the machine.[8] This is thought to stimulate the subcutaneous tissue structure and improve lymphatic drainage.[8,9] LPG® endermologie® (LPG Systems, Valence, France) was introduced by French engineer Louis-Paul Guitay.[9] Previously, LPG® was used to treat trauma and burn scars, but it has been approved by the U.S. Food and Drug Administration (FDA) as a non–invasive method to reduce the appearance of cellulite.[5] There is currently little published data to support the efficacy of lipomassage machines and the cost of treatment is relatively high.[10]

***Liposuction*:** Another mechanical method for removing subcutaneous adipose tissue introduced in the 1970s.[5,11] Liposuction has become well established, and standard suction lipoplasty has been claimed to improve body contouring.[12] Although others have suggested that liposuction may cause secondary cellulite (as a result of damage to the fibrous septae) and lead to an increased dimpled appearance after the procedure.[5,13] It has also been suggested that this procedure could be combined with ultrasonic stimulation, potentially resulting in a less destructive procedure compared with conventional liposuction.[14] However, liposuction is not recommended for diminishing the appearance of dimples due to a poor cosmetic outcome and the potential for minor trauma to surrounding connective tissue.[4]

***Subcision*:** A conventional procedure that can be performed manually by inserting a tri bevelled 16– or 18–G needle (BD Nokor Needle, Bectron, Dickinson and Company, Franklin Lakes, NJ) into the deep dermal layer to release the fibrous septae under a local anesthetic agent (lidocaine).[3] A new approach using a tissue stabilised-guided subsicion (TS-GS) system (Cellfina®; Ulthera/Merz, Meza, AZ), with a vacuum-assisted chamber and a microblade that can extend to precisely 6mm or 10mm in depth to mechanically release the fibrous septae through a forward and backward motion has been developed.[1,15] The manual procedure and vacuum-assisted subsicion have proven effective in smoothing the skin topography by releasing the collagen-rich subdermal septae.[5] Although controlled, vacuum-assisted subsicion has been approved by the U.S. FDA and reported positive lasting results > 3 years, there are potential negative effects associated with the treatment.[3] These include pain, bruising and bleeding under the skin (hematoma).[4]

Energy-based devices

Energy-based devices utilise power from various sources, including radiofrequency (R.F.), light amplification by stimulated emission of radiation (LASER) and light and acoustic wave therapy, extensively used to treat subcutaneous fat lobules and skin laxity improvement.[3]

***Radiofrequency (R.F.)*:** Two types of R.F. technology have been used to treat cellulite, first-generation (unipolar, monopolar and bipolar) systems and second-generation multipolar devices.[3] Some R.F. devices also include other energy systems, such as infrared light, vacuum suction and pulsed-electromagnetic fields.[3] Thermal energy is generated from the impedance electrodes and then delivered through the skin tissue, with different depths of penetration for monopolar (≥ 2cm) and multipolar (< 1 cm to > 4 cm) systems.[3,16] A combination R.F. technology had been approved by the U.S. FDA using bipolar and infrared light energy concurrently to target cellulite, particularly reduction in thigh circumference (Velasmooth™; Syneron Medical Ltd, Yokneam, Israel). The device creates heat when it penetrates adipose tissue, increasing oxygen uptake and fat metabolism. In addition, the negative tissue massage promotes lymphatic fluid drainage and stretches the fibrous septa network in connective tissue. Therefore, it has been suggested that Velasmooth™ can improve skin dimpling.[1,17]

***LASER and other light sources*:** Another minimally invasive technology that has been used to treat cellulite. Heat is produced from a 1440–nm Nd: YAG (neodymium-doped yttrium aluminium garnet) LASER combined with a side-firing fibre to distribute light energy laterally through the skin a thermal sensing cannula to avoid overheating. This system is thought to stimulate collagen production and increase microcirculation, improving the skin surface appearance.[3,5] Although this device's impact is not very substantial, it has demonstrated significant cellulite reduction.[3] Moreover, the benefits of LASER treatment requires only a single treatment with minimal side effects and good patient satisfaction related to the clinical outcome.[3] However, there are some limitations in terms of any quantitative changes in skin characteristics and LASER may have unpredictable effects on connective tissue characteristics.[18]

Acoustic wave therapy (AWT): An energy-based therapy consisting of two types, focused extracorporeal shock waves therapy (ESWT) and radial shock wave therapy. Both have been used to treat cellulite.[19] ESWT uses high–electrical energy pulses to trigger pressure waves

and create mechanical disruption without cytolysis (disruption of cells).[20] The pressure waves are transmitted into the tissues to penetrate the deeper skin layers (dermis, adipose and fibrous septae). ESWT improves local blood flow, promotes lipolysis, and stimulates collagen production.[3,5] Radial shock therapy produces dispersed form energy that can diffuse up to 25 mm, reaching connective tissue and subcutaneous fat lobules.[21] AWT requires several sessions to demonstrate its effectiveness in reducing cellulite, although the advantage of AWT is that each session does not require the application of a topical anesthetic.[22] Side effects of this treatment are minor pain, minor rashes, and minor bruising in the assigned area of treatment.[22,23]

Although the efficacy of these minimally–invasive procedures for cellulite reduction has been documented in peer-reviewed literature, most of these treatments exhibit complications in terms of pain,[4,23] erythema,[1,23] bruising,[4,23-26] and thermal skin injury.[27] Other limitations that need to be considered include relatively high cost,[10,28] multiple treatment sessions required,[27,29,30] some poor cosmetic outcomes,[4,9,31] suitability for pregnant women,[9,23] and monitoring and post-treatment follow–up requirements. [32-34]

As a result, alternative therapeutic approaches have been developed over the years. This chapter focuses on topical and transdermal treatment with minimal side effects.[35] Topical and transdermal delivery offers a comfortable route of administration for various types of clinical indications.[36] The other advantage is that it provides a safe, painless treatment for self-administration by clients.[37,38] Topical semisolid products, in this case, the cream products are well-accepted by patients.[39] Topical treatment may also show good results and require minimal follow-up.[23,38]

4.1.1.2 Pharmacological agent

Topical agents can provide noninvasive treatments for cellulite. Many topical treatments have been developed and evaluated over the years.[23] Methylxanthine alkaloids are commonly used as a natural topical treatment of cellulite.[40] Methylxanthine alkaloids are derived from *Coffea arabica,* L., *Camellia sinensis*, (L.) Kuntze, *Paullinia cupana* Kunth var. sorbilis (Mart.) Ducke and *Ilex paraguariensis* (A.) St. Hill.[38] Amongst other xanthine alkaloids, CAF is the safest, either extracted from plants or synthesised as a chemical compound.[38] CAF has also demonstrated its efficacy for cellulite reduction in many clinical trials.[23,41] The concentration

of CAF that is normally used to treat cellulite varies from 1-2 percent.[40,42] However, some marketed topical anticellulite products contain between 3% and 7% of CAF[43-45] CAF is used as a treatment because it prevents excessive fat accumulation in cells.[23] Topical CAF acts directly on adipose cells,[42] enhancing lipolysis,[35,42] stimulating the peripheral microcirculatory flow,[46] and reducing edema (inflammation).[40,47] The mechanism of action of CAF involves inhibition of phosphodiesterase activity, stimulation of cyclic adenosine monophosphate (cAMP) activity, [3,44,46,48] and activation of hormone-sensitive lipase (HSL).[35] This results in a breakdown of adipose tissue during the lipolytic process and improved blood flow.[42]

A summary of studies evaluating the efficacy of topically applied anticellulite creams and creams in combination with mechanical methods is presented in Table 4.1.

Table 4.1 Studies evaluating the efficacy of anticellulite products in humans

Study design; no of participant	Inclusion criteria (age; BMI; grade of cellulite)	Type of treatment	Formulation type-active ingredients	Frequency of application and duration treatment	Target specific of the body part	Outcomes	Ref
D.B., randomised, placebo-controlled study; 46 healthy women	≥ 18 years; 20-25 kg/m^2; moderate	Topical and mechanical	Cream containing retinol, CAF, alcohol and ruscogenine extract	Twice/day – 3 months	Entire thighs with circular massage	Significant reduction of the orange-peel appearance	[49]
D.B., single center, placebo-controlled study; 41 both men and women	18-65 years; slight to moderate cellulite	Topical	Liposome containing safflower oil, PEG-40 stearate, polysorbate 80, isopropyl myristate, butylene glycol, dimethicone, cyclomethicone, panthenol, imidazolidinyl urea, quaternium 15, tocopheryl acetate, CAF	Twice/day – 2 months	Tricep, hip, abdomen, lateral and posterior thigh	Significant reduction of subcutaneous adipose tissue for all areas using calipers; no significant reduction of subcutaneous adipose tissue for all areas using tape measurement	[28]
D.B., randomised, placebo-controlled study; 40 women	26-74 years; moderate to severe cellulite (minimun score II)	Topical-bioceramic-coated neoprene short	Cream containing botanical extracts and CAF	Once/day – 1 month	Lateral and posterior thigh	Significant reduction of cellulite appearance	[50]

Study design; no of participant	Inclusion criteria (age; BMI; grade of cellulite)	Type of treatment	Formulation type-active ingredients	Frequency of application and duration treatment	Target specific of the body part	Outcomes	Ref
D.B., randomised, placebo-controlled study;50 women	21-49 years	Topical	Solution containing sulfo-carrabiose and CAF	Twice/day – 2 months	Thigh with a small circular movement	Significant reduction in thigh circumference and volume of thighs using a combination of CAF and sulfo-carrabiose	[51]
DB, randomised, placebo-controlled study; 78 women	18-60 years; 20-26 kg/m^2	Topical	Cream containing retinol, carnitine, foskolin, tetrahydroxy ethylenediamine (THPE), CAF	Twice/day – 3 months	Thigh, buttock, hip, stomach	Significant reduction in circumference of waist, abdomen, hip, buttock; significant reduction of orange-peel appearance and improvement of skin tonicity	[52]
D.B., randomised, placebo-controlled study; 50 women	18-45 years; 20-27 kg/m^2	Topical	Cream containing a botanical extract and CAF	Twice/day – 1 month	Thigh, hip	Significant reduction in circumference of upper thigh, volume of thigh; significant improvement in skin tonicity	[53]

Study design; no of participant	Inclusion criteria (age; BMI; grade of cellulite)	Type of treatment	Formulation type-active ingredients	Frequency of application and duration treatment	Target specific of the body part	Outcomes	Ref
D.B., randomised, placebo-controlled study; 21 healthy women	20-55 years; grade ≥ 2 cellulite	Topical	Compress containing 5 additional herbals, CAF from tea and coffee	Twice/day – 2 months	Thigh	Significant reduction in Nürnberger-Müller cellulite score; significant reduction of thigh circumference and skinfold fat thickness	[54]
DB, randomised, placebo-controlled study; 44 healthy women	25-55 years; 24.5-24.8 kg/m^2; slight to moderate cellulite	Topical	Gel containing CAF, retinol, carnitine, escin and a range of botanical extracts	Twice/day – 3 months	Thigh, hip and buttock and stomach with gently massage	Significant improvement in skin tonicity (thigh, hip and buttock); significant reduction of orange-peel appearance in thigh, hip and buttock; significant reduction of stubborn cellulite (thigh, hip and buttock);	[55]

Study design; no of participant	Inclusion criteria (age; BMI; grade of cellulite)	Type of treatment	Formulation type-active ingredients	Frequency of application and duration treatment	Target specific of the body part	Outcomes	Ref
						significant reduction in circumference of thigh and abdomen	
D.B., randomised, placebo-controlled study; 12 healthy women	22-58 years; mild to moderate cellulite	Topical	Cream	Twice/day – 2 months	Thigh and buttock	No significant reduction of cellulite score, thigh circumference, skinfold fat thickness and dermis density thickness; degree of satisfaction to the active product compared with placebo	[56]

Notes: DB= double-blind

A range of studies have evaluated the efficacy of topical products to improve the appearance of cellulite.[28,49-56] For example, a cream containing retinol, CAF and ruscogenine has been proven effective to reduce the orange-peel appearance within 3 months, in combination with several non-invasive methods.[49] Rao et al.[50] also demonstrated the efficacy of a herbal topical cream, concurrently used with bioceramic-coated neoprene shorts that could reduce the appearance of cellulite in a shorter period. The shorts were made from neoprene synthetic rubber embedded with bioceramic technology. The shorts were worn immediately after applying the cream and left overnight for a minimum of 6 hours, thus forming an occlusive membrane and enhancing penetration of the cream. It appears that a combination of topical application and mechanical stimulation may have synergistic activity in human clinical studies.[57]

In combination with multiple active ingredients and a range of botanical extracts, CAF has also been incorporated into a gel formulation, which was evaluated by Dupont et al. to reduce cellulite.[55] These multiple cosmetic active ingredients also cover skin biological ageing mechanisms[58] since cellulite impacts skin ageing.[59] Dupont's study did not evaluate for individual active ingredients. Although, many previous studies have supported that multiple active ingredients can give synergetic action to improve cellulite appearance.[49,51-53,57] Moreover, a mixture of CAF with retinol and carnitine was able to reduce the orange-peel appearance and increase microcirculation.[52] Those ingredients improved the skin tonicity and diminished orange-peel appearance in thigh, hip and buttock after 3-months. Although this study provided a promising approach, it was difficult to distinguish either the performance of a single ingredient or multi-active ingredients due to the complexity of cellulite. There is a clear need for a simple method that can effectively deliver CAF to the skin in a formulation that could be made commercially available.

We found most published human clinical trials carried out the same parameters to assess the efficacy of anticellulite creams. Clinical assessments mainly determined the efficacy of the topical products. Clinical parameters included assessing reduction in thigh circumference measurements, in skinfold cutaneous thickness, and reduction of scoring the orange-peel appearance.[46]

In this current study, our novel topical creams were specifically designed with a combination of chemical penetration enhancers to increase CAF penetration and reduce cellulite. Prior to examining the efficacy of CAF creams, skin permeation studies were carried out to determine the fluxes through porcine skins. Roure et al.[52] and Al-Bader et al.[57] carried out the same principle. The *in vitro* and *ex vivo* experiments showed that a combination of ingredients gave synergistic effects on stimulating keratinocyte proliferation and pro-collagen I production. In combination with LAN, we proved our CAF nano-cream formulation showed higher flux on porcine skin (see Chapter 2).

Therefore, the current study was a proof of concept trial to determine the clinical effectiveness of our CAF formulation, compared to a vehicle placebo, in human participants. The primary objective was to investigate the effect of the optimised CAF cream relative to placebo cream on cellulite appearance over 12 weeks. The secondary objective was to assess whether the formulated CAF cream could reduce thigh circumference (T.C.) and skinfold thickness (S.T.) over the 12 weeks. In addition, the study assessed participants' perception of the sensory qualities of the cream products.

4.1.2 Research questions

Research questions addressed in this study included:

1. Does daily topical application of the CAF cream reduce the severity score for cellulite on the posterior thigh of female participants in comparison to a placebo cream?
2. Does daily topical application of the CAF cream reduce T.C. of female participants in comparison to a placebo cream?
3. Does daily topical application of the CAF cream can reduce S.T. on the posterior thigh of female participants in comparison to a placebo cream?
4. Does daily topical application of the CAF cream improve participants' perception of cellulite appearance?
5. Do the participants have positive perceptions of the products?

4.2 Experimental design

4.2.1 Materials and Methods

4.2.1.1 Study design

This study was a randomised, double-blind, placebo-controlled proof of concept trial. Each participant applied the CAF cream and the placebo to regions on their posterior thighs twice daily based on a random allocation. The study utilised a repeated measures design to evaluate the intervention over 12-weeks.

4.2.1.2 Participant' recruitment

24 healthy female participants aged between 18 to 55 years, with a BMI > 22, were recruited via advertisements on noticeboards around the Bentley and Victoria Park areas, and online advertising via Curtin weekly and the School of Pharmacy and Biomedical Sciences Facebook pages (sample of the flyer attached in APPENDICES page 175). We referred to a previous study,[41,54] in which power was calculated at 84% for a total sample size of 42 legs (21 participants) with an effect size (E.S.) of 0.33 between 2 treatments (6 measurements) over 6-time points.

Therefore, in our study, we calculated that an E.S. of 0.33 could be detected with a sample size of 24 participants equal to 48 legs (80% power) and repeated measures of 2 treatments (active vs placebo) over 4-time points (G*Power 3.1.9.4).

Participants were excluded if they had used anticellulite treatment in the past 3 months or had major surgery in the past year, including liposuction, or had any scarring of the skin tissues in the posterior thigh area. At the start of the study, a pre-screening process was carried out to determine the eligibility of participants. Participants who met the selection criteria and decided to participate then provided written consent. Participants received a gift card amount of A$20 for their participation in the study. The Ethics Committee of Curtin University (HSE2019-0521) approved the study and the trial was also registered on Australia and New Zealand Clinical Trials Registry (ANZCTR) (ACTRN12619001547134). The study also followed the Declaration of Helsinki (DoH) version 7 (Brazil, 2013) guidelines for human subjects' medical research.

4.2.1.3 Preparation of cream formulations

A batch of the optimised nano-cream formulation containing LAN (2% CAF) and placebo nano-cream (cream base with no CAF) was prepared and packaged into cream jars in the Skin Delivery laboratory, building 306 Room 102 at the Curtin Medical School, Curtin University. The formula was stated in Chapter 2 (Table 2.4). Participants were provided with two jars of cream (active and placebo) and with two spatulas for every 4 weeks application period. The cream jars were marked as "A" and "B" by one member of the study team (A.W.), who prepared the randomisation schedule (Figure 4.1). Participants were advised individually to apply cream A and cream B to specific legs. Randomisation was carried out using computer-generated random numbers based on the randomisation schedule. A.W. did not participate in any data collection for the trials. All ingredients used in the creams were pharmaceutical grade and were categorised as GRAS (Generally Regarded as Safe) by the U.S. FDA.

Figure 4.1 Topical cream formulations: (A) Caffeine (CAF) (B) placebo (vehicle only)

4.2.1.4 Study site

The study was conducted in the Curtin Health Innovation Research Institute (CHIRI) clinical research facility in Building 305, Room 128, equipped with individual rooms with a treatment plinth. The temperature and humidity of the facility were controlled, and the light was suitable for photographic assessments. An example of the photography room set-up in the clinical trial laboratory is shown in Figure 4.2.

4.2.1.5 Cream effect testing protocols

At day 0 (baseline) and 4, 8 and 12 weeks, a standardised group of testing procedures were conducted:

4.2.1.5.1 Standardised cellulite photographs and scoring

A standardised series of photographs were taken using a digital SLR camera (Canon type EOS 550D (Rebel T2i / Kiss X4 Digital) (serial no. 2432309240) made in Japan) and a high-quality LED ring light (LUVO, Qld, Australia) placed on a tripod at a predetermined height and distance from the treatment site. Participants wore a standardised black thong for all photographic sessions for the measurement process. The participant then stood with their feet placed in a marked position on the floor. Images were coded and used to evaluate cellulite severity. Two evaluators and an independent moderator carried out cellulite severity scoring to determine a severity score for each participant at each testing session. The reliability of the cellulite severity scoring process has been described in Chapter 3.

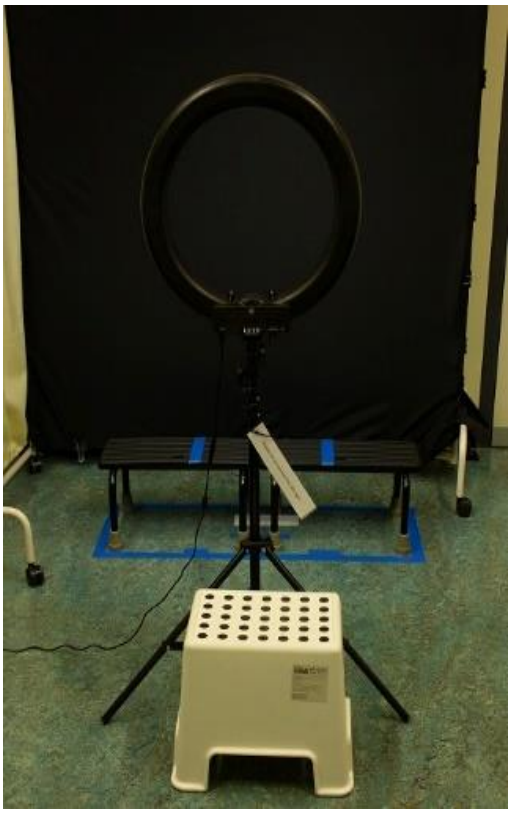

Figure 4.2 Image of photography room set up in the clinical trial laboratory

4.2.1.5.2 Measurement of thigh circumference

The thigh circumference was measured in millimetres at a distance of 150 mm proximal to the patella, which was a mid-way point in the treatment site, using a standard measuring tape (Figure 4.3). Triplicate measurements were conducted by the study coordinator (TP).

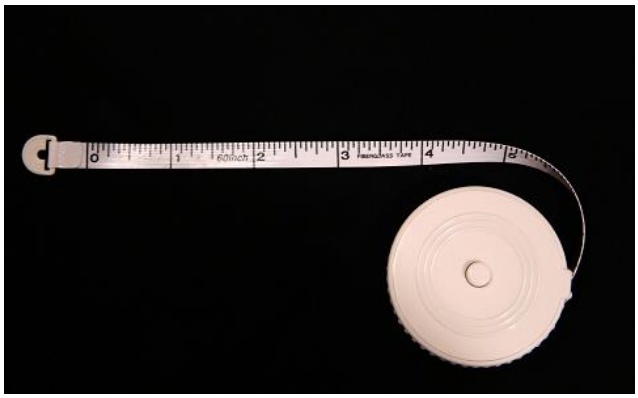

Figure 4.3 Image of the flexible measuring tape

4.2.1.5.3 Measurement of skinfold thickness

The skin-fold thickness was measured at a mid-way point within the treatment site (as described in 4.2.1.5.2 above). Each skin-fold measurement was taken by gripping the skin with the thumb and index finger, 1 cm away from the measurement point, then measuring the skinfold thickness with a Harpenden body fat plicometer (calliper; Figure 4.4) (Baty International, Sussex, UK). Triplicate measurements were conducted by the same evaluator (TP).

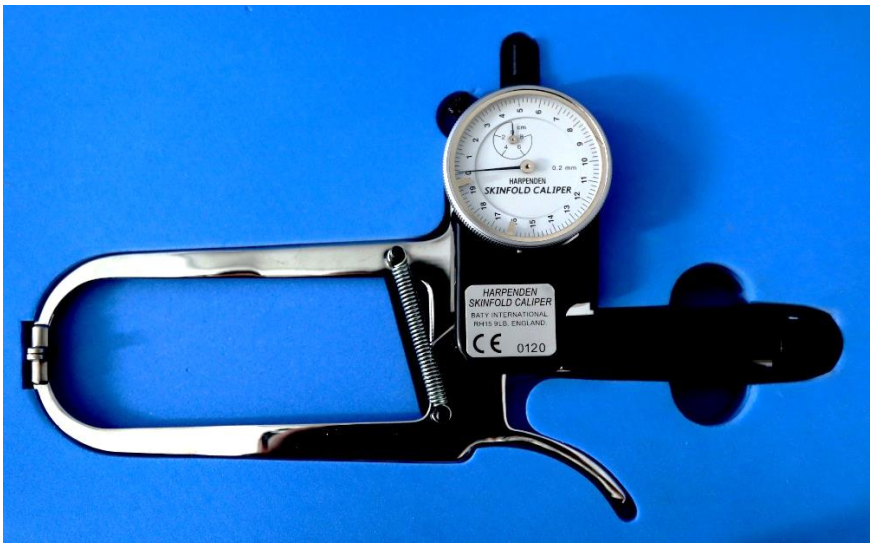

Figure 4.4 Image of Harpenden body fat plicometer (calliper)

4.2.1.5.4 Participant self-assessment

At weeks 4, 8 and 12, participants completed a questionnaire to assess their perception of the suitability of the cream products and the effects on their skin. Participants answered a five-point Likert scale questionnaire concerning colour, smell, absorption, spreadability, stickiness and skin feeling of the products. They also answered a five-point Likert scale questionnaire

concerning the subjective change in dimpled appearance, degree of moisture, elasticity and smoothness of the skin.

At week 12, participants also completed a seven-point global rating of change (GROC) scale ("since applying the creams, the cellulite on my thigh is: much worse, worse, somewhat worse, the same, somewhat better, better, much better than before application") (sample questionnaires attached in APPENDICES page 175).

4.2.1.6 Study procedure

At the start of the study, participants were screened to ensure they met the inclusion criteria. An initial study data sheet was completed in conjunction with the study coordinator. Participants were advised not to change their normal daily routine (diet, exercise, tea and coffee consumption) during the 12-week study period. The daily cream application was explained, and they were advised of the 4-weekly assessment protocols.

The participant was informed that the two cream formulations should be applied twice daily to the posterior thigh areas, morning and night. They were supplied with two cream jars and two separate spatulas and shown the amount of cream to be removed by the spatula and applied to the treatment area. They were advised which cream should be applied to which leg. Each application was applied for approximately 30 seconds rubbing into the assigned area until the creams were wholly absorbed.

After taking baseline measurements (including height, weight, thigh circumference and skin for thickness) and photographs for cellulite evaluation, a time was arranged for the 4–week measurement and photo session. The study coordinator contacted the participant via social media as a reminder prior to each session. This process was repeated at 8 and 12 weeks.

At each visit, participants were asked to return their cream jars and these were weighed to determine the amount of cream usage. Additional jars of cream were provided for the subsequent treatment period. A summary of the clinical trial activities is provided in Table 4.2.

Table 4.2 Clinical trial timetable during the 12–week intervention

Activities	WEEK												
	0	1	2	3	4	5	6	7	8	9	10	11	12
Recruitment and briefing	B												
Discussions					D				D				
Treatments		T	T	T	T	T	T	T	T	T	T	T	T
Measurements	M				M				M				M
Photo sessions	P				P				P				P
Patient satisfaction measure					Q				Q				Q

Notes: B= briefing; D= discussions; T= treatments; M= measurements; P= photo sessions; Q= participant satisfaction questionnaire

4.2.1.7 Management of skin reaction

Participants were asked if they had experienced any skin reaction at each visit. If they did experience any skin reaction, the study coordinator advised them to discontinue the application of the cream. They were then monitored over the following 2 days to resolve the skin reaction. Once the skin reaction resolved, they continued to apply the cream.

4.2.1.8 Statistical analysis

The primary outcome measure was the cellulite severity score. The secondary outcome measures included thigh circumference and skinfold thickness. The participants were included in the analysis if the creams were applied during the 12–week study period and they completed the photo sessions and assessment for each study period. Participants who withdrew and failed to complete the trial were replaced and their data were excluded from the analysis.

For continuous outcomes, means ± S.D. were calculated. Data were analysed using Linear Mixed Models, comparing the effects of the placebo and CAF creams over time. Effect sizes (Cohen's d) were calculated comparing CAF and placebo data at week 12.[60] GROC was assessed with an independent t-test. Stata® version 16.0 (StataCorp, College Station, TX, USA) was used for the analyses.

4.3 Results

4.3.1 Participants

Of the 29 female participants initially screened, 24 participants completed the study (Figure 4.5). The age range was from 18–51 years (mean age 31.68 ± 9.03) and the mean BMI was 29.04 ± 6.52 kg/m^2. Seventeen participants were of Asian or South Asian descent, six were of European descent and 1 was of African descent. Twenty-nine participants completed the pre-screening requirements. Three participants withdrew due to study commitments; one participant withdrew because of a family issue and another participant was excluded because she had tattoos on her posterior thigh.

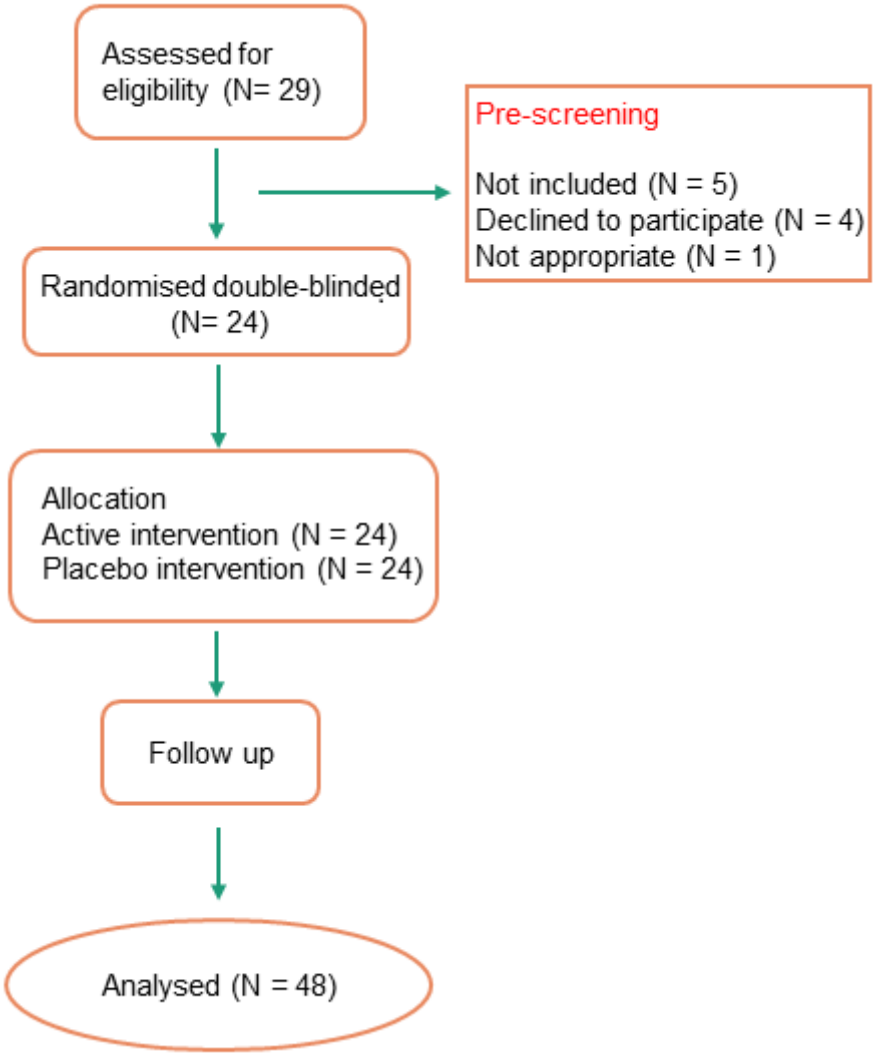

Figure 4.5. CONSORT flow chart. This figure shows the flow of participants through the trial

In the pre-screening session, we found 87.5% of participants had consumed a balanced diet of meat and vegetables. Half of the participants consumed 1 to 2 liters of water per day. The most popular beverages consumed were coffee and tea. The majority of participants consumed more than one beverage. Table 4.3 includes further information regarding the participants' diet and exercise preferences.

Table 4.3 Pre-screening questions on daily diet and exercise

	Pre-screening questions	**N (%)**
1	Usual diet	
	Balanced-meat and vegetables	21 (87.5)
	Vegetarian	2 (8.3)
	Vegan	1 (4.2)
2	Water consumption	
	Less than a litre	7 (29.2)
	1-2 litres	15 (62.5)
	More than 2 litres	2 (8.3)
3	Drinking beverages	
	Coffee	18 (75)
	Tea	18 (75)
	Chocolate	13 (54.2)
	Soda drinks	11 (45.8)
	Energy drinks	4 (16.7)
4	Regular physical exercise	
	Yes	12 (50)
	No	12 (50)

4.3.2 Primary outcome measure

The primary outcome measure of cellulite severity grade was significantly reduced for the CAF cream relative to the placebo cream. After 12 weeks of twice-daily treatment, the CAF cream significantly reduced cellulite severity grade relative to baseline ($p < 0.05$). Placebo treatment resulted in a limited reduction of cellulite (Table 4.4). There was a significant formula*time interaction effect for this measure from week 4 to week 12 (Table 4.4) (Figure 4.6). The Cohen *d* effect size at 12-weeks was 0.475 (Table 4.5), indicating a moderate effect size for a reduction in cellulite severity grade with the CAF cream relative to the placebo cream.

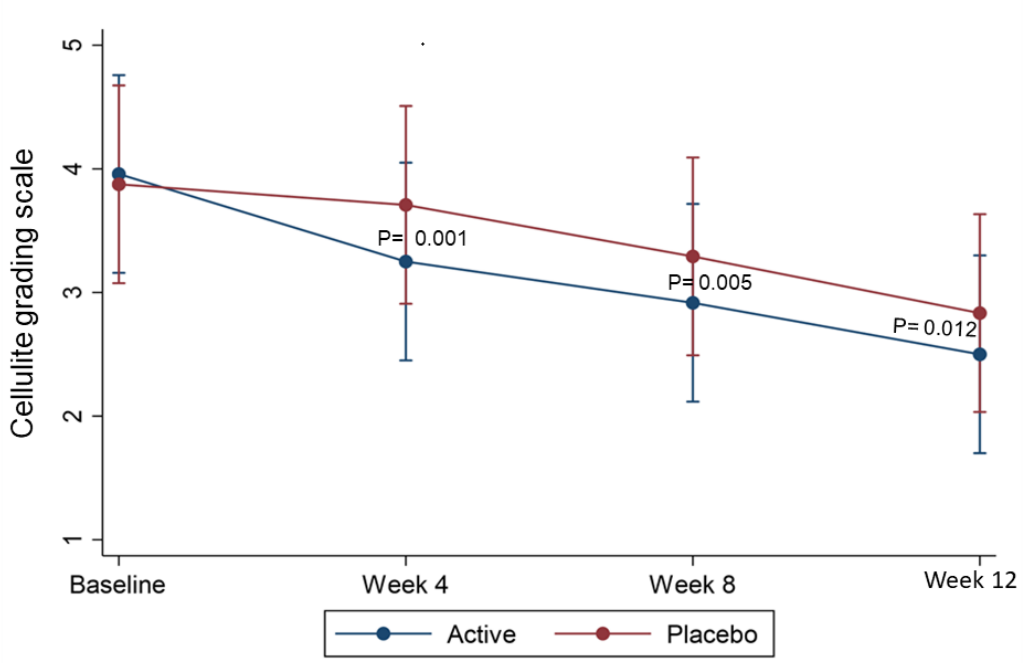

Figure 4.6 Mean (95% CI) cellulite severity grade from the female posterior thighs at baseline (week 0), with 12 weeks of treatment with active and placebo creams

Table 4.4 Mean change of cellulite grading scale, thigh circumference and skinfold fat thickness at baseline, week 4, week 8 and week 12

Measure	Week	CAF cream	*p*-value	Placebo cream	*p*-value	*p*-value
		Mean (95%CI)	baseline to each time point	Mean (95%CI)	baseline to each time point	cross-sectional between-group treatments each time point
Primary outcome measure						
Cellulite grading scale	0	3.96 (3.16-4.76)	-	3.88 (3.08-4.67)	-	0.530
	4	3.25 (2.45-4.05)	< 0.001	3.71 (2.91-4.51)	< 0.001	0.001
	8	2.92 (2.12-3.72)	< 0.001	3.29 (2.49-4.09)	< 0.001	0.005
	12	2.50 (1.70-3.30)	< 0.001	2.83 (2.03-3.63)	< 0.001	0.012
Secondary outcome measures						
Thigh circumference (T.C.)	0	56.56 (59.45-54.05)	-	56.21 (59.05-53.74)	-	0.157
	4	56.09 (58.89-53.64)	0.050	55.96 (58.76-53.53)	0.295	0.613
	8	56.13 (58.96-53.68)	0.081	56.06 (58.86-53.61)	0.519	0.753
	12	56.01 (58.81-53.57)	0.023	55.70 (58.45-53.30)	0.031	0.195
Skinfold thickness (S.T.)	0	13.43 (12.15-14.72)	-	13.47 (12.19-14.76)	-	0.418
	4	13.33 (12.05-14.60)	0.041	13.49 (12.20-14.78)	0.714	< 0.001
	8	13.30 (12.03-14.57)	0.012	13.53 (12.24-14.82)	0.280	< 0.001
	12	13.25 (11.99-14.52)	< 0.001	13.54 (12.25-14.84)	0.168	< 0.001

Table 4.5 Effect size (Cohen's d) calculations for the CAF cream relative to the placebo cream

Measure	Cohen's d
Cellulite grading scale	0.475
Thigh circumference	0.068
Skinfold fat thickness	0.041

4.3.3 Secondary outcome measures

Of the secondary outcome measures related to reducing cellulite appearance, T.C. and S.T. were assessed for the CAF cream compared to the placebo cream (Table 4.4).

Evaluation of T.C.

Table 4.4 summarises the mean circumference measurements for the CAF cream and placebo at each time point at the posterior thighs. After 12 weeks of treatment with the CAF cream, there was a significant reduction of thigh size relative to baseline (mean 56.01; 95%CI: 58.81-53.57; *p*= 0.023). The placebo group however, also showed substantial thigh size reduction (mean 55.70; 95%CI: 58.45-53.30; *p*= 0.031). There was no significant formula*time interaction effect for this measure at week 12 (*p* = 0.195) (Figure 4.7).

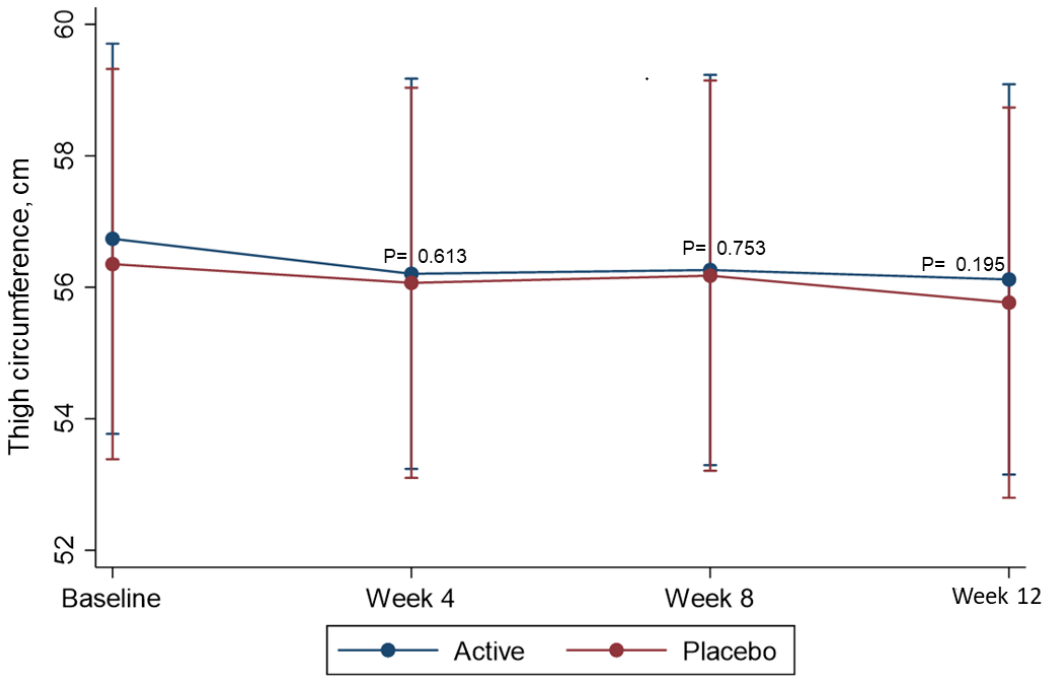

Figure 4.7 Mean (95% CI) of the evolution of thigh circumference (in cm) from the female posterior thighs at baseline (week 0), with 12 weeks of treatment with CAF and placebo creams

Evaluation of S.T.

Table 4.4 shows the mean S.T. measures for the CAF cream and placebo cream at each time point. Starting from week 4 with the anticellulite cream, the S.T. of the posterior thighs significantly reduced in the CAF group relative to the placebo. That difference was maintained until the end of treatment ($p < 0.001$). After 12 weeks of twice-daily application, the millimetric decreases were significant over baseline (mean 13.25; 95%CI: 11.99-14.52; $p < 0.001$) (Table 4.4). The average mean measured reduction was –0.18 mm for posterior thighs (80% of participants improved). The placebo group had no significant reduction on S.T. over baseline. The comparison of the two groups showed a significant formula*time interaction effect for this measure ($p < 0.001$) (Figure 4.8).

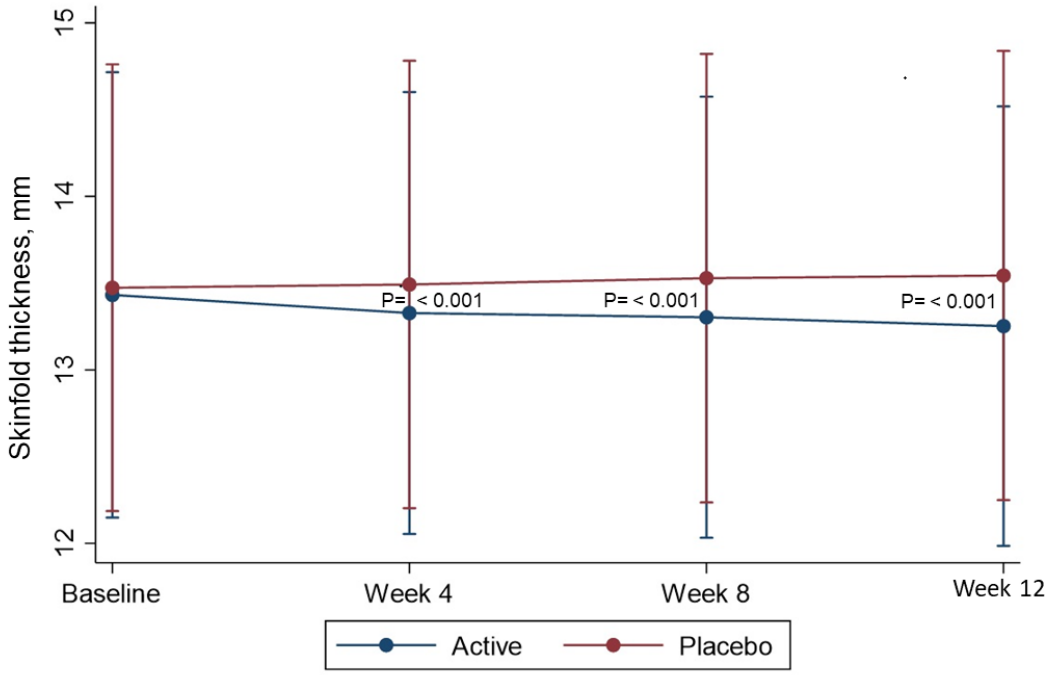

Figure 4.8 Mean (95% CI) of the evolution of skinfold thickness (in mm) from the female posterior thighs at baseline (week 0), with 12 weeks of treatment with CAF and placebo creams

4.3.4 Participant self-measures

Participants completed questionnaires regarding their satisfaction with treatment and the nature of the products. Questionnaires were distributed and completed every 4 weeks.

About the treatment

Mean values for evaluation of hydration, elasticity, and smoothness and dimpled appearance for both creams collected from self-evaluation questionnaires are presented in Table 4.6.

After 4 weeks of using CAF cream, participants indicated that their skin was better hydrated (mean 3.50; 95%CI: 3.17-3.83) than baseline ($p < 0.001$). They also indicated that the CAF cream provided a smoother feeling on their skin (mean 3.71; 95%CI: 3.40-4.02) over baseline ($p < 0.001$). Placebo treatment slightly improved skin hydration (mean 2.33; 95%CI: 2.00-2.66) and provided a less smooth surface on the skin (mean 2.83; 95%CI: 2.53-3.14). Both groups showed a significant formula*time interaction in improving skin hydration ($p= 0.010$; Table 4.6). Conversely, there was no significant difference between the two groups in the perception of improved skin texture ($p= 0.809$; Table 4.6).

At the end of the clinical trial, statistical analysis showed that the CAF cream (mean 3.83; 95% CI: 3.54-4.12) performed significantly better than the placebo (mean 3.08; 95%CI: 2.79-3.37) in terms of participants' perceptions of skin elasticity. The participants expressed that "orange peel" dimpled appearance decreased on their posterior thighs following CAF cream use (mean 3.96; 95%CI: 3.67-4.25). The comparison of the two groups showed a significant formula*time interaction effect for the elasticity measure and the dimpled appearance measure ($p= 0.005$; $p < 0.001$; Table 4.6)

About the products

Table 4.7 summarises participants' perceptions of the products. Most participants agreed or strongly agreed that the products had good colour for both creams. Half of the participants neither agreed nor disagreed about the product having a very pleasant smell for CAF cream and placebo. Thirteen participants agreed that the CAF cream was absorbed perfectly and strongly agreed that the CAF cream spread quickly. The majority of participants agreed that the products did not leave a sticky sensation on the skin. More than 90% of participants commented that the products left a smooth feeling on the CAF cream or placebo skin.

Table 4.6 Mean of evaluation of hydration, elasticity, smoothness and dimpled appearance at baseline, week 4, week 8 and week 12

Measure	Week	CAF cream	P-value	Placebo cream	P-value	P-value
		Mean (95%CI)	baseline to each time point	Mean (95%CI)	baseline to each time point	cross-sectional between-group treatments each time point
Evaluation						
Hydration	0	2.29 (1.96-2.62)	-	2.08 (1.75-2.41)	-	0.286
	4	3.50 (3.17-3.83)	< 0.001	2.33 (2.00-2.66)	0.201	< 0.001
	8	3.75 (3.42-4.08)	< 0.001	3.25 (2.92-3.58)	< 0.001	0.010
	12	4.08 (3.75-4.41)	< 0.001	3.58 (3.25-3.91)	< 0.001	0.010
Elasticity	0	2.50 (2.21-2.79)	-	2.42 (2.13-2.71)	-	0.621
	4	3.33 (3.04-3.62)	< 0.001	2.67 (2.38-2.96)	0.138	< 0.001
	8	3.67 (3.38-3.96)	< 0.001	2.79 (2.50-3.08)	0.026	< 0.001
	12	3.83 (3.54-4.12)	< 0.001	3.08 (2.79-3.37)	< 0.001	< 0.001
Smoothness	0	2.50 (2.19-2.81)	-	2.38 (2.07-2.68)	-	0.468
	4	3.71 (3.40-4.02)	< 0.001	2.83 (2.53-3.14)	0.008	< 0.001
	8	3.88 (3.57-4.18)	< 0.001	3.42 (3.11-3.72)	< 0.001	0.008
	12	4.00 (3.69-4.31)	< 0.001	3.96 (3.65-4.27)	< 0.001	0.809
Dimpled appearance	0	1.58 (1.29-1.87)	-	1.63 (1.33-1.93)	-	0.801
	4	2.50 (2.21-2.79)	< 0.001	2.00 (1.71-2.29)	0.023	0.002
	8	3.33 (3.04-3.62)	< 0.001	2.71 (2.42-3.00)	< 0.001	< 0.001
	12	3.96 (3.67-4.25)	< 0.001	3.17 (2.88-3.46)	< 0.001	< 0.001

Notes: Responses to the questionnaires on the CAF cream and placebo cream. Close-ended questions using Likert scale 5-point scale. A numerical value of 1 to 5, where 1= strongly disagree; 2= disagree; 3= neither agree/nor disagree; 4= agree; 5= strongly agree

Table 4.7 Summary of generalised perception from participants on the suitability of the CAF and placebo creams

Generalised perception	About CAF cream					About placebo cream				
	1	**2**	**3**	**4**	**5**	**1**	**2**	**3**	**4**	**5**
The product is a good colour			2	11	11			2	11	11
The product has a very pleasant smell			11	7	6			12	7	5
The product absorbs perfectly		1	3	13	7		2	2	11	9
The product spreads easily		1	1	8	14			3	9	12
The product leaves sticky on the skin	4	9	3	7	1	4	10	4	4	2
The product leaves the skin feeling smooth			2	10	12			3	10	11

Notes: Close-ended questions using Likert scale 5-point scale. A numerical value of 1 to 5, where 1= strongly disagree; 2= disagree; 3= neither agree/nor disagree; 4= agree; 5= strongly agree

4.3.5 Global rating of change

At the end of treatment (week 12), only one participant indicated that overall the cellulite on their posterior thigh was about the same (no change), following the CAF cream application, with four participants indicating that the cellulite on their posterior thigh was much better following the placebo cream application (Table 4.8). There was a significant difference in participants' rating of reduced cellulite appearance within 12 weeks of cream containing CAF (mean 6.08; 95%CI: 5.72-6.45) relative to placebo (*p*= 0.035).

Table 4.8 Global rating of change (GROC) following either CAF cream or placebo cream application

	CAF cream	Placebo cream
Much worse	0	0
Worse	0	0
Somewhat worse	0	1
About the same	1	2
Somewhat better	4	9
Better	11	8
Much better	8	4

Notes: close-ended questions using Likert scale 7-point GROC ("since applying the products, the cellulite on my thigh was: much worse, worse, somewhat worse, the same, somewhat better, better, much better than before application")

4.3.6 Skin irritation

There were no major side effects recorded during the study. The majority of participants experienced no skin reactions to either active or placebo creams (79% – 19/24). Two participants with the CAF creams reported itching and prickling sensation on their thigh skin and three participants with the placebo creams (Table 4.9). Most of them experienced skin reactions in the first 4 weeks. We advised stopping for the creams and applying them when the skin reaction was resolved.

Table 4.9 Skin reaction to creams application

	CAF cream	Placebo cream
Itching	1	3
Prickling	1	

4.4 Discussion

Chapter 2 demonstrated that our CAF creams gave good penetration/permeation into and through the skin. Therefore, this present study evaluated the potential beneficial effects of a topical CAF formulation in reducing the appearance of cellulite, T.C. and thigh S.T. following a 12-week intervention.

Compared with baseline (week 0), the cellulite severity scale score was significantly reduced after 12 weeks ($p < 0.001$; Table 4.4) in the active group. Similarly, the placebo group also showed a decrease in the cellulite grading score relative to baseline ($p < 0.001$; Table 4.4). However, at week 12, there was a significant difference ($p= 0.012$) in cellulite severity scores between the active and placebo creams (Figure 4.6). It indicates that the inclusion of CAF resulted in a clinical improvement in terms of reducing visible signs of cellulite.

Saman et al. [56] investigated an anticellulite cream containing 1% caffeine, 5% L-carnitine and 0.015% coenzyme A. Their findings showed that placebo cream had the same effect as active cream applied topically twice a day over a two month treatment period. However, 90% of participants in the study had an overall satisfaction score of 5 for both creams, placebo and active.

Throughout the 12-week treatment, the study also demonstrated that our novel cream formulation combined with CAF significantly decreased skinfold thickness relative to baseline ($p < 0.001$; Table 4.4). However, no statistically significant decrease was seen in the placebo group. A significant ($p < 0.001$) treatment*time interaction effect favoured the active treatment. Approximately 80% of participants showed a consistent reduction of skinfold thicknesses for all treatment time points over baseline with a relatively small effect size (ES= 0.041). The Ngamdokmai group developed a herbal compress that contained 6-gingerol, piperine and caffeine from tea and coffee sources. The findings showed a similar result, with 85-90% of participants demonstrating skinfold thickness reduction with a more substantial effect size (ES= 1.72).[54] When considering differences in the studies, various factors need to be considered, such as the number of participants involved, the total treatment time, and the number of measurements. For example, the Ngamdokmai study was completed over 11 weeks with six-time points; two additional weeks were used to measure post-treatment

efficacy. The differences can also be considered in the method, compliance, and intervals of applying the topical herbal compress and the number of participants involved.

The effect of the CAF cream was also assessed through the measurement of T.C. By the end of the treatment period (week 12), a significant reduction in T.C. was observed over baseline for the active (mean -0.55) and placebo (mean -0.51) groups. There was no treatment*time interaction effect indicating a similar improvement for both groups.

Reduction in thigh measurement is one of the parameters mainly used to measure the effectiveness of anticellulite agents. In contrast, several studies using either CAF alone or combined with botanical extracts have reported that T.C. measurements decreased significantly relative to placebo groups. [28,53-55,61] Only Saman et al.[56] reported that the reduction in the T.C. was not significant compared with the placebo.

The participants themselves evaluated treatment efficacy through survey questionnaires. Participants indicated that the active and placebo creams showed significant improvement in skin hydration, skin elasticity, smoothness of their thigh skin and visible reduction of cellulite appearance after week 8 and week 12 of application (Table 4.6). However, there was a significant difference in efficacy perception in terms of improvements in skin moisture and skin elasticity and smoothness of the skin after using the CAF cream relative to placebo. The participants also felt satisfied with a diminished skin dimpled appearance at the end of treatment (Table 4.6). However, slight differences between the two groups started emerging in weeks 8 and 12, with the same performance for both creams. It may be speculated that the placebo treatment also contained the identical vehicle ingredients applied in the CAF cream and presumably, those ingredients provided the same result for skin hydration and skin-smoothing.

Byun et al.[61] reported that although, participants expressed their satisfaction with the cellulite treatment, the skin firmness improvement was similar for both active and placebo products.[49] Their cream contained 3.5% CAF and xanthenes. They suggested that the placebo had the same effect on skin firmness as the active product due to the massage effect related to cream application.[49,55]

The self-evaluation questionnaire was also designed to assess the overall performance of the products (active and placebo). All participants agreed or strongly agreed that both products

had good colour and a very pleasant cream smell. Most participants agreed that the active cream containing CAF was very well absorbed. A similar number of participants expressed that the products spread quickly upon application on the skin during the period of treatment. More than 90% of the study participants were satisfied with the smoothing effect of the products. Some participants enjoyed using both anticellulite cream and placebo and requested additional containers of cream when cream application finished. Most of them reported both creams had similar texture properties. This suggests that the participants could not distinguish between the two creams due to the compounds' characteristics.[50]

At the end of the study, the participants assessed GROC evaluating the overall anticellulite effect. Participants rated a higher score at 6.08 (95%CI: 5.72-6.45) for the CAF cream over the placebo at 5.50 (95%CI: 5.14-5.86). There was a statistically significant difference between the active and placebo cream ($p < 0.001$) in the overall impression of the anticellulite effect.

Two participants developed minor side effects from the anticellulite cream and three from the placebo. The prickling and itching sensations were familiar side effects for products applied topically to the skin. However, no serious adverse events led to treatment interruption by decreasing the cream usage.

Cellulite is a complex condition that does not tend to improve rapidly.[55] No treatment is entirely successful as none are more than mildly and temporarily effective.[62] A number of topical creams with an anticellulite effect are available on the market. Most of the products are from the methylxanthine family. This study demonstrated that the initial evaluation of our novel CAF cream in a clinical setting provided an indication that it could be an effective cellulite treatment.

There were a few limitations of our study, such as participants' compliance since each participant was responsible for daily applying the creams and applying the appropriate amount of cream to the designated thigh site. Another contributory factor to error is that daily weight fluctuation led to a perceived variability in thigh measurements. However, the reduction in T.C. was not due to weight loss since no overall reduction in weight occurred.

The flexible tape measure was used to quantify changes in T.C. and there may have been some limitations to the precision of this measure. Lesser et al.[28] compared two devices to measure subcutaneous adipose tissue. They found the calliper was a precise device that showed a significant reduction in subcutaneous adipose tissue whilst the tape measure

showed no significant change. This was similar to our findings. Overall, our anticellulite cream proved effective and tolerable, both objectively (Table 4.4) and subjectively (Table 4.6).

There are a limited number of tools available to treat cellulite and some are complicated to implement. The use of a reliable evaluation process plays a vital role in giving outcome measures for assessing visual changes in clinical trials. Previous studies [53,55-57,61,63] evaluated the efficacy of an anticellulite topical cream containing CAF by using rating scores from a couple of standard visual scales that had been validated.[53,55,57,63-67] Most of them did not conduct inter-rater and intra-rater (test/re-test) reliability of the method when a standardised grading system was used for scoring changes in the appearance of cellulite.[53-57,61] To verify the results that were produced, we generated an iterative process with a relatively simple and reliable method for evaluating intervention effects during the clinical trial. This process can be adapted to assess other skin conditions using visual images. To the best of our knowledge, only the Roure group conducted a similar approach with our experiment, which started from developing the formula creams, *ex vivo* testing and then testing the efficacy of the CAF creams in an *in vivo* study.[52] In addition, the Yoo group used the visual assessment grading scales from DERMAPRO SOP and conducted reliability testing to validate the process.[63]

Various treatments, either topical alone or combinations between topical and mechanical, offer advantages and disadvantages. Topical applications provide safe and relatively inexpensive treatments and do not require follow-up post-treatment compared to other treatments, which may involve significant costs and unfavourable risk profiles.[50,61]

We did not continue the measurement post-treatment. Therefore, we cannot guarantee the CAF cream produces a permanent result. The use of creams may provide only minor short-term improvements.[15] However, we demonstrated that our novel topical cream containing CAF effectively reduced the visible appearance of cellulite and skinfold fat thickness when used continuously for 12 weeks. We noted it was difficult to control for many factors involved, such as age, weight, body density, and skin condition. Other external factors that may have contributed to the result that we cannot control include diet and exercise for the participants and human errors in each measurement session.

Further research is now needed to gather additional clinical data to evaluate this treatment with a larger sample size, longer duration of treatment and follow-up post-treatment. The

treatment could also be evaluated at different body sites (buttock and abdomen) and comparisons could be made with other existing treatments.

4.5 References

1. Davis DS, Boen M, Fabi SG. Cellulite: Patient Selection and Combination Treatments for Optimal Results-A Review and Our Experience. *Dermatol Surg*. 2019;45(9):1171-1184. doi:10.1097/dss.0000000000001776
2. Khan MH, Victor F, Rao B, Sadick NS. Treatment of cellulite: Part II. Advances and controversies. *J Am Acad Dermatol*. 2010;62(3):373-384; quiz 385-376. doi:10.1016/j.jaad.2009.10.041
3. Sadick N. Treatment for cellulite. *International journal of women's dermatology*. 2019;5(1):68-72.doi:10.1016/j.ijwd.2018.09.002
4. Avram MM. Cellulite: a review of its physiology and treatment. *J Cosmet Laser Ther*. 2004;6(4):181-185.doi:10.1080/14764170410003057
5. Bass LS, Kaminer MS. Insights Into the Pathophysiology of Cellulite: A Review. *Dermatol Surg*. 2020;46 Suppl 1(1):S77-s85.doi:10.1097/dss.0000000000002388
6. Tülin Güleç AJIjod. Treatment of cellulite with LPG endermologie. 2009;48(3):265-270.doi:10.1111/j.1365-4632.2009.03898.x
7. Kutlubay Z, Songur A, Engin B, et al. An alternative treatment modality for cellulite: LPG endermologie. 2013;15(5):266-270.doi:10.3109/14764172.2013.787801
8. Draelos ZD, Marenus KDJDs. Cellulite: etiology and purported treatment. 1997;23(12):1177-1177.doi:10.1111/j.1524-4725.1997.tb00468.x
9. Collis N, Elliot L-A, Sharpe C, Sharpe DTJP. Cellulite treatment: a myth or reality: a prospective randomized, controlled trial of two therapies, endermologie and aminophylline cream. 1999;104(4):1110-1114.https://pubmed.ncbi.nlm.nih.gov/10654755/
10. Greenway FL, Bray GA. Regional fat loss from the thigh in obese women after adrenergic modulation. *Clin Ther*. 1987;9(6):663-669. https://pubmed.ncbi.nlm.nih.gov/2894247/
11. Karnes J, Salisbury M, Schaeferle M, Beckham P, Ersek RA. Hip lift. *Aesthetic Plast Surg*. 2002;26(2):126-129.doi:10.1007/s00266-002-1373-7
12. Gasparotti M. Superficial liposuction: a new application of the technique for aged and flaccid skin. *Aesthetic Plast Surg*. 1992;16(2):141-153.doi:10.1007/BF00450606
13. Coleman WP, Hanke CW. *Cosmetic surgery of the skin: principles and techniques*. Mosby Incorporated; 1997.Accessed June 06, 2021. https://www.goodreads.com/book/show/2130369.Cosmetic_Surgery_of_the_Skin
14. Adamo C, Mazzocchi M, Rossi A, Scuderi N. Ultrasonic liposculpturing: extrapolations from the analysis of in vivo sonicated adipose tissue. *Plast Reconstr Surg*. 1997;100(1):220-226.doi:10.1097/00006534-199707000-00033
15. Kaminer MS, Coleman III WP, Weiss RA, Robinson DM, Coleman IV WP, Hornfeldt C. Multicenter pivotal study of vacuum-assisted precise tissue release for the treatment of cellulite. *Dermatol Surg*. 2015;41(3):336-347.doi:10.1097/DSS.0000000000000280
16. Narsete T, Narsete DS. Evaluation of Radiofrequency Devices in Aesthetic Medicine: A Preliminary Report. 2017. Accessed June 08, 2021. https://www.shape-up.eu/wp-content/uploads/2019/05/07-Evaluation-of-Radiofrequency-Devices-in-Aesthetic-Medicine.pdf
17. Wanitphakdeedecha R, Manuskiatti W. Treatment of cellulite with a bipolar radiofrequency, infrared heat, and pulsatile suction device: a pilot study. *J Cosmet Dermatol*. 2006;5(4):284-288.doi:10.1111/j.1473-2165.2006.00271.x
18. Sasaki GH. Single treatment of grades II and III cellulite using a minimally invasive 1,440-nm pulsed Nd: YAG laser and side-firing fiber: an institutional review board-approved study with a 24-month follow-up period. *Aesthetic Plast Surg*. 2013;37(6):1073-1089. doi:10.1007/s00266-013-0219-9
19. Knobloch K, Kraemer R. Extracorporeal shock wave therapy (ESWT) for the treatment of cellulite – A current metaanalysis. *International Journal of Surgery*. 2015;24:210-217. doi:10.1016/j.ijsu.2015.07.644

20. Kuhn C, Angehrn F, Sonnabend O, Voss A. Impact of extracorporeal shock waves on the human skin with cellulite: a case study of an unique instance. *Clin Interv Aging*. 2008;3(1):201.doi: 10.2147/cia.s2334
21. Russe-Wilflingseder K, Russe E. Acoustic Wave Treatment For Cellulite—A New Approach. *American Institute of Physics*; 2010:25-30.doi:10.1063/1.3453782
22. Schlaudraff KU, Kiessling MC, Császár NBM, Schmitz C. Predictability of the individual clinical outcome of extracorporeal shock wave therapy for cellulite. *Clin Cosmet Investig Dermatol*. 2014;7:171-182.doi:10.2147/CCID.S59851
23. Zerini I, Sisti A, Cuomo R, et al. Cellulite treatment: a comprehensive literature review. *J Cosmet Dermatol*. 2015;14(3):224-240.doi:10.1111/jocd.12154
24. Goldberg DJ, Fazeli A, Berlin AL. Clinical, laboratory, and MRI analysis of cellulite treatment with a unipolar radiofrequency device. *Dermatol Surg*. 2008;34(2):204-209; discussion 209.doi:10.1111/j.1524-4725.2007.34038.x
25. Emilia del Pino M, Rosado RH, Azuela A, et al. Effect of controlled volumetric tissue heating with radiofrequency on cellulite and the subcutaneous tissue of the buttocks and thighs. *Journal of drugs in dermatology: JDD*. 2006;5(8):714-722. https://pubmed.ncbi.nlm.nih.gov/16989185/
26. Alexiades-Armenakas M, Dover JS, Arndt KA. Unipolar radiofrequency treatment to improve the appearance of cellulite. *J Cosmet Laser Ther*. 2008;10(3):148-153. doi:10.1080/14764170802279651
27. Mulholland RS, Paul MD, Chalfoun C. Noninvasive body contouring with radiofrequency, ultrasound, cryolipolysis, and low-level laser therapy. *Clin Plast Surg*. 2011;38(3):503-520.doi 10.1016/j.cps.2011.05.002
28. Lesser T, Ritvo E, Moy LS. Modification of Subcutaneous Adipose Tissue by a Methylxanthine Formulation: A Double-Blind Controlled Study. *Dermatol Surg*. 1999;25(6):455-462.doi:10.1046/j.1524-4725.1999.08243.x
29. Anolik R, Chapas AM, Brightman LA, Geronemus RG. Radiofrequency devices for body shaping: a review and study of 12 patients. *Semin Cutan Med Surg*. 2009;28(4):236-243. doi:10.1016/j.sder.2009.11.003
30. Sadick N, Magro C. A study evaluating the safety and efficacy of the VelaSmooth system in the treatment of cellulite. *J Cosmet Laser Ther*. 2007;9(1):15-20. doi:10.1080/14764170601134461
31. Güleç AT. Treatment of cellulite with LPG endermologie. *Int J Dermatol*. 2009;48(3):265-270.doi:10.1111/j.1365-4632.2009.03898.x
32. Goldman A, Gotkin RH, Sarnoff DS, Prati C, Rossato F. Cellulite: a new treatment approach combining subdermal Nd: YAG laser lipolysis and autologous fat transplantation. *Aesthet Surg J*. 2008;28(6):656-662.doi:10.1016/j.asj.2008.09.002
33. DiBernardo B, Sasaki G, Katz BE, Hunstad JP, Petti C, Burns AJ. A multicenter study for a single, three-step laser treatment for cellulite using a 1440-nm Nd:YAG laser, a novel side-firing fiber, and a temperature-sensing cannula. *Aesthet Surg J*. 2013;33(4):576-584. doi:10.1177/1090820x13480858
34. Hexsel DM, Mazzuco R. Subcision: a treatment for cellulite. *Int J Dermatol*. 2000;39(7):539-544.doi:10.1046/j.1365-4362.2000.00020.x
35. Abosabaa SA, Arafa MG, ElMeshad AN. Drug delivery systems integrated with conventional and advanced treatment approaches toward cellulite reduction. *Journal of Drug Delivery Science and Technology*. 2020;60:102084.doi:10.1016/j.jddst.2020.102084
36. Benson HA. Transdermal drug delivery: penetration enhancement techniques. *Current drug delivery*. 2005;2(1):23-33.doi:10.2174/1567201052772915
37. Sengar V, Jyoti K, Jain UK, Prakash Katare O, Chandra R, Madan J. Chapter 10 - Lipid nanoparticles for topical and transdermal delivery of pharmaceuticals and cosmeceuticals: A glorious victory. In: Grumezescu AM, ed. *Lipid Nanocarriers for Drug Targeting*. William Andrew Publishing; 2018:413-436.
doi:10.1016/B978-0-12-813687-4.00010-4
38. Marchei E, De Orsi D, Guarino C, Dorato S, Pacifici R, Pichini S. Measurement of iodide and caffeine content in cellulite reduction cosmetic products sold in the European market. *Analytical Methods*. 2013;5(2):376-383.doi:10.1039/C2AY25761K
39. Zsikó, Csányi, Kovács, Budai S, Gácsi, Berkó. Methods to Evaluate Skin Penetration In Vitro. *Sci Pharm*. 2019;87(3):19.doi:10.3390/scipharm87030019

40. Hexsel D, Orlandi C, Zechmeister do Prado D. Botanical extracts used in the treatment of cellulite. *Dermatol Surg*. 2005;31(7 Pt 2):866-872; discussion 872.doi:10.1111/j.1524-4725.2005.31733
41. Turati F, Pelucchi C, Marzatico F, et al. Efficacy of cosmetic products in cellulite reduction: systematic review and meta-analysis. *J Eur Acad Dermatol Venereol*. 2014;28(1):1-15.doi:10.1111/jdv.12193
42. Hexsel D, Soirefmann M. Cosmeceuticals for cellulite. *Semin Cutan Med Surg*. 2011;30(3):167-170.doi:10.1016/j.sder.2011.06.005
43. Dwornicka D, Wojciechowska K, Zun M, et al. The inflluence of emulsifiers on physical properties and release parameters of creams with caffeine. *Current Issues in Pharmacy and Medical Sciences*. 2015;28(2):81-84.doi:10.1515/cipms-2015-0049
44. Herman A, Herman AP. Caffeine's mechanisms of action and its cosmetic use. *Skin Pharmacol Physiol*. 2013;26(1):8-14.doi:10.1159/000343174
45. Dias M, Farinha A, Faustino E, Hadgraft J, Pais J, Toscano C. Topical delivery of caffeine from some commercial formulations. *Int J Pharm*. 1999;182(1):41-47. doi:10.1016/S0378-5173(99)00067-8
46. Luebberding S, Krueger N, Sadick NS. Cellulite: an evidence-based review. *Am J Clin Dermatol*. 2015;16(4):243-256.doi:10.1007/s40257-015-0129-5
47. Green JB, Cohen JL, Kaufman J, Metelitsa AI, Kaminer MS. Therapeutic approaches to cellulite. *Semin Cutan Med Surg*. 2015;34(3):140-143.doi:10.12788/j.sder.2015.0169
48. Rawlings AV. Cellulite and its treatment. *Int J Cosmet Sci*. 2006;28(3):175-190. doi:10.1111/j.1467-2494.2006.00318.x
49. Bertin C, Zunino H, Pittet JC, et al. A double-blind evaluation of the activity of an anti-cellulite product containing retinol, caffeine, and ruscogenine by a combination of several non-invasive methods. *J Cosmet Sci*. 2001;52(4):199-210. https://pubmed.ncbi.nlm.nih.gov/11479653/
50. Rao J, Gold MH, Goldman MP. A two-center, double-blinded, randomized trial testing the tolerability and efficacy of a novel therapeutic agent for cellulite reduction. *J Cosmet Dermatol*. 2005;4(2):93-102.doi:10.1111/j.1473-2165.2005.40208.x
51. Vogelgesang B, Bonnet I, Godard N, Sohm B, Perrier E. In vitro and in vivo efficacy of sulfo-carrabiose, a sugar-based cosmetic ingredient with anti-cellulite properties. *Int J Cosmet Sci*. 2011;33(2):120-125. doi:10.1111/j.1468-2494.2010.00593.x
52. Roure R, Oddos T, Rossi A, Vial F, Bertin C. Evaluation of the efficacy of a topical cosmetic slimming product combining tetrahydroxypropyl ethylenediamine, caffeine, carnitine, forskolin and retinol, In vitro, ex vivo and in vivo studies. *Int J Cosmet Sci*. 2011;33(6):519-526.doi:10.1111/j.1468-2494.2011.00665.x
53. Escudier B, Fanchon C, Labrousse E, Pellae M. Benefit of a topical slimming cream in conjunction with dietary advice. *Int J Cosmet Sci*. 2011;33(4):334-337.doi: 10.1111/j.1468-2494.2010.00630.x
54. Ngamdokmai N, Waranuch N, Chootip K, Jampachaisri K, Scholfield CN, Ingkaninan K. Cellulite Reduction by Modified Thai Herbal Compresses A Randomized Double-Blind Trial. *Journal of evidence-based integrative medicine*. 2018;23:2515690X1879415. doi:10.1177/2515690X18794158
55. Dupont E, Journet M, Oula ML, et al. An integral topical gel for cellulite reduction: results from a double-blind, randomized, placebo-controlled evaluation of efficacy. *Clin Cosmet Investig Dermatol*. 2014;7:73-88. doi:10.2147/ccid.S53580
56. Saman Ahmad N, Hournaz H, Marjan A, et al. Assessment of an anti-cellulite cream: A randomized, double-blind, placebo controlled, right-left comparison, clinical trial. *Iranian Journal of Dermatology*. 2015;18(4):145-150. http://www.iranjd.ir/article_98269_90da3c38b42169c1588b386678286e2e.pdf
57. Al-Bader T, Byrne A, Gillbro J, et al. Effect of cosmetic ingredients as anticellulite agents: synergistic action of actives with in vitro and in vivo efficacy. *J Cosmet Dermatol*. 2012;11(1):17-26. doi:10.1111/j.1473-2165.2011.00594.x
58. Dupont E, Gomez J, Léveillé C, Bilodeau D. From hydration to cell turnover: an integral approach to antiaging. *Cosmetics & Toiletries*. 2010;125(8):50.
59. Ortonne JP, Zartarian M, Verschoore M, Queille-Roussel C, Duteil L. Cellulite and skin ageing: is there any interaction? *J Eur Acad Dermatol Venereol*. 2008;22(7):827-834. doi:10.1111/j.1468-3083.2007.02570.x
60. Durlak JA. How to Select, Calculate, and Interpret Effect Sizes. *J Pediatr Psychol*. 2009;34(9):917-928.doi:10.1093/jpepsy/jsp004

61. Byun S-Y, Kwon S-H, Heo S-H, Shim J-S, Du M-H, Na J-I. Efficacy of Slimming Cream Containing 3.5% Water-Soluble Caffeine and Xanthenes for the Treatment of Cellulite: Clinical Study and Literature Review. *Annals of dermatology*. 2015;27(3):243-249. doi:10.5021/ad.2015.27.3.243
62. Wanner M, Avram M. An evidence-based assessment of treatments for cellulite. *J Drugs Dermatol*. 2008;7(4):341-345. https://europepmc.org/article/med/18459514
63. Yoo MA, Seo YK, Ryu JH, Back JH, Koh JS. A validation study to find highly correlated parameters with visual assessment for clinical evaluation of cosmetic anti-cellulite products. *Skin Res Technol*. 2014;20(2):200-207.doi:10.1111/srt.12106
64. Longhitano S, Galadari H, Cascini S, et al. A validated photonumeric cellulite severity scale for the area above the knees: the knee cellulite severity score. *J Eur Acad Dermatol Venereol*. 2020;34(9):2152-2155.doi:10.1111/jdv.16269
65. Hexsel D, Dal'forno T, Hexsel C. A validated photonumeric cellulite severity scale. *J Eur Acad Dermatol Venereol*. 2009;23(5):523-528 doi:10.1111/j.1468-3083.2009.03101.x
66. Nürnberger F, Müller G. So-called cellulite: an invented disease. *J Dermatol Surg Oncol*. 1978;4(3):221-229.doi:10.1111/j.1524-4725.1978.tb00416.x
67. Bielfeldt S, Buttgereit P, Brandt M, Springmann G, Wilhelm KP. Non-invasive evaluation techniques to quantify the efficacy of cosmetic anti-cellulite products. *Skin Res Technol*. 2008;14(3):336-346.doi:10.1111/j.1600-0846.2008.00300.x

Chapter 5. Novel Self-Nano Emulsifying Drug Delivery Systems (SNEDDS) Containing Astaxanthin for Topical Skin Delivery (Published paper)

Ponto T, Latter G, Luna G, Leite-Silva VR, Benson HAE and Wright A. Novel Self-Nano Emulsifying Drug Delivery Systems (SNEDDS) Containing Astaxanthin for Topical Skin Delivery. *Pharmaceutics*. 2021;13(5):649.doi.org/10.3390/pharmaceutics13050649.

Abstract

Background: Astaxanthin (ASX) is a potent lipophilic antioxidant derived from the natural pigment that gives marine animals their distinctive red-orange colour and confers protection from ultraviolet radiation. ***Objectives:*** Self nano-emulsifying drug delivery systems (SNEDDS) have been successfully developed and evaluated to increase the skin penetration of ASX and target its antioxidant and anti-inflammatory potential to the epidermis and dermis. ***Methods:*** SNEDDS were prepared using a low-temperature spontaneous emulsification method, and their physical characteristics, stability, antioxidant activity, and skin penetration were characterised. Terpenes (D-limonene, geraniol, and farnesol) were included in the SNEDDS formulations to evaluate their potential skin penetration enhancement. An HPLC assay was developed that allowed ASX recovery from skin tissues and quantification. ***Results:*** All SNEDDS formulations had droplets in the 20 nm range, with low polydispersity. ASX stability over 28 days storage in light and dark conditions was improved and antioxidant activity was high. SNEDDS-L1 (no terpene) gave significantly increased ASX penetration to the stratum corneum (SC) and the epidermis-dermis-follicle region (E + D + F) compared to an ASX in oil solution and a commercial ASX facial serum product. The SNEDDS-containing D-limonene gave the highest ASX permeation enhancement, with 3.34- and 3.79-fold the amount in the SC and E + D + F, respectively, compared to a similar applied dose of ASX in oil. ***Conclusions:*** We concluded that SNEDDS provide an effective formulation strategy for enhanced skin penetration of a highly lipophilic molecule, and when applied to ASX, have the potential to provide topical formulations for UV protection, anti-ageing, and inflammatory conditions of the skin.

pharmaceutics

MDPI

Article

Novel Self-Nano-Emulsifying Drug Delivery Systems Containing Astaxanthin for Topical Skin Delivery

Thellie Ponto [1], Gemma Latter [1], Giuseppe Luna [1], Vânia R. Leite-Silva [2], Anthony Wright [3] and Heather A. E. Benson [1,*]

[1] Curtin Medical School, Curtin Health Innovation Research Institute (CHIRI), Curtin University, GPO Box U1987, Perth, WA 6845, Australia; thellie.ponto@postgrad.curtin.edu.au (T.P.); gemma.latter@postgrad.curtin.edu.au (G.L.); giuseppe.luna@curtin.edu.au (G.L.)
[2] Instituto de Ciências Ambientais, Químicas e Farmacêuticas, Departamento de Ciências Farmacêuticas, Universidade Federal de São Paulo, UNIFESP-Diadema, São Paulo 09913-030, Brazil; vaniarleite@uol.com.br
[3] School of Allied Health, Curtin University, GPO Box U1987, Perth, WA 6845, Australia; t.wright@curtin.edu.au
* Correspondence: h.benson@curtin.edu.au; Tel.: +61-8-9266-2338

Abstract: Astaxanthin (ASX) is a potent lipophilic antioxidant derived from the natural pigment that gives marine animals their distinctive red-orange colour and confers protection from ultraviolet radiation. Self nano-emulsifying drug delivery systems (SNEDDS) have been successfully developed and evaluated to increase the skin penetration of ASX and target its antioxidant and anti-inflammatory potential to the epidermis and dermis. SNEDDS were prepared using a low-temperature spontaneous emulsification method, and their physical characteristics, stability, antioxidant activity, and skin penetration were characterized. Terpenes (D-limonene, geraniol, and farnesol) were included in the SNEDDS formulations to evaluate their potential skin penetration enhancement. An HPLC assay was developed that allowed ASX recovery from skin tissues and quantification. All SNEDDS formulations had droplets in the 20 nm range, with low polydispersity. ASX stability over 28 days storage in light and dark conditions was improved and antioxidant activity was high. SNEDDS-L1 (no terpene) gave significantly increased ASX penetration to the stratum corneum (SC) and the epidermis-dermis-follicle region (E + D + F) compared to an ASX in oil solution and a commercial ASX facial serum product. The SNEDDS-containing D-limonene gave the highest ASX permeation enhancement, with 3.34- and 3.79-fold the amount in the SC and E + D + F, respectively, compared to a similar applied dose of ASX in oil. We concluded that SNEDDS provide an effective formulation strategy for enhanced skin penetration of a highly lipophilic molecule, and when applied to ASX, have the potential to provide topical formulations for UV protection, anti-aging, and inflammatory conditions of the skin.

Keywords: skin targeting; antioxidant; terpenes; penetration enhancement; SNEDDS; nano-delivery; cosmeceutical; dermatological

Citation: Ponto, T.; Latter, G.; Luna, G.; Leite-Silva, V.R.; Wright, A.; Benson, H.A.E. Novel Self-Nano-Emulsifying Drug Delivery Systems Containing Astaxanthin for Topical Skin Delivery. *Pharmaceutics* **2021**, *13*, 649. https://doi.org/10.3390/pharmaceutics13050649

Academic Editors: Donatella Paolino, Jelena Filipović-Grčić and Cinzia Anna Ventura

Received: 2 March 2021
Accepted: 28 April 2021
Published: 3 May 2021

1. Introduction

There is increasing consumer demand for effective, natural-based products to protect the skin from environmental assault and treat dermatological conditions related to skin aging, irritancy, and inflammation [1]. Astaxanthin (3,3′-dihydroxy-β,β-carotene-4,4′-dione; ASX: Figure 1) is a carotenoid from the xanthophylls family with potent antioxidant activity [2]. ASX is commonly found in nature and is best known as the red-orange pigment that contributes the distinctive colour to many marine animals such as salmon, shrimp, and crayfish, and the flamingo birds that feast on them. It has many important biological functions in marine animals including pigmentation, protection against ultraviolet (UV) light effects, communication, immune response, reproductive capacity, stress tolerance, and protection against oxidation of macromolecules [3]. This keto-carotenoid is synthesized

by a variety of green microalgae/phytoplankton, and also red yeast, bacteria, and other plants [4].

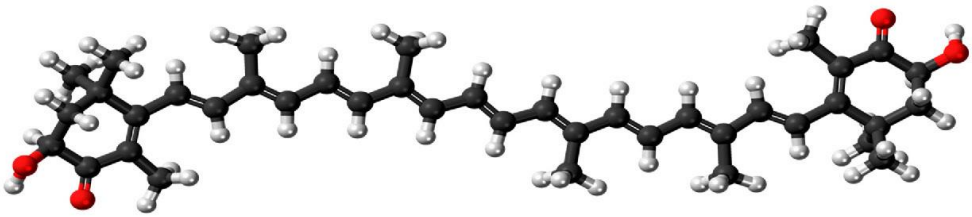

Figure 1. Structure of all-*trans* astaxanthin ($C_{40}H_{52}0_4$: carbon—black, hydrogen—white, oxygen—red). By Jynto: this image was created with Discovery Studio Visualizer, CC0, https://commons.wikimedia.org/w/index.php?curid=16311511 (accessed on 9 February 2021).

ASX has attracted interest due to its reported therapeutic effects in a range of health conditions [5]. This includes the prevention and treatment of cardiovascular diseases [2,6–8], neurological diseases [9–11], ocular disorders [12,13], cancer [14] and improving dermal health [15,16]. ASX derived from the green microalga *Haematococcus pluvialis* is the main source for human applications including dietary supplements, cosmetics, and food. It has shown antiaging potential in an experimental model of oxidative stress [17]. This suggests its potential in protecting human skin from environmental-derived stress, such as cigarette smoking and ultraviolet (UV) exposure, that contributes to and accelerates the skin-aging effects.

Skin aging has both cosmetic and health implications. The molecular and morphological changes that occur as the skin ages reduce its barrier function and protective role, and contribute to a range of skin symptoms including the formation or deepening of wrinkles, dyspigmentation, excessive dryness and pruritus, fragility, and difficulty in healing following skin injuries, skin sensitivity and irritation, and tumor incidence [15]. A range of positive effects on human skin has been reported following dietary supplementation with ASX [18–23]. In particular, ASX has shown to suppress hyperpigmentation and melanin synthesis, improve skin elasticity, inhibit photoaging associated with UV light exposure, and reduce wrinkle formation [18–23]. For example, in a double-blind, placebo-controlled trial, Ito et al. [18] showed that dietary supplementation with ASX for 9 weeks reduced the UV-induced changes in skin moisture and texture in 23 healthy volunteers. In another study conducted in Japan on 65 healthy female participants, those in the placebo group showed worsening wrinkle parameters, skin moisture decrease, and increase in the inflammatory marker interleukin-1α over a 16 week period from August to December [22]. Those receiving oral ASX showed no change in these skin parameters. The authors concluded that oral ASX supplementation may inhibit age-related skin deterioration via its anti-inflammatory effect. In most cases, these studies involve dietary supplementation rather than topical administration of ASX directly to the skin.

ASX (MW: 596.84 g/mol; Figure 1) has a high log P (octanol/water) of 13.27 [24], exhibiting low water solubility and limited bioavailability [25]. When applied to the skin, the ASX may not be efficiently released from an oil-based formulation, or may form a reservoir in the lipid-rich regions of the stratum corneum and not permeate further into the viable skin tissues, thus limiting its accessibility to its site of therapeutic activity. ASX is highly sensitive to light, heat, and oxygen due to its unsaturated molecular form [26]. Consequently, ASX presents significant challenges for the development of a successful formulation that will optimize stability and bioavailability within the skin. Commercially available topical formulations of ASX are primarily oil-based serums such as astaxanthin in argan oil (Skin Actives Scientific L.L.C., Gilvert, AZ, USA), Astalift Essence Destiny (Fuji-Film Healthcare Laboratory Co., Ltd., Minato-ku, Tokyo, Japan), and Astarism (AstaREAL Co., Ltd., Minato-ku, Tokyo, Japan). A number of novel delivery systems have been inves-

tigated to facilitate the formulation of ASX, improve stability and skin permeation. These include micro/nanoemulsions [27,28], hydrogels/lipogels [29], liposomes [30], and nanostructured lipid carriers (NLCs) [31]. Whilst some of these approaches appear promising, there remains limited information based on robust in vitro permeation tests (IVPT) with appropriate IVPT protocols and skin membranes, to properly assess ASX delivery into skin target sites where it can exert its therapeutic activity. For example, in some studies, IVPT was conducted using rat [27,28,31] or mouse skin [30], which are widely acknowledged to be more permeable than human skin; and in one case, only an in vitro release test (IVRT) was performed [29].

In the current study, we have formulated self-nano-emulsifying drug delivery systems (SNEDDS) and evaluated the inclusion of terpene components on the skin permeation, stability, and antioxidant activity of ASX. SNEDDS are isotropic mixtures of an active compound in a combination of lipids, surfactants, and hydrophilic co-solvents/solubilizers that produce spontaneous ultrafine emulsions upon gentle agitation in the water phase (typically <50 nm in size) [32–34]. SNEDDS have a high solubilizing capacity for lipophilic compounds, are thermodynamically stable, provide simplicity of fabrication, and have an elegant appearance [35,36]. They have been shown to enhance skin delivery of lipophilic solutes such as curcumin [37] and clofazimine [38]. When applied topically, a SNEDDS may be diluted by an aqueous phase coming to the skin surface from the secretion of sweat or trans epidermal water loss, and then form an occlusive topical system that has a high thermodynamic driving force for skin delivery [34,39,40]. We suggest that the SNEDDS approach is ideally suited to deliver the highly lipophilic ASX into the skin to target sites of therapeutic action such as melanocytes located in the basal layer of the epidermis, collagen and elastin synthesis by fibroblasts located in the dermis and UV induced inflammatory processes in the epidermis and dermis [19,23,30]. SNEDDS also has potential advantages for ASX stability, as the elimination of water during preparation and storage reduces the potential for dissolved oxygen in the water phase of an emulsion to degrade ASX [28].

We have developed and characterized the physical characteristics, stability, skin permeation, and distribution, and antioxidant activity of SNEDDS composed of oil, non-ionic surfactants, and cosurfactants and incorporating ASX. We have also evaluated the inclusion of terpenes as potential skin penetration enhancers. To facilitate this study, we have developed a simple and accurate HPLC assay for ASX determination with suitable extraction protocols for quantifying ASX in skin layers.

2. Material and Methods

2.1. Chemicals and Materials

Astaxanthin of analytical grade (CAS# 472-61-7) (SML0982) with a purity of 99.7%, Kolliphor® EL (Polyoxyl 35 castor oil–CAS# 61791-12-6), D-limonene (CAS# 5989-27-5), geraniol (CAS# 106-24-1), farnesol (CAS# 4602-84-0), L-ascorbic acid (CAS# 50-81-7), potassium persulfate (CAS# 7727-21-1), and ABTS (Roche-Diagnostics GmbH) (CAS# 30931-67-0) were purchased from Sigma-Aldrich (North Ryde, Australia). Labrafil® M 1944 CS (Oleoyl polyoxyl-6 glycerides–CAS# 69071-70-1) and Transcutol® P (Ethoxydiglycol–CAS# 111-90-0) were kind gifts from Gattefossé (Saint-Priest, France). Astarism® facial serum was a gift from AstaREAL Co. Ltd., Minato-ku, Tokyo, Japan. Veet™ hair removal cream (containing potassium thioglycolate) was purchased from Reckitt Benckiser Pty Ltd. (Sydney, Australia). HPLC-grade methanol and ethanol were from Thermo Fisher Scientific (Scoresby, Australia). HPLC-grade solvents (including acetone (ACT) and dichloromethane (DCM) were purchased from RCI Labscan Ltd. (Pathumwan, Bangkok, Thailand) distributed by Chem-Supply Pty Ltd., Gillman, Australia. Potassium chloride and sodium chloride were purchased from Chem-Supply Australia Pty Ltd. Potassium dihydrogen orthophosphate was purchased from Thermo Fisher Scientific (Scoresby, Australia). Di-sodium hydrogen orthophosphate anhydrous was purchased from Merck Pty Ltd (Bayswater, Australia). Deionised water was produced using a Milli-Q RC apparatus (Millipore Corporation, Bedford, MA, USA).

2.2. Standard Solution Preparation

A stock standard solution of astaxanthin was prepared by weighing exactly 3.75 mg of astaxanthin into a 25 mL volumetric flask, dissolving the astaxanthin in a mixture (15 mL) of acetone and dichloromethane (50:50), and adding a mobile-phase solution to 25 mL. The solution was sonicated for 1 minute in a warm water bath at 60 °C, and allowed to equilibrate to ambient temperature for 15 min. Working solutions of individual standards were prepared by diluting the freshly prepared stock solution with the mobile phase to required concentration.

2.3. HPLC Instrumentation and Conditions

Chromatographic separation was performed using an Agilent™ 1200 system (Agilent Technologies, Waldbronn, Germany), using a Jupiter C18 5 µm column, (150 mm × 4.6 mm) protected by a Security Guard Cartridge (C18, 4 × 3 mm) both from Phenomenex (Lane Cove, Australia), and isocratic flow of mobile phase (methanol:water:dichloromethane = 85:13:2) at 1 mL/min (chromatography adapted from Yuan et al. [41]. Samples were maintained at 10 °C within the autoinjector. Full assay conditions and protocols for extraction from skin tissues are available in the Supplementary Materials.

2.4. Design of Self-Nanoemulsifying Drug Delivery Systems (SNEDDS)

SNEDDS were formulated with Labrafil® M 1944 CS (constituting oil phase) and Kolliphor® EL (non-ionic surfactant), and Transcutol® P as a co-surfactant. Three terpenes (D-limonene, geraniol, and farnesol) were added, as 5% *w*/*w* of the oil phase, to determine their ASX skin permeation enhancement capability within the SNEDDS formulation. The physical characteristics and ASX skin delivery of all formulations were characterized, including the droplet size, polydispersity index (PDI), viscosity, ASX solubility, stability, oxidative inhibition values, and amount of ASX retained in the skin (IVPT).

The ratio of Labrafil® M 1944 CS, Kolliphor® EL, and Transcutol® P was determined from ASX solubility experiments. The SNEDDS were prepared based on the method of Hong et al. [27], using a spontaneous emulsification method, and high energy input. Briefly, ASX (3 mg) was dissolved in 4 g of surfactant, stirred with magnetic stirring at 1000 rpm for 10 min. The mixture was then dissolved in 1 g of the oil phase, with magnetic stirring at 1000 rpm for 10 min. This mixture was then combined with 1 g of co-surfactant using magnetic stirring for 10 min, then sonicated in a water bath for 1 h at room temperature. The formulation vehicle addition sequence was based on preliminary ASX solubility determination in each vehicle component. A nanoemulsion formulation (L1-NE) was made by the same method but with an initial 6 mg ASX and then a 50:50 dilution with water as the final step to provide a nanoemulsion with the same ASX concentration as the SNEDDS formulations.

The composition of the SNEDDS formulations is documented in Table 1 with the initial SNEDDS formulation designated L1 and the terpene-containing formulation designated T1 (D-limonene), T2 (geraniol), and T3 (farnesol). All ASX SNEDDS were protected from light exposure at room temperature for further use.

Table 1. ASX-SNEDDS formulation compositions (all excipients as *w*/*w*).

Codes	ASX	Labrafil® M 1944 CS	Kolliphor® EL	Transcutol	D-Limonene	Geraniol	Farnesol	Water
SNEDDS–L1	0.003	1.00	4.00	1.00				
SNEDDS–T1	0.003	0.95	4.00	1.00	0.05			
SNEDDS–T2	0.003	0.95	4.00	1.00		0.05		
SNEDDS–T3	0.003	0.95	4.00	1.00			0.05	
L1-NE	0.006	1.00	4.00	1.00				6.00

SNEDDS = self-nanoemulsifying drug delivery systems. L1 = initial formulation; T1 = addition D-limonene in oil phase; T2 = addition geraniol in oil phase; T3 = addition farnesol in oil phase. NE = nanoemulsion (50% water added to the oil/surfactant-cosurfactant mixture immediately before use). The final concentration of ASX in L1–NE was same concentration the SNEDDS.

2.5. *Physical Characterization, Stability, and Antioxidant Activity*

The ASX SNEDDS were visually observed to describe the physical appearance (colour, clarity, single phase), and viscosity (Bohlin Visco 88, Malvern Instruments, Malvern, Worcestershire, UK), and refractive index (Atago refractometer, Minato-ku, Tokyo, Japan) were determined. The pH measurement was determined using a pH meter (Hanna Instruments, Woonsocket, RI, USA) for all SNEDDS anhydrous formulations and after 100-fold dilution with deionized water. The droplet size and polydispersity index (PDI) were examined using a Zetasizer Nano™ ZSP (Malvern Instruments, Malvern, Worcestershire, UK) with aqueous dilution 100-fold to avoid multiple scattering.

Robustness to dilution was assessed in different volumes (1 part to 50, 100, and 250) using deionized water. This parameter provides a prediction of the potential for phase separation of a system generated by spontaneous emulsification. After the dilution process, the droplet size should remain uniform [33].

The stability of ASX SNEDDS was determined over 4 weeks of storage at room temperature to provide a preliminary indication of the stability of ASX in the SNEDDS formulations, when exposed to or protected from light. Physical appearance and the ASX content were determined after storage at 22–25 °C in clear vials and protected from light in amber vials. ASX in oil solution was used as a control.

2.6. *In Vitro Skin Penetration (IVPT) Study*

Due to the lack of availability of human skin, newborn pig skin was used as a previously validated human skin surrogate [42,43]. Full-thickness skin was obtained from newborn Yorkshire piglets that had died at or within 24 h of birth, as supplied by a local veterinary service. The skin was peeled from the body and extraneous tissue was removed by surgical scalpel. Hair was removed using Veet™ hair removal cream applied for 10 min and then thoroughly removed. This method has been previously validated on piglet skin and shown no skin damage [43]. The skin surface was rinsed with phosphate-buffered saline solution at pH 7.4 (PBS), wrapped in aluminum foil, and stored in a polyethylene bag at −20 °C until use. Three different donors were used for each experiment (9 replications).

The skin was defrosted at ambient temperature immediately before each experiment. Skin thickness was determined by digital vernier caliper (Kincrome Australia Pty Ltd., Scoresby, Australia) and was 400–600 µm. The skin was mounted in Franz diffusion cells with the stratum corneum (SC) side facing the donor. PBS solution was placed in the donor and receptor compartments and allowed to equilibrate at 35 °C prior to determining the electrical resistance (UNI-T®, UT58 series), as a measure of skin barrier integrity. Skin was included that provided a maximum resistance of 1 MΩ and minimum value of 50 kΩ [44]. PBS was removed and the skin surface touched dry (Kimtech Science Kimwipes®, Kimberly-Clark Professional, Milsons Point, Australia). The receptor compartment was filled with a mixture of PBS and ethanol (7:3 *v/v*) to facilitate ASX solubility [28,29], stirred by magnetic stirring at 600 rpm/min, and maintained in a water bath system at 35 °C to provide skin surface temperature of 32 °C. Parafilm M® (Sigma-Aldrich Pty Ltd, North Ryde, Australia) was used to cover the donor and receptor cells to minimize evaporation and to facilitate the process of total replacement sampling. 0.5 g of ASX SNEDDS formulation, marketed ASX product or ASX in oil solution (control) was applied to the donor compartment as an infinite dose. Samples (total receptor fluid volume) were withdrawn for HPLC analysis and immediately replaced by pre-warmed receptor solution, over an 8 h period.

Skin Distribution Study

After 8 h, the skin was washed to remove any remaining formulation (washing fluid retained), dried, and treated to separate SC and remaining skin tissue (epidermis/dermis). To obtain SC samples, D-Squame® adhesive tapes with a diameter of 22 mm (CuDerm, Dallas, TX, USA) were applied on the skin surface with a D-Squame disc® applicator following the method of Davies et al. [45] with modification. The total of 10 tapes strips comprised the first two tapes (assumed to include unabsorbed ASX) and remaining 8 tapes

as absorbed into the SC. The remaining skin was cut into pieces and weighed. ASX was extracted by soaking in acetone: dicloromethane 50:50 mixture prior to sonication in a water bath for 1 h at room temperature. The supernatant fluid was collected and then centrifuged to remove the precipitation of fat tissue. The tapes were soaked in methanol, vortex mixed for 30 min, then removed and the soaking solution centrifuged for 10 min. All samples were analyzed as soon as possible by HPLC.

2.7. Antioxidant Activity

The antioxidant activity of ASX was determined by the ABTS (2,2′-azino-bis(3-ethylben zothiazoline-6-sulfonic acid)) radical scavenging assay according to Chintong et al. [46] with minor modification. ABTS provides radicals that can be easily observed by a colour change from almost colourless to deep bluish-green in the absorbance wavelength at 734 nm [47].

Briefly, 7 mM ABTS and 2 mM $K_2S_2O_8$, both in aqueous solution and equal quantities, were allowed to stand in the dark at room temperature for 16 h. ABTS working solution was then diluted with distilled water to obtain an absorbance of 0.70 ± 0.03 units at 734 nm using a UV–Vis spectrophotometer (UV-1280, Shimadzu, Nakagayo-ku, Kyoto, Japan). Twenty microliters of different concentrations of the SNEDDS and ASX in ethanol 95% solution (200–1000 µg/mL) was mixed with 200 µL of the working ABTS solution. The absorbance of the mixture was measured after 6 min at wavelength 734 nm. Ascorbic acid and the marketed ASX topical product were compared as positive controls. Water and ethanol 95% were used as blanks. The scavenging rate of ABTS was calculated as:

$$\%\text{ABTS radical scavenging} = [(A_{\text{sample}} - A_{\text{sample blank}})/A_{\text{control}}] \times 100$$

where A_{control}, A_{sample}, and $A_{\text{sample blank}}$ are the absorbance of the ABTS solution, ASX solution with ABTS, and ASX solution without ABTS, respectively.

2.8. Data Analysis

For the in vitro skin permeation study, the amount of ASX in the skin tissues was calculated from the HPLC analysis of extract solutions giving the amount of ASX retained in the SC (tape strips 2–10) and the amount of ASX present in the skin tissue (epidermis, dermis).

Mass balance of in vitro permeation experiments was determined by comparison of the initial applied amount of ASX with the combination of ASX in the wash, tape strips 1/2 and 3–10 samples, the remaining skin tissue extracts, and the receptor compartment.

2.9. Statistical Analysis

All experiments were carried out in triplicate. The data are expressed as the mean ± SD (non-biologically related measurements) and the mean ± SEM (biologically related measurements). All data were analyzed using GraphPad Prism™ 9 software (GraphPad Software Inc., San Diego, CA, USA), using two-way ANOVA with Tukey post hoc test. Data were considered to be statistically significant if $p < 0.05$.

3. Results

3.1. HPLC Assay Method Development

The HPLC method provided a single ASX peak for the stock solution at 8.3 ± 0.1 min and good separation from any skin sample-related peaks (see Figure S1). The details of the assay development and outcomes are provided in the Supplementary Materials.

3.2. Preparation of ASX-Loaded SNEDDS

The initial SNEDDS formulation was developed based on solubility studies of ASX with the three core excipients of Labrafil® M 1944 CS (constituting the oil phase), Kolliphor® EL (non-ionic surfactant), and Transcutol® P as a co-surfactant. The optimal ratio was 1:4:1 (oil:surfactant:co-surfactant) providing the SNEDDS-L1 formulation. This ratio provided a

transparent SNEDDS formulation that readily dispersed in water to produce a nanoemulsion with suitably small droplet size. The SNEDDS-L1 formulation was then adapted to include a terpene in the oil phase, providing SNEDDS-T1 (D-limonene), T2 (geraniol), and T3 (farnesol). The addition of 5% D-limonene, geraniol, and farnesol generated transparent nanoformulations with excellent clarity and similar physical characteristics to the SNEDDS-L1 formulation.

3.3. Physical Characteristics of ASX Nanoformulations

All SNEDDS formulations were a darkish red-orange colour that formed a pale orange transparent nanoemulsion system when diluted 100-fold by deionized water (Figure 2A). The colour is associated with the ASX. Addition of terpenes did not alter the physical appearance of the SNEDDS. There was no sedimentation or phase separation in any SNEDDS formulation when observed immediately after formulation or after up to 28 days storage at room temperature.

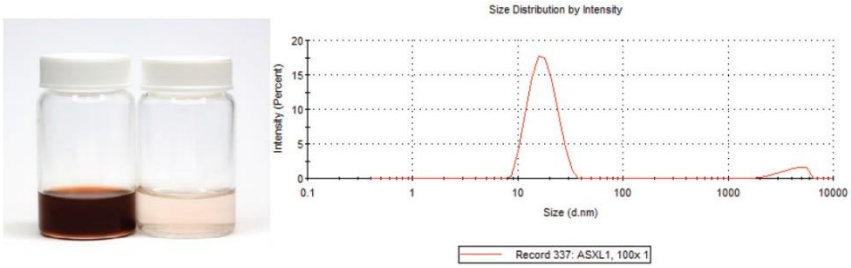

(A) **(B)**

Figure 2. (**A**) Photographic image of SNEDDS–L1 (left) and SNEDDS–L1 diluted 100-fold by water (right). (**B**) Size distribution of SNEDDS–L1.

The droplet size and PDI were measured immediately after the preparation of each SNEDDS. In all cases the SNEDDS exhibited a monomodal distribution reflecting uniform size distribution, as shown for SNEDDS-L1 in Figure 2B. All SNEDDS formulations had a droplet size below 20 nm and with a polydispersity index of less than 0.25, indicating a narrow distribution pattern and homogeneity (Table 2). At ambient temperature, the SNEDDS were viscous and spread easily and smoothly on the skin surface. The viscosity ranged from 0.19 ± 0.01 Pas to 0.23 ± 0.01 Pas (Table 2). The pH for all SNEDDS was in the range of 6.17–8.01 and reduced to 4.43–5.42 after dilution, bringing them close to the pH range of the skin and similar to the marketed ASX product (Table 2).

Table 2. Physical characteristics of ASX self-nanoemulsifying formulations (mean ± SD; $n = 3$).

Codes	Droplet Size (nm)	PDI	Zeta Potential (mV)	Viscosity (Pas)	Refractive Index	pH	
						Before Dilution	After Dilution
SNEDDS–L1	18.79 ± 0.54	0.24 ± 0.02	−12.40 ± 0.20	0.19 ± 0.01	1.46 ± 0.01	8.01 ± 0.02	5.42 ± 0.01
SNEDDS–T1	18.44 ± 0.41	0.21 ± 0.00	−12.67 ± 0.21	0.19 ± 0.01	1.46 ± 0.01	8.01 ± 0.03	4.97 ± 0.04
SNEDDS–T2	18.95 ± 1.48	0.25 ± 0.02	−12.80 ± 0.35	0.20 ± 0.01	1.46 ± 0.01	7.97 ± 0.02	5.06 ± 0.03
SNEDDS–T3	17.75 ± 0.21	0.26 ± 0.02	−13.10 ± 0.52	0.23 ± 0.01	1.46 ± 0.01	7.89 ± 0.02	4.98 ± 0.08
L1-NE	87.13 ± 2.44	0.28 ± 0.00	−12.53 ± 0.55	0.22 ± 0.01	1.40 ± 0.01	6.17 ± 0.01	4.43 ± 0.01
Marketed ASX	160.00 ± 3.44	0.20 ± 0.00	−41.57 ± 2.46	0.01 ± 0.01	1.34 ± 0.01	5.40 ± 0.02 (no dilution)	

The zeta potential of all SNEDDS formulations, determined after dilution with distilled water, were −13.10 ± 0.52 to −12.40 ± 0.20 mV, and results are summarised in Table 2. The relatively low value of zeta potential in the prepared self-nanoemulsifying

formulations may be due to the presence of a relatively higher amount of Kolliphor® EL used in formulations so that the surface charge was contributed only by co-surfactant.

The robustness to dilution test showed minimal change in the droplet size and PDI of the SNEDDS formulation upon dilution with 50-, 100-, and 250-fold deionised water with the droplet size remaining approximately 20 nm for all formulations (Table 3).

Table 3. Robustness to dilution studies of ASX-loaded SNEDDS (mean ± SD; $n = 3$).

Codes	Droplet Size (nm)		
	1:50	1:100	1:250
SNEDDS–L1	21.57 ± 0.05	18.79 ± 0.54	19.70 ± 0.27
SNEDDS–T1	19.30 ± 1.33	18.44 ± 0.41	18.47 ± 0.32
SNEDDS–T2	19.53 ± 1.35	18.95 ± 1.48	18.89 ± 0.50
SNEDDS–T3	18.08 ± 0.78	17.75 ± 0.21	19.03 ± 0.99
L1-NE	88.00 ± 3.71	87.13 ± 2.44	84.44 ± 4.52

3.4. In Vitro Skin Penetration/Permeation Study

No detectible ASX permeated through the skin to the receptor fluid from any of the SNEDDS, commercial formulation or ASX in oil (control) over the 8 h topical application period. In contrast, ASX was present in the SC and remaining skin comprised of the epidermis, dermis, and associated follicular regions (Table 4).

Table 4. Skin distribution of ASX from SNEDDS formulations, marketed product, and oil solution control (mean ± SEM; $n = 9$).

Codes	ASX Distribution in the Skin (μg/cm^2, mean ± SEM)		ER
	SC	E + D + F	
Control: ASX in oil	0.42 ± 0.01	0.56 ± 0.07	1.00
Marketed ASX product	0.67 ± 0.03	0.36 ± 0.03	1.05
SNEDDS–L1	1.48 ± 0.31	1.28 ± 0.29	2.82
SNEDDS–T1	1.40 ± 0.14	2.12 ± 0.19	3.59
SNEDDS–T2	1.09 ± 0.14	1.75 ± 0.10	2.90
SNEDDS–T3	0.82 ± 0.10	1.40 ± 0.06	2.27
L1–NE	0.50 ± 0.08	0.63 ± 0.24	1.15

ER = ratio of the mean total amount of ASX in skin (SC and E + D + F) from SNEDDS/ASX in oil solution. SC = stratum corneum; E + D + F = epidermis, dermis and follicles.

Figure 3 shows a comparison of the skin distribution of ASX following administration of the SNEDDS formulations, commercial topical product, and ASX in oil solution control. The SNEDDS–L1, comprised of Labrafil® M 1944 CS, Kolliphor® EL, Transcutol® P, showed statistically significantly greater penetration of ASX into the SC compared to the marketed commercial product and control ASX in oil solution (1.48 ± 0.31; 0.67 ± 0.03; 0.42 ± 0.01 μg/cm^2, respectively; $p < 0.05$). The SNEDDS also deposited statistically significantly more ASX in the deeper skin (E + D + F) than the commercial product and the oil solution control (1.28 ± 0.29; 0.36 ± 0.03; 0.56 ± 0.07 μg/cm^2, respectively; $p < 0.05$). Overall, there was a 2.2-fold increase in ASX in the SC and a 3.6-fold increase in the amount of ASX in the (E + D + F) from SNEDDS–L1 compared to marketed ASX nanoformulation product.

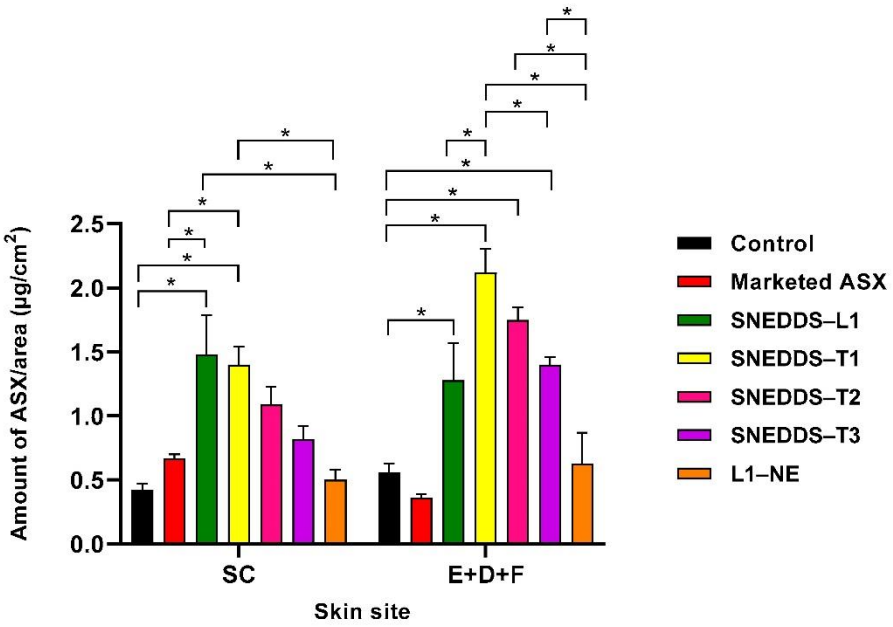

Figure 3. Skin penetration profile of SNEDDS formulations compared to marketed topical product and ASX in oil control: the distribution of ASX in the SC and E + D + F; (mean ± SEM; $n = 9$; * $p < 0.05$).

3.5. *Effect of D-Limonene, Geraniol, and Farnesol Incorporated into SNEDDS on Skin Penetration*

Three terpenes were added to the oil phase of the SNEDDS-L1 formulation to create SNEDDS-T1 (D-limonene), SNEDDS-T2 (geraniol), and SNEDDS-T3 (farnesol), and their effect on skin penetration determined (Table 4; Figure 3). No ASX was detected in the receptor fluid after 8 h application of any of the SNEDDS-containing terpenes.

All SNEDDS-containing terpenes increased ASX permeation into the SC compared to ASX in oil solution control and marketed topical product. However, the ASX penetration was significantly greater only from the SNEDDS-T1 formulation. In comparison to the SNEDDS-L1, only the SNEDDS-T1 provided similar ASX penetration into the SC, with the SNEDDS-containing geraniol and farnesol showing lower but not significantly different ASX penetration. When considering ASX penetration into the deeper skin tissues (E + D + F), the terpene-containing SNEDDS all showed statistically significantly greater ASX penetration than the control and marketed topical product, with penetration in the rank order of SNEDDS-T1 > T2 > T3. In addition, all terpene-containing SNEDDS showed greater penetration than SNEDDS-L1, although the difference was significantly different only for the D-limonene formulation.

The SNEDDS-L1 formulation was converted to an aqueous bearing nanoemulsion (designated L1-NE) by the addition of 50% water whilst maintaining the ASX concentration of the final nanoemulsion formulation. Addition of water significantly reduced the ASX penetration to the SC and (E + D + F) in comparison to the SNEDDS-L1 formulation (Table 4). ASX penetration from the L1-NE was reduced compared to all SNEDDS formulations (Figure 3).

3.6. *Preliminary Stability Study of ASX SNEDDS during Storage*

ASX stability was determined for all SNEDDS formulations and a control solution of ASX in oil, over 1 month storage at 22–25 °C with light-protected (dark) and unprotected light conditions. ASX% remaining after 30 days was in the range of 86.67–93.33% for both dark and light conditions for the SNEDDS formulations (Figure 4A,B). The ASX in oil

solution was relatively stable for 30 days at 22–25 °C when in the dark (80.74 ± 11.55%) but was reduced significantly when exposed to the light (58.75 ± 9.55%).

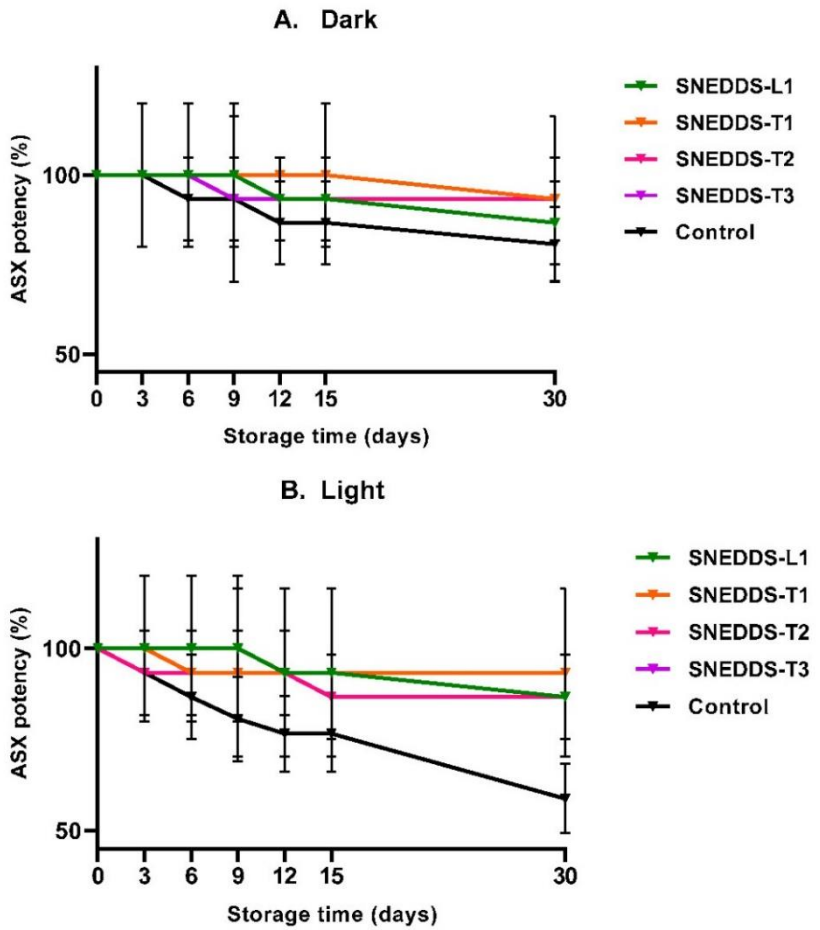

Figure 4. % ASX remaining after 30 day storage of SNEDDS formulations and ASX in oil (control) at room temperature in the dark (**A**) and light (**B**) conditions (mean ± SD; $n = 3$).

3.7. Antioxidant Activity of ASX SNEDDS Formulations

The ABTS radical scavenging assay was performed to investigate the antioxidant activity of all SNEDDS formulations and the SNEDDS-based nanoemulsion (L1-NE), and compared to the marketed topical product and ascorbic acid (Figure 5). The ABTS radical scavenging was stable across the concentration range of the formulations. At 1000 µg/mL, % scavenging activity in all SNEDDS was from 68.13 ± 0.44 µg/mL to 66.79 ± 0.08 µg/mL, and the L1-NE was approximately 20% lower at 57.79 ± 0.58 µg/mL. All SNEDDS-containing ASX had significantly greater ABTS scavenging activity than the ascorbic acid control (39.53 ± 0.61 µg/mL) and marketed topical product (53.00 ± 0.08 µg/mL; $p < 0.05$; Figure 5).

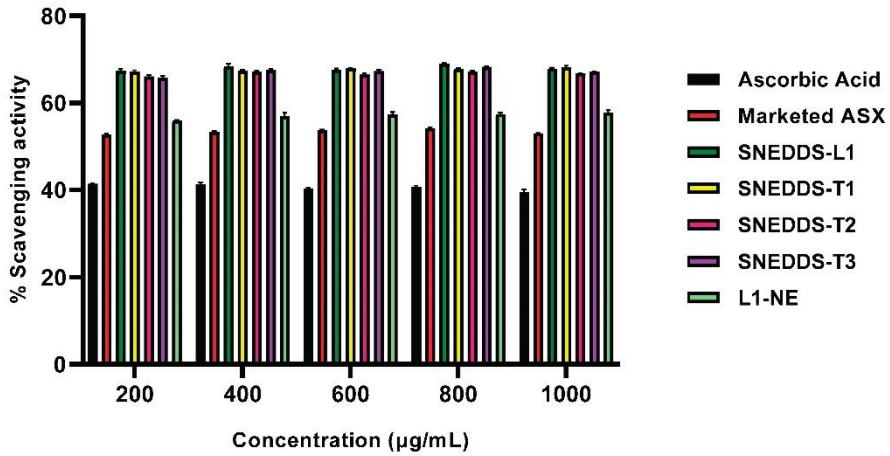

Figure 5. % ABTS-radical scavenging activity of 200–1000 µg/mL concentrations of SNEDDS formulations, SNEDDS-based nanoemulsion (L1-NE), marketed ASX topical product and ascorbic acid solution as positive control (mean ± SD; n = 3).

4. Discussion

The therapeutic potential of ASX has been investigated for a wide range of conditions and administration routes including oral and topical delivery [5]. Topical administration to the skin has been primarily for cosmeceutical purposes such as anti-aging with a number of facial serum products available. There is great potential to use the high antioxidant and anti-inflammatory capability of ASX for dermatological conditions such as repair of UV damage, dermatitis, and rashes. To fully utilise its potential, an effective delivery system is needed that targets ASX to the skin in therapeutic quantities. Targeted delivery of ASX to the epidermis and dermis, where it will exert its antioxidant and anti-inflammatory therapeutic activity, requires facilitating drug entry to these skin tissues whilst minimising uptake by the cutaneous circulation. The high lipophilicity of ASX is challenging as it requires formulating to enhance the solubility and delivery to the SC whilst also facilitating partitioning to the deeper more aqueous tissues of the epidermis and dermis. Previous reports have demonstrated the ability of self-emulsifying and self nano-emulsifying drug delivery systems (SEDDS and SNEDDS) to increase the solubility and bioavailability of lipophilic drugs including sesamin [32], clofazimine [38], meloxicam [34], and curcumin [48]. We proposed SNEDDS as a formulation approach to solubilize the highly lipophilic ASX and provide a delivery system that is simple to produce, has an attractive appearance, good spreadability on the skin, is stable (physically and chemically), and provides effective delivery of ASX into the skin to target its antioxidant/anti-inflammatory activity to its site of action in the epidermis and dermis. These criteria constituted the quality target product profile (QTPP) for assessing a successful formulation strategy [49,50]. We also proposed that the anhydrous SNEDDS formulations would perform better than a nanoemulsion composed from the same components as a SNEDDS formulation. Overall, in this study, the SNEDDS formulations containing ASX met the QTPP, with differences in the level of performance based on the choice of formulation excipients. All SNEDDS formulations performed better than the corresponding nanoemulsion, a marketed ASX facial serum product, and a solution of ASX in oil.

SNEDDS formulations incorporating ASX composed of Labrafil® M 1944 CS (constituting the oil phase), Kolliphor® EL (non-ionic surfactant), and Transcutol® P as a co-surfactant (designated SNEDDS-L1) were successfully formulated and provided statistically significant enhancement of skin permeation of ASX compared to a marketed ASX facial serum formulation and ASX in oil solution (Figure 3).

Labrafil® M 1944 CS consists of mono-, di- and triglycerides and PEG-6 mono- and diesters of oleic (C18:1) acid. It is a nonionic water-dispersible surfactant for lipid-based formulations that is commonly used as a co-emulsifier in topical formulations, and provides the oil phase for the current SNEDDS formulations. The selected surfactant, Kolliphor® EL (polyoxyl-35 hydrogenated castor oil), is a non-ionic solubilizer and emulsifying agent with hydrophile-lipophile balance (HLB) of 12. Its hydrophobic moiety is a combination of glycerol polyethylene glycol ricinoleate and fatty acid esters of polyethylene glycol, while the hydrophilic moiety is a combination of polyethylene glycols and glycerol ethoxylate [51]. Transcutol® P, a high purity grade of diethylene glycol monoethyl ether (DEGEE), was selected as the co-surfactant because of its properties as a hydroalcoholic solubilizer [51] and skin permeation enhancer without compromising skin integrity [52,53]. All components are categorised as Generally Recognised as Safe and Effective (GRASE) by the U.S. Food and Drug Administration (FDA) [54].

The SNEDDS formulations provided excellent physical characteristics for skin application. The SNEDDS-L1 formulation showed small droplet size in the order of 18 nm, a negative zeta potential (12.40 $\pm$ 0.20 mV), and a viscosity (0.19 $\pm$ 0.01 Pas) that provided good spreadability and retention on the skin surface. Kaur and Ajitha reported that the delivery of fluvastatin increased when the droplet size and zeta potential are reduced and viscosity increased, suggesting that this was due to higher occlusivity on the skin [55]. The droplet size has also been shown to be an important parameter to enhance the release of the drug from the formulation [34,56]. Smaller droplet size resulted in a large surface area that provided high drug release of meloxicam from a SNEDDS for transdermal delivery [34]. In our preliminary studies, manufacturing without the high-energy ultrasonic homogenization step provided slightly larger droplets of approximately 26 nm. As this is still an acceptable size for skin delivery, it suggests that the SNEDDS formulations could be manufactured by a lower energy method that could be beneficial for industrial scale-up. The negative zeta potential (Table 2) increased electrostatic repulsion between droplets to enhance physical stability.

All ASX-containing SNEDDS formulations showed good physical stability over 30 days and significantly improved the chemical stability of ASX in the formulation compared to ASX in oil solution, particularly when exposed to light (Figure 4). Whilst this provides a preliminary indication of the stability of ASX in the SNEDDS formulations, a full stability study over a longer-term is required to assess the formulations for use as commercial products. As ASX confers its therapeutic effects via its antioxidant activity this was assessed in all SNEDDS formulations and a range of controls including ascorbic acid as the antioxidant standard. The SNEDDS formulations all demonstrated higher antioxidant activity than ASX in oil solution and an ascorbic acid standard (Figure 5), showing that the SNEDDS formulations provided ASX inactive form more readily than when ASX was dissolved in oil. The SNEDDS-based nanoemulsion showed lower antioxidant activity than its corresponding anhydrous SNEDDS formulation. This suggests that the ASX is more available from the SNEDDS formulation or that the ASX could have been partially degraded by the presence of dissolved oxygen in that water phase of the nanoemulsion, as has been suggested by Sun et al. [28]. In addition, it has been reported that ASX can self-assemble in polar solvents to form tightly packed stacks of individual molecules [57], potentially reducing its availability and activity.

The SNEDDS-L1 formulation enhanced the penetration of ASX in the skin, providing a 2.2-fold increase and a 3.6-fold increase in the SC and (E + D + F), respectively compared to marketed ASX product. As ASX is highly lipophilic, it is expected to penetrate the lipid bilayer regions of the SC, but have poor partitioning to the more aqueous deeper epidermal and dermal tissues that constitute the target site for the ASX antioxidant and anti-inflammatory activity. When applied as the commercial formulation, the deposition of ASX in the E + D + F was lowest, followed by the oil solution. The SNEDDS-L1 formulation significantly increased ASX penetration to the target tissues compared to both the marketed topical product and a solution of ASX in oil. This demonstrates that

the SNEDDS formulation components and their nanosystem structure has the ability to enhance skin penetration by a number of mechanisms. First, the oil can solubilize the lipophilic ASX thus presenting it to the skin in a form that can access the lipid domains in the SC. However, that would not explain the significant improvement in comparison to the ASX in oil solution. Second, the oil, surfactant, and co-surfactant components can modify the SC lipid structure to facilitate permeation within the SC and entry to the viable epidermal regions. Third, presenting the ASX as a nanosystem optimizes ASX presentation to the skin, and facilitates diffusion and partitioning within the epidermal layers. Indeed, it has been postulated that SNEDDS formulations act by taking up moisture from the skin surface to form an occlusive topical system that has a high thermodynamic driving force for skin delivery [34,39,40]. We investigated formation of a SNEDDS-based nanoemulsion by addition of water to form L1-NE. However, when applied to the skin this nanoemulsion formulation showed significantly lower ASX penetration to the SC and (E + D + F) than the anhydrous SNEDDS-L1. This may be due to the increase in droplet size of the nanoemulsion compared to the SNEDDS-L1 (87.13 $\pm$ 2.44 and 18.79 $\pm$ 0.54 nm, respectively), or possibly a reduction in ASX degradation due to the presence of dissolved oxygen in the water phase. We did prepare all formulations immediately before administration in the IVPT studies so as to minimise any stability effects, but our antioxidant study did demonstrate a small reduction in ASX activity in the hydrous nanoemulsion compared to its corresponding anhydrous SNEDDS formulation (Figure 5).

Terpenes have demonstrated penetration enhancement activity by disruption of the intercellular lipid structure in the SC [58,59] to increase permeant diffusivity. Here, we investigated the addition of three terpenes into the oil phase to create three SNEDDS formulations: SNEDDS-T1 (D-limonene), SNEDDS-T2 (geraniol), and SNEDDS-T3 (farnesol). D-limonene (MW 1.36.23 g/mol; log Po/w 4.57) [60], geraniol (MW 154.25 g/mol; log Po/w 3.56) [61], farnesol (227.37 g/mol; log Po/w 5.77) [62] provide a range of chemical structures and properties that can influence their role in the formulation.

Incorporation of terpenes increased ASX penetration to the deeper skin target site (E + D + F) compared to the SNEDDS-L1 formulation, with the following order of penetration SNEDDS-T1 > T2 > T3, although only the SNEDDS-T1 was significantly greater ASX penetration ($p < 0.05$: Figure 3). There was no significant difference in ASX penetration to the SC across the SNEDDS formulations, although again the order of ASX penetration was SNEDDS-T1 > T2 > T3. It is interesting to note that the presence of terpenes resulted in greater deep tissue penetration compared to SC deposition in all cases, suggesting that the terpenes are facilitating ASX diffusion within the skin tissues. Overall, the data suggest that inclusion of terpene does not increase release from the SNEDDS to the skin surface or penetration into the SC, but can improve partitioning from the SC into the more aqueous epidermal tissues and diffusion within the skin tissues. Previous studies have demonstrated a correlation between drug permeation from nanoemulsions with partition coefficient of the terpene in the formulation [63,64]. For example, El-Kattan et al. reported a positive correlation between the lipophilicity of the terpenes and the cumulative amount of hydrocortisone (log P 1.43) permeating through hairless mouse skin [63]. However, we did not see a similar correlation for the highly lipophilic ASX. El-Kattan et al. also examined the effect of terpene enhancers on solutes with a range of lipophilicities (-1 to 8 approximately) showing that terpenes-based skin permeation enhancement (range 135-fold to 2-fold) was inversely correlated with log P [65].

We have demonstrated that SNEDDS are an effective formulation for enhanced skin delivery of the highly lipophilic ASX to the deeper skin tissues that constitute the target site for therapeutic antioxidant and anti-inflammatory activity. We have also shown that they provide the ASX in active form with high antioxidant activity (Figure 5) and help to preserve stability of this active ingredient that is prone to degradation (Figure 4). As has been previously stated [38], the simplicity and ease of preparation of SEDDS and SNEDDS, compared to the manufacture of liposomes and nanoemulsions, provides advantages for

topical/transdermal delivery systems of lipophilic molecules and has potential for poorly stable drugs and biologics.

Supplementary Materials: The following are available online at https://www.mdpi.com/article/10.3390/pharmaceutics13050649/s1, Figure S1: HPLC chromatograms (peak area versus time) of: (A) 0.75 µg/mL ASX solution as prepared for the calibration curve; (B) SNEDDS-L1 formulation matrix without ASX; (C) SNEDDS-L1 formulation matrix with ASX incorporated; (D) Skin extract following administration of SNEDDS L1-NE in IVPT experiment.

Author Contributions: Conceptualization, T.P. and H.A.E.B.; methodology, T.P., G.L. (Gemma Latter), G.L. (Giuseppe Luna), V.R.L.-S., A.W. and H.A.E.B.; data curation and analysis, T.P., G.L. (Gemma Latter), G.L. (Giuseppe Luna), V.R.L.-S., A.W. and H.A.E.B; writing—original draft preparation, T.P. and H.A.E.B.; writing—review and editing, T.P., G.L. (Gemma Latter), G.L. (Giuseppe Luna), V.R.L.-S., A.W. and H.A.E.B; project administration, H.A.E.B.; funding acquisition, T.P. and H.A.E.B. All authors have read and agreed to the published version of the manuscript.

Funding: This research was funded by Curtin University and T.P received an RTP scholarship from the Australian government.

Institutional Review Board Statement: Not applicable.

Informed Consent Statement: Not applicable.

Data Availability Statement: Data available by email request.

Acknowledgments: The authors would like to thank Behin Sundara Raj for technical support with the antioxidant studies and the veterinary staff at Portec Veterinary Services for collection of stillborn piglets. We are also grateful to AstaREAL Co., Ltd., Japan for gifts of commercial products.

Conflicts of Interest: The authors declare no conflict of interest.

References

1. Ramos-e-Silva, M.; Celem, L.R.; Ramos-e-Silva, S.; Fucci-da-Costa, A.P. Anti-aging cosmetics: Facts and controversies. *Clin. Dermatol.* **2013**, *31*, 750–758. [CrossRef]
2. Higuera-Ciapara, I.; Felix-Valenzuela, L.; Goycoolea, F.M. Astaxanthin: A review of its chemistry and applications. *Crit. Rev. Food Sci. Nutr.* **2006**, *46*, 185–196. [CrossRef]
3. Lim, K.C.; Yusoff, F.M.; Shariff, M.; Kamarudin, M.S. Astaxanthin as feed supplement in aquatic animals. *Rev. Aquac.* **2018**, *10*, 738–773. [CrossRef]
4. Shah, M.; Mahfuzur, R.; Liang, Y.; Cheng, J.J.; Daroch, M. Astaxanthin-producing green microalga Haematococcus pluvialis: From single cell to high value commercial products. *Front. Plant Sci.* **2016**, *7*, 531–558. [CrossRef] [PubMed]
5. Donoso, A.; González, J.; Muñoz, A.A.; González, P.A.; Agurto-Muñoz, C. Therapeutic uses of natural astaxanthin: An evidence-based review focused on human clinical trials. *Pharmacol. Res.* **2021**, *166*, 1–12. [CrossRef]
6. Ambati, R.R.; Phang, S.M.; Ravi, S.; Aswathanarayana, R.G. Astaxanthin: Sources, extraction, stability, biological activities and its commercial applications—A review. *Mar. Drugs* **2014**, *12*, 128–152. [CrossRef] [PubMed]
7. Pereira, C.P.M.; Souza, A.C.R.; Vasconcelos, A.R.; Prado, P.S. Antioxidant and anti-inflammatory mechanisms of action of astaxanthin in cardiovascular diseases. *Int. J. Mol. Med.* **2020**, *47*, 37–48. [CrossRef]
8. Xia, W.; Tang, N.; Varkaneh, H.K.; Low, T.Y.; Tan, S.C.; Wu, X.; Zhu, Y. The effects of astaxanthin supplementation on obesity, blood pressure, CRP, glycemic biomarkers, and lipid profile: A meta-analysis of randomized controlled trials. *Pharmacol. Res.* **2020**, *161*, 1–11. [CrossRef]
9. Fanaee-Danesh, E.; Gali, C.C.; Tadic, J.; Zandl-Lang, M.; Kober, A.C.; Agujetas, V.R.; de Dios, C.; Tam-Amersdorfer, C.; Stracke, A.; Albrecher, N.M. Astaxanthin exerts protective effects similar to bexarotene in Alzheimer's disease by modulating amyloid-beta and cholesterol homeostasis in blood-brain barrier endothelial cells. *Biochim. Biophys. Acta (BBA) Mol. Basis Dis.* **2019**, *1865*, 2224–2245. [CrossRef] [PubMed]
10. Cakir, E.; Cakir, U.; Tayman, C.; Turkmenoglu, T.T.; Gonel, A.; Turan, I.O. Favorable Effects of Astaxanthin on Brain Damage due to Ischemia-Reperfusion Injury. *Comb. Chem. High Throughput Screen.* **2020**, *23*, 214–224. [CrossRef] [PubMed]
11. Fleischmann, C.; Shohami, E.; Trembovler, V.; Heled, Y.; Horowitz, M. Cognitive effects of astaxanthin pretreatment on recovery from traumatic brain injury. *Front. Neurol.* **2020**, *11*, 1–14. [CrossRef]
12. Xu, L.; Yu, H.; Sun, H.; Yu, X.; Tao, Y. Optimized nonionic emulsifier for the efficient delivery of astaxanthin nanodispersions to retina: In vivo and ex vivo evaluations. *Drug Deliv.* **2019**, *26*, 1222–1234. [CrossRef] [PubMed]
13. Giannaccare, G.; Pellegrini, M.; Senni, C.; Bernabei, F.; Scorcia, V.; Cicero, A.F.G. Clinical Applications of Astaxanthin in the Treatment of Ocular Diseases: Emerging Insights. *Mar. Drugs* **2020**, *18*, 239. [CrossRef] [PubMed]

14. Faraone, I.; Sinisgalli, C.; Ostuni, A.; Armentano, M.F.; Carmosino, M.; Milella, L.; Russo, D.; Labanca, F.; Khan, H. Astaxanthin anticancer effects are mediated through multiple molecular mechanisms: A systematic review. *Pharmacol. Res.* **2020**, *155*, 1–13. [CrossRef] [PubMed]
15. Davinelli, S.; Nielsen, M.E.; Scapagnini, G. Astaxanthin in Skin Health, Repair, and Disease: A Comprehensive Review. *Nutrients* **2018**, *10*, 522. [CrossRef]
16. Singh, K.N.; Patil, S.; Barkate, H. Protective effects of astaxanthin on skin: Recent scientific evidence, possible mechanisms, and potential indications. *J. Cosmet. Dermatol.* **2020**, *19*, 22–27. [CrossRef] [PubMed]
17. Huangfu, J.; Liu, J.; Sun, Z.; Wang, M.; Jiang, Y.; Chen, Z.-Y.; Chen, F. Antiaging Effects of Astaxanthin-Rich Alga Haematococcus pluvialis on Fruit Flies under Oxidative Stress. *J. Agric. Food Chem.* **2013**, *61*, 7800–7804. [CrossRef] [PubMed]
18. Ito, N.; Seki, S.; Ueda, F. The Protective Role of Astaxanthin for UV-Induced Skin Deterioration in Healthy People-A Randomized, Double-Blind, Placebo-Controlled Trial. *Nutrients* **2018**, *10*, 817. [CrossRef]
19. Imokawa, G. The xanthophyll carotenoid astaxanthin has distinct biological effects to prevent the photoaging of the skin even by its postirradiation treatment. *Photochem. Photobiol.* **2019**, *95*, 490–500. [CrossRef]
20. Seki, T.; Sueki, H.; Kono, H.; Suganuma, K.; Yamashita, E. Effects of astaxanthin from Haematococcus pluvialis on human skin-patch test; skin repeated application test; effect on wrinkle reduction. *Fragr. J.* **2001**, *12*, 98–103.
21. Tominaga, K.; Hongo, N.; Karato, M.; Yamashita, E. Cosmetic benefits of astaxanthin on humans subjects. *Acta Biochim. Pol.* **2012**, *59*, 43–47. [CrossRef] [PubMed]
22. Tominaga, K.; Hongo, N.; Fujishita, M.; Takahashi, Y.; Adachi, Y. Protective effects of astaxanthin on skin deterioration. *J. Clin. Biochem. Nutr.* **2017**, *61*, 33–39. [CrossRef] [PubMed]
23. Yoon, H.-S.; Cho, H.H.; Cho, S.; Lee, S.-R.; Shin, M.-H.; Chung, J.H. Supplementing with Dietary Astaxanthin Combined with Collagen Hydrolysate Improves Facial Elasticity and Decreases Matrix Metalloproteinase-1 and -12 Expression: A Comparative Study with Placebo. *J. Med. Food* **2014**, *17*, 810–816. [CrossRef]
24. Jannel, S.; Caro, Y.; Bermudes, M.; Petit, T. Novel Insights into the Biotechnological Production of Haematococcus pluvialis-Derived Astaxanthin: Advances and Key Challenges to Allow Its Industrial Use as Novel Food Ingredient. *J. Mar. Sci. Eng.* **2020**, *8*, 789. [CrossRef]
25. Anarjan, N.; Tan, C.P.; Ling, T.C.; Lye, K.L.; Malmiri, H.J.; Nehdi, I.A.; Cheah, Y.K.; Mirhosseini, H.; Baharin, B.S. Effect of organic-phase solvents on physicochemical properties and cellular uptake of astaxanthin nanodispersions. *J. Agric. Food Chem.* **2011**, *59*, 8733–8741. [CrossRef] [PubMed]
26. Pan, L.; Zhang, S.; Gu, K.; Zhang, N. Preparation of astaxanthin-loaded liposomes: Characterization, storage stability and antioxidant activity. *CyTA J. Food* **2018**, *16*, 607–618. [CrossRef]
27. Hong, L.; Zhou, C.L.; Chen, F.P.; Han, D.; Wang, C.Y.; Li, J.X.; Chi, Z.; Liu, C.G. Development of a carboxymethyl chitosan functionalized nanoemulsion formulation for increasing aqueous solubility, stability and skin permeability of astaxanthin using low-energy method. *J. Microencapsul.* **2017**, *34*, 707–721. [CrossRef]
28. Sun, R.; Xia, N.; Xia, Q. Non-aqueous nanoemulsions as a new strategy for topical application of astaxanthin. *J. Dispers. Sci. Technol.* **2019**, *41*, 1777–1788. [CrossRef]
29. Eren, B.; Tuncay Tanriverdi, S.; Aydin Kose, F.; Ozer, O. Antioxidant properties evaluation of topical astaxanthin formulations as anti-aging products. *J. Cosmet. Dermatol.* **2019**, *18*, 242–250. [CrossRef]
30. Hama, S.; Takahashi, K.; Inai, Y.; Shiota, K.; Sakamoto, R.; Yamada, A.; Tsuchiya, H.; Kanamura, K.; Yamashita, E.; Kogure, K. Protective effects of topical application of a poorly soluble antioxidant astaxanthin liposomal formulation on ultraviolet-induced skin damage. *J. Pharm. Sci.* **2012**, *101*, 2909–2916. [CrossRef]
31. Geng, Q.; Zhao, Y.; Wang, L.; Xu, L.; Chen, X.; Han, J. Development and Evaluation of Astaxanthin as Nanostructure Lipid Carriers in Topical Delivery. *AAPS PharmSciTech* **2020**, *21*, 1–12. [CrossRef] [PubMed]
32. Kazi, M.; Al-Swairi, M.; Ahmad, A.; Raish, M.; Alanazi, F.K.; Badran, M.M.; Khan, A.A.; Alanazi, A.M.; Hussain, M.D. Evaluation of Self-Nanoemulsifying Drug Delivery Systems (SNEDDS) for Poorly Water-Soluble Talinolol: Preparation, in vitro and in vivo Assessment. *Front. Pharmacol.* **2019**, *10*, 459–471. [CrossRef] [PubMed]
33. Elnaggar, Y.S.R.; Massik, M.A.E.; Abdallah, O.Y. Sildenafil citrate nanoemulsion vs. self-nanoemulsifying delivery systems: Rational development and transdermal permeation. *Int. J. Nanotechnol* **2011**, *8*, 749–763. [CrossRef]
34. Badran, M.M.; Taha, E.I.; Tayel, M.M.; Al-Suwayeh, S.A. Ultra-fine self nanoemulsifying drug delivery system for transdermal delivery of meloxicam: Dependency on the type of surfactants. *J. Mol. Liq.* **2014**, *190*, 16–22. [CrossRef]
35. van Staden, D.; du Plessis, J.; Viljoen, J. Development of Topical/Transdermal Self-Emulsifying Drug Delivery Systems, Not as Simple as Expected. *Sci. Pharm.* **2020**, *88*, 17. [CrossRef]
36. Nastiti, C.M.R.R.; Ponto, T.; Abd, E.; Grice, J.E.; Benson, H.A.E.; Roberts, M.S. Topical nano and microemulsions for skin delivery. *Pharmaceutics* **2017**, *9*, 37. [CrossRef]
37. Khan, M.; Ali, M.; Shah, W.; Shah, A.; Yasinzai, M.M. Curcumin-loaded self-emulsifying drug delivery system (cu-SEDDS): A promising approach for the control of primary pathogen and secondary bacterial infections in cutaneous leishmaniasis. *Appl. Microbiol. Biotechnol.* **2019**, *103*, 7481–7490. [CrossRef]
38. van Staden, D.; du Plessis, J.; Viljoen, J. Development of a Self-Emulsifying Drug Delivery System for Optimized Topical Delivery of Clofazimine. *Pharmaceutics* **2020**, *12*, 523. [CrossRef]

39. El Maghraby, G.M. Self-microemulsifying and microemulsion systems for transdermal delivery of indomethacin: Effect of phase transition. *Colloids Surf. B Biointerfaces* **2010**, *75*, 595–600. [CrossRef]
40. Kogan, A.; Garti, N. Microemulsions as transdermal drug delivery vehicles. *Adv. Colloid Interface Sci.* **2006**, *123–126*, 369–385. [CrossRef]
41. Yuan, J.-P.; Chen, F. Chromatographic separation and purification of trans-astaxanthin from the extracts of Haematococcus pluvialis. *J. Agric. Food Chem.* **1998**, *46*, 3371–3375. [CrossRef]
42. Cilurzo, F.; Minghetti, P.; Sinico, C. Newborn pig skin as model membrane in in vitro drug permeation studies: A technical note. *AAPS PharmSciTech* **2007**, *8*, 97–100. [CrossRef]
43. Nastiti, C.; Mohammed, Y.; Telaprolu, K.C.; Liang, X.; Grice, J.E.; Roberts, M.S.; Benson, H.A.E. Evaluation of Quantum Dot Skin Penetration in Porcine Skin: Effect of Age and Anatomical Site of Topical Application. *Skin Pharmacol. Physiol.* **2019**, *32*, 182–191. [CrossRef] [PubMed]
44. Davies, D.J.; Ward, R.J.; Heylings, J.R. Multi-species assessment of electrical resistance as a skin integrity marker for in vitro percutaneous absorption studies. *Toxicology* **2004**, *18*, 351–358. [CrossRef]
45. Davies, D.J.; Heylings, J.R.; McCarthy, T.J.; Correa, C.M. Development of an in vitro model for studying the penetration of chemicals through compromised skin. *Toxicology* **2015**, *29*, 176–181. [CrossRef]
46. Chintong, S.; Phatvej, W.; Rerk-Am, U.; Waiprib, Y.; Klaypradit, W. In Vitro Antioxidant, Antityrosinase, and Cytotoxic Activities of Astaxanthin from Shrimp Waste. *Antioxidants* **2019**, *8*, 128. [CrossRef] [PubMed]
47. Prior, R.L.; Wu, X.; Schaich, K. Standardized methods for the determination of antioxidant capacity and phenolics in foods and dietary supplements. *J. Agric. Food Chem.* **2005**, *53*, 4290–4302. [CrossRef] [PubMed]
48. Altamimi, M.A.; Kazi, M.; Hadi Albgomi, M.; Ahad, A.; Raish, M. Development and optimization of self-nanoemulsifying drug delivery systems (SNEDDS) for curcumin transdermal delivery: An anti-inflammatory exposure. *Drug Dev. Ind. Pharm.* **2019**, *45*, 1073–1078. [CrossRef] [PubMed]
49. International Council for Harmonisation (ICH). ICH Expert Working Group Harmonised Tripartite Guideline: Quality Risk Management Q8 (R2). Available online: https://www.ich.org/fileadmin/Public_Web_Site/ICH_Products/Guidelines/Quality/Q8_R1/Step4/Q8_R2_Guideline.pdf (accessed on 9 February 2021).
50. International Council for Harmonisation (ICH). ICH Expert Working Group Harmonised Tripartite Guideline: Pharmaceutical Development Q9. Available online: https://www.ich.org/fileadmin/Public_Web_Site/ICH_Products/Guidelines/Quality/Q9/Step4/Q9_Guideline.pdf (accessed on 9 February 2021).
51. https://pharmaceutical.basf.com/. Kolliphor®EL. Available online: https://pharmaceutical.basf.com/global/en/drug-formulation/products/kolliphor-el.html (accessed on 9 February 2021).
52. Osborne, D.W.; Musakhanian, J. Skin Penetration and Permeation Properties of Transcutol(R)-Neat or Diluted Mixtures. *AAPS PharmSciTech* **2018**, *19*, 3512–3533. [CrossRef] [PubMed]
53. Yousef, S.A.; Mohammed, Y.H.; Namjoshi, S.; Grice, J.E.; Benson, H.A.; Sakran, W.; Roberts, M.S. Mechanistic evaluation of enhanced curcumin delivery through human skin in vitro from optimised nanoemulsion formulations fabricated with different penetration enhancers. *Pharmaceutics* **2019**, *11*, 639. [CrossRef]
54. Fiume, M.Z. Final report on the safety assessment of triacetin. *Int. J. Toxicol.* **2003**, *22* (Suppl. 2), 1–10.
55. Kaur, R.; Ajitha, M. Transdermal delivery of fluvastatin loaded nanoemulsion gel: Preparation, characterization and in vivo anti-osteoporosis activity. *Eur. J. Pharm. Sci.* **2019**, *136*, 1–10. [CrossRef]
56. Anton, N.; Gayet, P.; Benoit, J.-P.; Saulnier, P. Nano-emulsions and nanocapsules by the PIT method: An investigation on the role of the temperature cycling on the emulsion phase inversion. *Int. J. Pharm.* **2007**, *344*, 44–52. [CrossRef]
57. Brotosudarmo, T.H.P.; Limantara, L.; Setiyono, E. Structures of Astaxanthin and Their Consequences for Therapeutic Application. *Int. J. Food Sci.* **2020**, *2020*, 1–16. [CrossRef]
58. Herman, A.; Herman, A.P. Essential oils and their constituents as skin penetration enhancer for transdermal drug delivery: A review. *J. Pharm. Pharmacol.* **2015**, *67*, 473–485. [CrossRef] [PubMed]
59. Williams, A.C.; Barry, B.W. Terpenes and the Lipid–Protein–Partitioning Theory of Skin Penetration Enhancement. *Pharm. Res.* **1991**, *8*, 17–24. [CrossRef]
60. National Library of Medicine: National Center for Biotechnology Information. PubChem Compound Summary for CID 440917, D-Limonene. Available online: https://pubchem.ncbi.nlm.nih.gov/compound/D-Limonene (accessed on 9 February 2021).
61. National Library of Medicine: National Center for Biotechnology Information. PubChem Compound Summary for CID 445070, Geraniol. 2020. Available online: https://pubchem.ncbi.nlm.nih.gov/compound/637566 (accessed on 9 February 2021).
62. National Library of Medicine: National Center for Biotechnology Information. PubChem Compound Summary for CID 445070, Farnesol. 2020. Available online: https://pubchem.ncbi.nlm.nih.gov/compound/445070 (accessed on 9 February 2021).
63. El-Kattan, A.F.; Asbill, C.S.; Michniak, B.B. The effect of terpene enhancer lipophilicity on the percutaneous permeation of hydrocortisone formulated in HPMC gel systems. *Int. J. Pharm.* **2000**, *198*, 179–189. [CrossRef]
64. Nastiti, C.M.R.R.; Ponto, T.; Mohammed, Y.; Roberts, M.S.; Benson, H.A.E. Novel Nanocarriers for Targeted Topical Skin Delivery of the Antioxidant Resveratrol. *Pharmaceutics* **2020**, *12*, 108. [CrossRef]
65. El-Kattan, A.F.; Asbill, C.S.; Kim, N.; Michniak, B.B. The effects of terpene enhancers on the percutaneous permeation of drugs with different lipophilicities. *Int. J. Pharm.* **2001**, *215*, 229–240. [CrossRef]

pharmaceutics

MDPI

Supplementary Materials: Novel Self-Nano-Emulsifying Drug Delivery Systems Containing Astaxanthin for Topical Skin Delivery

Thellie Ponto, Gemma Latter, Giuseppe Luna, Vânia R. Leite-Silva, Anthony Wright and Heather A. E. Benson

Methods

HPLC instrumentation and conditions

Chromatographic separation was performed using an Agilent™ 1200 system (Agilent Technologies, Waldbronn, Germany), equipped with a degasser, binary pump, autosampler, multiple wavelength detector (at 476 nm UV detection), and Chemstation Rev B.04.03-SP1 software. A Jupiter C18 5 µm column, (150 mm × 4.6 mm) protected by a Security Guard Cartridge (C18, 4 × 3 mm) both from Phenomenex (Lane Cove, NSW, Australia), was used with isocratic flow of mobile phase (methanol: water: dichloromethane (DCM) = 85:13:2) at a flow rate of 1 mL/min (chromatography adapted from Yuan *et al.* [1]. The autosampler temperature was under a controlled temperature of 10 °C with an illuminator setting.

HPLC analysis method development

The HPLC method was developed for analysis of ASX in pharmaceutical formulations and extraction of ASX from skin tissues.

Linearity—Two series of ASX concentrations. System X (0.75–15 µg/mL) represented samples for determination of the solubility and stability of ASX, and the higher concentration tissue extract samples from skin permeation experiments with SNEDDS formulations. System Y (0.105–1.05 µg/mL) was for analysis of tissue sample extracts from commercial topical product administration in skin experiments.

Precision—ASX solutions at four concentrations (15, 3.75, 0.75 and 0.105 µg/mL) were analyzed in six replicates for each concentration. This provided concentrations from the two calibration curves used across the experimental samples. The acceptable relative standard deviation (RSD) < 5% [2].

Sensitivity—The blank solvent, a mixture of 15 mL of acetone and dichloromethane (50:50) and 10 mL mobile phase, was injected 6 times. The limit of detection (LOD) and LOQ (limit of quantification) were determined as three times and ten times the baseline noise level in the assay, respectively.

Accuracy—A mass balance study of ASX extracts from skin tissue samples that had been exposed to a SNEDDS formulation was carried out to assess the accuracy of the assay. The solvent extraction system was 50:50 ACT: DCM. The extraction procedure developed for the study involved soaking a pre-weighed section of skin tissue in 5 mL of an aqueous solution containing the SNEDDS-L1 formulation at a concentration of 0.0758 mg ASX/mL (equivalent to the theoretical concentration that would be present in an IVPT experiment) at 35 °C for 4h, then removing it, blotting dry and sectioning. The ASX was extracted from the skin sections (as per extraction protocol described in Section 2.6) and quantified by HPLC assay.

Results

HPLC assay method development

The HPLC method provided a single ASX peak for stock solution and good separation from any skin sample related peaks. ASX retention time was 8.3 ± 0.1 minutes with a

total analysis time of 13 minutes (Figure 1S). Two calibration curves were generated to allow for the larger volume injections in the lower concentration range calibration curve.

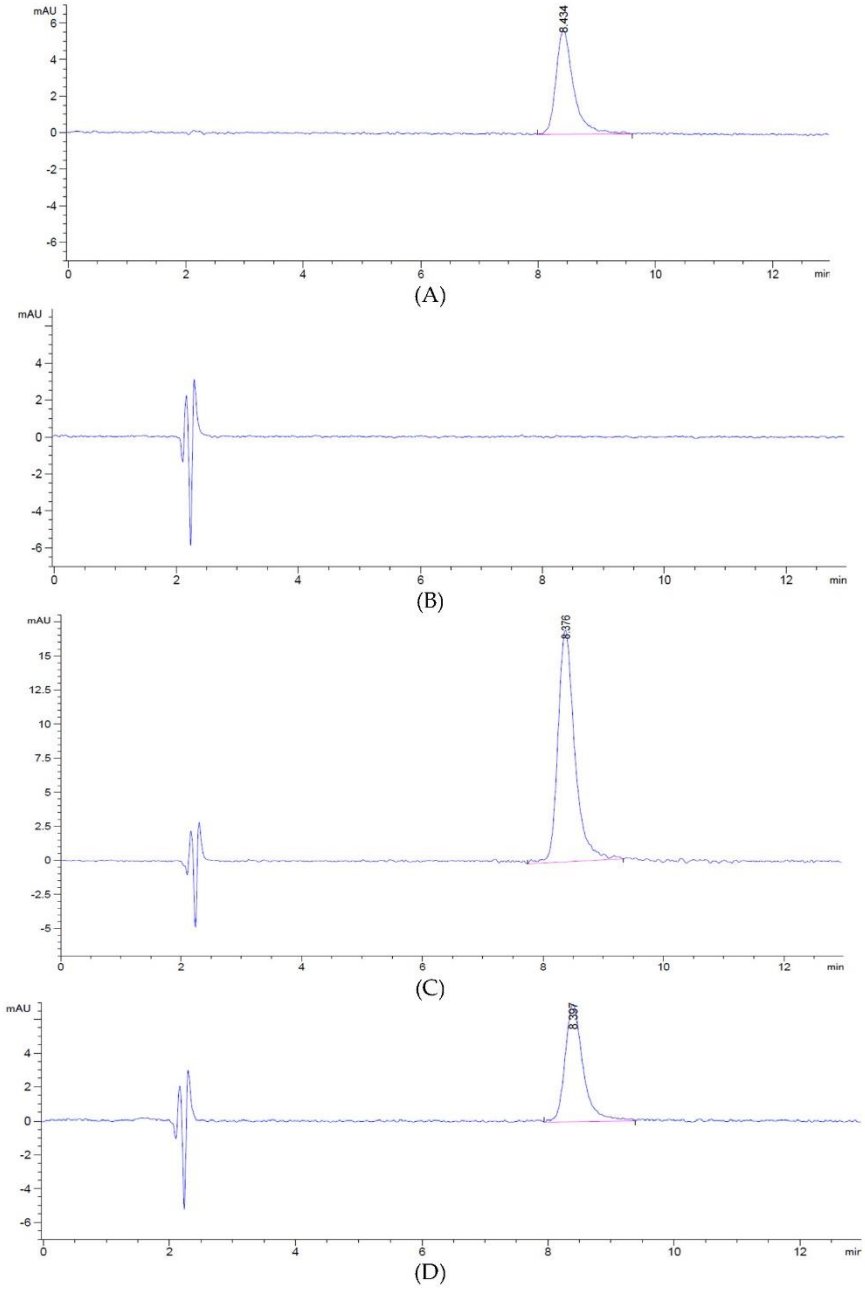

Figure S1. HPLC chromatograms (peak area versus time) of: (**A**) 0.75 µg/mL ASX solution as prepared for the calibration curve; (**B**) SNEDDS-L1 formulation matrix without ASX; (**C**) SNEDDS-L1 formulation matrix with ASX incorporated; (**D**) Skin extract following administration of SNEDDS L1-NE in IVPT experiment.

Linearity

The assay showed good linearity (regression coefficient of 0.99) for both concentration series.

Assay precision

The coefficient of variation precision parameters calculated from the relative standard deviation ($n = 6$) were 1.57% for 15 μg/mL, 4.18% for 0.105 μg/mL, 1.09% for 0.75 μg/mL, and 1.00% for 3.75 μg/mL. The acceptability criterion of precision repeatability has been fulfilled with R.S.D. < 5% in the high, medium, and low concentrations.

Sensitivity

The minimum LOD and LOQ for determination of ASX, calculated by injecting samples and blank solution six times were 41.7 ng/mL and 72.2 ng/mL respectively.

Accuracy

Figure S1 shows representative chromatograms for ASX analysis and control samples from the formulation development and IVPT experiments. This includes samples of the SNEDDS-L1 formulation without and with incorporation of ASX (B and C respectively), showing that there was no peak in the ASX region for the formulation matrix. The extraction fluid from skin that had been processed as per IVPT skin samples did not provide a peak in the ASX region (chromatogram not shown). The accuracy of the assay was determined from the recovery of ASX in the extraction from the skin permeation samples following administration of one SNEDDS formulation type. The amount of ASX recovered from the donor including washings, SC and skin extractions and receptor fluid samples was subtracted from the initial donor ASX applied gave a mass balance recovery of 88.87 ± 0.48% ASX compared to the amount of ASX applied.

Reference

1. Yuan, J.-P.; Chen, F. Chromatographic separation and purification of trans-astaxanthin from the extracts of Haematococcus pluvialis. *J. Agric. Food Chem.* **1998**, *46*, 3371–3375.
2. Namjoshi, S.; Caccetta, R.; Edwards, J.; Benson, H.A.E. Liquid chromatography assay for 5-aminolevulinic acid: application to in vitro assessment of skin penetration via Dermaportation. *J. Chromatogr. B Analyt. Technol. Biomed. Life Sci.* **2007**, *852*, 49–55.

Chapter 6. Conclusions

6.1 General discussion

The QbD approach is a systematic process to pharmaceutical product development that identifies the desired qualities in the final product and establishes a formulation program to achieve a defined QTPP.[1-3] In this thesis, the principles of the QbD approach were applied to the development of topical semisolid products to optimise drug delivery, product sensory qualities, and stability. The thesis describes the formulation process for developing two nanocosmeceuticals products, achieving optimised clinical outcomes in the case of CAF for management of cellulite and enhanced in vitro skin delivery of CAF and ASX, an antioxidant with applications in antiageing and skin health. Simply, the aims of the project were to develop and optimise novel nanocosmeceutical products, develop tools for clinical assessment and evaluate the efficacy of the novel CAF product in the clinical setting.

Chapters 2 and 4 focus on applying QbD principles to develop, characterise, and clinical test a novel nano-cream incorporating CAF as an anticellulite topical product. The process, summarised in Figure 6, included the selection of formulation ingredients and the manufacturing process to optimise the final product's physical, chemical, and skin delivery characteristics. We successfully developed nano-cream formulations containing CAF that met the QTPP criteria and fulfilled the CQA of a topical product. This was accomplished by the incorporation of one or more chemical penetration enhancers. We employed piglet skin mounted on Franz-type diffusion cells to determine CAF penetration/permeation through and into the skin. CAF was quantified in the SC, in the epidermal-dermal-follicle region and the cumulative amount in the receptor compartment after 8h. All CPEs significantly enhanced CAF penetration/permeation through and into the skin compared to control (nanoemulsion with no additional permeation enhancers) and a topical CAF product that is marketed for cellulite reduction. Nano-cream formulations containing LAN and TR showed maximum deposition of CAF in the deeper skin, with 2.30-fold and 2.51-fold permeation enhancement, respectively, compared to the control nanoformulation with no chemical permeation enhancer.

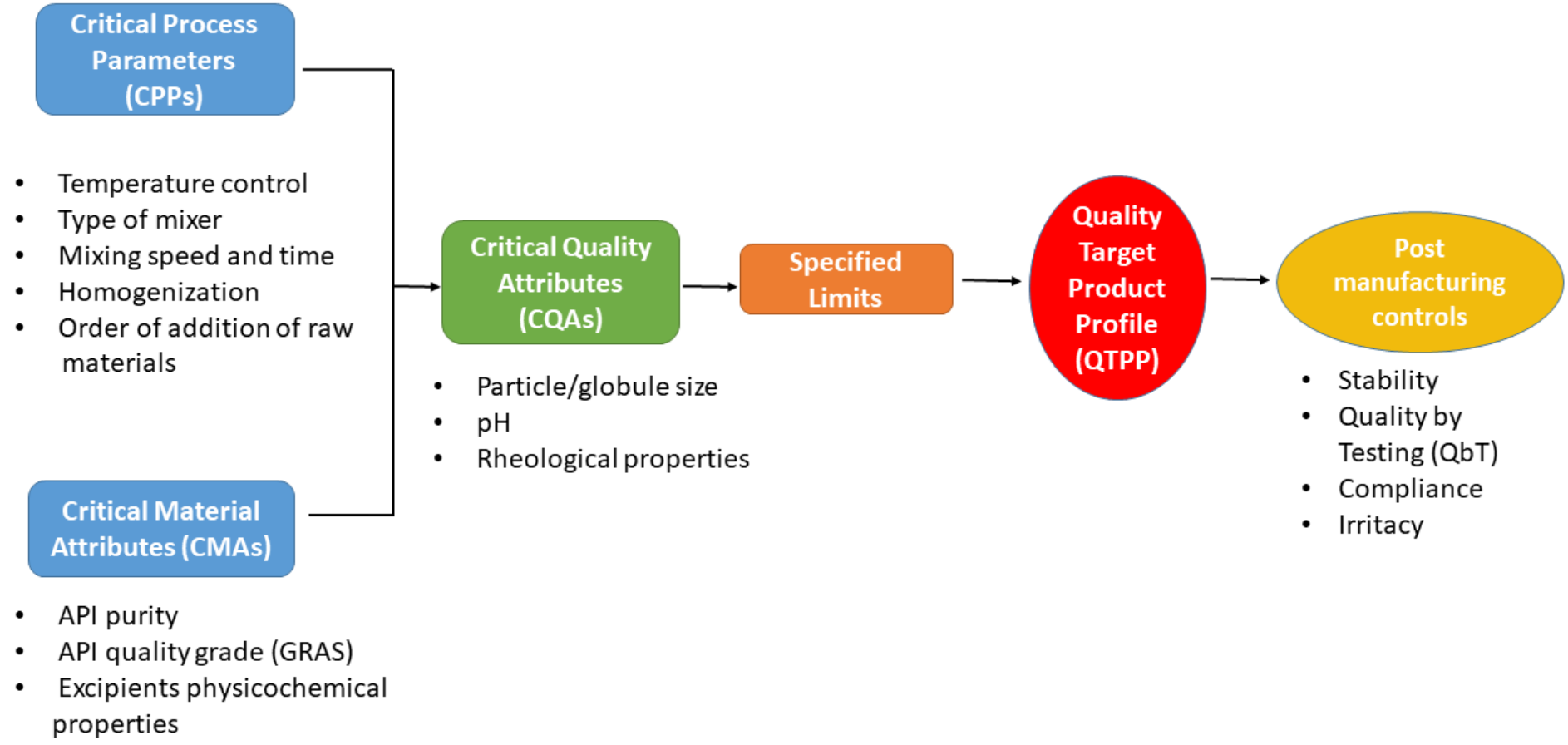

Figure 6. Flowchart summarising the current research project, modified from Namjoshi et al.[4]

Indeed, the LAN-based nano cream provided a 3.49-fold higher CAF delivery than a currently marketed anticellulite cream containing the same concentration of CAF. All nano-cream formulations were physically and chemically stable after 4 months of storage. Our findings confirm that the inclusion of LAN enhanced the skin delivery of CAF compared to the marketed product. This enhancement may be due to the chemical structure of LAN mimicking the human lipidic matrix of SC.[5,6] Therefore, the influence of LAN can potentially be used as a skin penetration enhancer for cosmetic products.[7]

The optimised nano-cream was evaluated for its anticellulite efficacy and sensory qualities in a clinical study of 24 female volunteers. To facilitate the clinical assessment of cellulite efficacy, we developed and validated an improved assessment methodology (described in Chapter 3). The validation process plays a pivotal role to develop a reliable, protocol to assess changes in the appearance of cellulite. The importance of the validation phase is to ensure the standardised measurement in a clinical setting, ensuring the results are accurate, precise and reproducible when used with different people from time to time. The result is trusted to compare for critical evaluation. Two stages were involved in the validation process. The first stage was a non-training involvement. The second stage was a more controlled process with training and moderator involvement to review grade selections. The participation of evaluators in training proved that inter-rater reliability improved from 0.838 to 0.978 and the moderation process test/retest reliability was excellent. The iterative process was used to evaluate the effects of these interventions. Using a simple rating of overall cellulite severity [8] provided a reliable outcome measure. This validation protocol could be implemented for assessing cellulite treatment in future clinical trials. It also could be applied to other visual analysis methods to evaluate drug or physical treatments on skin conditions.

In Chapter 4, human *in vivo* efficacy studies of the optimised nano-cream formulation was evaluated for targeted skin delivery of CAF.[9] The effect of the creams on skin appearance was monitored over 12 weeks. Participants completed a satisfaction questionnaire regarding the treatment and the nature of the products. The primary outcome measure was reduced cellulite scores from 3.96 to 2.50 (active) compared with placebo from 3.88 to 2.83. The secondary outcome measures were reduced thigh size relative to baseline (p= 0.023) for the CAF cream compared to the placebo cream. The study also demonstrated that our novel nano-cream

formulations combined with CAF significantly decreased skinfold thickness relative to baseline ($p < 0.001$). At the end of the clinical trial, participants expressed that "orange peel" dimpled appearance decreased on their posterior thighs following CAF cream use. Participants indicated that the active and placebo creams showed significant improvement in skin hydration, skin elasticity, smoothness of their thigh skin and visible reduction of cellulite appearance after week 8 and week 12 of application. Overall, participants rated reducing cellulite appearance within 12 weeks of cream containing CAF relative to placebo ($p= 0.035$). This project proved that applying CQA

SNEDDS for skin delivery of the potent lipophilic natural pigment ASX were developed and evaluated in Chapter 5.[10] ASX has potential as a topical antiageing in the experimental oxidative stress model.[11] This suggests its possibility in protecting human skin from environmental-derived stress, such as cigarette smoking and UV exposure that contributes to and accelerates the skin ageing effects. We used the QbD approach principles[3] to develop nanoformulations containing biocompatible components, including Labrafil and Kolliphor as surfactants and Transcutol [12] as cosurfactants, to enhance the solubility and incorporate materials to enhance the skin delivery of ASX. SNEDDS were prepared using a low-temperature spontaneous emulsification method and their physical characteristics, viscosity, refractive index, stability and antioxidant activity. ASX skin penetration/permeation studies were determined across porcine skin mounted Franz-type diffusion cells. Terpenes (D-limonene, geraniol and farnesol) were included in the SNEDDS formulations to evaluate their potential skin penetration enhancement. All SNEDDS were successfully formulated within nano-sized (~ 20nm). ASX was quantified in the SC and the area of the epidermis-dermis-follicle region (E+D+F). The ASX SNEDDS was visually observed to describe natural red-orange colour, excellent clarity and single-phase. ASX permeation was higher for SNEDDS containing terpenes and no correlation between lipophilicity of the terpenes and the cumulative amount of ASX permeating through porcine skin. The SNEDDS-L1 showed maximum deposition in the skin (2.76 ± 0.60 µg/cm^2) with 2.82-fold enhancement compared to the control. The SNEDDS containing D-limonene gave the highest ASX permeation enhancement with 3.34 and 3.79 times the amount in the SC and E+D+F, respectively, compared to a similarly applied dose of ASX in oil. We have demonstrated our SNEDDS development with

less oil and S/CoS enhanced the skin delivery of a potent lipophilic like ASX. We also showed that SNEDDS form can preserve ASX stability. These findings can implement to other active compound that also possess with high lipophilicity.

6.2 Future outlook

The development of nanoformulations based on a semisolid nano-cream and a liquid nanoemulsion appeared to be a promising topical formulation. Further investigation is needed to repeat human clinical trials with large sample sizes, longer treatment duration, other body areas with cellulite and post-treatment follow-up. Providing sufficient clinical data can be used to undertake research commercialisation.

6.3 Conclusions

The research in this thesis has highlighted the importance of implementing a pharmaceutical QbD approach to formulate suitable nanocosmeceuticals as high-quality final products for enhanced anticellulite and antiageing. The QbD framework drives the rational choice of formulation ingredients to focus on the effects of a range of S/CoS and oils, including ingredients with the potential to act as topical penetration/permeation enhancers. We defined a QTPP and identified several CQAs for nanoformulations-based topical products that included optimal globule sizes, solubility, viscosity, good physical and chemical stability, and good safety profile with low irritancy, and have an excellent skin delivery. In addition, human *in vivo* studies demonstrated the efficacy of topical anticellulite agents, which is a part of post-manufacturing control.

6.4 References

1. ICH Expert Working Group Harmonised Tripartite Guideline: Quality Risk Management Q8(R2). 2009. Accessed December 08, 2021. https://database.ich.org/sites/default/files/Q8_R2_Guideline.pdf
2. ICH Expert Working Group Harmonised Tripartite Guideline: Pharmaceutical Development Q9. 2005. Accessed 08 December 2021. https://database.ich.org/sites/default/files/Q9_Guideline.pdf
3. Zhang L, Mao S. Application of quality by design in the current drug development. *Asian J Pharm Sci*. 2017;12(1):1-8.doi:10.1016/j.ajps.2016.07.006
4. Namjoshi S, Dabbaghi M, Roberts MS, Grice JE, Mohammed Y. Quality by Design: Development of the Quality Target Product Profile (QTPP) for Semisolid Topical Products. *Pharmaceutics*. 2020;12(3).doi:10.3390/pharmaceutics12030287
5. Carrer V, Guzmán B, Martí M, Alonso C, Coderch L. Lanolin-Based Synthetic Membranes as Percutaneous Absorption Models for Transdermal Drug Delivery. *Pharmaceutics*. 2018;10(3).doi:10.3390/pharmaceutics10030073

6. Alonso C, Collini I, Martí M, Barba C, Coderch L. Lanolin-Based Synthetic Membranes for Transdermal Permeation and Penetration Drug Delivery Assays. *Membranes*. 2021;11(6):444.doi:10.3390/membranes11060444
7. Pavlou P, Siamidi A, Varvaresou A, Vlachou M. Skin Care Formulations and Lipid Carriers as Skin Moisturizing Agents. *Cosmetics*. 2021;8(3):89. doi:10.3390/cosmetics8030089
8. Dupont E, Journet M, Oula ML, et al. An integral topical gel for cellulite reduction: results from a double-blind, randomized, placebo-controlled evaluation of efficacy. *Clin Cosmet Investig Dermatol*. 2014;7:73-88. doi:10.2147/ccid.S53580
9. Ngamdokmai N, Waranuch N, Chootip K, Jampachaisri K, Scholfield CN, Ingkaninan K. Cellulite Reduction by Modified Thai Herbal Compresses; A Randomized Double-Blind Trial. *Journal of evidence-based integrative medicine*. 2018;23:2515690X1879415.doi:10.1177/2515690X18794158
10. Ponto T, Latter G, Luna G, Leite-Silva VR, Wright A, Benson HA. Novel Self-Nano-Emulsifying Drug Delivery Systems Containing Astaxanthin for Topical Skin Delivery. *Pharmaceutics*. 2021;13(5):649.doi:10.3390/pharmaceutics13050649
11. Huangfu J, Liu J, Sun Z, et al. Antiaging Effects of Astaxanthin-Rich Alga Haematococcus pluvialis on Fruit Flies under Oxidative Stress. *J Agric Food Chem*. 2013;61(32):7800-7804.doi:10.1021/jf402224w
12. Osborne DW, Musakhanian J. Skin Penetration and Permeation Properties of Transcutol(R)-Neat or Diluted Mixtures. *AAPS PharmSciTech*. 2018;19(8):3512-3533. doi:10.1208/s12249-018-1196-8

APPENDICES

Appendix 1. Attribution statement for co-authors of additional publication by candidate

To Whom It May Concern

I, Thellie Ponto, as one of the first authors, contributed the following to a review article: Topical Nano and Microemulsions for Skin Delivery

- Conception and design
- Literature search and review
- Data conditioning
- Manuscript preparation
- Final approval

_____

I as a first/co-author, endorse that this level of contribution by the candidate indicated above is appropriate.

Christofori M.R.R. Nastiti _____

Dr. Eman Abd _____

Dr. Jeffrey E. Grice _____

A/P Dr. Heather A.E Benson _____

Prof. Michael S. Roberts _____

Review article: Topical Nano and Microemulsions for Skin Delivery

Pharmaceutics 2017, 9(4), 37; pages 1-25; https://doi.org/10.3390/pharmaceutics9040037

Christofori M. R. R. Nastiti [1,2,†], Thellie Ponto [1,†], Eman Abd [3], Jeffrey E. Grice [3], Heather A. E. Benson [1] and Michael S. Roberts [3,4,*]

[1] School of Pharmacy, Curtin Health Innovation Research Institute, Curtin University, G.P.O. Box U1987, Perth, WA 6845, Australia

[2] Faculty of Pharmacy, Sanata Dharma University, Yogyakarta 55282, Indonesia

[3] Therapeutics Research Centre, The University of Queensland Diamantina Institute, Faculty of Medicine, Translational Research Institute, Woolloongabba, QLD 4102, Australia

[4] School of Pharmacy and Medical Sciences, University of South Australia, Adelaide, SA 5000, Australia

* Correspondence: m.roberts@uq.edu.au; Tel.: +61-7-34438031; Fax +61-7-34437779

† These authors contributed equally to this work.

	Conception and design	Literature search and review	Data conditioning	Manuscript preparation	Final approval
Christofori M.R.R. Nastiti	✓	✓	✓	✓	✓
I acknowledge that these represent my contribution to the above research output					
Dr. Eman Abd		✓	✓		✓
I acknowledge that these represent my contribution to the above research output					
Dr. Jeffrey E Grice		✓	✓	✓	✓
I acknowledge that these represent my contribution to the above research output					

A/P Dr. Heather A.E. Benson	✓	✓	✓	✓	✓
I acknowledge that these represent my contribution to the above research output					
Prof. Michael S. Roberts	✓	✓	✓	✓	✓
I acknowledge that these represent my contribution to the above research output					

pharmaceutics

MDPI

Review

Topical Nano and Microemulsions for Skin Delivery

Christofori M. R. R. Nastiti [1,2,†], Thellie Ponto [1,†], Eman Abd [3], Jeffrey E. Grice [3], Heather A. E. Benson [1] and Michael S. Roberts [3,4,*]

1 School of Pharmacy, Curtin Health Innovation Research Institute, Curtin University, G.P.O. Box U1987, Perth, WA 6845, Australia; c.nastiti@postgrad.curtin.edu.au (C.M.R.R.N.); thellie.ponto@postgrad.curtin.edu.au (T.P.); H.Benson@curtin.edu.au (H.A.E.B.)
2 Faculty of Pharmacy, Sanata Dharma University, Yogyakarta 55282, Indonesia
3 Therapeutics Research Centre, The University of Queensland Diamentina Institute, Faculty of Medicine, Translational Research Institute, Woolloongabba, QLD 4102, Australia; e.abd@uq.edu.au (E.A.); jeff.grice@uq.edu.au (J.E.G.)
4 School of Pharmacy and Medical Sciences, University of South Australia, Adelaide, SA 5000, Australia
* Correspondence: m.roberts@uq.edu.au; Tel.: +61-7-34438031; Fax: +61-7-34437779
† These authors contributed equally to this work.

Received: 11 August 2017; Accepted: 13 September 2017; Published: 21 September 2017

Abstract: Nanosystems such as microemulsions (ME) and nanoemulsions (NE) offer considerable opportunities for targeted drug delivery to and via the skin. ME and NE are stable colloidal systems composed of oil and water, stabilised by a mixture of surfactants and cosurfactants, that have received particular interest as topical skin delivery systems. There is considerable scope to manipulate the formulation components and characteristics to achieve optimal bioavailability and minimal skin irritancy. This includes the incorporation of established chemical penetration enhancers to fluidize the stratum corneum lipid bilayers, thus reducing the primary skin barrier and increasing permeation. This review discusses nanosystems with utility in skin delivery and focuses on the composition and characterization of ME and NE for topical and transdermal delivery. The mechanism of skin delivery across the stratum corneum and via hair follicles is reviewed with particular focus on the influence of formulation.

Keywords: microemulsion; nanoemulsion; transdermal; skin penetration; penetration enhancer; nanosystem

1. Introduction

The skin provides an effective barrier to protect the body from the penetration of molecules and micro-organisms in the external environment, and from excessive loss of water to maintain homeostasis. The main skin barrier resides in the stratum corneum (Figure 1) due to its unique structure of layers of flattened corneocytes surrounded by lipid bilayers composed primarily of ceramides [1]. Penetration of most topically applied compounds follows the tortuous route of the stratum corneum lipid bilayers (intercellular) [2], although the transcellular route through the corneocytes may contribute in some circumstances [3]. Although hair follicles (and associated sebaceous glands) and sweat glands account for only about 0.1% of the total skin surface area [4], these appendages are potential routes of access into the skin, and may be important for nanosystems.

Compounds that successfully diffuse across the stratum corneum are typically relatively small (up to about 500 Da), lipophilic (logP 1–3) and water soluble, thus excluding many potentially useful therapeutic compounds with properties that do not fit these criteria. A range of micro- and nanosystems has been investigated as potential delivery vehicles that could enhance the skin penetration of both small and macromolecules that do not otherwise permeate the stratum corneum in sufficient quantities to provide a therapeutic outcome. Here, we review micro and nanosystems that have been applied to

skin delivery and focus particularly on micro- and nanoemulsions, as these present an extension of the most commonly applied topical formulations used in pharmaceutical, cosmeceutical and personal care products.

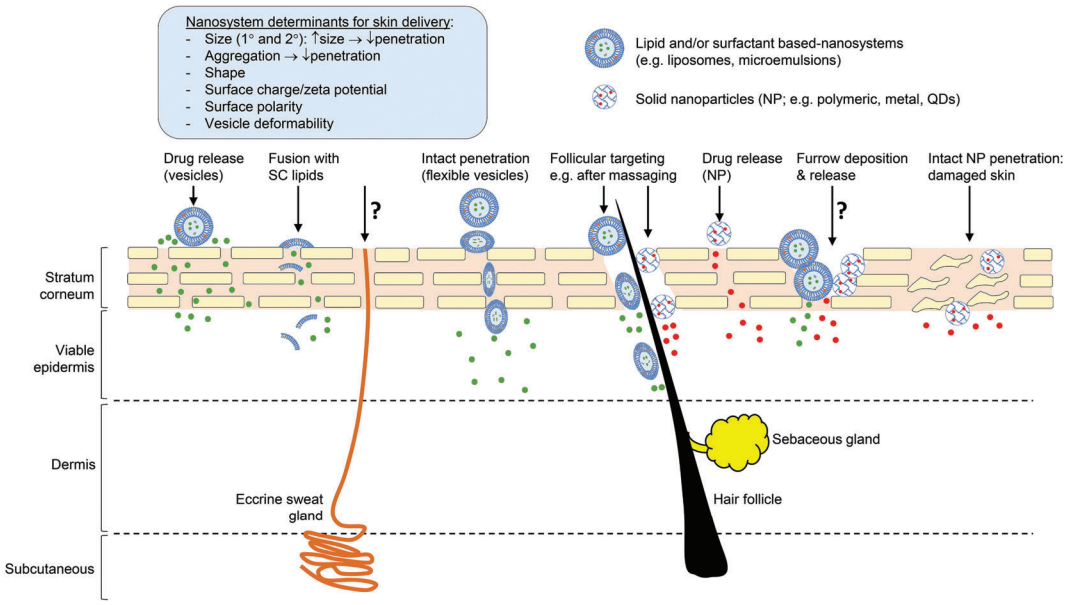

Figure 1. Properties of nanosystems determining skin absorption and potential routes of penetration (skin layer thicknesses not drawn to scale). Reproduced with permission from [5].

2. Classification of Nano and Microsystems Used for Skin Delivery

Nanosystems that have been investigated for enhanced skin permeation include microemulsions (ME), nanoemulsions (NE), nanoparticles of various compositions including solid lipid nanoparticles (SLN), nanostructured lipid carriers (NLC), liposomes and vesicles [5]. These nanosystems can offer significant advantages in the formulation of hydrophobic molecules, enhancing their solubility and thus bioavailability. This approach has been used to formulate hydrophobic actives for a range of routes of administration, including topical application to the skin. An example is Estrasorb® (Novavax Inc., Malvern, PA, USA), which contains oestradiol hemihydrate (logP 3.3) in a nanoemulsion composed of soybean oil, water, polysorbate 80 and ethanol, packed in single dose foil pouches for application to the legs in the management of vasomotor symptoms associated with menopause. Topicaine® (ESBA Laboratories Inc., Jupiter, FL, USA) is a microemulsion-based gel product (composed of jojoba oil, aloe vera oil, ethanol, benzyl alcohol, glycerine and water emulsified by glyceryl monostearate, and gelled with carbomer 940) containing lidocaine for localised pain relief. There are also examples of nanosystems designed to enhance delivery of hydrophilic compounds. Ameluz® topical gel (Biofrontera Pharma GmbH, Leverkusen, Germany) containing aminolevulinic acid (logP 1.5) in a nanoemulsion composed of soybean phosphatidylcholine, water, polysorbate, propylene glycol and isopropyl alcohol for the treatment of actinic keratosis and basal cell carcinoma. The range of nanosystems used for skin delivery is classified below. Figure 1 summarises the suggested and/or established mechanisms of skin permeation of nanosystems. While some routes are well described in the literature, the extent to which other routes, such as the eccrine sweat glands and via skin furrows (designated as ? in Figure 1), contribute to skin permeation is less well established. We have demonstrated that topically applied zinc oxide nanoparticles deposit in the skin furrows, but this does not contribute to permeation to deeper skin tissues [6,7].

Microemulsions (ME): transparent, monophasic, optically isotropic and thermodynamically stable colloidal dispersions composed of oil, water, surfactant and cosurfactant with droplet sizes in the range 10–100 nm [8].

Nanoemulsions (NE): transparent, monophasic, optically isotropic and kinetically stable colloidal dispersions composed of oil, water, surfactant and cosurfactant with droplet sizes less than 100 nm.

Solid Nanoparticles: Discrete particles in the size range up to 1000 nm composed of inorganic materials such as metal oxides (e.g., zinc oxide, titanium dioxide) or polymers. There is a considerable body of evidence to show that these nanoparticles do not permeate human skin under a range of administration conditions [6,7]. Their primary application is as sunscreen products.

Solid Lipid Nanoparticles (SLN): composed of lipids that are solid at room temperature with a surface covering of surfactant to stabilise them as a nano-dispersion [9]. SLN enhance skin permeation by prolonging contact with the skin surface, providing an occlusive barrier that hydrates the skin, and interacting with the lipids in the stratum corneum bilayers. They are particularly useful for formulation of hydrophobic actives such as vitamin A, E and coenzyme Q in cosmetically elegant products, and maintaining the stability of compounds such as retinol that are prone to decomposition by light and oxygen [9].

Nanostructured lipid carriers (NLC): colloid systems composed of a fluid lipid phase embedded into a solid lipid matrix or localized at the surface of solid platelets and the surfactant layer [9,10]. The spatial structure of the lipids allows greater drug loading and better stability compared to SLN.

Liposomes: spherical vesicles composed of amphiphilic phospholipids and cholesterol, self-associated into multilamellar, large unilamellar and small unilamellar vesicles.

Flexible vesicles: composed of materials that will associate into bilayer structures but incorporate components that confer flexibility, thereby allowing the vesicles to deform in shape. Compositions that associate into flexible vesicles include ethosomes (phospholipids with a high proportion of ethanol) [11], niosomes (non-ionic surfactants) [12], invasomes (phospholipids, ethanol and a mixture of terpene penetration enhancers) [13], SECosomes (surfactant, ethanol and cholesterol) [14] and PEV (penetration enhancer vesicles, for which a range of penetration enhancers have been investigated including oleic acid, limonene, propylene glycol, Transcutol®) [15,16]. Multiple mechanisms are likely to contribute to enhanced skin permeation including the effect of the vesicle components on the stratum corneum lipids and the potential, as proposed by Cevc, that the vesicles have sufficient flexibility to squeeze through the stratum corneum intact [17,18].

Polymeric micelles and dendrimers: nanosized, colloidal carriers with a hydrophilic exterior shell and a hydrophobic interior core, comprised of two main categories of hydrophobically assembled micelles and polyion-complex micelles [19]. Dendrimers are highly branched polymer structures incorporating drug and potentially, penetration enhancer molecules [20].

3. Formulation of Micro and Nanoemulsions

The focus of this review is the application of ME and NE in dermal and transdermal drug delivery. In comparison to many of the nanosystems outlined above, ME and NE offer advantages in terms of simplicity and stability. Coarse emulsions are composed of oil and water phases, with one dispersed as droplets in the other, and stabilised by a surfactant. In addition to their obvious droplet size difference, ME are clear/transparent, form spontaneously, have low interfacial energy and are thermodynamically stable, unlike emulsions that are cloudy, require energy in preparation, have high interfacial energy and are kinetically stable [21]. While the terminology suggests that NE would have a smaller particle size than ME, based on nano and micro referring to 10^{-9} and 10^{-6} respectively, this is a quirk of the history of the development of colloidal dispersions, and the size range of NE and ME is similar. Essentially, the terms ME and NE entered widespread usage before they were properly defined or distinguished from each other [22]. Both NE and ME typically have low polydispersity (up to about 10%) compared to the much higher polydispersity exhibited by emulsions (>40%).

NE are thermodynamically unstable but kinetically stable, and can be prepared by both low and high energy methods. Given sufficient time, an NE will phase separate. Destabilization mechanisms include flocculation, coalescence, Ostwald ripening and creaming, with Ostwald ripening being the dominant mechanism of destabilization for NE [22–24]. The systems also differ when exposed to dilution and temperature fluctuations. ME are affected and potentially broken by temperature changes and/or dilution, whereas NE droplets will remain stable under these physical stresses [23]. Thus, the primary difference between NE and ME is their thermodynamic stability [22], which also results in the higher energy input required to form NE compared to ME. Detailed examination of the terminology, differences and similarities of NE and ME, with particular focus on their physical chemistry, is provided by McClements [22], Anton and Vandamme [23] and Gupta et al. [24]. The similarities and differences between emulsions, ME and NE are summarized in Table 1.

Table 1. Comparison of the properties of emulsions, microemulsions and nanoemulsions.

	Emulsion	Microemulsion	Nanoemulsion
Physical description	Coarse dispersion	Colloidal dispersion	Colloidal dispersion
Particle size range	>500 nm	<100 nm	<100 nm
Polydispersity	High	Low	Low
Thermodynamic stability	Unstable	Stable	Unstable
Preparation	High energy	Low energy	Low/high energy
Composition: surfactant to oil ratio	Low	High	Moderate
Physical appearance	Creamy	Transparent	Transparent
Texture	Semi-solid	Fluid	Fluid

The low interfacial tension and small particle size in ME and NE is due to their composition; in particular, the presence of cosurfactants such as short or medium chain alcohols or polyglyceryl derivatives working in combination with the primary surfactant [25]. The surfactant to oil ratio is much higher in ME (see examples in Table 2) than in coarse emulsions (typically 2–10%). While coarse emulsions are creamy in appearance and tend to adhere well to the skin, NE and ME are more fluid. To achieve an appropriate consistency of ME or NE on the skin, a viscosity enhancing polymer is added to form a gel.

In general, non-ionic surfactants are favoured as they are less irritating to human skin. A wide range of non-ionic surfactants and the amphiphilic surfactant lecithin have been investigated, together with a variety of oils and cosurfactants (Table 2). The development of NE and ME formulations is based on ternary diagrams to determine the optimal component ratios.

4. Formulation Parameters: Composition and Preparation Methods

ME can be formed spontaneously at optimal component ratios and temperature, although in practice, low energy such as heat or stirring is generally applied to facilitate formation. ME and NE are classified as water in oil (w/o) or oil in water (o/w), each designating the dispersed phase within the continuous phase. Some more complex systems also exist such as o/w/o and w/o/w. Bicontinuous ME in which the aqueous and oil phases are intertwined and stabilized by sheet-like surfactant areas in the areas between the phases [26] can also exist. Lindman et al. [27] demonstrated that continuous pathways can exist between interconnected-sphere structures, lamellar-like structures, tubule structures and other structures in ME systems. Bicontinuous structures are dynamic and are characterized by a higher amphiphilic character, greater fluctuation at the interface, lower interfacial tension and better solubilizing properties compared to globular w/o or o/w ME [28,29]. Naoui et al. [29] compared the penetration of the hydrophilic drug caffeine across excised pig skin, when applied in o/w, w/o and bicontinuous ME having the same ingredients. Transdermal flux of caffeine was in the order w/o < bicontinuous < o/w ME, with the o/w ME providing permeation of 50% of the applied dose within 24 h. In contrast, Bhatia et al. [28] reported that, for the lipophilic drug adapalene, the penetration in hair follicles increased by almost three times as the microstructure of the applied

ME shifted from o/w to bicontinuous, with an increase in water content of the ME. In both cases, presentation of the drug in the continuous phase of the ME provided the greatest drug delivery, with the bicontinuous system acting as an intermediate system.

4.1. Preparation Methods

NE formation is generally a two-step process with the initial preparation of a macroemulsion that is then converted to a NE. This requires external energy applied by high-energy (HEE) or low-energy (LEE) methods (Figure 2). HEE methods such as high-pressure homogenizers, microfluidizers and ultrasonicators generate highly disruptive forces that break down the oil and water phases, causing them to intersperse and form nanometer-sized droplets. LEE methods include heat, stirring and phase inversion. Control of NE droplet size is related to both the preparation method and the formulation components.

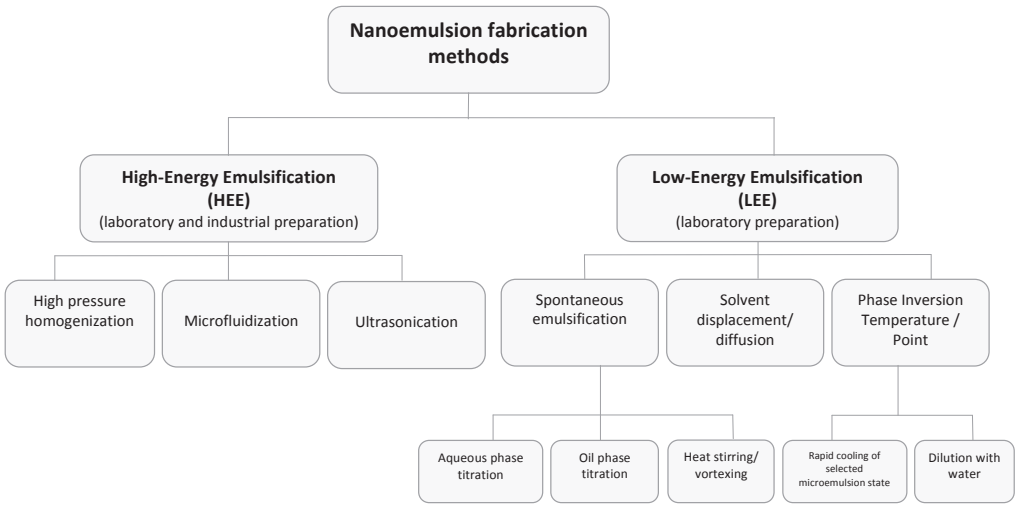

Figure 2. Schematic representation of nanoemulsion preparation methods adapted from [30,31].

Dilution can be used as a method of forming a final ME or NE product. NE can be prepared by diluting o/w microemulsions, bicontinuous microemulsions, or w/o ME with water [32]. Dilution of an o/w ME with water induces a proportion of the surfactants to dissolve into the aqueous phase. The surfactant molecules remaining at the oil/water interface cannot maintain the low interfacial tension required for thermodynamic stability and the ME droplets give rise to nanoemulsion droplets [33].

When diluting bicontinuous ME, the homogeneous nucleation that occurs during the spontaneous emulsification process leads to the formation of NE [34] Despite this mechanism, NE may be formed by the migration of surfactants or cosurfactants through the oil-water interface due to the "ouzo effect" when diluting bicontinuous ME or w/o ME [35]. When diluting w/o ME, the oil may act as nuclei, leading to heterogeneous nucleation, resulting in droplets with larger sizes and polydispersity [36]. NE formed by diluting o/w ME or bicontinuous ME are more stable and have smaller droplets [37].

Sole et al. [32] reported that NE with droplet diameters of 20 nm were obtained when diluting o/w ME regardless of the ME composition or dilution procedure (incremental or all at once). In contrast, when the starting emulsion was a w/o ME, NE were only obtained if the emulsification conditions allowed the establishment of an equilibrium in an o/w ME domain during the process. These conditions required the stepwise addition of water and w/o ME with specific oil to surfactant ratios.

4.2. Composition

The choice of emulsion components and ratios of these components is critical in generating stable emulsion systems with appropriate particle sizes. A wide range of components and combinations has been investigated (Table 2).

Oil phase components include fatty acids (e.g., oleic acid), esters of fatty acids and alcohols (e.g., isopropyl myristate, isopropyl palmitate, ethyl oleate), medium chain triglycerides, triacetin, terpenes (e.g., limonene, menthol, cineole) and other penetration enhancers. These may be used alone or in combination to form the oil phase. The aqueous phase may include sodium chloride and buffer salts, preservatives and penetration enhancers. Viscosity enhancing agents (e.g., Carbopol®, Aerosil®, gelatin) are incorporated to reduce the fluidity and generate the desired final consistency of the product.

A wide range of materials has been used as surfactants and cosurfactants (see examples in Table 2). Consideration must be given to combinations that effectively reduce interfacial tension and produce stable emulsions with appropriate particle size, but which also ensure minimal skin irritancy; thus, the preference for non-ionic surfactants. Commonly used surfactants include Tween® (polysorbates), Cremophor® (mixture of macrogol glycerol hydroxystearate, PEG-40 castor oil, polyoxyl 40 hydrogenated castor oil), Transcutol® P (diethylene glycol monoethyl ether), Plurol Oleique® (polyglyceryl-3-oleate), Plurol Isostearique® (isostearic acid ester of poly-glycerols and higher oligomers) and Labrasol® (mixture of mono-, di- and tri-glycerides of C8 and C10 fatty acids, and mono- and di-esters of PEG) [38]. Lecithin, an amphiphilic compound, has been widely investigated as the "ideal" surfactant because it is a natural compound with a low skin irritancy profile. Organogels are w/o ME based on lecithin and an apolar organic solvent, that form gel-like reverse micellar systems with high viscosity, solubilisation capacity and thermodynamic stability, and are transparent and biocompatible [39]. Cosurfactants are generally short and medium chain alcohols and polyglyceryl derivatives, including ethanol, isopropanol, isopropyl myristate and propylene glycol (PG). Nonionic surfactants have also been used to provide low irritancy cosurfactants [38,40]. Table 2 shows examples of the range of NE and ME compositions and their skin delivery. Lopes provides an excellent review focused on the formulation and physical characterisation of ME [41].

5. Physical Characterisation of Nano- and Microemulsions

5.1. Pseudo Ternary Phase Diagrams

NE and ME are characterised by a range of physical properties that are important determinants of their structure, drug release and stability. Pseudo ternary phase diagrams are often constructed to indicate the boundaries of the different phases as a function of the composition of the aqueous, oil and surfactant/cosurfactant components [21,42]. Mixtures of the oil, surfactant and cosurfactant at certain weight ratios at ambient temperature (25 °C) are diluted with the aqueous solution under moderate agitation. After equilibrium, the combinations of the three components that give rise to clear emulsions, shown by visual inspection or polarised light microscopy, are mapped on the phase diagram. Examples of pseudo-ternary phase diagrams showing regions of various phases for mixtures of oil and water and different ratios of surfactant and cosurfactant (Tween 80 and Brij 52) are shown in Figure 3 [43].

5.2. Particle Size, Polydispersity and Zeta Potential

Particle/droplet size and polydispersity index can be determined by microscopic and scattering techniques. Dynamic light scattering, also called photon correlation spectroscopy (PCS), is used to analyse the fluctuations in intensity of incident laser light as it passes through droplets or particles that are subject to Brownian motion. A number of instruments are available that can provide rapid analysis of the particle/droplet size (down to about 1 nm), polydispersity (a measure of the broadness

of the size distribution derived from the cumulative analysis of dynamic light scattering: indicates the quality or homogeneity of the dispersion) and zeta potential (surface charge).

Freeze fracture transmission electron microscopy (TEM) and cryo-TEM allow the direct imaging of nanostructures at high resolution [44]. Laser light scattering, photon correlation spectroscopy (PCS), small angle X-ray scattering (SAXS), small angle neutron scattering (SANS) are useful for determining particle size distribution [45]. Consideration of particle interactions within the emulsion systems, and understanding the limitations of these techniques, is critical to ensure accurate measurements [21].

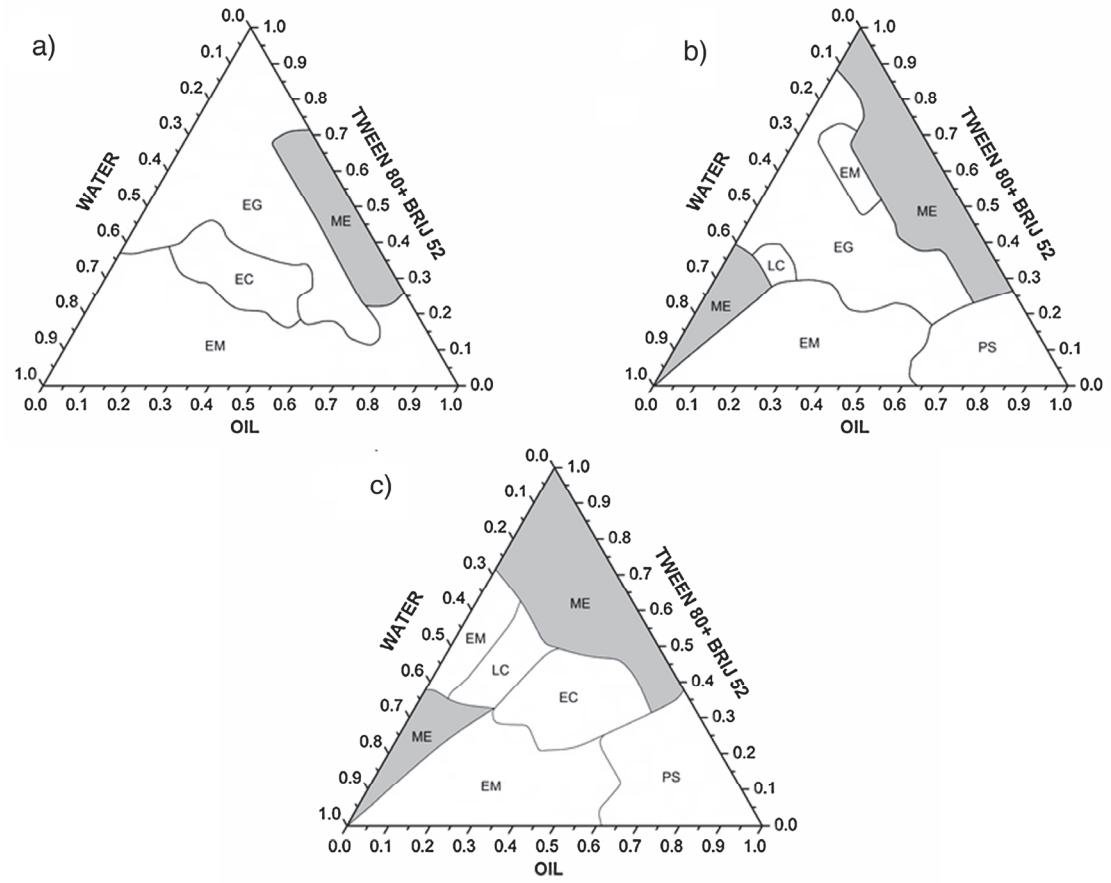

Figure 3. Pseudo-ternary phase diagrams formed by a mixture of caprylic/capric triglycerides as the oil phase, Tween 80: Brij 52 at 7:3 (**a**), 8:2 (**b**) and 9:1 (**c**) surfactant mix-ratio and water. Gray area represents the microemulsion systems (ME). Liquid crystal (LC), emulsion (EM), emollient gel (EG), emollient cream (EC), phase separation (PS). Reproduced with permission from [43].

5.3. Viscosity and Electrical Conductivity

Viscosity and conductivity measurements provide information on the emulsion structure and can be used to detect phase inversion phenomena [45]. High conductivity values demonstrate a water continuous phase, whilst an oil continuous phase will have low or no conductivity. Where the conductivity increases this may demonstrate the percolation effect caused by the attractive interactions between water droplets, that is characteristic of a bicontinuous structure [46,47]. These measurements can also be useful in predicting drug release from the NE or ME.

Electrical conductivity meaurements are simple and inexpensive, involving the insertion of conductometer electodes into the NE/ME formulation. High conductivity is obtained for an aqueous continuous phase, and phase inversion in response to formulation or temperature change can be monitored by the change in electrical conductivity. The technique is therefore useful for determining emulsion type, and monitoring changes during preparation or storage [48].

Viscosity is an important property that influences the stability and drug release of NE and ME formulations. The viscosity of an emulsion is a function of the surfactant, water and oil components and their concentrations. An increase in the water content will lead to a lowering of the viscosity, while decreasing the surfactant and co surfactant content increases interfacial tension between the water and oil, causing increased viscosity. Monitoring of viscosity changes is a method of assessing the stability of liquid and semi-solid preparations, including nanoemulsion formulations [49]. In general, cone and plate type rheometers are used for rheological evaluation of NE and ME [50].

Podlogar et al. [45] provide an excellent example of how the data from a range of these techniques can be collectively interpreted to provide the structural characterisation of ME. They found good agreement in their measurements of density and surface tension, and by viscometry, conductivity, DSC and SAXS techniques, for their ME (composed of IPM and water with Tween 40® and Imwitor 308® [glyceryl caprylate] surfactant/cosurfactant mix). The SAXS data showed a monodisperse w/o ME with strong attractive interactions. The type of ME was confirmed by DSC by demonstrating the degree of interaction between water and surfactants. Conductivity, viscosity, density and surface tension measurements confirmed a percolation transition to a bicontinuous structure. The authors concluded that these techniques could be applied to determine the type and structure of more complex systems, and could enable partitioning and release rates of drugs from ME to be predicted.

6. Skin Delivery from Nano and Microemulsions

NE and ME systems have been developed for the delivery of a wide range of compounds to the skin for dermatological, cosmetic/cosmeceutical and transdermal outcomes. Enhanced skin delivery has been demonstrated in comparison to conventional emulsions and gels. This has been attributed both to the action of their components on the skin and their phase structure and particle size. We have evaluated the literature on in vitro and in vivo studies of skin permeation of compounds applied as NE and ME systems, with particular focus on the formulation composition and properties, and skin permeation experimental design. The choice of appropriate models for skin permeation evaluation is critical to the accurate assessment of the potential of these systems as future therapeutic products. Ideally, studies are conducted on human excised skin or volunteers, although pig and piglet skin does provide a reasonable surrogate. In studies of follicular penetration, Lademann has suggested that pig ear skin is a superior in vitro model, as it does not contract and close the follicle openings, as excised human skin does [51]. Animal models such as rat, mouse and rabbit have a weaker barrier than human skin and their use tends to over-estimate skin permeation relative to humans. In addition, experimental parameters such as the appropriate choice of receptor solutions that do not damage skin membranes, while providing sufficient receptor phase solubility to achieve sink conditions and suitable hydrodynamics to limit the formation of aqueous diffusion layers [52] need to be scrutinized, along with validated analytical methods and application protocols. In some cases high proportions of alcohols [53–57] or other known penetration enhancers such as DMSO [58] have been used to provide sink conditions in the receptor phase, with the potential to compromise the skin barrier and lead to over-estimation of drug flux. Our work has also shown that even when non-sink conditions are used in in vitro permeation experiments, the results can be corrected to derive the equivalent sink condition data, provided the effects of aqueous diffusion layers are minimised [52].

Given the presence of sebum in hair follicles it is likely that oil, surfactant and alcohol based vehicles such as NE/ME could facilitate transfollicular transport of both hydrophilic and lipophilic compounds. Bhatia et al. [28] indicated that ME not only increased the permeation of adapalene in the stratum corneum, but also demonstrated optimal penetration into the hair follicles. The permeation of adapalene in the stratum corneum increased from 1.40 to 3.37 μg and penetration in the hair follicles increased significantly from 0.017 to 0.292 μg in ME treated skin compared with the control. This represents a 17-fold increase in penetration in the hair follicles compared with the control. Teichmann et al. [59] compared the skin penetration of the lipophilic dye curcumin incorporated in an o/w ME and a coarse emulsion/cream applied to human volunteers. Using the method of tape

stripping to remove the stratum corneum (SC), the depth profiles of the dye within the horny layer were compared. The depth of penetration, determined both by tape stripping and laser scanning microscopy, was greater with the ME than the cream. In addition, when applied in the ME, curcumin penetrated into the complete follicular infundibula, whereas with the cream a fluorescence signal was only received from the follicular orifices.

While some hair follicles are open, others are plugged with shed corneocytes and dry sebum [60], which can particularly restrict the permeation of hydrophilic compounds. Hair follicles can be opened by a mechanical peeling technique applied prior to the administration of a topical formulation [61]. We investigated the follicular delivery of the hydrophilic compound caffeine from NE composed of penetration enhancer chemicals (unpublished data). We found that when we open the hair follicles, the increase in caffeine permeation relative to control (aqueous solution) was greater for oleic acid and eucalyptol NE. The cumulative amount and flux of caffeine increased by 27- and 23-fold with oleic acid NE relative to control. Eucalyptol NE increased the cumulative amount of caffeine penetrated by 43-fold and flux by 31-fold compared to control.

In the following section, we discuss representative literature on a range of formulations, focused on the anti-inflammatory drug class. Examples of NE formulations evaluated for a broad range of therapeutic classes relevant to topical and transdermal delivery are also summarised in Table 2.

Anti-Inflammatory Drugs

Non-steroidal anti-inflammatory drugs (NSAIDs) are widely used in the management of musculoskeletal and arthritic pain. These drugs often create gastro-intestinal side effects when taken orally, thus application to the skin over the painful site is an attractive alternative. A number of NSAIDs have been available as gel and cream formulations for many years. There is extensive literature focused on the development and evaluation of ME and NE systems for topical delivery of a number of NSAIDs including diclofenac [62,63], aceclofenac [57,64,65], piroxicam [66], indomethacin [67–69], ibuprofen, celecoxib [70,71], etoricoxib [72], naproxen [73], flufenamic acid [50,74,75], ketoprofen [39,76,77], flurbiprofen [78], lornoxicam [79], and meloxicam [80]. Consequently, we have focused our discussion on this drug class to illustrate the development and potential of ME/NE formulations for topical and transdermal delivery.

ME composed of oleic acid as the internal phase, Labrasol® /Cremophor® RH as the cosolvent mixture and water were shown to enhance skin permeation of the lipophilic NSAID ketoprofen [76]. Increasing the water content (from 5 to 64%) and reducing the surfactant content (from 80 to 30%) increased ketoprofen skin permeation. This increased permeation is achieved by reducing the solubility of the drug and hence increasing its thermodynamic activity in the external phase, and has been reported for other lipophilic compounds [74,81]. Hoppel et al. [74] evaluated a lecithin related, naturally derived monoacyl phosphatidycholine (MAPL) surfactant, with the aim of reducing the irritancy associated with many conventional ionic surfactants. The in vitro skin permeation of flufenamic acid across dermatomed porcine skin was evaluated from ME composed of oleic acid, water, MAPL and isopropanol as co-surfactant. Attenuated total reflectance–fourier transform infrared spectrometry (ATR-FTIR) analysis and tape stripping of the stratum corneum demonstrated that the MAPL itself did not penetrate beyond the superficial layers of the stratum corneum. This superficial penetration is likely to minimise irritancy. NSAID skin permeation was significantly greater for the water-rich ME than other ME compositions and a commercial flufenamic acid product. When applied to the skin the isopropanol evaporated, leaving crystal-like structures of MAPL on the skin surface and forming a barrier to skin permeation. However, the ME with high water content prevented the formation of these MAPL structures. In a subsequent study exploring the influence of MAPL content it was confirmed that higher MAPL content resulted in lower skin permeation of flufenamic acid, most likely due to the MAPL acting as a hydrophilic barrier to the permeation of the lipophilic drug [50].

Duangjit et al. [82] applied a simple lattice statistical design approach to provide a more rational choice of ME composition. The physical properties (size, charge, conductivity, pH, viscosity,

drug content and loading capacity) and skin permeation were determined for ketoprofen-loaded ME composed of oleic acid, Cremophor® RH, ethanol and water. The authors reported that the experimentally determined skin permeation correlated well with their predictions using Design-Expert® software (Stat-ease, Minneapolis, MN, USA), and allowed optimisation of skin delivery via rational design.

Oleic acid-based ME have also been investigated for skin delivery of flufenamic acid [74,75,83]. Mahrhauser et al. [75] combined a fluorosurfactant (Hexafor™670 or Chemguard S-550-100) with isopropyl alcohol as cosurfactant (total S + CoS 65% *w*/*w*) to form an anisotropic ME with oleic acid (10% *w*/*w*) and water (25% *w*/*w*), loaded with flurbiprofen. Physical characterisation using conductivity, SAXS and NMR showed that the ME was oil in water with spherical or rod-shaped microstructures. In vitro porcine skin penetration demonstrated enhanced permeation for the ME with elongated rather than spherical microstructures, suggesting that the shape of the ME particles is an important determinant in skin delivery. In a parallel study incorporating diclofenac sodium in the ME, increased deposition into the stratum corneum of porcine ear skin was demonstrated by tape stripping [83]. ATR-FTIR studies showed significant shifts of the CH_2 stretching absorbance when the ME was applied to the skin, demonstrating increased disorder of the stratum corneum lipids that was indicative of reduced barrier function. Similar shifts were not seen when pure fluorosurfactant was applied, suggesting that the permeation enhancement was a feature of the ME and not simply the surfactant constituent.

Sugar-based esters have been investigated as another source of low irritancy surfactants [84]. Sucrose esters [laurate (SL) or myristate (SM)] were shown to be superior surfactants to Tween® 80 (T80) for the delivery of aceclofenac from ME composed of isopropyl myristate, water and co-surfactant of isopropyl alcohol or Transcutol®P. Aceclofenac release from the ME was determined across cellulose membranes and in vivo tape stripping (12 strips) was performed on human volunteers. An in vivo pharmacokinetic study was conducted in rats and skin irritancy of blank ME determined on human volunteers by measuring trans epidermal water loss (TEWL), erythema and hydration. The ME incorporating sugar esters released significantly more aceclofenac over 6h than Tween 80-based ME (87.28 ± 4.89 and 70.66 ± 4.46 compared to 53.65 ± 5.62% for SL, SM and T80 respectively). Aceclofenac penetration into the stratum corneum (by tape stripping) from the sugar ester ME was approximately two times that of the T80 ME (60.81 ± 5.97, 60.86 ± 3.67, 27.00 ± 5.09 mg/cm^2 for SL, SM, T80 respectively), and this was reflected in the maximum plasma concentrations and lag times measured in the rats (275.57 ± 109.49, 281.32 ± 6.76, 150.23 ± 69.74 ng/mL and 0.44 ± 0.19, 0.74 ± 0.32, 2.41 ± 2.70 h for SL, SM, T80 respectively). Not only were the sugar ester-based ME effective in the transdermal delivery of aceclofenac, but they also showed better skin tolerability [84].

Kriwet and Müller–Goyman [85] explored the mechanism of lecithin-based permeation enhancement by altering the ratio of diclofenac diethylamine, lecithin (soybean phosphatidylcholine) and water to develop a range of colloidal structures including ME, liposomes and lamellar liquid crystals. As diclofenac diethylamine is an amphiphilic molecule it interacts with the colloidal microstructure. At lecithin concentrations below 6% low viscosity ME were formed which gave rapid release of diclofenac diethylamine across a silicone impregnated dialysis membrane. Increasing the lecithin concentration led to phase transition into isotropic gels containing droplets with few lamellar layers surrounding the droplets. The increased viscosity of these systems resulted in decreased drug release. ME also gave higher permeation of diclofenac across human stratum corneum membranes than the other formulations tested, including a simple aqueous solution. The authors suggested that the increased permeation resulted from interaction between the lecithin phospholipids and the stratum corneum lipid bilayers, but this occurred only when presented as a ME and not as gel or liposomal formulations. In the liposomal formulations, the drug and phospholipids are too tightly held within the colloidal microstructure to effectively interact with the stratum corneum [85]. Further investigation of the interaction of lecithin-based ME and the stratum corneum was undertaken using FTIR and differential scanning calorimetry (DSC) [86]. In this case they used isopropyl palmitate as the oil phase

(alone and in the lecithin-based ME) and investigated the in vitro permeation of indomethacin and diclofenac across full-thickness human skin and the interactions on isolated stratum corneum sheets. ME formulations provided much higher permeation compared to isopropyl palmitate solutions, for both drugs. ME and isopropyl palmitate alone gave similar temperature shifts of the stratum corneum lipid transitions so they could not distinguish the penetration enhancement role of lecithin.

Viscosity enhancing agents are often added to convert the ME into a gel consistency suitable for retention on the skin surface. Naeem et al. [87] compared gels composed of Carbopol® 934P and Xanthan gum bases containing ME (5% *w*/*w* oleic acid, 46% *w*/*w* Tween®20:ethanol 2:1, 44% *w*/*w* water) or hydroalcoholic solution (ethanol/water) incorporating 5% *w*/*w* flurbiprofen. The transdermal flux of flurbiprofen across excised rabbit skin was 18.75 ± 0.08, 15.72 ± 0.05, 9.80 ± 0.09, 4.76 ± 0.07 and 2.70 ± 0.05 μg/cm^2/h over 24 h for the un-gelled ME, ME gelled with Carbopol and Xanthan, and hydroalcoholic solution gelled with Carbopol and Xanthan respectively. This clearly demonstrates that the ME delivers more NSAID than the hydroalcoholic solutions and that addition of a gelling agent reduces transdermal delivery. Similar findings were reported for lornoxicam [79] and aceclofenac [57], although it is interesting to note that this group have reported identical transdermal flux values for the two NSAIDs in these separately published manuscripts, despite the different drugs, compositions and experimental models. Shakeel et al. [67] also reported lower transdermal flux of indomethacin across rat skin from ME composed of 5% Labrafil®, 50% water and 45% of a 3:1 ratio of Tween® 80 and Transcutol®, when gelled with 1% Carbopol® 940 (73.96 ± 2.89 and 61.64 ± 2.38 μg/cm^2/h). It should be noted that there are other reports in which the addition of gelling agent did not significantly change the skin delivery (e.g., diclofenac diethylamine [63]) or indeed resulted in an increase in transdermal flux (e.g., amphotericin [58]).

The incorporation of additional chemical penetration enhancers [dimethyl sulfoxide (DMSO) and propylene glycol (PG)] in w/o ME compositions has been shown to further increase skin permeation across excised rabbit skin [88]. The relative effects of DMSO and PG were shown to be dependent on the cosurfactant in the ME formulation. PG gave better skin permeation of diclofenac sodium than DMSO when incorporated into isopropyl alcohol ME, whereas DMSO was superior to PG in propanol ME. Overall the ME containing isopropyl alcohol and PG gave greatest enhancement, although all ME formulations provided higher skin permeation of diclofenac than the commercial products tested.

We examined the skin permeation enhancement of the lipophilic NSAID naproxen and the hydrophilic drug caffeine applied in NE incorporating skin penetration enhancers oleic acid or eucalyptol as oil phases, with Volpo-N10 (an ethoxylated fatty alcohol) and ethanol as the surfactant and cosurfactant in a 1:1 ratio [73]. Caffeine and naproxen fluxes across human epidermal membranes were determined over 8 h. All NE formulations significantly enhanced the skin penetration of both caffeine and naproxen, compared to aqueous control solutions. Caffeine maximum flux enhancement was associated with a synergistic increase in both caffeine stratum corneum solubility and skin diffusivity, whereas a formulation-increased solubility in the stratum corneum was the dominant mechanism for increased naproxen fluxes. Enhancements in stratum corneum solubility were related to the uptake into the stratum corneum of the formulation excipients containing the active compounds. We concluded that enhanced skin penetration from NE is primarily due to uptake of formulation excipients containing the active compounds into the stratum corneum with consequent impacts on stratum corneum solubility and diffusivity.

A number of in vivo pharmacokinetic studies have supported the enhanced skin delivery effects of ME demonstrated in vitro. For example, an eight-fold higher permeation of diclofenac from ME (w/o; 2:3 PEG-40 stearate/glyceryl oleate as surfactant mix, tetraglycol as cosurfactant, S/CoS ratio 8:1, isopropyl myristate as oil phase and water than Voltaren® Emulgel (commercial coarse emulsion gel product) was demonstrated in a rat pharmacokinetic study [89]. Constant plasma diclofenac levels of 0.7–0.9 μg/mL were maintained for at least 8 h following ME administration. In contrast, a subcutaneous injection of diclofenac solution (3.5 mg/kg) resulted in a peak plasma level of 0.94 μg/mL at 1 h, which decreased rapidly to 0.19 μg/mL by 6 h.

Table 2. Examples of nanoemulsion (NE) formulations evaluated for topical and transdermal delivery: hydrophilic (H) and lipophilic (L) nature of active compound, composition (detail where available), preparation method and physical characterisation of emulsion formulation, and skin permeation experimental details and data.

Therapeutic Class and Active Compound	H/L	Composition	Preparation Method	Physical Characterisation				Skin Permeation Evaluation		Ref
				Particle Size (nm)	Surface Charge (mV)	Poly Dispersity	Viscosity (mPa s)			
NON-STEROIDAL ANTI-INFLAMMATORY DRUGS (NSAID)										
Aceclofenac	L	Nanoemulsion NE31 (O/W) Triacetin 13.6% Water 54.6% Cremophor EL® 23.9% PEG-400 7.9% Nanoemulsion gel NG31 NE31 gelled with Carbopol 934® 1% Drug load (DL): 1.5 mg%	Spontaneous aqueous phase titration	NE31 39.48		NE31 0.230	NE31 339.51 ± 0.31	Method (M) Results (R)	Full thickness rat abdominal skin Receptor: methanol-PBS (pH 7.4) (3:7) *Flux J* ($\mu g \cdot cm^{-2} \cdot h^{-1}$) *in 24 h* NE31: 254.90 ± 1.25 NG31: 199.60 ± 6.93 *Control* (Hiffenac™ Gel) 43.67 ± 2.11 *Enhancement ratio* (*ER*) NE31: 5.84 NG31: 4.57	[57]
Aceclofenac (ACF)	L	Nanoemulsion $L_{1.5}$ $S_{0.5}$ P_2A Medium chain triglycerides (MCT) Castor oil 1:1 20% Water 76% Lecithin 80 1.5% Sucrose stearate S-970 0.5% Sucrose palmitate P-1670 2% Drug load (DL): 1% *w*/*w*	High pressure homogenization	181.2 ± 0.8	−39.2 ± 1.5	0.110 ± 0.006	3.60 ± 0.23	(M) (R)	Human skin (in vivo 12 times tape stripping) *Amount of drug in SC strips* ($\mu g/cm^2$) $L_{1.5}$ $S_{0.5}$ P_2A 39.85 ± 1.29 *Control* L_2 $P80_2$A 28.32 ± 4.39	[65]
Lornoxicam	L	Nanoemulsion NE8 Labrafac® Tween 80 Pluronic F-68® S_{mix} 3:1 Oil: S_{mix} 2:8 Nanoemulsion gel NG8 NE 8 gelled with Carbopol 934® 1% Drug load (DL): 1.5%	Spontaneous aqueous phase titration	139 ± 29		0.233	23.87 ± 1.86	(M) (R)	Full thickness pig abdominal skin Receptor: PBS (pH 7.4) *Flux J* ($\mu g \cdot cm^{-2} \cdot h^{-1}$) *in 24 h* NE8: 254.90 ± 1.25 NG8: 199.60 ± 6.93 *Control* (gel) 43.67 ± 2.11	[79]
Indomethacin	L	Nanoemulsion F6 (O/W) Labrafil® 5% Water 50% Tween 80 33.75% Transcutol-HP® 11.25% S_{mix} ratio 3:1 S_{mix}/oil ratio 4.00 Nanoemulsion gel NG6 F6 gelled with Carbopol 940® 1% Triethanolamine 0.5% Drug load (DL): 0.5%	Spontaneous aqueous phase titration	F6 25.53 ± 2.22		F6 0.087	F6 14.32 ± 1.12	(M) (R)	Full thickness rat abdominal skin Receptor: methanol-PBS (pH 7.4) (1:9) *Flux J* ($\mu g \cdot cm^{-2} \cdot h^{-1}$) F6: 73.96 ± 2.89 NG6: 61.64 ± 2.38 *Control* Indobene gel (Indo Gel™) 9.38 ± 0.41 *ER* F6: 7.88 NG6: 6.57	[67]

Table 2. *Cont.*

Therapeutic Class and Active Compound	H/L	Composition	Preparation Method	Physical Characterisation				Skin Permeation Evaluation		Ref
				Particle Size (nm)	Surface Charge (mV)	Poly Dispersity	Viscosity (mPa s)			
NON-STEROIDAL ANTI-INFLAMMATORY DRUGS (NSAID)										
Naproxen and Caffeine	L, H	Nanoemulsions with penetration enhancers in oil phase E1 Eucalyptol (EU) 15.93% Water 30.97% Volpo-N10® 26.55% Ethanol 26.55% E2 Eucalyptol (EU) 14.63% Water 36.59% Volpo-N10® 24.39% Ethanol 24.39% O1 Oleic acid (OA) 15.93% Water 30.97% Volpo-N10® 26.55% Ethanol 26.55% O2 Oleic acid (OA) 14.63% Water 36.59% Volpo-N10® 24.39% Ethanol 24.39% Drug load (DL): Caffeine 3% Naproxen 2% *Controls:* $C1^{C}$: water 100% $C2^{C,N}$: water 40%, ethanol 60% $C3^{C}$: water 75%, PEG-6000 25% $C4^{N}$: water 50%, ethanol 25%, Volpo-N10 25%	Spontaneous aqueous phase titration and moderate agitation	Caffeine E1: 19.3 ± 4.0 E2: 16.0 ± 3.6 O1: 5.9 ± 2.4 O2: 1.2 ± 0.1 Naproxen E1: 37.8 ± 5.9 E2: 25.0 ± 3.0 O1: 11.6 ± 3.8 O2: 13.5 ± 4.5	Caffeine/ Naproxen-EU 15.3 Caffeine/ Naproxen-OA 15.3		Caffeine/ Naproxen-EU 13.7 ± 4.5 15.1 ± 4.0 Caffeine/ Naproxen-OA 23.7 ± 4.7 28.3 ± 4.5	(M)	Full thickness human skin Receptor: PBS (pH 7.4)	[73]
								(R)	*Flux J* ($\mu g \cdot cm^{-2} \cdot h^{-1}$) *in 24 h* (Caffeine) E1: 263.6 ± 1.2 E2: 267.7 ± 24.0 O1: 118.8 ± 57.3 O2: 136.4 ± 95.2 *Control* (Caffeine) C1: 2.2 ± 0.8 C2: 25.6 ± 3.1 C3: 2.5 ± 0.7 C4: not identified *Flux J* (Naproxen) E1: 122.4 ± 27.1 E2: 86.6 ± 8.9 O1: 101.2 ± 41.7 O2: 74.0 ± 2.3 *Control* (Naproxen) C1: not identified C2: 23.4 ± 4.8 C3: 6.2 ± 0.3 C4: 7.3 ± 2.7	
Diclofenac diethylamine (DDEA)	L	Nanoemulsion F1 Oleic acid 15% Water 30% Polysorbate 20 18.3% Ethanol 36.7% S_{mix} 1:2 55% Nanoemulsion gel NE F1 gelled with Carbopol 971P® 0.75% added Propylene glycol 10.0% Methyl paraben 0.18% Propyl paraben 0.02% Drug load (DL): 1.16% w/w DDEA (equivalent to 1% *w/w* diclofenac)	Spontaneous aqueous phase titration and vortex mixing	59.97 ± 3.22		0.28 ± 0.07	1.002	(M)	Strat-M® membrane Receptor: PBS (pH 7.4): methanol (70:30)	[63]
								(R)	*Flux J* ($\mu g \cdot cm^{-2} \cdot h^{-1}$) *in 12 h* F1: 11.5 NE gel: 12.0 *Controls* DDEA solution: 1.71 Conventional gel: 11.7 Emulgel: 12.5 (coarse emulsion gel)	

Table 2. *Cont.*

Therapeutic Class and Active Compound	H/L	Composition	Preparation Method	Physical Characterisation				Skin Permeation Evaluation		Ref
				Particle Size (nm)	Surface Charge (mV)	Poly Dispersity	Viscosity (mPa s)			
NON-STEROIDAL ANTI-INFLAMMATORY DRUGS (NSAID)										
Indomethacin	L	Nanoemulsion Triacetin® Capryol 90® 1:1 10% Water 40% Tween 80 25% Transcutol 25%	Spontaneous aqueous phase titration and vortex mixing	101.1	n.a	n.a	60 ± 2.1	(M)	Full thickness hairless new born albino rat Receptor: PBS (pH 7.4)	[90]
								(R)	*Flux J* ($\mu g \cdot cm^{-2} \cdot h^{-1}$) *in 6 h* 55.81 ± 4.65 No control	
Meloxicam (MLX)	L	Drug load (DL): 1% Nanoemulsion gel Caprylic acid 0.95% Water 70%Tween 80 20% Propylene glycol 10% Carbopol 940® 0.05%	Spontaneous aqueous phase titration	125 ± 1.9	−31.85 ± 0.61	0.193 ± 0.01		(M)	Abdominal rat skin Receptor: Acetate buffer (pH 6.0)	[80]
								(R)	*Flux J* ($\mu g \cdot cm^{-2} \cdot h^{-1}$) 6.407 ± 0.0911 Control (MLX solution): not identified *Amount in skin layers in 24 h* Tape strips: SC level *Control* > MLX-NE gel (1.02 folds) Epidermal level MLX-NE gel > *Control* (3.24 folds) Dermal level MLX-NE gel > *Control* (1.42 folds)	
Flufenamic acid	L	Nanoemulsion Potassium sorbate 0.1% γ-Cyclodextrin 1.0% Water to 100% PCL-liquid (cetearyl ethyl hexanoate, isopropyl myristate) 20% Sucrose stearate S-970 2.5% Drug load (DL): 1%	High pressure homogenization	-	-	-	-	(M)	Dermatomed pig abdominal skin (1.2 mm) Receptor: PBS (pH 7.4)	[91]
								(R)	*Flux J* ($\mu g \cdot cm^{-2} \cdot h^{-1}$) γ–SN Fluf 1.83 ± 0.87 No control	

Table 2. *Cont.*

Therapeutic Class and Active Compound	H/L	Composition	Preparation Method	Physical Characterisation				Skin Permeation Evaluation		Ref
				Particle Size (nm)	Surface Charge (mV)	Poly Dispersity	Viscosity (mPa s)			
ANTIFUNGAL AGENTS										
Terbinafine (TER) Citral (CIT)	L L	Nanoemulsion (NE) CIT 4% Water 71% Cremophor EL-40® 18% 1,2-propylene glycol 6% S_{mix} 3:1 NG1 NE gelled with Carbopol 934® 1% 1:1 (NG2 and NG3 contain 2% and 3% Carbopol 934®, respectively, at the same ratio with NE) Drug load (DL) in NE TER 1% and CIT 4% (oil phase) Controls: TER-CIT in Conventional gels (1.5% Carbopol 934®)	Spontaneous aqueous phase titration	NE 15.53 ± 3.32 NG1 14.88 ± 3.11	NE −7.4 ± 1.8 NG1 −6.5 ± 2.3	NE 0.074 ± 0.009 NG1 0.084 ± 0.025		(M)	Guinea pig abdominal skin Receptor: PBS (pH 7.4)	[93]
								(R)	*Flux J* ($\mu g \cdot cm^{-2} \cdot h^{-1}$) (TER) NE: 11.30 ± 0.56 NG1: 11.50 ± 0.43 *Control:* 1.48 ± 0.34 *Flux J* (CIT) NE: 54.71 ± 1.34 NG1: 55.01 ± 1.67 *Control:* 10.55 ± 0.87 *Amount in stratum corneum in 12 h* ($\mu g \cdot cm^{-2}$) NE-TER: 1.65 ± 0.29 NG1-TER: 6.27 ± 1.03 *Control TER:* 5.63 ± 0.76 NE-CIT: 0.95 ± 0.52 NG1-CIT: 10.88 ± 5.80 *Control CIT:* 13.68 ± 1.91 *Amount in epidermis-dermis in 12 h* ($\mu g \cdot cm^{-2}$) NE-TER: 73.5 ± 8.23 NG1-TER: 75.25 ± 9.52 *Control TER:* 17.42 ± 5.63 NE-CIT: 210.71 ± 12.38 NG1-CIT: 214.64 ± 0.92 *Control CIT:* 39.47 ± 5.51	
Fluconazole	H	Lecithin based NE PCL-liquid (cetearyl ethyl hexanoate, isopropyl myristate) 20% Potassium sorbate 0.1% γ-Cyclodextrin 1.0% Water to 100% Lipoid E-80® 2.5% Drug load (DL): 1%	High pressure homogenization	LN Fluc 156.87 ± 09.73 γ-LN Fluc 155.60 ± 07.96	LN Fluc −24.70 ± 3.41 γ-LN Fluc −22.50 ± 2.20	LN Fluc 0.05 ± 0.01 γ-LN Fluc 0.07 ± 0.02		(M)	Dermatomed pig abdominal skin (1.2mm) Receptor: PBS (pH 7.4)	[91]
								(R)	*Flux J* ($\mu g \cdot cm^{-2} \cdot h^{-1}$) LN Fluc: 109.55 ± 11.30 γ-LN Fluc: 93.63 ± 3.80 No control	

Table 2. *Cont.*

Therapeutic Class and Active Compound	H/L	Composition	Preparation Method	Physical Characterisation				Skin Permeation Evaluation		Ref
				Particle Size (nm)	Surface Charge (mV)	Poly Dispersity	Viscosity (mPa s)			
CORTICOSTEROIDS										
Fludrocortisone acetate	L	Lecithin based NE PCL-liquid (cetearyl ethyl hexanoate, isopropyl myristate) 20% Potassium sorbate 0.1% γ-Cyclodextrin 0.5% or 1.0% Water to 100% Lecithin E-80® 2.5% Drug load (DL): 1%	High pressure homogenization	γ-0.5% NE 171.03 ± 0.32 γ-1% NE 169.73 ± 2.35	γ-0.5% NE −33.17 ± 0.75 γ-1% NE −31.73 ± 1.52	γ-0.5% NE 0.098 ± 0.042 γ-1% NE 0.033 ± 0.049		(M)	Dermatomed pig abdominal skin (1.2mm) Receptor: PBS (pH 7.4)	[94]
								(R)	*Flux J* ($\mu g \cdot cm^{-2} \cdot h^{-1}$)*in 24 h* Finite dose γ-1% NE 0.067 ± 0.047 *NE Control:* 0.008 ± 0.007 Infinite dose γ-1% NE 2.48 ± 0.68 *NE Control:* 0.09 ± 0.07 *ER* of γ-1% NE: finite dose 8.38 infinite dose 27.55 *Control:* NE without cyclodextrin Applied as finite (5mg/cm^2) and infinite doses (500mg/cm^2) No significant different in drug flux between γ-1% NE and γ-0.5% NE	
Fludrocortisone acetate (FA) Flumethasone pivalate (FP)	L	Nanoemulsion (positive charge) PCL-liquid (cetearyl ethyl hexanoate, isopropyl myristate) 20% Lipoid S-75® 4% α tocopherol 1% Phytosphingosine (PS) 0.4% or 0.6% Water to 100% Sucrose laurate L-1695 1% *or* Tween 80 1% Drug load (DL): 1% FA NL: FA NE with sucrose laurate L-1695 FA NT: FA NE with tween 80 FP NL: FP NE with sucrose laurate L-1695 FP NT: FP NE with tween 80	High pressure homogenization	FA NL 161 ± 0.7 FA NL-0.4PS 215 ± 2.8 FA NL-0.6PS 254 ± 2.2 FA NT 170 ± 3.8 FA NT-0.4PS 216 ± 26.6 FA NT-0.6PS 170 ± 2.1	FA NL −6.2 ± 0.4 FA NL-0.4PS +46 ± 0.4 FA NL-0.6PS +48 ± 0.7 FA NT −55 ± 0.7 FA NT-0.4PS +45 ± 0.7 FA NT-0.6 PS +48 ± 1.1	FA NL 0.12–0.22 FA NL-0.4PS 0.22–0.25 FA NL-0.6 PS 0.06–0.1 FA NT 0.15–0.18 FA NT-0.4PS 0.13–0.18 FA NT-0.6 PS 0.10–0.14		(M)	Dermatomed pig abdominal skin (1 mm) Receptor: PBS (pH 7.4)	[95]
								(R)	*Flux J* ($\mu g \cdot cm^{-2} \cdot h^{-1}$) *in 48 h* FA NL 0.126 ± 0.027 FA NL-0.4PS 0.150 ± 0.010 FA NL-0.6 PS 0.189 ± 0.012 FA NT 0.263 ± 0.043 FA NT-0.4PS 0.353 ± 0.018 FA NT-0.6 PS 0.377 ± 0.038 FP NT 2.290 ± 0.313 FP NT-0.4PS 2.698 ± 0.117 FP NT-0.6 PS 3.073 ± 0.104 No control Flux increased with PS concentration; Tween 80 > sucrose laurate	

Table 2. *Cont.*

Therapeutic Class and Active Compound	H/L	Composition	Preparation Method	Physical Characterisation				Skin Permeation Evaluation		Ref
				Particle Size (nm)	Surface Charge (mV)	Poly Dispersity	Viscosity (mPa s)			
CORTICOSTEROIDS										
Prednicarbate (PC)	L	Positively charged NE (PCNE) Phytosphingosine (PS) 0.6% Lecithin E-80®, Tween 80 2% Ethanol 20% α tocopherol 0.03% Potassium sorbate 0.1% Negatively charged NE (NCNE) Myristic acid 1% was used to replace PS Drug load (DL): 0.25%	High pressure homogenization	PCNE: 157 NCNE: 136	PCNE: 50–60 NCNE: −(40–50)	0.05–0.1		(M)	Full thickness human skin Receptor: Ethanol-PBS (1:1) No PC detected in receptor in 24 h	[53, 54]
								(R)	*Amount PC in skin in 24 h* PCNE: 18.4 ± 3.4 µg/mL NCNE : 11.7 ± 2.5 µg/mL No control Positive > negative charged NE	
Fludrocortisone acetate (FA)	L	Lecithin based NE PCL-liquid (cetearyl ethyl hexanoate, isopropyl myristate) 20% Lecithin E-80® 2.5% Potassium sorbate 0.1% γ-Cyclodextrin 1.0% Water to 100% Drug load (DL): 1%	High pressure homogenization	γ-LN Flud 175.82 ± 00.47	γ-LN Flud −30.19 ± 4.12	γ-LN Flud 0.09 ± 0.04		(M)	Dermatomed pig abdominal skin (1.2mm thick) Receptor: PBS (pH 7.4)	[91]
								(R)	*Flux J* ($\mu g \cdot cm^{-2} \cdot h^{-1}$) (FA) γ-LN Flud: 4.53 ± 0.99 No control	
VITAMINS										
α tocopherol (vitamin E)	L	Hyaluronic acid-based NE (L6) Methylene oxide (O) Tween 80-Span 20 (S) HA-GMS solution (A) Mass ratio O:S:A 2:3:95 Drug load (DL): 0.1% HA-GMS is water soluble amphiphile from crosslinking esterification of hyaluronic acid and glycerol α-mono stearate (stearin)	Oil/water/surfactant emulsifying system and solvent evaporation	57.3 ± 0.2		0.260		(M)	Full thickness Wistar rat dorsal skin Receptor: PBS (pH 7.4)	[96]
								(R)	*Flux J* ($\mu g \cdot cm^{-2} \cdot h^{-1}$) *in 24 h* L6: 14.68 ± 4.13 *Control*: not detected *Control*: 0.1% vitamin E in ethanol solution	
α tocopherol (vitamin E) and Vitamin K1 (VK1)	L	Nanoemulsions α-tocopherol (α-TOC), VK1 10% Water 64% Tween 80 10% Ethanol 16% Drug load (DL): 3% or 5%	Spontaneous aqueous phase titration and Ultrasonic nebulization NE-neb-VK1 = ultrasonic nebulizer	NE-VK1 3% 254.8 ± 10.7 NE-neb-VK1 3% 259.4 ± 4.1 NE-VK1 5% 215.7 ± 2.3 NE-neb-VK1 5% 233.2 ± 0.2	NE-VK1 3% −14.89 ± 2.68 NEs-neb-VK1 3% −16.60 ± 1.01 NE-VK1 5% −14.14 ± 0.29 NE-neb-VK1 5% −15.4 ± 0.1	NE-VK1 3% 0.22 ± 0.05 NEs-neb-VK1 3% 0.19 ± 0.14 NE-VK1 5% 0.23 ± 0.02 NE-neb-VK1 5% 0.26 ± 0.02		(M)	Pig ear skin (thickness 1.7–2.3 mm) Receptor: PBS : Ethanol (7:3 *v*/*v*)	[56]
								(R)	*Amount in epidermis in 24 h (ng/mg)* NEs-VK1 3%: 46.7 NEs-neb-VK1 3%: 72.8 NEs-VK1 5%: 55.6 NEs-neb-VK1 5%: 51.4 *Amount in dermis in 24 h (ng/mg)* NEs-neb-VK1 3%: 27.9 NEs-neb-VK1 5%: 24.8 No control	

Table 2. *Cont.*

Therapeutic Class and Active Compound	H/L	Composition	Preparation Method	Physical Characterisation				Skin Permeation Evaluation		Ref
				Particle Size (nm)	Surface Charge (mV)	Poly Dispersity	Viscosity (mPa s)			
MISCELLANEOUS										
Thiocolchicoside (TCC) anti inflammatory, analgesic, muscle relaxant	H	Nanoemulsion C1 (W/O type) Linseed oil : Sefsol® 1:1 35.44% Water 10.81% Span 80 40.53% Transcutol P® 13.51% S_{mix} 3:1 C3 (W/O type) Linseed oil : Sefsol® 1:1 35.19% Water 9.26% Span 80 41.67% Transcutol P® 13.89% S_{mix} 3:1 Drug load (DL): 0.2%	Spontaneous aqueous phase titration	C1 117.73 ± 13.71 C3 131.43 ± 15.15		C1 0.285 C3 0.311	C1 61.12 ± 5.28 C3 65.75 ± 6.08	(M)	Full thickness weanling pig abdominal skin Receptor: PBS (pH 7.4)	[97]
								(R)	*Flux J* ($\mu g \cdot cm^{-2} \cdot h^{-1}$) *in 24 h* (TCC) C1: 30.63 ± 4.18 C3: 28.01 ± 3.41 *Control* (TCC aqueous solution) 5.99 ± 0.73 *ER* C1: 5.114 C3: 4.676 Type of NE did not influence *ER*	
Curcumin natural anti-inflammatory	L	Nanoemulsion NE gel Glyceryl monooleate (GMO) Water Cremophor RH40® PEG 400 O:S:CoS 1:8:1 Water: oil phase 5:1 NE gelled with Viscolam AT 100P® 5% and added: Methyl paraben 0.2% Propyl paraben 0.05% Glycerine 5% Propylene glycol 15% Drug load (DL): 0.35%	Spontaneous aqueous phase titration with 1 h ultrasonic sonication	85.0 ± 1.5	0.18 ± 0.0	−5.9 ± 0.3	2000–2700	(M)	Shed snake skin Receptor: PBS (pH 7.4)	[91]
								(R)	*Flux J* ($\mu g \cdot cm^{-2} \cdot h^{-1}$) NE gel: 1.699 ± 0.050 *Control gel* 0.836 ± 0.004	

Table 2. *Cont.*

Therapeutic Class and Active Compound	H/L	Composition	Preparation Method	Physical Characterisation				Skin Permeation Evaluation		Ref
				Particle Size (nm)	Surface Charge (mV)	Poly Dispersity	Viscosity (mPa s)			
MISCELLANEOUS										
Bovine albumin-fluorescein isothiocyanate conjugate (FITC-BSA) vaccine model	L	Nanoemulsion Squalene 37.5% Water 52.5% Span 80, Tween 80 10% S_{mix} 1:1 Drug load (DL): 0.25%	Spontaneous aqueous phase titration with high pressure homogenization	85.2 ± 15.5	−45.17 ± 4.77	0.186 ± 0.026	14.6 ± 0.026	(M)	Mouse skin Receptor: PBS (pH 7.4)	[69]
								(R)	*Flux J* ($\mu g \cdot cm^{-2} \cdot h^{-1}$) *in 48 h* NE: 23.44 ± 17.230 *Controls* CE: 6.10 ± 0.977 CA: 3.15 ± 0.897 *Controls* CE: emulsifiers solution (10% of S_{mix}) CA: aqueous solution	
Granisetron HCl (GHCl) anti emetic drug	H	Nanoemulsion with penetration enhancer NMP Isopropyl myristate (IPM) 4% Tween 85 20% Ethanol 20% N-methyl pyrrolidone (NMP) 10% Water up to 100% Drug load (DL): 2.5%	Spontaneous aqueous phase titration	48.3 ± 1.7		0.27 ± 0.02		(M)	Full thickness rat abdominal skin Receptor: saline solution	[98]
								(R)	*Flux J* ($\mu g \cdot cm^{-2} \cdot h^{-1}$) NMP NE: 85.39 ± 2.90 *Control*: 71.17 ± 3.54 *Amount in skin in 12 h* ($\mu g \cdot cm^{-2}$) NMP NE: 891.8 ± 2.86 *Control*: 889.1 ± 2.24 NMP NE ≅ NE Control: NE without NMP	
Minoxidil (Min) antihypertensive vasodilator (stimulate hair growth)	H	Lecithin based NE PCL-liquid (cetearyl ethyl hexanoate, isopropyl myristate) 20% Potassium sorbate 0.1% γ-Cyclodextrin 1.0% Water to 100% Lecithin E-80® 2.5% Drug load (DL): 1%	High pressure homogenization	-	-	-		(M)	Dermatomed pig abdominal skin (1.2mm thick) Receptor: PBS (pH 7.4)	[91]
								(R)	*Flux J* ($\mu g \cdot cm^{-2} \cdot h^{-1}$) 102.56 ± 9.41 No control	

Ensuring that any novel formulation maintains the stability and therapeutic activity of the drug is essential. The anti-inflammatory activity of NSAIDs applied in ME formulations has been demonstrated in a number of studies. For example, ME [o/w: composed of isopropyl myristate, water, Capmul MCM® (mixture of medium chain glycerides), Tween 80], gel (added Carbopol® 934), and cream (anionic emulsifying ointment and water) formulations containing celecoxib were compared for permeation across excised full-thickness rat skin [70]. Selected formulations were evaluated using the arachidonic acid induced ear edema model in Swiss albino mice. The skin permeation of celecoxib from the ME formulations was 3 to 5-fold greater than ME gels, and 7 to 11-fold greater than the cream. Increasing the concentration of Capmul MCM® in the ME resulted in an increase of droplet size and viscosity and decrease in celecoxib diffusion coefficient. Administration of selected ME formulations reduced ear edema by up to 55% demonstrating that the celecoxib ME was an effective anti-inflammatory formulation.

7. Conclusions and Future Directions

ME and NE have a clear place in the delivery of active compounds to and through the skin for a range of therapeutic purposes. They are elegant, relatively simple and inexpensive to manufacture and offer significant delivery advantages over coarse emulsions. Over the past few decades, there has been extensive research demonstrating the effectiveness of these delivery technologies. In addition, the development of new excipients with potential utility in NE and ME formulations continues to offer new opportunities for formulations with high delivery capacity coupled with low irritancy and toxicity. Although it has been explored, the precise mechanism of delivery of these formulations remains controversial, but it is likely to be a combination of the effect of the formulation components on stratum corneum diffusivity of the active compounds. The increase in transfollicular penetration from NE and ME is well established and is again likely due to both the formulation components facilitating penetration through the sebum and within the follicle. Given the advantages of these systems and the continued development of low toxicity excipients, it is likely that we will continue to see new NE and ME products for topical and transdermal delivery into the future.

Acknowledgments: Michael Roberts acknowledges the support of grants from the National Health and Medical Research Council of Australia (APP1049906; 1002611) and the US FDA (U01FD005226; U01FD005232). Christofori Nastiti acknowledges the Australia Awards Scholarship from the Department of Foreign Affairs and Trade, Australia.

Author Contributions: All authors contributed to the literature review and critical analysis, drafting and editing of this manuscript.

Conflicts of Interest: The authors declare no conflicts of interest.

References

1. Scheuplein, R.J. Analysis of permeability data for the case of parallel diffusion pathways. *Biophys. J.* **1966**, *6*, 1–17. [CrossRef]
2. Scheuplein, R.J.; Blank, I.H. Permeability of the skin. *Physiol. Rev.* **1971**, *51*, 702–747. [PubMed]
3. Kasting, G.B.; Barai, N.D.; Wang, T.F.; Nitsche, J.M. Mobility of water in human stratum corneum. *J. Pharm. Sci.* **2003**, *92*, 2326–2340. [CrossRef] [PubMed]
4. Illel, B.; Schaefer, H.; Wepierre, J.; Doucet, O. Follicles play an important role in percutaneous absorption. *J. Pharm. Sci.* **1991**, *80*, 424–427. [CrossRef] [PubMed]
5. Roberts, M.S.; Mohammed, Y.; Pastore, M.N.; Namjoshi, S.; Yousef, S.; Alinaghi, A.; Haridass, I.N.; Abd, E.; Leite-Silva, V.R.; Benson, H.; et al. Topical and cutaneous delivery using nanosystems. *J. Control. Release* **2017**, *247*, 86–105. [CrossRef] [PubMed]
6. Leite-Silva, V.R.; Liu, D.C.; Sanchez, W.Y.; Studier, H.; Mohammed, Y.H.; Holmes, A.; Becker, W.; Grice, J.E.; Benson, H.A.; Roberts, M.S. Effect of flexing and massage on in vivo human skin penetration and toxicity of zinc oxide nanoparticles. *Nanomedicine (Lond.)* **2016**, *11*, 1193–1205. [CrossRef] [PubMed]

7. Leite-Silva, V.R.; Sanchez, W.Y.; Studier, H.; Liu, D.C.; Mohammed, Y.H.; Holmes, A.M.; Ryan, E.M.; Haridass, I.N.; Chandrasekaran, N.C.; Becker, W.; et al. Human skin penetration and local effects of topical nano zinc oxide after occlusion and barrier impairment. *Eur. J. Pharm. Biopharm.* **2016**, *104*, 140–147. [CrossRef] [PubMed]
8. Danielsson, I.; Lindman, B. The definition of microemulsion. *Colloid Surf.* **1981**, *3*, 391–392. [CrossRef]
9. Muller, R.H.; Radtke, M.; Wissing, S.A. Solid lipid nanoparticles (SLN) and nanostructured lipid carriers (NLC) in cosmetic and dermatological preparations. *Adv. Drug Deliv. Rev.* **2002**, *54* (Suppl. 1), S131–S155. [CrossRef]
10. Jores, K.; Haberland, A.; Wartewig, S.; Mader, K.; Mehnert, W. Solid lipid nanoparticles (SLN) and oil-loaded SLN studied by spectrofluorometry and Raman spectroscopy. *Pharm. Res.* **2005**, *22*, 1887–1897. [CrossRef] [PubMed]
11. Touitou, E.; Dayan, N.; Bergelson, L.; Godin, B.; Eliaz, M. Ethosomes—Novel vesicular carriers for enhanced delivery: Characterization and skin penetration properties. *J. Control. Release* **2000**, *65*, 403–418. [CrossRef]
12. Uchegbu, I.F.; Vyas, S.P. Non-ionic surfactant based vesicles (niosomes) in drug delivery. *Int. J. Pharm.* **1997**, *172*, 33–70. [CrossRef]
13. Dragicevic-Curic, N.; Scheglmann, D.; Albrecht, V.; Fahr, A. Temoporfin-loaded invasomes: Development, characterization and in vitro skin penetration studies. *J. Control. Release* **2008**, *127*, 59–69. [CrossRef] [PubMed]
14. Geusens, B.; van Gele, M.; Braat, S.; de Smedt, S.C.; Stuart, M.C.; Prow, T.W.; Sanchez, W.; Roberts, M.S.; Sanders, N.; Lambert, J. Flexible Nanosomes (SECosomes) Enable Efficient siRNA Delivery in Cultured Primary Skin Cells and in the Viable Epidermis of Ex Vivo Human Skin. *Adv. Funct. Mater.* **2010**, *20*, 4077–4090. [CrossRef]
15. Mura, S.; Manconi, M.; Fadda, A.M.; Sala, M.C.; Perricci, J.; Pini, E.; Sinico, C. Penetration enhancer-containing vesicles (PEVs) as carriers for cutaneous delivery of minoxidil: In vitro evaluation of drug permeation by infrared spectroscopy. *Pharm. Dev. Technol.* **2013**, *18*, 1339–1345. [CrossRef] [PubMed]
16. Manconi, M.; Caddeo, C.; Sinico, C.; Valenti, D.; Mostallino, M.C.; Biggio, G.; Fadda, A.M. Ex vivo skin delivery of diclofenac by transcutol containing liposomes and suggested mechanism of vesicle-skin interaction. *Eur. J. Pharm. Biopharm.* **2011**, *78*, 27–35. [CrossRef] [PubMed]
17. Williams, A.C.; Barry, B.W. Penetration enhancers. *Adv. Drug Deliv. Rev.* **2004**, *56*, 603–618. [CrossRef] [PubMed]
18. Cevc, G.; Blume, G. Lipid vesicles penetrate into intact skin owing to the transdermal osmotic gradients and hydration force. *Biochim. Biophys. Acta* **1992**, *1104*, 226–232. [CrossRef]
19. Kim, S.; Shi, Y.; Kim, J.Y.; Park, K.; Cheng, J.X. Overcoming the barriers in micellar drug delivery: Loading efficiency, in vivo stability, and micelle-cell interaction. *Exp. Opin. Drug Deliv.* **2010**, *7*, 49–62. [CrossRef] [PubMed]
20. Borowska, K.; Wolowiec, S.; Glowniak, K.; Sieniawska, E.; Radej, S. Transdermal delivery of 8-methoxypsoralene mediated by polyamidoamine dendrimer G2.5 and G3.5—In vitro and in vivo study. *Int. J. Pharm.* **2012**, *436*, 764–770. [CrossRef] [PubMed]
21. Santos, P.; Watkinson, A.C.; Hadgraft, J.; Lane, M.E. Application of microemulsions in dermal and transdermal drug delivery. *Skin Pharmacol. Physiol.* **2008**, *21*, 246–259. [CrossRef] [PubMed]
22. McClements, D.J. Nanoemulsions versus microemulsions: Clarification of critical differences. *Soft Matter* **2012**, *8*, 1719–1729. [CrossRef]
23. Anton, N.; Vandamme, T.F. Nano-emulsions and micro-emulsions: Clarifications of the critical differences. *Pharm. Res.* **2011**, *28*, 978–985. [CrossRef] [PubMed]
24. Gupta, A.; Eral, H.B.; Hatton, T.A.; Doyle, P.S. Nanoemulsions: Formation, properties and applications. *Soft Matter* **2016**, *12*, 2826–2841. [CrossRef] [PubMed]
25. Heuschkel, S.; Goebel, A.; Neubert, R.H. Microemulsions—Modern colloidal carrier for dermal and transdermal drug delivery. *J. Pharm. Sci.* **2008**, *97*, 603–631. [CrossRef] [PubMed]
26. Scriven, L.E. Equilibrium bicontinuous structure. *Nature* **1976**, *263*, 123–125. [CrossRef]
27. Lindman, B.; Shinoda, K.; Olsson, U.; Anderson, D.; Karlström, G.; Wennerström, H. On the demonstration of bicontinuous structures in microemulsions. *Colloids Surf. A Physicochem. Eng. Asp.* **1989**, *38*, 205–224. [CrossRef]

28. Bhatia, G.; Zhou, Y.; Banga, A.K. Adapalene microemulsion for transfollicular drug delivery. *J. Pharm. Sci.* **2013**, *102*, 2622–2631. [CrossRef] [PubMed]
29. Naoui, W.; Bolzinger, M.A.; Fenet, B.; Pelletier, J.; Valour, J.P.; Kalfat, R.; Chevalier, Y. Microemulsion microstructure influences the skin delivery of an hydrophilic drug. *Pharm. Res.* **2011**, *28*, 1683–1695. [CrossRef] [PubMed]
30. Anton, N.; Benoit, J.P.; Saulnier, P. Design and production of nanoparticles formulated from nano-emulsion templates-a review. *J. Control. Release* **2008**, *128*, 185–199. [CrossRef] [PubMed]
31. Jasmina, H.; Džana, O.; Alisa, E.; Edina, V.; Ognjenka, R. Preparation of nanoemulsions by high-energy and low energy emulsification methods. In *CMBEBIH 2017, Proceedings of the International Conference on Medical and Biological Engineering (IFMBE), Sarajevo, Bosnia and Herzegovina, 16–18 March 2017*; Badnjevic, A., Ed.; Springer: Singapore, 2017.
32. Sole, I.; Solans, C.; Maestro, A.; Gonzalez, C.; Gutierrez, J.M. Study of nano-emulsion formation by dilution of microemulsions. *J. Colloid Interface Sci.* **2012**, *376*, 133–139. [CrossRef] [PubMed]
33. Wang, L.; Tabor, R.; Eastoe, J.; Li, X.; Heenan, R.K.; Dong, J. Formation and stability of nanoemulsions with mixed ionic-nonionic surfactants. *Phys. Chem. Chem. Phys.* **2009**, *11*, 9772–9778. [CrossRef] [PubMed]
34. Pons, R.; Carrera, I.; Caelles, J.; Rouch, J.; Panizza, P. Formation and properties of mini-emulsions formed by microemulsions dilution. *Adv. Colloid Interface Sci.* **2003**, *106*, 129–146. [CrossRef]
35. Vitale, S.A.; Katz, J.L. Liquid droplet dispersions formed by homogeneous liquid—Liquid nucleation: "The ouzo effect". *Langmuir* **2003**, *19*, 4105–4110. [CrossRef]
36. Wang, L.; Mutch, K.J.; Eastoe, J.; Heenan, R.K.; Dong, J. Nanoemulsions prepared by a two-step low-energy process. *Langmuir* **2008**, *24*, 6092–6099. [CrossRef] [PubMed]
37. Lee, H.S.; Morrison, E.D.; Frethem, C.D.; Zasadzinski, J.A.; McCormick, A.V. Cryogenic electron microscopy study of nanoemulsion formation from microemulsions. *Langmuir* **2014**, *30*, 10826–10833. [CrossRef] [PubMed]
38. Kreilgaard, M.; Pedersen, E.J.; Jaroszewski, J.W. NMR characterisation and transdermal drug delivery potential of microemulsion systems. *J. Control. Release* **2000**, *69*, 421–433. [CrossRef]
39. Paolino, D.; Ventura, C.A.; Nistico, S.; Puglisi, G.; Fresta, M. Lecithin microemulsions for the topical administration of ketoprofen: Percutaneous adsorption through human skin and in vivo human skin tolerability. *Int. J. Pharm.* **2002**, *244*, 21–31. [CrossRef]
40. Hua, L.; Weisan, P.; Jiayu, L.; Ying, Z. Preparation, evaluation, and NMR characterization of vinpocetine microemulsion for transdermal delivery. *Drug Dev. Ind. Pharm.* **2004**, *30*, 657–666. [CrossRef] [PubMed]
41. Lopes, L.B. Overcoming the Cutaneous Barrier with Microemulsions. *Pharmaceutics* **2014**, *6*, 52–77. [CrossRef] [PubMed]
42. Ita, K. Progress in the use of microemulsions for transdermal and dermal drug delivery. *Pharm. Dev. Technol.* **2017**, *22*, 467–475. [CrossRef] [PubMed]
43. Cavalcanti, A.L.; Reis, M.Y.; Silva, G.C.; Ramalho, I.M.; Guimaraes, G.P.; Silva, J.A.; Saraiva, K.L.; Damasceno, B.P. Microemulsion for topical application of pentoxifylline: In vitro release and in vivo evaluation. *Int. J. Pharm.* **2016**, *506*, 351–360. [CrossRef] [PubMed]
44. Danino, D.; Bernheim-Groswasser, A.; Talmon, Y. Digital cryogenic transmission electron microscopy: An advanced tool for direct imaging of complex fluids. *Colloids Surf. A Physicochem. Eng. Asp.* **2001**, *183–185*, 113–122. [CrossRef]
45. Podlogar, F.; Gasperlin, M.; Tomsic, M.; Jamnik, A.; Rogac, M.B. Structural characterisation of water-Tween 40/Imwitor 308-isopropyl myristate microemulsions using different experimental methods. *Int. J. Pharm.* **2004**, *276*, 115–128. [CrossRef] [PubMed]
46. Bhattacharya, S.; Stokes, J.P.; Kim, M.W.; Huang, J.S. Percolation in an oil-continuous microemulsion. *Phys. Rev. Lett.* **1985**, *55*, 1884–1887. [CrossRef] [PubMed]
47. Thevenin, M.A.; Grossiord, J.L.; Poelman, M.C. Sucrose esters/cosurfactant microemulsion systems for transdermal delivery: Assessment of bicontinuous structures. *Int. J. Pharm.* **1996**, *137*, 177–186. [CrossRef]
48. Lutz, R.; Aserin, A.; Wachtel, E.J.; Ben-Shoshan, E.; Danino, D.; Garti, N. A Study of the Emulsified Microemulsion by SAXS, Cryo-TEM, SD-NMR, and Electrical Conductivity. *J. Dispers. Sci. Technol.* **2007**, *28*, 1149–1157. [CrossRef]
49. Acharya, D.P.; Hartley, P.G. Progress in microemulsion characterization. *Curr. Opin. Colloid Interface Sci.* **2012**, *17*, 274–280. [CrossRef]

50. Hoppel, M.; Juric, S.; Ettl, H.; Valenta, C. Effect of monoacyl phosphatidylcholine content on the formation of microemulsions and the dermal delivery of flufenamic acid. *Int. J. Pharm.* **2015**, *479*, 70–76. [CrossRef] [PubMed]
51. Lademann, J.; Richter, H.; Meinke, M.; Sterry, W.; Patzelt, A. Which skin model is the most appropriate for the investigation of topically applied substances into the hair follicles? *Skin Pharmacol. Physiol.* **2010**, *23*, 47–52. [CrossRef] [PubMed]
52. Yousef, S.; Liu, X.; Mostafa, A.; Mohammed, Y.; Grice, J.E.; Anissimov, Y.G.; Sakran, W.; Roberts, M.S. Estimating Maximal In Vitro Skin Permeation Flux from Studies Using Non-sink Receptor Phase Conditions. *Pharm. Res.* **2016**, *33*, 2180–2194. [CrossRef] [PubMed]
53. Baspinar, Y.; Borchert, H.H. Penetration and release studies of positively and negatively charged nanoemulsions—Is there a benefit of the positive charge? *Int. J. Pharm.* **2012**, *430*, 247–252. [CrossRef] [PubMed]
54. Baspinar, Y.; Keck, C.M.; Borchert, H.H. Development of a positively charged prednicarbate nanoemulsion. *Int. J. Pharm.* **2010**, *383*, 201–208. [CrossRef] [PubMed]
55. Lu, W.C.; Chiang, B.H.; Huang, D.W.; Li, P.H. Skin permeation of D-limonene-based nanoemulsions as a transdermal carrier prepared by ultrasonic emulsification. *Ultrason. Sonochem.* **2014**, *21*, 826–832. [CrossRef] [PubMed]
56. Campani, V.; Biondi, M.; Mayol, L.; Cilurzo, F.; Pitaro, M.; de Rosa, G. Development of nanoemulsions for topical delivery of vitamin K1. *Int. J. Pharm.* **2016**, *511*, 170–177. [CrossRef] [PubMed]
57. Dasgupta, S.; Dey, S.; Choudhury, S.; Mazumder, B. Topical delivery of aceclofenac as nanoemulsion comprising excipients having optimum emulsification capabilities: Preparation, characterization and in vivo evaluation. *Exp. Opin. Drug Deliv.* **2013**, *10*, 411–420. [CrossRef] [PubMed]
58. Hussain, A.; Samad, A.; Singh, S.K.; Ahsan, M.N.; Haque, M.W.; Faruk, A.; Ahmed, F.J. Nanoemulsion gel-based topical delivery of an antifungal drug: In vitro activity and in vivo evaluation. *Drug Deliv.* **2016**, *23*, 642–647. [CrossRef] [PubMed]
59. Teichmann, A.; Heuschkel, S.; Jacobi, U.; Presse, G.; Neubert, R.H.; Sterry, W.; Lademann, J. Comparison of stratum corneum penetration and localization of a lipophilic model drug applied in an o/w microemulsion and an amphiphilic cream. *Eur. Pharm. Biopharm.* **2007**, *67*, 699–706. [CrossRef] [PubMed]
60. Wosicka, H.; Cal, K. Targeting to the hair follicles: Current status and potential. *J. Dermatol. Sci.* **2010**, *57*, 83–89. [CrossRef] [PubMed]
61. Lademann, J.; Knorr, F.; Richter, H.; Blume-Peytavi, U.; Vogt, A.; Antoniou, C.; Sterry, W.; Patzelt, A. Hair follicles—An efficient storage and penetration pathway for topically applied substances. Summary of recent results obtained at the Center of Experimental and Applied Cutaneous Physiology, Charite-Universitatsmedizin Berlin, Germany. *Skin Pharmacol. Physiol.* **2008**, *21*, 150–155. [CrossRef] [PubMed]
62. Kweon, J.H.; Chi, S.C.; Park, E.S. Transdermal delivery of diclofenac using microemulsions. *Arch. Pharm. Res.* **2004**, *27*, 351–356. [CrossRef] [PubMed]
63. Hamed, R.; Basil, M.; AlBaraghthi, T.; Sunoqrot, S.; Tarawneh, O. Nanoemulsion-based gel formulation of diclofenac diethylamine: Design, optimization, rheological behavior and in vitro diffusion studies. *Pharm. Dev. Technol.* **2016**, *21*, 980–989. [CrossRef] [PubMed]
64. Lee, J.; Lee, Y.; Kim, J.; Yoon, M.; Choi, Y.W. Formulation of microemulsion systems for transdermal delivery of aceclofenac. *Arch. Pharm. Res.* **2005**, *28*, 1097–1102. [CrossRef] [PubMed]
65. Isailovic, T.; Ethordevic, S.; Markovic, B.; Randelovic, D.; Cekic, N.; Lukic, M.; Pantelic, I.; Daniels, R.; Savic, S. Biocompatible Nanoemulsions for Improved Aceclofenac Skin Delivery: Formulation Approach Using Combined Mixture-Process Experimental Design. *J. Pharm. Sci.* **2016**, *105*, 308–323. [CrossRef] [PubMed]
66. Park, E.S.; Cui, Y.; Yun, B.J.; Ko, I.J.; Chi, S.C. Transdermal delivery of piroxicam using microemulsions. *Arch. Pharm. Res.* **2005**, *28*, 243–248. [CrossRef] [PubMed]
67. Shakeel, F.; Ramadan, W.; Ahmed, M.A. Investigation of true nanoemulsions for transdermal potential of indomethacin: Characterization, rheological characteristics, and ex vivo skin permeation studies. *J. Drug Target.* **2009**, *17*, 435–441. [CrossRef] [PubMed]
68. Shakeel, F.; Ramadan, W.; Gargum, H.M.; Singh, R. Preparation and in vivo evaluation of indomethacin loaded true nanoemulsions. *Sci. Pharm.* **2010**, *78*, 47–56. [CrossRef] [PubMed]

69. Ledet, G.; Pamujula, S.; Walker, V.; Simon, S.; Graves, R.; Mandal, T.K. Development and in vitro evaluation of a nanoemulsion for transcutaneous delivery. *Drug Dev. Ind. Pharm.* **2014**, *40*, 370–379. [CrossRef] [PubMed]
70. Subramanian, N.; Ghosal, S.K.; Moulik, S.P. Enhanced in vitro percutaneous absorption and in vivo anti-inflammatory effect of a selective cyclooxygenase inhibitor using microemulsion. *Drug Dev. Ind. Pharm.* **2005**, *31*, 405–416. [CrossRef] [PubMed]
71. Shakeel, F.; Baboota, S.; Ahuja, A.; Ali, J.; Shafiq, S. Enhanced anti-inflammatory effects of celecoxib from a transdermally applied nanoemulsion. *Die Pharm.* **2009**, *64*, 258–259.
72. Lala, R.R.; Awari, N.G. Nanoemulsion-based gel formulations of COX-2 inhibitors for enhanced efficacy in inflammatory conditions. *Appl. Nanosci.* **2014**, *4*, 143–151. [CrossRef]
73. Abd, E.; Namjoshi, S.; Mohammed, Y.H.; Roberts, M.S.; Grice, J.E. Synergistic Skin Penetration Enhancer and Nanoemulsion Formulations Promote the Human Epidermal Permeation of Caffeine and Naproxen. *J. Pharm. Sci.* **2016**, *105*, 212–220. [CrossRef] [PubMed]
74. Hoppel, M.; Ettl, H.; Holper, E.; Valenta, C. Influence of the composition of monoacyl phosphatidylcholine based microemulsions on the dermal delivery of flufenamic acid. *Int. J. Pharm.* **2014**, *475*, 156–162. [CrossRef] [PubMed]
75. Mahrhauser, D.S.; Kahlig, H.; Partyka-Jankowska, E.; Peterlik, H.; Binder, L.; Kwizda, K.; Valenta, C. Investigation of microemulsion microstructure and its impact on skin delivery of flufenamic acid. *Int. J. Pharm.* **2015**, *490*, 292–297. [CrossRef] [PubMed]
76. Rhee, Y.S.; Choi, J.G.; Park, E.S.; Chi, S.C. Transdermal delivery of ketoprofen using microemulsions. *Int. J. Pharm.* **2001**, *228*, 161–170. [CrossRef]
77. Kim, B.S.; Won, M.; Lee, K.M.; Kim, C.S. In vitro permeation studies of nanoemulsions containing ketoprofen as a model drug. *Drug Deliv.* **2008**, *15*, 465–469. [CrossRef] [PubMed]
78. Park, K.M.; Lee, M.K.; Hwang, K.J.; Kim, C.K. Phospholipid-based microemulsions of flurbiprofen by the spontaneous emulsification process. *Int. J. Pharm.* **1999**, *183*, 145–154. [CrossRef]
79. Dasgupta, S.; Ghosh, S.K.; Ray, S.; Kaurav, S.S.; Mazumder, B. In vitro & in vivo studies on lornoxicam loaded nanoemulsion gels for topical application. *Curr. Drug Deliv.* **2014**, *11*, 132–138. [PubMed]
80. Khurana, S.; Jain, N.K.; Bedi, P.M. Nanoemulsion based gel for transdermal delivery of meloxicam: Physico-chemical, mechanistic investigation. *Life Sci.* **2013**, *92*, 383–392. [CrossRef] [PubMed]
81. Sintov, A.C.; Shapiro, L. New microemulsion vehicle facilitates percutaneous penetration in vitro and cutaneous drug bioavailability in vivo. *J. Control. Release* **2004**, *95*, 173–183. [CrossRef] [PubMed]
82. Duangjit, S.; Mehr, L.M.; Kumpugdee-Vollrath, M.; Ngawhirunpat, T. Role of simplex lattice statistical design in the formulation and optimization of microemulsions for transdermal delivery. *Biol. Pharm. Bull.* **2014**, *37*, 1948–1957. [CrossRef] [PubMed]
83. Mahrhauser, D.; Hoppel, M.; Scholl, J.; Binder, L.; Kahlig, H.; Valenta, C. Simultaneous analysis of skin penetration of surfactant and active drug from fluorosurfactant-based microemulsions. *Eur. J. Pharm. Biopharm.* **2014**, *88*, 34–39. [CrossRef] [PubMed]
84. Todosijevic, M.N.; Savic, M.M.; Batinic, B.B.; Markovic, B.D.; Gasperlin, M.; Randelovic, D.V.; Lukic, M.Z.; Savic, S.D. Biocompatible microemulsions of a model NSAID for skin delivery: A decisive role of surfactants in skin penetration/irritation profiles and pharmacokinetic performance. *Int. J. Pharm.* **2015**, *496*, 931–941. [CrossRef] [PubMed]
85. Kriwet, K.; Muller-Goyman, C.C. Diclofenac release from phospholipid drug systems and permeation through excised human stratum corneum. *Int. J. Pharm.* **1995**, *135*, 231–242. [CrossRef]
86. Dreher, F.; Walde, P.; Walther, P.; Wehrli, E. Interaction of a lecithin microemulsion gel with human stratum corneum and its effect on human stratum corneum transport. *J. Control. Release* **1997**, *45*, 131–140. [CrossRef]
87. Naeem, M.; Rahman, N.U.; Tavares, G.D.; Barbosa, S.F.; Chacra, N.B.; Lobenberg, R.; Sarfraz, M.K. Physicochemical, in vitro and in vivo evaluation of flurbiprofen microemulsion. *An. Acad. Bras. Cienc.* **2015**, *87*, 1823–1831. [CrossRef] [PubMed]
88. Kantarci, G.; Ozguney, I.; Karasulu, H.Y.; Guneri, T.; Basdemir, G. In vitro permeation of diclofenac sodium from novel microemulsion formulations through rabbit skin. *Drug Dev. Res.* **2005**, *65*, 17–25. [CrossRef]
89. Sintov, A.C.; Botner, S. Transdermal drug delivery using microemulsion and aqueous systems: Influence of skin storage conditions on the in vitro permeability of diclofenac from aqueous vehicle systems. *Int. J. Pharm.* **2006**, *311*, 55–62. [CrossRef] [PubMed]

90. El-Leithy, E.S.; Ibrahim, H.K.; Sorour, R.M. In vitro and in vivo evaluation of indomethacin nanoemulsion as a transdermal delivery system. *Drug Deliv.* **2015**, *22*, 1010–1017. [CrossRef] [PubMed]
91. Klang, V.; Matsko, N.; Raupach, K.; El-Hagin, N.; Valenta, C. Development of sucrose stearate-based nanoemulsions and optimisation through gamma-cyclodextrin. *Eur. J. Pharm. Biopharm.* **2011**, *79*, 58–67. [CrossRef] [PubMed]
92. Hussain, A.; Samad, A.; Nazish, I.; Ahmed, F.J. Nanocarrier-based topical drug delivery for an antifungal drug. *Drug Dev. Ind. Pharm.* **2014**, *40*, 527–541. [CrossRef] [PubMed]
93. Zheng, Y.; Ouyang, W.Q.; Wei, Y.P.; Syed, S.F.; Hao, C.S.; Wang, B.Z.; Shang, Y.H. Effects of Carbopol(R) 934 proportion on nanoemulsion gel for topical and transdermal drug delivery: A skin permeation study. *Int. J. Nanomed.* **2016**, *11*, 5971–5987. [CrossRef] [PubMed]
94. Klang, V.; Haberfeld, S.; Hartl, A.; Valenta, C. Effect of gamma-cyclodextrin on the in vitro skin permeation of a steroidal drug from nanoemulsions: Impact of experimental setup. *Int. J. Pharm.* **2012**, *423*, 535–542. [CrossRef] [PubMed]
95. Hoeller, S.; Sperger, A.; Valenta, C. Lecithin based nanoemulsions: A comparative study of the influence of non-ionic surfactants and the cationic phytosphingosine on physicochemical behaviour and skin permeation. *Int. J. Pharm.* **2009**, *370*, 181–186. [CrossRef] [PubMed]
96. Kong, M.; Chen, X.G.; Kweon, D.K.; Park, H.J. Investigations on skin permeation of hyaluronic acid based nanoemulsion as transdermal carrier. *Carbohydr. Polym.* **2011**, *86*, 837–843. [CrossRef]
97. Kumar, D.; Ali, J.; Baboota, S. Omega 3 fatty acid-enriched nanoemulsion of thiocolchicoside for transdermal delivery: Formulation, characterization and absorption studies. *Drug Deliv.* **2016**, *23*, 591–600. [CrossRef] [PubMed]
98. Zheng, W.W.; Zhao, L.; Wei, Y.M.; Ye, Y.; Xiao, S.H. Preparation and the in vitro evaluation of nanoemulsion system for the transdermal delivery of granisetron hydrochloride. *Chem. Pharm. Bull.* **2010**, *58*, 1015–1019. [CrossRef] [PubMed]

Appendix 3. Attribution statement for co-authors for published article presented in Chapter 5

To Whom It May Concern

I, Thellie Ponto, as one of the first authors, contributed the following to a research article: Novel Self-Nano-Emulsifying Drug Delivery Systems Containing Astaxanthin for Topical Skin Delivery

- Conception and design
- Literature search and review
- Data conditioning
- Manuscript preparation
- Final approval

_____

I as a first/co-author, endorse that this level of contribution by the candidate indicated above is appropriate.

Gemma Latter _____

Giuseppe Luna _____

Prof. Vânia R. Leite-Silva _____

Prof. Anthony Wright _____

A/P Dr. Heather A.E Benson _____

Research article: Novel Self-Nano-Emulsifying Drug Delivery Systems Containing Astaxanthin for Topical Skin Delivery

Pharmaceutics 2021, 13(5), 649; pages 1-16; https://doi.org/10.3390/pharmaceutics13050649

Thellie Ponto [1] , Gemma Latter [1] , Giuseppe Luna [1] , Vânia R. Leite-Silva [2] , Anthony Wright [3] and Heather A. E. Benson [1],*

[1] Curtin Medical School, Curtin Health Innovation Research Institute (CHIRI), Curtin University, GPO Box U1987, Perth, WA 6845, Australia

[2] Instituto de Ciências Ambientais, Químicas e Farmacêuticas, Departamento de Ciências Farmacêuticas,
Universidade Federal de São Paulo, UNIFESP-Diadema, São Paulo 09913-030, Brazil

[3] School of Allied Health, Curtin University, GPO Box U1987, Perth, WA 6845, Australia;

* Correspondence: h.benson@curtin.edu.au; Tel.: +61-8-9266-2338

	Conception and design	Literature search and review	Data conditioning	Manuscript preparation	Final approval
Gemma Latter			✓		✓
I acknowledge that these represent my contribution to the above research output					
Giuseppe Luna	✓		✓		✓
I acknowledge that these represent my contribution to the above research output					
Prof. Vânia R. Leite-Silva	✓				✓
I acknowledge that these represent my contribution to the above research output					

Prof. Anthony Wright	✓				✓
I acknowledge that these represent my contribution to the above research output					
A/P Dr. Heather A.E Benson	✓	✓	✓	✓	✓
I acknowledge that these represent my contribution to the above research output					

Appendix 4. First page of publication, as presented in Chapter 5

pharmaceutics

MDPI

Article

Novel Self-Nano-Emulsifying Drug Delivery Systems Containing Astaxanthin for Topical Skin Delivery

Thellie Ponto [1], Gemma Latter [1], Giuseppe Luna [1], Vânia R. Leite-Silva [2], Anthony Wright [3] and Heather A. E. Benson [1,*]

[1] Curtin Medical School, Curtin Health Innovation Research Institute (CHIRI), Curtin University, GPO Box U1987, Perth, WA 6845, Australia; thellie.ponto@postgrad.curtin.edu.au (T.P.); gemma.latter@postgrad.curtin.edu.au (G.L.); giuseppe.luna@curtin.edu.au (G.L.)
[2] Instituto de Ciências Ambientais, Químicas e Farmacêuticas, Departamento de Ciências Farmacêuticas, Universidade Federal de São Paulo, UNIFESP-Diadema, São Paulo 09913-030, Brazil; vaniarleite@uol.com.br
[3] School of Allied Health, Curtin University, GPO Box U1987, Perth, WA 6845, Australia; t.wright@curtin.edu.au
* Correspondence: h.benson@curtin.edu.au; Tel.: +61-8-9266-2338

Abstract: Astaxanthin (ASX) is a potent lipophilic antioxidant derived from the natural pigment that gives marine animals their distinctive red-orange colour and confers protection from ultraviolet radiation. Self nano-emulsifying drug delivery systems (SNEDDS) have been successfully developed and evaluated to increase the skin penetration of ASX and target its antioxidant and anti-inflammatory potential to the epidermis and dermis. SNEDDS were prepared using a low-temperature spontaneous emulsification method, and their physical characteristics, stability, antioxidant activity, and skin penetration were characterized. Terpenes (D-limonene, geraniol, and farnesol) were included in the SNEDDS formulations to evaluate their potential skin penetration enhancement. An HPLC assay was developed that allowed ASX recovery from skin tissues and quantification. All SNEDDS formulations had droplets in the 20 nm range, with low polydispersity. ASX stability over 28 days storage in light and dark conditions was improved and antioxidant activity was high. SNEDDS-L1 (no terpene) gave significantly increased ASX penetration to the stratum corneum (SC) and the epidermis-dermis-follicle region (E + D + F) compared to an ASX in oil solution and a commercial ASX facial serum product. The SNEDDS-containing D-limonene gave the highest ASX permeation enhancement, with 3.34- and 3.79-fold the amount in the SC and E + D + F, respectively, compared to a similar applied dose of ASX in oil. We concluded that SNEDDS provide an effective formulation strategy for enhanced skin penetration of a highly lipophilic molecule, and when applied to ASX, have the potential to provide topical formulations for UV protection, anti-aging, and inflammatory conditions of the skin.

Keywords: skin targeting; antioxidant; terpenes; penetration enhancement; SNEDDS; nano-delivery; cosmeceutical; dermatological

Citation: Ponto, T.; Latter, G.; Luna, G.; Leite-Silva, V.R.; Wright, A.; Benson, H.A.E. Novel Self-Nano-Emulsifying Drug Delivery Systems Containing Astaxanthin for Topical Skin Delivery. *Pharmaceutics* **2021**, *13*, 649. https://doi.org/10.3390/pharmaceutics13050649

Academic Editors: Donatella Paolino, Jelena Filipović-Grčić and Cinzia Anna Ventura

Received: 2 March 2021
Accepted: 28 April 2021
Published: 3 May 2021

1. Introduction

There is increasing consumer demand for effective, natural-based products to protect the skin from environmental assault and treat dermatological conditions related to skin aging, irritancy, and inflammation [1]. Astaxanthin (3,3′-dihydroxy-β,β-carotene-4,4′-dione; ASX: Figure 1) is a carotenoid from the xanthophylls family with potent antioxidant activity [2]. ASX is commonly found in nature and is best known as the red-orange pigment that contributes the distinctive colour to many marine animals such as salmon, shrimp, and crayfish, and the flamingo birds that feast on them. It has many important biological functions in marine animals including pigmentation, protection against ultraviolet (UV) light effects, communication, immune response, reproductive capacity, stress tolerance, and protection against oxidation of macromolecules [3]. This keto-carotenoid is synthesized

pharmaceutics

MDPI

Supplementary Materials: Novel Self-Nano-Emulsifying Drug Delivery Systems Containing Astaxanthin for Topical Skin Delivery

Thellie Ponto, Gemma Latter, Giuseppe Luna, Vânia R. Leite-Silva, Anthony Wright and Heather A. E. Benson

Methods

HPLC instrumentation and conditions

Chromatographic separation was performed using an Agilent™ 1200 system (Agilent Technologies, Waldbronn, Germany), equipped with a degasser, binary pump, autosampler, multiple wavelength detector (at 476 nm UV detection), and Chemstation Rev B.04.03-SP1 software. A Jupiter C18 5 µm column, (150 mm × 4.6 mm) protected by a Security Guard Cartridge (C18, 4 × 3 mm) both from Phenomenex (Lane Cove, NSW, Australia), was used with isocratic flow of mobile phase (methanol: water: dichloromethane (DCM) = 85:13:2) at a flow rate of 1 mL/min (chromatography adapted from Yuan *et al.* [1]. The autosampler temperature was under a controlled temperature of 10 °C with an illuminator setting.

HPLC analysis method development

The HPLC method was developed for analysis of ASX in pharmaceutical formulations and extraction of ASX from skin tissues.

Linearity—Two series of ASX concentrations. System X (0.75–15 µg/mL) represented samples for determination of the solubility and stability of ASX, and the higher concentration tissue extract samples from skin permeation experiments with SNEDDS formulations. System Y (0.105–1.05 µg/mL) was for analysis of tissue sample extracts from commercial topical product administration in skin experiments.

Precision—ASX solutions at four concentrations (15, 3.75, 0.75 and 0.105 µg/mL) were analyzed in six replicates for each concentration. This provided concentrations from the two calibration curves used across the experimental samples. The acceptable relative standard deviation (RSD) < 5% [2].

Sensitivity—The blank solvent, a mixture of 15 mL of acetone and dichloromethane (50:50) and 10 mL mobile phase, was injected 6 times. The limit of detection (LOD) and LOQ (limit of quantification) were determined as three times and ten times the baseline noise level in the assay, respectively.

Accuracy—A mass balance study of ASX extracts from skin tissue samples that had been exposed to a SNEDDS formulation was carried out to assess the accuracy of the assay. The solvent extraction system was 50:50 ACT: DCM. The extraction procedure developed for the study involved soaking a pre-weighed section of skin tissue in 5 mL of an aqueous solution containing the SNEDDS-L1 formulation at a concentration of 0.0758 mg ASX/mL (equivalent to the theoretical concentration that would be present in an IVPT experiment) at 35 °C for 4h, then removing it, blotting dry and sectioning. The ASX was extracted from the skin sections (as per extraction protocol described in Section 2.6) and quantified by HPLC assay.

Results

HPLC assay method development

The HPLC method provided a single ASX peak for stock solution and good separation from any skin sample related peaks. ASX retention time was 8.3 ± 0.1 minutes with a

Appendix 5. Licence agreement for CC-BY

According to MDPI Terms of Use, unless otherwise stated, articles published on the MDPI websites are labelled as "Open Access" and licensed by the respective authors by the Creative Commons Attribution (CC-BY) license. Within the limitations mentioned in §4 of their Terms of Use, the "Open Access" license allows for unlimited distribution and reuse as long as appropriate credit is given to the source and any changes made compared to the original are indicated.

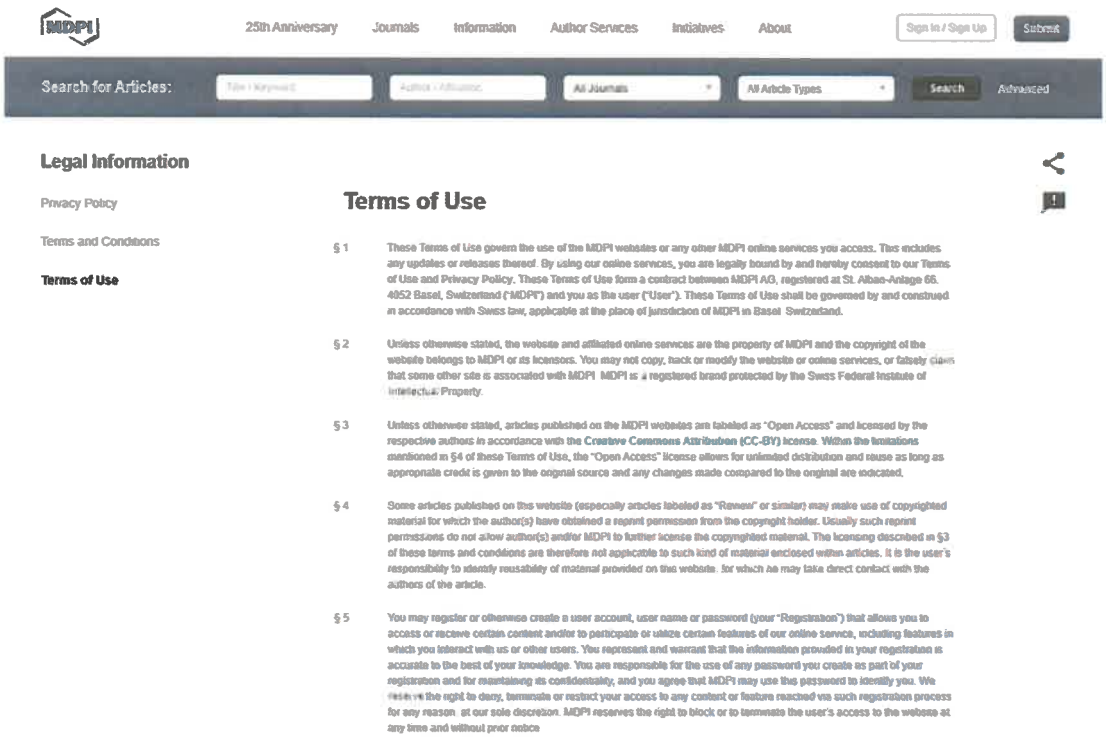

Appendix 6. Clinical study advertising flyer for recruitment (Chapter 4)

Curtin University

Can we melt away your cellulite?

We are conducting a research study to test if a new cream can improve skin circulation and appearance, particularly the presence of cellulite on the upper thighs area.

We need healthy women, between 18 to 55 years old. The study involves applying the formulation on your upper thigh areas twice a day, and attending 4 assessment sessions, that will each last about 30 mins. **A gift voucher** will be provided to thank you for assisting in the study.

For further information please contact Thellie Ponto on **0422018311** or thellie.ponto@postgrad.curtin.edu.au or Heather Benson on 92662338 or h.benson@curtin.edu.au.

This study has been approved by Curtin University Human Research Ethics Committee (HRE2019 - 0521).

0	0	0	0	0	0	0	0	0	0
4	4	4	4	4	4	4	4	4	4
2	2	2	2	2	2	2	2	2	2
2	2	2	2	2	2	2	2	2	2
0	0	0	0	0	0	0	0	0	0
1	1	1	1	1	1	1	1	1	1
8	8	8	8	8	8	8	8	8	8
3	3	3	3	3	3	3	3	3	3
1	1	1	1	1	1	1	1	1	1
1	1	1	1	1	1	1	1	1	1

Appendix 7. Patient information form (Chapter 4)

Curtin University

Investigation of a new caffeine cream on cellulite appearance

Principal Investigators: Thellie Ponto, Dr. Heather Benson and Prof. Anthony Wright

Location: CHIRI Clinical Research Facility Building 305, Curtin University (Bentley campus)

You are invited to participate in a research study to assess the effect of an anti-cellulite topical cream applied twice daily to both upper thighs. The project is being conducted by Thellie Ponto and is supervised by Dr. Heather Benson. Please read this information carefully and ask questions about anything that you do not understand.

1. What is the purpose of this research project?

Topical products containing coffee/caffeine are used to improve skin circulation and appearance. We have developed a cream that may improve caffeine permeation to its site of action in the skin and therefore its effectiveness. We will monitor its effect on the appearance of the skin that is most easily seen with the cellulite present on the upper thighs area. We also want to assess your perception of the skin as a routine cosmetic application.

2. Why have I been asked to participate in this research project?

You have been asked to participate in this research because you are a healthy adult aged between 18 and 55 with no history of anti-cellulite treatment in the past 3 months or major surgery within the past year including liposuction; and no appearance of scarring on the thigh area.

3. What will I have to do if I decide to participate?

If you decide to take part, you will be asked to sign a participant consent form and will be provided with a copy of this information sheet to keep. You will be asked to attend four research sessions that will last for approximately 30 minutes per session on four separate days (Day 0, Week 4, 8 and 12). You will be advised to discontinue any topical products you normally use on the skin at the treatment site for the duration of the 12 weeks study. On each day you will apply the assigned creams on the left and right upper thighs, twice daily, in the morning and at night before bedtime. We will take some baseline measurements and photos before you apply the products. Then another 3 sets of measurements and photos will be taken every four weeks (week 4, week 8 and week 12). These measurements will include your weight, thigh circumference and skin fat fold thickness. During each session your upper thighs will also be photographed.
You will be given a diary to monitor the cream applications and you will be asked to evaluate the products and the treatment through questionnaires on week 4, 8 and 12. The diary will be collected on the completion of the study. We will give you a gift voucher to thank you for participating in the study. The cream used in the study will not be available after completion of the study.

4. What are the benefits of participation?

There are no direct benefits for you in participating in the study. The results of the study will assist us in developing a new formulation that could be more effective in reducing cellulite and improving skin circulation. The test product will not be available after the study period is completed.

5. What are the risks of participation?

There are minimal risks involved in this study. The active cream contains caffeine, which is most commonly taken in caffeinated drinks such as coffee, tea and cola, but also available in topical creams and scrubs to improve the skin.

6. Do I have to take part in this research project? What happens if I withdraw?

You are not obliged to take part in this research and your decision to participate is entirely voluntary. You will be asked to sign a consent form prior to research commencement and you do not have to take part if you do not wish to. Please take your time and ask any questions. You can withdraw at any time during the study without prejudice.

7. Will my participation be kept confidential?

You will be given a unique identification number which will be linked to the data collected from you to keep your information confidential. Soft copies of data will be stored on a spreadsheet that will be saved on a password protected Curtin server while hard copies of data will be stored at the Curtin School of Pharmacy and Biomedical Sciences, in a locked cupboard. All data will only be used for research purposes and will only be accessible to the research team. Once the study is completed, the hard copies of data will be stored securely in a locked cupboard for 7 years before being destroyed.

8. What will happen to the results from the research project?

Results from this study will be published in a research journal and/or presented at a conference. Your individual data will not be identifiable and only overall results will be presented.

9. How is this study being paid for?

This study is being funded by Curtin University.

10. Further information and who to contact?

Curtin University's School of Pharmacy and Biomedical Sciences is responsible for the research project. Approval for this study will be sought from the Human Research Ethics Committee (HREC) at Curtin University. If you have any questions or would like further clarification on aspects of this research project you are more than welcome to contact Thellie Ponto or Dr. Heather Benson. We would be more than happy to discuss any issues you have regarding this project.

Contact details

Name	**Thellie Ponto**	**Dr. Heather Benson**	**Prof. Tony Wright**
Position	PhD student	Supervisor	Investigator
Telephone	08-92661357	9266 2833	9266 3675
Email	thellie.ponto@postgrad.curtin.edu.au	H.Benson@curtin.edu.au	t.wright@curtin.edu.au

Ethics review and complaints

Curtin University Human Research Ethics Committee (HREC) has approved this study (HRE2019 - 0521). Should you wish to discuss the study with someone not directly involved, in particular, any matters concerning the conduct of the study or your rights as a participant, or you wish to make a confidential complaint, you may contact the Ethics Officer on (08) 9266 9223 or the Manager, Research Integrity on (08) 9266 7093 or email hrec@curtin.edu.au.

Thank you for considering participation in this study. If you wish to participate please complete the attached consent form

Appendix 8. Patient consent form (Chapter 4)

Curtin University

HRE2019-0521

CONSENT FORM

Contact details

Name	**Thellie Ponto**	**Dr. Heather Benson**	**Prof. Anthony Wright**
Position	PhD student	Supervisor	Investigator
Telephone	08-92661357	9266 2833	9266 3675
Email	thellie.ponto@postgrad.curtin.edu.au	H.Benson@curtin.edu.au	t.wright@curtin.edu.au

- I have read the participant information sheet and I understand its contents.
- I believe I understand the purpose, extent and possible risks of my involvement in this project.
- I voluntarily consent to take part in this research project and I can withdraw at any time of the study without consequences.
- I have had an opportunity to ask questions and I am satisfied with the answers I have received.
- I understand that my data will be de-identified at all times to ensure my privacy.
- I understand that this project has been approved by Curtin University Human Research Ethics Committee and will be carried out in line with the National Statement on Ethical Conduct in Human Research (2007).
- I understand I will receive a copy of this Information Sheet and Consent Form.
- I do consent to the storage and use of my information in future ethically-approved research projects related to this study.

Participant Name	
Participant Signature	
Date	

Declaration by researcher: I have supplied an Information Sheet and Consent Form to the participant who has signed above, and believe that they understand the purpose, extent and possible risks of their involvement in this project.

Researcher Name	Thellie Ponto
Researcher Signature	
Date	2019

Appendix 9. Study questionnaire used for collection of participant responses (Chapter 4)

Curtin University

Principal Investigators: Thellie Ponto, Dr. Heather Benson and Prof Anthony Wright

Location: CHIRI Clinical Research Facility Building 305, Curtin University (Bentley campus)

Each questionnaire will take about 10 minutes.
Questionnaire for WEEK 0

A.	**Participant information**
Instructions: For section (A), please fill out your personal information.	

Name : Mobile number :
Date of birth :
Race/skin type : Caucasian / Asian / African / Other – please specify
Height : cms
Weight : kgs
BMI :

B.	**DIET AND EXERCISE**
Instructions: This section, for each question that contains the box (☐), please only tick (✓) **ONE BOX** for each question.	

1. Please indicate your usual diet:
   ☐ balanced – meat and vegetable
   ☐ vegetarian
   ☐ vegan
   ☐ other – please specify

2. How much water do you drink per day?
   ☐ less than a litre ☐ 1-2 litres ☐ more than 2 litres

3. Which caffeinated drinks do you have? (*Please tick all that apply*)
   ☐ coffee ☐ tea ☐ chocolate ☐ soda drinks ☐ energy drinks

4. Do you do regular physical exercise? ☐ Yes ☐ No
   If "Yes", please describe:

5. Have you used anti-cellulite treatment in the past 3 months?

☐ Yes ☐ No

6. Have you had a major surgery in the past year including liposuction or skincare treatment?

☐ Yes ☐ No

7. Have you any scarring of the skin tissues in the upper thigh area?

☐ Yes ☐ No

8. Have you any scarring of the skin tissues in the buttock?

☐ Yes ☐ No

Thank you for completing these questions

Curtin University

Investigation of a new caffeine cream on cellulite appearance

Name: **Weight:** **kgs** **Code:** **Date:**
Week: 4 / 8 / 12
Left leg / Right leg *(Please circle as appropriate)*

Instructions:
This section, for each question that contains the box (□), please only tick (✓) **ONE BOX** for each question how much you agree or disagree with it.

C.	**The suitability of the products** Section C is to determine your perceptions of the product.

		Strongly disagree 1	Disagree 2	Neither agree/ nor disagree 3	Agree 4	Strongly agree 5
1.	The product is a good colour	□ 1	□ 2	□ 3	□ 4	□ 5
2.	The product has a very pleasant smell	□ 1	□ 2	□ 3	□ 4	□ 5
3.	The product absorbs perfectly	□ 1	□ 2	□ 3	□ 4	□ 5
4.	The product spreads easily	□ 1	□ 2	□ 3	□ 4	□ 5
5.	The product leaves sticky on the skin	□ 1	□ 2	□ 3	□ 4	□ 5
6.	The product leaves the skin feeling smooth	□ 1	□ 2	□ 3	□ 4	□ 5

Instructions:
This section, for each question that contains the box (□), please only tick (✓) **ONE BOX** that best describes your answer.

D.	**Customer's perception on effect of the products** This part is to assess if the product you used had an effect on your skin.

		Poor 1	Fair 2	Good 3	Very good 4	Excellent 5
7.	The hydration (moisture) of my skin is	□ 1	□ 2	□ 3	□ 4	□ 5
8.	The smoothness of my skin is	□ 1	□ 2	□ 3	□ 4	□ 5
9.	The elasticity of my skin is	□ 1	□ 2	□ 3	□ 4	□ 5
10.	The dimpled appearance (”orange peel”) on my thigh skin is	□ 1	□ 2	□ 3	□ 4	□ 5

Thank you for completing these questions

Curtin University

Investigation of a new caffeine cream on cellulite appearance

Name: **Weight:** **kgs** **Code:**
Date:
Week: 4 / 8 / 12
Left leg / Right leg *(Please circle as appropriate)*

Instructions:
This section, for each question that contains the box (□), please only tick (✓) **ONE BOX** that best describes your answer.

D.	**Customer's perception on effect of the products** This part is to assess if the product you used had an effect on your skin.

	Poor 1	Fair 2	Good 3	Very good 4	Excellent 5
11. The hydration (moisture) of my skin is	□ 1	□ 2	□ 3	□ 4	□ 5
12. The smoothness of my skin is	□ 1	□ 2	□ 3	□ 4	□ 5
13. The elasticity of my skin is	□ 1	□ 2	□ 3	□ 4	□ 5
14. The dimpled appearance ("orange peel") on my thigh skin is	□ 1	□ 2	□ 3	□ 4	□ 5

E.	**Overall impression of the products**

	Much worse 1	Worse 2	Somewh at worse 3	About the same 4	Somewh at better 5	Better 6	Much better 7
The cellulite on my thigh is	□ 1	□ 2	□ 3	□ 4	□ 5	□ 6	□ 7

F.	**Additional feedback** (*Please describe if you have comments on the products during your treatment)*

Appendix 10. Instructions provided to evaluators to grade degree of cellulite from photographs (Chapter 3 - validation phase)

Grading of photos: Instructions for validation phase

Thank you for assisting our study by providing independent validation of our cellulite grading process.

You have been provided a cellulite grading scale chart showing images of the upper thigh, 24 photos of the upper thigh area of study participants, and a table for recording of cellulite grades for each photo against the grading scale chart. The cellulite grading scale chart shows 9 images, grouped in 3 lines, that have been scored on a scale of 0 “no intensity” to 8 “maximum intensity” based on the “orange peel” appearance of cellulite.

Please follow the protocol below to grade the cellulite appearance of each of the 24 photos independently.

1. Review the grading system prior to viewing the first photo. Note that there are 3 rows of images depicting cellulite on upper thighs. The severity of the cellulite images increases from left to right.
2. Turn over the first photo and note the code. Review the photo and focus on the most severe area of cellulite on the posterior upper thigh in between the area of the black marker to the back of the knee.
3. Compare the cellulite appearance on the photo to the images on the cellulite grading chart. Based on appearance of the most severe cellulite area decide which row of images on the grading chart is closest.
4. Next compare the photo with the 3 grade images within the chosen row and decide which is most comparable.
5. If you are in doubt between two grades, **select the higher grade**.
6. Write the chosen cellulite grade next to the photo code on the table.
7. Repeat the steps 2 – 6 for each photo, viewing only **one photo at a time**.

Appendix 11. Example of reporting sheets (0,4,8 and 12 weeks for evaluation of cellulite grading by evaluators (Chapter 3)

Curtin University

Example of cellulite grading table at baseline

Assessor:			Date:
Table of celululite grading			
Photo code	Cellulite Grade	Photo code	Cellulite Grade
S01_RL_WK0		S15_RL_WK0	
S02_RL_WK0		S16_RL_WK0	
S03_RL_WK0		S18_RL_WK0	
S04_RL_WK0		S19_RL_WK0	
S05_RL_WK0		S20_RL_WK0	
S06_RL_WK0		S21_RL_WK0	
S07R_RL_WK0		S22_RL_WK0	
S08_RL_WK0		S23_RL_WK0	
S09_RL_WK0		S24_RL_WK0	
S10_RL_WK0		S19R_RL_WK0	
S12_RL_WK0		S20R_RL_WK0	
S13_RL_WK0			
S14_RL_WK0			

Notes: S= subject; R= replacement code when the participant was replaced

Example of cellulite grading table at WK8

Assessor:			Date:
Table of celululite grading			
Photo code	Cellulite Grade	Photo code	Cellulite Grade
S01_LL_WK8		S15_LL_WK8	
S02_LL_WK8		S16_LL_WK8	
S03_LL_WK8		S18_LL_WK8	
S04_LL_WK8		S19_LL_WK8	
S05_LL_WK8		S20_LL_WK8	
S06_LL_WK8		S21_LL_WK8	
S07R_LL_WK8		S22_LL_WK8	
S08_LL_WK8		S23_LL_WK8	
S09_LL_WK8		S24_LL_WK8	
S10_LL_WK8		S19R_LL_WK8	
S12_LL_WK8		S20R_LL_WK8	
S13_LL_WK8			
S14_LL_WK8			

Notes: cellulite grading table form is based on the right leg (RL) and left leg (LL) at WK0= baseline; WK4= week 4; WK8= week 8; WK12= week 12

Appendix 12. Elsevier license agreement for use of published figures/tables/illustrations

ELSEVIER LICENSE TERMS AND CONDITIONS

Nov 03, 2021

This Agreement between Curtin University – Thellie Ponto ("You") and Elsevier ("Elsevier") consists of your license details and the terms and conditions provided by Elsevier and Copyright Clearance Center.

License Number	5181421407587
License date	Nov 03, 2021
Licensed Content Publisher	Elsevier
Licensed Content Publication	International Journal of Pharmaceutics
Licensed Content Title	Microemulsion for topical application of pentoxifylline: In vitro release and in vivo evaluation
Licensed Content Author	Airlla L.M. Cavalcanti,Mysrayn Y.F.A. Reis,Geilza C.L. Silva,İzola M.M. Ramalho,Geovani P. Guimarães,José A. Silva,Karina L.A. Saraiva,Bolívar P.G.L. Damasceno
Licensed Content Date	Jun 15, 2016
Licensed Content Volume	506
Licensed Content Issue	1-2
Licensed Content Pages	10
Start Page	351
End Page	360
Type of Use	reuse in a thesis/dissertation
Portion	figures/tables/illustrations
Number of figures/tables/illustrations	1
Format	both print and electronic
Are you the author of this Elsevier article?	No
Will you be translating?	No
Title	Development of Novel Nanocosmeceuticals for Skin Delivery
Institution name	Curtin University
Expected presentation date	Jan 2022
Portions	Figure 1 on page 354
Requestor Location	Curtin University Bld 306-102, Curtin Medical School Kent Street, Bentley Perth, WA 6102 Australia Attn: Thellie Ponto
Publisher Tax ID	GB 494 6272 12
Total	**0.00 AUD**

Terms and Conditions

INTRODUCTION

1. The publisher for this copyrighted material is Elsevier. By clicking "accept" in connection with completing this licensing transaction, you agree that the following terms and conditions apply to this transaction (along with the Billing and Payment terms and conditions established by Copyright Clearance Center, Inc. ("CCC"), at the time that you opened your Rightslink account and that are available at any time at http://myaccount.copyright.com).

GENERAL TERMS

2. Elsevier hereby grants you permission to reproduce the aforementioned material subject to the terms and conditions indicated.
3. Acknowledgement: If any part of the material to be used (for example, figures) has appeared in our publication with credit or acknowledgement to another source, permission must also be sought from that source. If such permission is not obtained then

ELSEVIER LICENSE
TERMS AND CONDITIONS

Nov 03, 2021

This Agreement between Curtin University – Thellie Ponto ("You") and Elsevier ("Elsevier") consists of your license details and the terms and conditions provided by Elsevier and Copyright Clearance Center.

License Number	5181381042674
License date	Nov 03, 2021
Licensed Content Publisher	Elsevier
Licensed Content Publication	European Journal of Pharmaceutical Sciences
Licensed Content Title	Novel mechanisms and devices to enable successful transdermal drug delivery
Licensed Content Author	B.W Barry
Licensed Content Date	Sep 1, 2001
Licensed Content Volume	14
Licensed Content Issue	2
Licensed Content Pages	14
Start Page	101
End Page	114
Type of Use	reuse in a thesis/dissertation
Portion	figures/tables/illustrations
Number of figures/tables/illustrations	1
Format	both print and electronic
Are you the author of this Elsevier article?	No
Will you be translating?	No
Title	Development of Novel Nanocosmeceuticals for Skin Delivery
Institution name	Curtin University
Expected presentation date	Jan 2022
Portions	Figure 3 summarises some ways for circumventing the stratum corneum barrier.
Requestor Location	Curtin University Bld 306-102, Curtin Medical School Kent Street, Bentley Perth, WA 6102 Australia Attn: Thellie Ponto
Publisher Tax ID	GB 494 6272 12
Total	**0.00 AUD**

Terms and Conditions

INTRODUCTION

1. The publisher for this copyrighted material is Elsevier. By clicking "accept" in connection with completing this licensing transaction, you agree that the following terms and conditions apply to this transaction (along with the Billing and Payment terms and conditions established by Copyright Clearance Center, Inc. ("CCC"), at the time that you opened your Rightslink account and that are available at any time at http://myaccount.copyright.com).

GENERAL TERMS

2. Elsevier hereby grants you permission to reproduce the aforementioned material subject to the terms and conditions indicated.
3. Acknowledgement: If any part of the material to be used (for example, figures) has appeared in our publication with credit or acknowledgement to another source, permission must also be sought from that source. If such permission is not obtained then

ELSEVIER LICENSE
TERMS AND CONDITIONS

Nov 03, 2021

This Agreement between Curtin University – Thellie Ponto ("You") and Elsevier ("Elsevier") consists of your license details and the terms and conditions provided by Elsevier and Copyright Clearance Center.

License Number	5181290275422
License date	Nov 03, 2021
Licensed Content Publisher	Elsevier
Licensed Content Publication	Journal of Controlled Release
Licensed Content Title	Topical and cutaneous delivery using nanosystems
Licensed Content Author	MS Roberts,Y Mohammed,MN Pastore,S Namjoshi,S Yousef,A Alinaghi,IN Haridass,E Abd,VR Leite-Silva,HAE Benson,JE Grice
Licensed Content Date	Feb 10, 2017
Licensed Content Volume	247
Licensed Content Issue	n/a
Licensed Content Pages	20
Start Page	86
End Page	105
Type of Use	reuse in a thesis/dissertation
Portion	figures/tables/illustrations
Number of figures/tables/illustrations	2
Format	both print and electronic
Are you the author of this Elsevier article?	No
Will you be translating?	No
Title	Development of Novel Nanocosmeceuticals for Skin Delivery
Institution name	Curtin University
Expected presentation date	Jan 2022
Portions	Figure 1 and Figure 2. Images on page 89 and 90
Requestor Location	Curtin University Bld 306-102, Curtin Medical School Kent Street, Bentley Perth, WA 6102 Australia Attn: Thellie Ponto
Publisher Tax ID	GB 494 6272 12
Total	**0.00 AUD**

Terms and Conditions

INTRODUCTION

1. The publisher for this copyrighted material is Elsevier. By clicking "accept" in connection with completing this licensing transaction, you agree that the following terms and conditions apply to this transaction (along with the Billing and Payment terms and conditions established by Copyright Clearance Center, Inc. ("CCC"), at the time that you opened your Rightslink account and that are available at any time at http://myaccount.copyright.com).

GENERAL TERMS

2. Elsevier hereby grants you permission to reproduce the aforementioned material subject to the terms and conditions indicated.
3. Acknowledgement: If any part of the material to be used (for example, figures) has appeared in our publication with credit or acknowledgement to another source, permission must also be sought from that source. If such permission is not obtained then

Appendix 13. Dove Medical press license agreement for use of published image and figure

04th November 2021

Dear Thellie Ponto,

ACI212991 - Drug development/Abd - Permission Granted

Thank you for your below enquiry.

I am pleased to confirm that we grant permission to use figure 1 from the below article for your thesis aimed at researchers and examiners and at no cost.

Skin models for the testing of transdermal drugs
Abd E et al
Clinical Pharmacology: Advances and Applications 2016 8 163-176

Please note:

- The figure must be fully cited
- Dove Medical Press must be acknowledged as the original publisher
- Any other re-use in the future will require separate permission to be requested
- No transfer of copyright should be inferred or implied

Please let me know should you have any further questions.

Best regards
Kylie

Kylie Maden
Sales Administrator
Dove Medical Press Limited

Beechfield House,
Winterton Way,
Macclesfield SK11 0LP
United Kingdom
www.dovepress.com

T: +44 (0)1625 704501
F: +44 (0)1625 617933

E: kylie.maden@dovepress.co.uk

DOVE Medical Press

15th March 2022

Dear Thellie Ponto,

ACI221452 - Cellulite treatment/Dupont - Permission Granted

Many thanks for your pdf, we have reviewed the document and can confirm that this has now been approved and permission has been granted to re-use figure 3 from the below article;

An integral topical gel for cellulite reduction: results from a double-blind, randomized, placebo-controlled evaluation of efficacy
Dupont E et al
Clinical, Cosmetic and Investigational Dermatology 2014 7 73-88

Permission is granted on a one-time basis and any other request for re-use in the future will require separate permission.

We look forward to working with you again shortly.

Best regards
Kylie

Kylie Maden
Sales Administrator
Dove Medical Press Limited

T: +44 (0)1625 704501/ F: +44 (0)1625 617933/ E: kylie.maden@dovepress.co.uk / www.dovepress.com

Appendix 14. Future Science license agreement for use of published article

Permission to use Future Science Ltd copyright material

Request from:

- Contact name: Thellie Ponto
- Publisher/company name: Curtin University
- Address:
- Telephone/e-mail: thellie.ponto@postgrad.curtin.edu.au

Request details:

- Request to use the following content: Table 1, Future Science OA (2020) FSO613
- In the following publication: As part of a thesis
- In what media (print/electronic/print & electronic): Print and Electronic
- In the following languages: All

We, Future Science Ltd, grant permission to reuse the material specified above within the publication specified above.

Notes and conditions:

1. This permission is granted free of charge, for one-time use only.
2. Future Science Ltd grant the publisher non-exclusive world rights to publish the content in the publication/website specified above.
3. Future Science Ltd retains copyright ownership of the content.
4. Permission is granted on a one-time basis only. Separate permission is required for any further use or edition.
5. The publisher will make due acknowledgement of the original publication wherever they republish the content: citing the author, content title, publication name and Future Science Ltd as the original publisher.
6. The publisher will not amend, abridge, or otherwise change the content without authorization from Future Science Ltd.
7. Permission does not include any copyrighted material from other sources that may be incorporated within the content.
8. Failure to comply with the conditions above will result in immediate revocation of the permission here granted.

Date: 24th November 2021